

The effect of single tree morphology and forest structure on drought stress response of beech (*Fagus sylvatica* L.)

Thomas Willibald Mathes

Vollständiger Abdruck der von der TUM School of Life Sciences der Technischen Universität
München zur Erlangung eines

Doktors der Forstwissenschaft (Dr. rer. silv.)

genehmigten Dissertation.

Vorsitz:

Prof. Dr. Thomas Knoke

Prüfende der Dissertation:

1. Prof. Dr. Peter Annighöfer
2. Prof. Dr. Dominik Seidel

Die Dissertation wurde am 05.03.2024 bei der Technischen Universität München eingereicht
und durch die TUM School of Life Sciences am 24.06.2024 angenommen.

1 Acknowledgements

The year 2023 was the hottest year since the beginning of weather records. The climate crisis continues to worsen, with the long-warned effects of wildfires, droughts, and floods becoming increasingly visible. Between 2018 and 2020, parts of Germany experienced an exceptional drought. This series of drought events was the impetus for this thesis. I want to thank my supervisor, Prof. Dr. Peter Annighöfer, for his inspiring suggestions and invaluable support and guidance in investigating the effects of drought on beech forests. In addition, I would like to express my gratitude to my second supervisor, Prof. Dr. Dominik Seidel, for his excellent advice and supervision. I am grateful to them and all the co-authors of my publications for the opportunity to learn from their scientific experience and expertise. Further, I thank Prof. Dr. Thomas Knoke for chairing my examination committee.

Thanks also to my mentor, Dr. Heinz Utschig, for his valuable suggestions on how to view scientific results in the context of practical applications. Furthermore, I am indebted to my colleagues at the Professorship of Forest and Agroforestry Systems, especially Rudolf Harpaintner, for their indispensable support during the field and laboratory work. Many thanks also go to the students who contributed to the project's success with their bachelor and master theses and their work as student assistants.

As a field study, such work is inconceivable without the forest. I thank the Kitzingen-Würzburg Office for Food, Agriculture, and Forestry and the Bavarian State Forest Enterprise with its regional state forest enterprises Arnstein and Ebrach for access to experimental plots.

This study is the result of a research project funded by the Bavarian State Ministry of Food, Agriculture, and Forestry. I sincerely thank the Bavarian Forest Administration for making this work possible by seconding me to the Technical University of Munich. Additionally, I am grateful to the Bavarian Forest Institute (LWF), particularly its President, Dr. Peter Pröbstle, and the Board of Trustees, headed by Stefan Tretter, for their idealistic and financial support.

2 Content

1	Acknowledgements.....	I
2	Content.....	II
3	Summary.....	IV
4	Zusammenfassung.....	VI
5	Peer-reviewed paper	VIII
5.1	Paper I.....	IX
5.2	Paper II.....	X
5.3	Paper III	XII
6	Introduction.....	1
6.1	Impact of drought stress on European beech forests	1
6.2	Relationship between single tree morphology and drought stress.....	2
6.3	Relationship between forest structure and drought stress.....	3
6.4	Assessment of single tree morphology and forest structure using laser scanning technology.....	4
6.5	Research Objectives.....	6
7	Material and Methods	8
7.1	Study area	8
7.2	Data collection	10
7.3	Data processing.....	14
7.4	Statistical analysis.....	19
7.5	Overview.....	21
8	Results	22
8.1	Occlusion in laser scanning point clouds (Paper I)	22
8.2	Effect of single tree morphology on drought stress response of beech (Paper II).....	25
8.3	Effect of forest structure on drought stress response of beech (Paper III)	27
8.4	Intra-annual variation of the $\delta^{13}\text{C}$ signal.....	29
9	Discussion.....	31
9.1	Occlusion in laser scanning point clouds (Paper I)	31

9.2	Effect of single tree morphology on drought stress response of beech (Paper II)	34
9.3	Effect of forest structure on drought stress response of beech (Paper III)	38
9.4	Intra-annual variation of the $\delta^{13}\text{C}$ signal	40
9.5	Effect of drought stress on beech wood quality	40
9.6	Response of other tree species to the 2018-2020 drought event	41
9.7	Mitigating drought stress through species interactions	42
10	Conclusion	44
11	References	47
12	Appendices	63
12.1	Paper I	63
12.2	Paper II	84
12.3	Paper III	101
12.4	Student projects	113

3 Summary

The exceptional drought period between 2018 and 2020 has caused considerable damage to beech (*Fagus sylvatica* L.) forests in Central Europe. This thesis investigates the influence of tree morphology and forest structure on the response of beech trees to drought stress in northern Bavaria, Germany, using a combination of mobile laser scanning technology and retrospective analyses of radial increment and $\delta^{13}\text{C}$ signal. The thesis consists of two main parts:

In the first part, the influence of occlusion is investigated when recording single tree morphology and forest structure using mobile laser scanning technology. For this purpose, beech and spruce (*Picea abies* (L.) H. Karst.) stands were scanned at different times of the year, both in leaf-on (summer) and leaf-off (winter) conditions, from the ground as well as from the ground and from above using a crane. The analysis showed a substantial occlusion, especially in the canopy area. Although the influence of occlusion on single tree morphologies was less than expected, it still led, for example, to a reduction in measured tree heights. At the stand level, ground scanning alone led to a loss of information in the canopy space, reflected in changes in the point counts, the Clark-Evans index and the box-dimension. A voxel size of at least 20 cm was suitable for reducing occlusion effects while maintaining a high level of detail in the point clouds. These results were used to validate the laser scanner technology for the subsequent analysis of drought effects.

In the second part, the influence of single tree morphology and forest structure on the vulnerability of European beech to drought years 2018 to 2020 was investigated. For this purpose, 990 beech trees in 240 drought-affected forest plots were analyzed. Tree morphology, such as tree height and crown volume, was recorded using a mobile laser scanner, while drought stress was assessed by examining core samples, $\delta^{13}\text{C}$ signals, and crown defoliation. There were clear responses of beech trees to drought, including increased crown defoliation, reduced tree growth, and altered $\delta^{13}\text{C}$ signatures compared to pre-drought values.

In terms of tree morphology, core analysis showed that dominant trees were particularly affected by the drought. While these trees still showed increased growth in 2018, they showed significant decreases in radial growth in 2019 and 2020. The $\delta^{13}\text{C}$ signal increased with increasing drought, indicating more substantial drought stress. In extreme drought, the influence of competition on tree growth decreased. Morphological differences between trees had a minor impact on drought resistance. Understory trees, however, showed some stability in growth during drought years.

Concerning the stand structure, the results showed a correlation between crown closure and defoliation in beech, indicating an increased susceptibility to drought in more open stands. But the potential of silvicultural measures to reduce drought stress, as measured by

increment and $\delta^{13}\text{C}$ signal, seems limited. However, the results suggest that increasing structural complexity may increase drought resistance through compensatory effects of the understory. Future forest management strategies could include promoting structural diversity, promoting vital individuals during thinning, and actively enriching forests with drought-resistant tree species to improve the adaptive capacity of beech-dominated forests to climate change. Overall, the intensity of the 2018-2020 drought event was so severe that it appears to have overridden many known rules and drivers of forest ecology and forest dynamics (social position, morphology, competition).

This thesis provides insights into the complex effects of drought events on beech forests. It highlights the need to adapt forest management to changing climatic conditions, particularly by promoting structural diversity and selecting drought-resistant tree species to increase the resistance of beech-dominated forests.

4 Zusammenfassung

Die außergewöhnliche Dürreperiode zwischen 2018 und 2020 hat in Mitteleuropa erhebliche Schäden an Buchenwäldern (*Fagus sylvatica* L.) verursacht. Diese Arbeit untersucht den Einfluss der Baummorphologie und der Waldstruktur auf die Reaktion von Buchen auf Dürrestress in Nordbayern mittels einer Kombination von mobiler Laserscantechnik und retrospektiven Analysen des Radialzuwachses und des $\delta^{13}\text{C}$ -Signals. Die Arbeit gliedert sich in zwei Hauptabschnitte:

Im ersten Teil wird der Einfluss der Verdeckung (Okklusion) bei der Erfassung der Baummorphologie und der Waldstruktur mittels mobiler Laserscantechnik untersucht. Dazu wurden Buchen- und Fichtenbestände (*Picea abies* (L.) H. Karst.) zu verschiedenen Jahreszeiten sowohl im belaubten (Sommer) als auch im unbelaubten Zustand (Winter) vom Boden und mit Hilfe eines Krans auch von oben erfasst. Die Analyse zeigt, dass vor allem im Bereich der Baumkronen eine starke Okklusion vorherrscht. Der Einfluss der Okklusion auf die Einzelbaummorphologien war zwar geringer als erwartet, führte aber beispielsweise zu einer Reduktion der gemessenen Baumhöhen. Auf Bestandesebene führte der Informationsverlust im Kronenbereich zu einer verringerten Punktdichte, Veränderungen des Clark-Evans-Index und der Box-Dimension. Eine Voxelgröße von mindestens 20 cm erwies sich als geeignet, um Okklusionseffekte zu reduzieren und gleichzeitig einen hohen Detailgrad in den Punktwolken zu erhalten. Diese Erkenntnisse dienen der Validierung der Laserscantechnik für die anschließende Analyse der Dürreeffekte.

Im zweiten Teil wurde der Einfluss von Einzelbaummorphologie und Waldstruktur auf die Resistenz der Rotbuche gegenüber den Dürrejahren 2018 bis 2020 untersucht. Dazu wurden 990 Buchen auf 240 Plots in von Dürre betroffenen Waldgebieten (Fränkische Platte, Steigerwald) analysiert. Die Morphologie der Bäume, wie Baumhöhe und Kronenvolumen, wurde mit einem mobilen Laserscanner erfasst, während der Dürrestress durch Jahrringanalysen, $\delta^{13}\text{C}$ -Signalen und der Kronenverlichtung quantifiziert wurde. Es zeigten sich deutliche Reaktionen der Buchen auf die Trockenheit, darunter erhöhte Kronenverlichtung, reduziertes Wachstum und veränderte $\delta^{13}\text{C}$ -Signaturen im Vergleich zu den Werten vor der Dürre.

In Bezug auf die Baummorphologie zeigte die Jahrringanalyse, dass insbesondere dominante Bäume stark unter der Dürre litten. Während diese Bäume 2018 noch Mehrzuwächse aufwiesen, zeigten sie 2019 und 2020 deutliche Rückgänge. Mit zunehmender Trockenheit nahm das $\delta^{13}\text{C}$ -Signal zu, was auf verstärkten Dürrestress hinweist. Bei extremer Dürre nahm der Einfluss der Konkurrenz auf das Baumwachstum ab. Morphologische Unterschiede zwischen den Bäumen hatten nur einen geringen Einfluss auf die Dürre-resistenz. Die unterständigen Bäume hingegen zeigten in den Dürre-jahren eine gewisse Wachstumsstabilität.

Hinsichtlich der Bestandesstruktur zeigten die Ergebnisse eine Korrelation zwischen Kronenschluss und Kronenverlichtung bei Buchen, was auf eine erhöhte Dürreanfälligkeit in offeneren Beständen hindeutet. Das Potenzial waldbaulicher Maßnahmen zur Minderung von Trockenstress, gemessen am Zuwachs und am $\delta^{13}\text{C}$ -Signal, scheint allerdings begrenzt. Die Ergebnisse deuten darauf hin, dass eine Erhöhung der strukturellen Komplexität die Dürre-resistenz durch kompensatorische Effekte des Unter- und Zwischenstandes erhöhen kann. Zukünftige Waldbewirtschaftungsstrategien könnten darauf abzielen, die strukturelle Diversität zu erhöhen, vitale Individuen im Rahmen von Durchforstungen zu fördern und die Wälder aktiv mit dürreresistenten Baumarten anzureichern, um die Anpassungsfähigkeit buchendominierter Wälder an den Klimawandel zu verbessern. Insgesamt wird deutlich, dass die Intensität des Dürreereignisses 2018-2020 so gravierend war, dass viele bekannte Regeln der Walddynamik (soziale Stellung, Morphologie, Konkurrenz) an Bedeutung verlieren.

Diese Arbeit gibt einen Einblick in die komplexen Auswirkungen von Dürreereignissen auf Buchenwälder. Sie unterstreicht die Notwendigkeit, die Waldbewirtschaftung an die sich ändernden Klimabedingungen anzupassen, insbesondere durch die Förderung der Strukturvielfalt und die Auswahl dürreresistenter Baumarten, um die Resistenz buchendominierter Wälder zu erhöhen.

5 Peer-reviewed paper

This dissertation is presented as a cumulative dissertation based on the following three lead authorships. The original abstract and individual author contributions are provided for each paper. In addition, one peer-reviewed co-authored paper has been published during the time of this dissertation.

Lead authorships (Basis of the cumulative thesis)

Mathes, T., Seidel, D., Häberle, K.-H., Pretzsch, H. and Annighöfer, P. 2023 What Are We Missing? Occlusion in Laser Scanning Point Clouds and Its Impact on the Detection of Single-Tree Morphologies and Stand Structural Variables. *Remote Sensing* 15, 450.

Mathes, T., Seidel, D. and Annighöfer, P. 2023 Response to extreme events: do morphological differences affect the ability of beech (*Fagus sylvatica* L.) to resist drought stress? *Forestry: An International Journal of Forest Research* 96, 355–371.

Mathes, T., Seidel, D., Klemmt, H.-J., Thom, D. and Annighöfer, P. 2024 The effect of forest structure on drought stress in beech forests (*Fagus sylvatica* L.). *Forest Ecology and Management* 554, 121667.

Co-authorships

Mataruga, M., Cvjetković, B., De Cuyper, B., Aneva, I., Zhelev, P., **Mathes, T.**, ... & Villar-Salvador, P. (2023). Monitoring and control of forest seedling quality in Europe. *Forest Ecology and Management* 546, 121308.

5.1 Paper I

What Are We Missing? Occlusion in Laser Scanning Point Clouds and Its Impact on the Detection of Single-Tree Morphologies and Stand Structural Variables

Mathes, T.; Seidel, D.; Häberle, K.-H.; Pretzsch, H.; Annighöfer, P.

Published in 2023 in Remote Sensing 15, 450, <https://doi.org/10.3390/rs15020450>

Impact Factor (2022): 5.0

Abstract

Laser scanning has revolutionized the ability to quantify single-tree morphologies and stand structural variables. In this study, we address the issue of occlusion when scanning a spruce (*Picea abies* (L.) H.Karst.) and beech (*Fagus sylvatica* L.) forest with a mobile laser scanner by making use of a unique study site setup. We scanned forest stands (1) from the ground only and (2) from the ground and from above by using a crane. We also examined the occlusion effect by scanning in the summer (leaf-on) and in the winter (leaf-off). Especially at the canopy level of the forest stands, occlusion was very pronounced, and we were able to quantify its impact in more detail. Occlusion was not as noticeable as expected for crown-related variables but, on average, resulted in smaller values for tree height in particular. Between the species, the total tree height underestimation for spruce was more pronounced than that for beech. At the stand level, significant information was lost in the canopy area when scanning from the ground alone. This information shortage is reflected in the relative point counts, the Clark–Evans index and the box-dimension. Increasing the voxel size can compensate for this loss of information but comes with the trade-off of losing details in the point clouds. From our analysis, we conclude that the voxelization of point clouds prior to the extraction of stand or tree measurements with a voxel size of at least 20 cm is appropriate to reduce occlusion effects while still providing a high level of detail.

Author Contributions

Thomas Mathes (T.M.), Dominik Seidel (D.S.) and Peter Annighöfer (P.A.) conceived the ideas for the study; T.M., D.S., Hans Pretzsch (H.P.) and P.A. designed the methodology for the study; T.M., D.S. and P.A. analyzed the data; T.M. wrote the first draft of the manuscript; T.M., D.S., Karl-Heinz Häberle (K.-H.H.), H.P. and P.A. contributed to further versions of the manuscript.

5.2 Paper II

Response to extreme events: do morphological differences affect the ability of beech (*Fagus sylvatica* L.) to resist drought stress?

Mathes, T.; Seidel, D.; Annighöfer, P.

Published in 2023 in *Forestry: An International Journal of Forest Research*, 96, 3, Pages 355–371, <https://doi.org/10.1093/forestry/cpac056>

Impact Factor (2022): 2.8

Abstract

Adaptive silvicultural approaches intend to develop forests that can cope with changing climatic conditions. Just recently, many parts of Germany experienced 3 years of summer drought in a row (2018–2020). This study analyzed the effects of this event on beech (*Fagus sylvatica* L.) in two regions in northern Bavaria, Germany. For this purpose, 990 beech trees were studied on 240 plots in drought-stressed forests. We examined trees of different social position and different size. Their morphology (e.g., tree height, crown volume) was recorded by laser scanning, and drought stress was quantified by tree core sample analyses. In addition to increment analyses, the $\delta^{13}\text{C}$ signal was determined by year. Results show that the dominant tree collective was particularly affected by the drought. They still managed to perform well in 2018, but the radial growth decreased significantly in 2019 and 2020, partly resembling the performance values of subordinate trees. Subordinate trees, on the other hand, provide some consistency in growth during drought years. The drought was so severe that the effects of competition on tree growth began to disappear. The difference in growth of two geographically distinct study areas equalized due to drought. With continuing drought, increasing levels of the $\delta^{13}\text{C}$ signal were detected. Similar patterns at different $\delta^{13}\text{C}$ levels were found across the social positions of the trees. The influence of tree morphological variables on tree resistance to drought showed no clear pattern. Some trends could be found only by focusing on a data subset. We conclude that the intensity of the 2018–2020 drought event was so severe that many rules and drivers of forest ecology and forest dynamics (social position, morphology, and competition) were overruled. The influence of morphological differences was shown to be limited. The weakening of dominant trees could potentially be no longer linear and drought events like the one experienced in 2018–2020 have the potential of acting as tipping points for beech forests.

Author Contributions

Thomas Mathes (T.M.), Dominik Seidel (D.S.) and Peter Annighöfer (P.A.) conceived the ideas for the study; T.M., D.S. and P.A. designed the methodology for the study; T.M., D.S. and P.A. analyzed the data; T.M. wrote the first draft of the manuscript; T.M., D.S. and P.A. contributed to further versions of the manuscript.

5.3 Paper III

The effect of forest structure on drought stress in beech forests (*Fagus sylvatica* L.)

Mathes, T.; Seidel, D.; Klemmt, H.J.; Thom, D.; Annighöfer, P.

Published in 2024 in Forest Ecology and Management 554, 121667, <https://doi.org/10.1016/j.foreco.2023.121667>

Impact Factor (2022): 3.7

Abstract

The unprecedented drought between 2018 and 2020 had a significant impact on European beech (*Fagus sylvatica* L.) forests in Central Europe. The role of different forest structures in mitigating drought stress remains controversial. This contentious debate prompted our study, in which we aimed to quantify the effect of forest structure on drought stress in beech forests in two ecoregions of northern Bavaria, Germany. Using a mobile laser scanner, we surveyed 240 plots in drought-stressed forests. We analyzed the responses of beech trees to the drought period through radial growth, wood-derived $\delta^{13}\text{C}$ signal, and crown defoliation. Results revealed significant responses of beech forests in both regions to the drought event, including increased crown defoliation, reduced tree growth, and altered $\delta^{13}\text{C}$ signatures compared to pre-drought conditions. Our results show a relationship between crown closure and crown defoliation in beech, suggesting an increased vulnerability of beech to drought in more open canopies. However, the potential for silvicultural intervention to mitigate drought stress, as measured by BAI and $\delta^{13}\text{C}$ signal, appears limited. Neighboring trees and forest structure had little influence on average drought resistance. The $\delta^{13}\text{C}$ signal showed minimal responsiveness to variations in canopy openness, as well as to distinctions between single and multi-layered forests. However, increased structural complexity within stands tended to increase resistance due to the compensatory effects of understory trees. Future forest management strategies could focus on promoting structural diversity, selecting resilient individuals but also actively enrich the forests with more drought-adapted species to increase the adaptive capacity of beech-dominated forests in the face of changing climate conditions.

Author Contributions

Thomas Mathes (T.M.), Dominik Seidel (D.S.) and Peter Annighöfer (P.A.) conceived the ideas for the study; T.M., D.S. and P.A. designed the methodology for the study; T.M., D.S., Dominik Thom (D.T.) and P.A. analyzed the data; T.M. wrote the first draft of the manuscript; T.M., D.S., Hans-Joachim Klemmt (H.-J.K.), D.T. and P.A. contributed to further versions of the manuscript.

6 Introduction

6.1 Impact of drought stress on European beech forests

2023 was the hottest year since the beginning of weather records ([Copernicus Climate Change Service, 2024](#)). The climate crisis continues to worsen, and the long-predicted effects of wildfires, droughts, and floods are becoming increasingly visible. Yet, as in previous years, global greenhouse gas emissions continued to rise in 2023. 36.8 billion tons of carbon dioxide (CO₂) or its equivalent were emitted ([Friedlingstein et al., 2023](#)). To make matters worse, a significant portion of global warming is not directly attributable to current emissions but results from slow feedback mechanisms and delayed additional effects ([Hansen et al., 2023](#)). For Central Europe, a continuation of the trend towards more frequent and more intense droughts is predicted ([IPCC, 2018](#), [Hari et al., 2020](#), [Rakovec et al., 2022](#)). Between 2018 and 2020, for example, parts of Germany experienced an exceptional drought with significant impacts on forests ([Senf and Seidl, 2021](#), [Thonfeld et al., 2022](#), [Thom et al., 2023](#)). In total, 14 million cubic meters of broadleaf trees died, severely affecting European beech (*Fagus sylvatica* L.) ([BMEL, 2021](#)). Beech is sensitive to summer droughts such as those that occurred in Central Europe in 2003 and 2018 to 2020 ([Scharnweber et al., 2011](#), [Schuldt et al., 2020](#), [Del Martinez Castillo et al., 2022](#)). In addition to severe growth losses ([Scharnweber et al., 2020](#), [Leuschner et al., 2023](#)), partial or complete crown dieback, premature leaf drop, and leaf discoloration were observed ([Nussbaumer et al., 2020](#), [Bigler and Vitasse, 2021](#), [Arend et al., 2022](#)). Beech trees were also susceptible to secondary infestation leading to increased mortality ([Corcobado et al., 2020](#), [Langer and Bußkamp, 2023](#)). One of the major damage centers was located in northern Bavaria, Germany ([StMELF, 2023](#)).

The decline of beech is becoming increasingly critical, especially due to its position as Central Europe's most common broadleaf species ([Forest Europe, 2020](#)). Beech plays an important role from an ecological and economic point of view ([Ellenberg and Leuschner, 2010](#), [Yousefpour et al., 2018](#)). Beech forests of different types are Germany's dominant potential natural vegetation, forming complex and unique deciduous and mixed forest ecosystems associated with various faunistic and floristic species. The proportion of beech in Germany is currently increasing, mainly due to the conversion of coniferous forests into mixed deciduous forests. Consequently, the proportion of beech in the regeneration layer is significantly higher than in older stands ([Thünen-Institut, 2012](#)).

The sustainable use of beech is closely linked to the goal of climate neutrality in Germany and Europe ([European Commission, 2019](#)). Its contribution to climate protection results from the CO₂ sequestration potential of healthy beech forest ecosystems on the one hand ([van der Woude et al., 2023](#)), and from the use of wood as a renewable raw material on the

other. However, beech forests can only fulfill their expected role in climate protection if they are stable under climate change conditions. Studies show that different provenances have specific adaptations. For example, [Kramer et al. \(2017\)](#) found significant differences in temperature requirements for bud bursts, indicating local temperature adaptations. [Čortan et al. \(2019\)](#) observed morphological adaptations to different climatic conditions, highlighting the high adaptability of beech.

However, forest ecosystems are particularly vulnerable to extreme climate events due to their relatively slow natural rates of adaptation ([Allen et al., 2010](#)). During this slow adaptation process, extreme weather events, especially droughts, may increasingly act as tipping points for ecosystems ([Barnosky et al., 2012](#)). Evidence from recent years supports the prediction that the magnitude and speed of climate change will overwhelm the adaptive capacity of many tree species and pose major challenges for forest management ([Lindner et al., 2010](#)). A significant decline in growth is predicted for beech ([Del Martinez Castillo et al., 2022](#)).

Adapting beech forests to climate change raises the question of the importance of forest structures, such as layering or the degree of canopy closure, as well as about single tree morphology in the context of drought stress mitigation. This is even more relevant as many beech stands are in the mature phase ([Thünen-Institut, 2012](#)) and need adaptation to climate change. Against this background, the question arises of how existing stands can be silviculturally managed to prolong the lifespan of beech-dominated stands and gain time for a gradual conversion to other tree species. The targeted promotion of favorable structures and single tree morphologies could decisively influence climate-adapted forest management. These open questions are addressed in this dissertation.

6.2 Relationship between single tree morphology and drought stress

In this context, the influence of single tree morphology, such as tree height, crown volume, or leaf area index, on drought stress in trees is discussed ([Dobbertin et al., 2010](#), [Adams et al., 2015](#)). It is hypothesized that more giant trees may be more drought-resistant due to their extensive root systems and greater canopy surface area. Such trees may extract water from the soil more effectively than trees in denser stands ([Whitehead et al., 1984](#), [Aussenac and Granier, 1988](#)).

However, there are also studies suggesting that more giant trees may be significantly less resistant and subject to increased mortality during droughts ([Bennett et al., 2015](#), [Serra-Maluquer et al., 2018](#), [Stovall et al., 2019](#)), which could be due to increased sensitivity from higher radiation and evapotranspiration requirements. Exposed trees may have increased

water requirements as a result of increased light exposure and associated transpiration rates ([McDowell et al., 2006](#)). The increased transpiration rates of large trees may be related to increased hydraulic stress in situations of limited water availability ([Ruehr et al., 2014](#)).

The situation might be different for subordinate and smaller trees. These individuals also compete with dominant trees for limited resources above and below the ground, and their lower social position could be disadvantageous and lead to higher stress levels ([Diaconu et al., 2017](#)). [Lüttschwager and Jochheim \(2020\)](#) emphasize that thinning could stabilize forests under drought conditions by removing understory trees, arguing that dominant trees have better water storage behavior and higher adaptability to drought than understory trees.

However, despite their lower social position, understory trees may benefit from the shade and microclimate under the canopy of more dominant but exposed trees. This microclimatic potential could compensate for limitations imposed by their lower position and reduced access to resources ([Hardt Ferreira Dos Santos et al., 2020](#)). Heat and drought could reduce the growth of exposed tall trees relative to smaller trees, leading to a more even size distribution and a more homogeneous vertical structure of the stand ([Grote et al., 2016](#)). [van der Maaten \(2013\)](#) found that dominant beech trees were particularly sensitive to drought compared to understory trees. Correspondingly, [Meyer et al. \(2022\)](#) found a shift in tree mortality patterns from suppressed to more giant trees due to the 2018 to 2019 drought.

6.3 Relationship between forest structure and drought stress

Another possible strategy to increase the resistance of beech forests to climate extremes could be to modify the forest structure through silvicultural interventions, such as thinning ([Del Campo et al., 2022](#)). Several studies support thinning, including [Martín-Benito et al. \(2010\)](#), [Calev et al. \(2016\)](#), and [Sankey and Tatum \(2022\)](#). The beneficial effects of significantly reduced basal area, resulting in less dense forest stands, have been observed for deciduous trees ([Diaconu et al., 2017](#), [Klesse et al., 2022](#)) and conifer species ([Giuggiola et al., 2013](#), [Sohn et al., 2016](#)). According to [Lagergren et al. \(2008\)](#), the short-term benefits of thinning include reduced transpiration and resource competition, resulting in increased soil water availability. Positive effects of thinning during or after drought include improved tree growth performance, as reported by [Kohler et al. \(2010\)](#), [Brooks and Mitchell \(2011\)](#), and [McDowell et al. \(2007\)](#). In addition, the reduction in tree mortality and the increase in vigor ([Bréda et al., 1995](#)) and the improved root development ([Whitehead et al., 1984](#)) support thinning as a beneficial intervention.

Conversely, thinning can also lead to undesirable outcomes. Changes in the radiation budget of the stand or the growth of ground vegetation after thinning can reduce soil moisture and

increase the water requirements of the more exposed trees, which can negate the benefits of thinning ([Gebhardt et al., 2014](#), [Bosela et al., 2021](#)). Increased wind speeds and stronger solar radiation can increase transpiration and evaporation rates ([Bréda et al., 2006](#), [Lagergren et al., 2008](#)). In addition, the increased leaf area of the favored trees and ground vegetation can lead to increased transpiration and interception, counteracting the positive effects ([Hedwall et al., 2013](#)). The importance of forest structure is also reflected in its impact on the microclimate. As [Zellweger et al. \(2020\)](#) and [Frenne et al. \(2021\)](#) show, higher canopy cover can mitigate forest warming. [Thom et al. \(2020\)](#) suggest that foresters should take advantage of the buffering capacity of closed canopies in the face of climate change. Excessive thinning can also reduce the structural complexity of the stand, impairing its ability to moderate internal climatic conditions and potentially leading to greater temperature and moisture fluctuations ([Aussenac, 2000](#), [Thom et al., 2020](#)).

The importance of forest structure is, therefore, the result of a complex interplay of factors such as thinning intensity and site conditions ([Nilsen and Strand, 2008](#)), tree species ([Leuschner et al., 2024](#)), stand age ([D'Amato et al., 2013](#)), tree architecture and social position in the stand structure ([Bennett et al., 2015](#)). Hence, determining the optimal forest structure in beech stands is a complex balancing act. Therefore, this study aims to improve understanding of the interactions between forest structure and drought stress in beech forests.

6.4 Assessment of single tree morphology and forest structure using laser scanning technology

There are several methods for assessing single tree morphology and forest structure. Traditional approaches often rely on qualitative descriptions and variables, such as simple quantitative measures like diameter at breast height (DBH) or tree position. Quantifying features in vertical space, especially crown features such as crown delineation or crown volume, requires considerable effort, leading to frequent standardizations or approximations.

In contrast, terrestrial laser scanning (TLS) has in recent years enabled detailed capture of forest structure, providing previously unattainable insights into ecosystem dynamics, as demonstrated, for example, by studies by [Seidel et al. \(2015\)](#), [Hyypä et al. \(2012\)](#) or [Bayer et al. \(2013\)](#). For forest inventory purposes, TLS data allow for faster and more efficient derivation of single tree morphologies, such as tree height and DBH ([Liang et al., 2016](#)). This method not only streamlines the measurement of classical variables but also facilitates the quantification of previously difficult traits. The accuracy of crown morphology measurements, such as crown volume, has been improved, which is relevant to various tree

physiological studies ([Pretzsch et al., 2015](#), [Jacobs et al., 2021](#)) that used laser scan data to illustrate the effects of drought stress on crown size and tree height.

Lidar-based scanners dominate mobile mapping in the field ([Lee et al., 2019](#)). In forestry, laser scan data are typically collected from the ground or air. Ground-based scanning includes two approaches: Terrestrial Laser Scanning (TLS) and Mobile Laser Scanning (MLS), also known as Handheld Personal Laser Scanning. In TLS, three-dimensional point clouds are created by single scans from fixed viewpoints ([Lovell et al., 2011](#)) or by combining multiple scans ([Dassot et al., 2011](#)). However, this method is time-consuming and expensive, as various scan locations are required to capture forest structures accurately. Conversely, MLS is faster and less costly ([Ryding et al., 2015](#)).

When using TLS or MLS, scans are often performed from the ground. This leads to an occlusion effect ([van der Zande et al., 2008](#), [Trochta et al., 2013](#), [Ehbrecht et al., 2016](#), [Abegg et al., 2017](#)), which raises questions about the degree of information loss from a single perspective and its impact on derived tree and forest structure variables. The degree of information loss due to occlusion is likely to depend on the spatial distribution of biomass, with dense stands being particularly affected ([Li et al., 2021](#)).

Species such as beech form dense canopies due to high shade tolerance and the development of shade leaves, which can block laser beams even at lower stand heights ([Matyssek et al., 2010](#)). Norway spruce (*Picea abies* (L.) H. Karst.) also develops dense canopies but loses needles in lower stem sections due to light deficiency under dense conditions. In both cases, laser scanners may have difficulties detecting the upper parts of the crowns when scanning from the ground during the growing season. In winter, beech trees lose their leaves, which improves the accessibility of ground-based laser beams, unlike spruce trees, which keep their needles.

Strategies for dealing with occlusion in mobile laser scanning include reducing the spatial resolution of the point cloud through voxelization ([Stiers et al., 2020](#), [Willim et al., 2020](#)). Voxelization can partially compensate for occlusion and spatial variation in point cloud density, depending on voxel size. However, this also results in a loss of detail in the point cloud and increased space-filling estimates.

The methodological basis of this study focuses on the investigation of occlusion in ground-based mobile laser scanning, using a test setup that allows the scanning of forest stands from both ground level and above. The aim was to quantify potential information loss, identify patterns of this loss, and examine how these vary with different voxel sizes.

6.5 Research Objectives

This thesis analyzes the influence of single tree morphology and forest structure on the response of European beech to drought stress in the years 2018 to 2020 using a combination of mobile laser scanning technologies and retrospective analyses of radial increment and $\delta^{13}\text{C}$ signal. This work is divided into two main parts: The first part focuses on detecting single tree morphologies and forest structures using mobile laser scanning ([Paper I](#)). The second part is dedicated to investigating the influence of single tree morphology and forest structure on the response of European beech to drought stress ([Paper II](#) and [Paper III](#)).

6.5.1 Occlusion in laser scanning point clouds ([Paper I](#))

The first paper of this thesis focuses on the determination of single tree morphology and forest structure using a mobile laser scanner. It deals with the phenomenon of occlusion in beech and spruce. Scanning was performed on forest stands from ground level only and also from both ground level and above using the KROOF crane experiment ([Pretzsch *et al.*, 2014](#)). Seasonal scanning was performed in summer (leaf-on) and winter (leaf-off) to assess seasonal effects on beech trees. The specific hypotheses tested in this study were:

Seasonal comparison

H1.1) For beech, the occlusion effect leads to significant differences in single tree morphologies when comparing summer to winter ground scans; for spruce there are no significant differences.

H1.2) For beech stands, the occlusion effect results in a significant difference in stand complexity when comparing summer to winter scans; for spruce there is no significant difference.

Methodological comparison

H1.3) For single trees, the occlusion effect leads to smaller values for canopy morphologies of all trees (e.g., lower height, smaller crown volume) when scanned only from the ground.

H1.4) For stands, the occlusion effect results in an underestimation of the stand structural variables when scanned only from the ground.

H1.5) For stand specific variables, the occlusion effect is reduced in importance as the resolution of the data decreases (voxel size increases).

6.5.2 Effect of single tree morphology on drought stress response of beech (Paper II)

The second paper focuses on the relationship between individual tree morphology and drought stress in beech. By assessing numerous factors such as social position, structural characteristics, and competitive environment, the study aims to correlate these aspects with the drought stress response of beech. Two regions with different environmental conditions will be studied. A crucial part of this research is using $\delta^{13}\text{C}$ signals in annual rings as an indicator of drought stress, complementing traditional increment analysis. Hypotheses tested in this work include:

H2.1.1: The radial growth reaction of beech trees to drought stress depends on their social position

H2.1.2: Trees that are accustomed to a warm and dry climate, as well as shallow sites, do not react as strongly to drought events in their radial growth

H2.2: The drought-related $\delta^{13}\text{C}$ signal differs between different social positions

H2.3: Morphological differences affect resistance to drought indicated by: a) impact on tree-ring growth and b) differences in stable carbon isotope signatures

H2.4: A lower competitive environment mitigates adverse drought effects

6.5.3 Effect of forest structure on drought stress response of beech (Paper III)

The third paper investigates the role of forest structure and drought stress in beech forests. The hypotheses are based on the assumption that multi-layered forests are more resistant to drought events. The hypotheses tested are:

H3.1: Beech forests in both study regions responded to the drought period with (1) defoliation, (2) growth decline, and (3) an increase in the $\delta^{13}\text{C}$ signature.

H3.2: With increasing canopy openness, (1) defoliation and (2) growth decline was greater, and (3) the $\delta^{13}\text{C}$ signature was more pronounced.

H3.3: Multi-layered beech forests exhibited (1) lower canopy defoliation and (2) higher resistance (as measured by tree growth and $\delta^{13}\text{C}$ signature) to the drought period compared to single-layered forests.

7 Material and Methods

7.1 Study area

7.1.1 Occlusion in laser scanning point clouds (Paper I)

The study site for the first paper of this thesis was located in the Kranzberg forest near Munich in southern Germany ([Pretzsch et al., 2016](#)). The KROOF experiment takes place at this site on 0.5 ha, originally developed for drought stress research ([Grams et al., 2021](#)). A canopy crane allows studies to be conducted at heights of up to 45 m ([Figure 1c](#)) and was used in this study to complement ground scans with scans from above the forest canopy. The forest consists mainly of spruce and beech, planted in the 1930s and 1950s ([Pretzsch et al., 2014](#)). These species dominate Germany's forested areas ([Thünen-Institut, 2012](#)). Beech was chosen because its single tree morphology and forest structure were investigated concerning drought stress in papers 2 and 3. Inventory data show that beech trees reach 28 m and spruce trees 32 m, with an average diameter at breast height of 29 cm and 35 cm, respectively ([Grams et al., 2021](#)). The stand consists of 639-926 trees/ha, with a volume increase of 19.4-26.3 m³/ha*yr ([Pretzsch et al., 2020](#)).

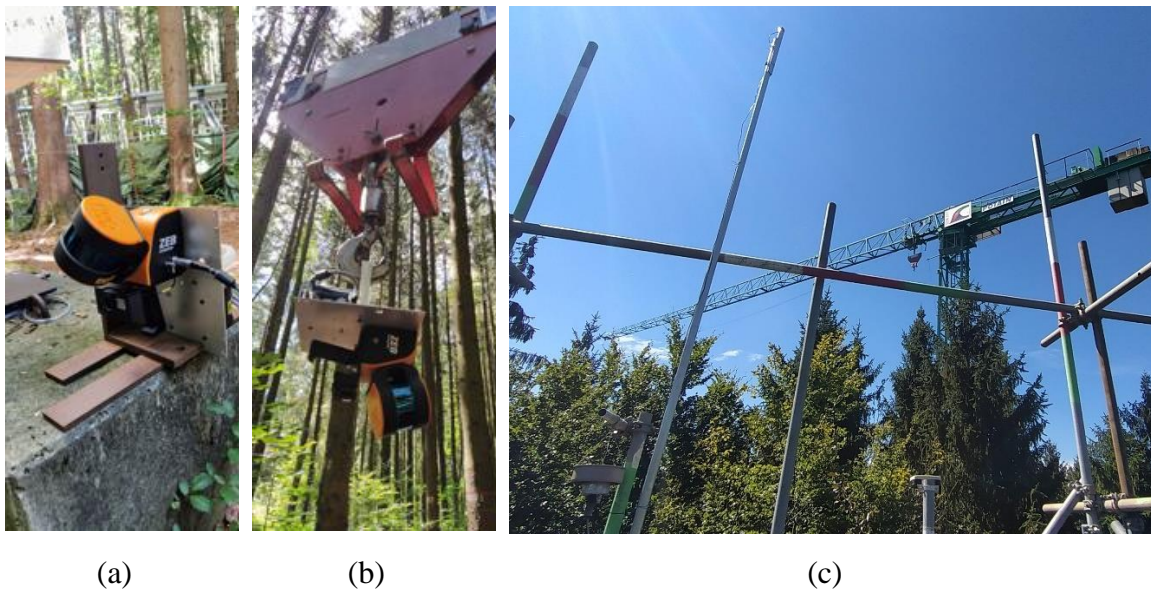


Figure 1 The mobile laser scanner in the start position a) and attached to the crane b). During operation, it was lifted over the canopy and moved smoothly over the canopy of the forest stand. Figure c) shows the crane itself. Figure taken from [Mathes et al. \(2023b\)](#).

7.1.2 Effect of single tree morphology and forest structure on drought stress response of beech (Paper II, III)

The second part of this thesis focused on two beech-dominated ecoregions in southern Germany: the "Plateau" near Würzburg and the "Steigerwald" near Bamberg (Figure 2). The Plateau, located in the Southern Franconian Plateau, is characterized by a warm, dry climate with an average annual temperature of 10.1 °C and precipitation of 576 mm (DWD, 2022a, 2022b). The soils formed from carbonate-rich limestone have limited water retention and are defined as Eutric Leptic Cambisol with a tendency towards Rendzic Leptic Phaeozem (FAO, 2014). This results in natural vegetation composed mainly of Hordelymo-Fagetum and Galio odorati-Fagetum (Walentowski, 2006).

The Steigerwald area contrasts with a cooler average temperature (8.6 °C) and higher precipitation (802 mm) (DWD, 2022a, 2022b). Its soils, formed on Keuper, are deeper than the Plateau's and are classified as Dystric Cambisol. This results in better water retention and predominant natural vegetation of Luzulo-Fagetum, accompanied by Galio odorati-Fagetum (Walentowski, 2006).

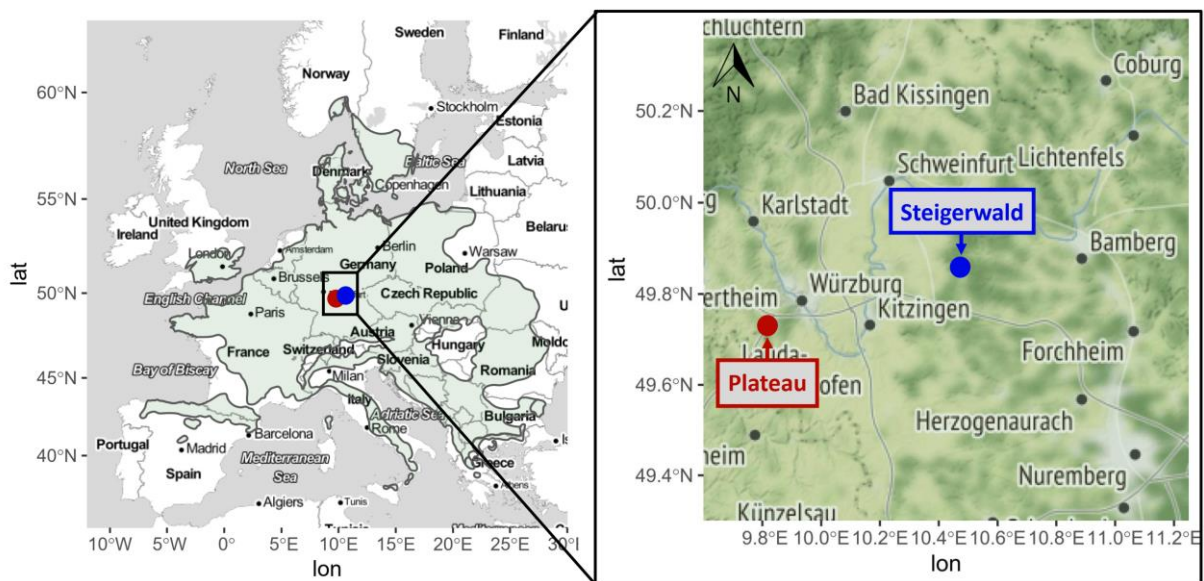


Figure 2 Geographic location of the study sites; the red dot represents the study area in the Plateau. This area is one of the warmest and driest areas in Germany. A bit more humid and cooler is the Steigerwald (blue dot). The green shading in the left map indicates the distribution pattern of European beech (*Fagus sylvatica* L.) in Europe, according to Caudullo et al. (2017). Map taken from Mathes et al. (2023a).

Both regions have sufficient nutrients for beech growth, but the summer water supply is limited. The Plateau and the Steigerwald experienced significant water deficits between 2018 and 2020 (Thom et al., 2023). Detailed site conditions are tabulated in Table 1.

Table 1 Main characteristics of Plateau and Steigerwald study sites presented by climatic, geographic, and soil data. The data basis is the Forest Atlas of Bavaria (LWF, 2005) and the climate stations of the German weather service (DWD, 2022a, 2022b). The climate data cited refer to the reference period 1991-2020. Table taken from Mathes et al. (2023a).

Study site	Plateau	Steigerwald
Latitude, longitude (WGS 84)	49.7286N, 9.8156E	49.8721N, 10.4724E
Elevation (m.a.s.l)	270-350	400-460
Geology	Muschelkalk	Keuper
Soils, according to the WRB	Eutric Leptic Cambisol (Clayic) with a tendency to Rendzic Leptic Phaeozem (Clayic)	Dystric Cambisol (Loamic)
Climate	suboceanic	suboceanic
Mean annual temperature	10.1 °C	8.6 °C
Mean annual precipitation	576 mm	802 mm
Potential vegetation/ plant association	Hordelymo-Fagetum and Galio odorati-Fagetum	Luzulo-Fagetum, but also Galio odorati-Fagetum

7.2 Data collection

7.2.1 Occlusion in laser scanning point clouds (Paper I)

The data were obtained from pure spruce and beech stands sections in two 30 m x 40 m plots. Scanning was conducted in summer 2020 (leaf-on) and winter 2020/2021 (leaf-off for broadleaves). Due to the lack of growth between these periods, the effects of the drought experiment treatments were excluded. The ZEB HORIZON mobile laser scanner (GeoSLAM Ltd., UK) was used, which can scan objects up to 100 m distance using the time-of-flight principle and SLAM (simultaneous localization and mapping) technology (Bauwens et al., 2016). This device, embedded with the Velodyne VLP-16 multibeam LiDAR, operated at a wavelength of 903 nm and scanned 300,000 points per second with a system accuracy of 1-3 cm.

Scanning was initially performed at ground level in a predetermined pattern, called the 'ground scan' (Figure 3a). This was followed by a 'full scan' using the same path as the first scan (under identical conditions) but supplemented by a canopy scan. For this, the scanner was attached to a crane and moved vertically over the canopy and horizontally, capturing data from the ground and above in one scan (Figure 3b). Consistency was ensured by using a single starting point for each scan. Eight different scans were conducted for the two tree species (beech and spruce), two methods (ground and full scan), and two seasons (summer and winter). All scans were conducted under ideal weather conditions.

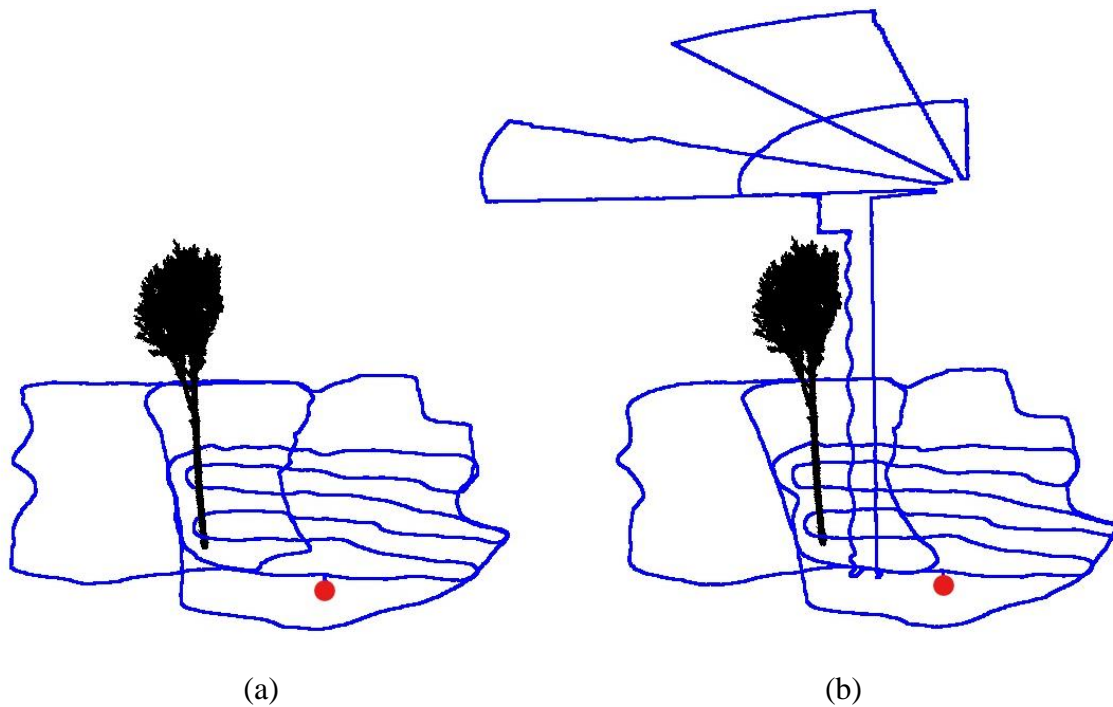


Figure 3 The walking paths (blue lines) for the beech plot for the two scan conditions a) ground scan and b) full scan. The red dot indicates the same starting point in each scan. The walking path on the ground is identical. A beech tree is shown as an example for better orientation. Figure taken from [Mathes et al. \(2023b\)](#).

7.2.2 Effect of single tree morphology and forest structure on drought stress response of beech (Paper II, III)

Stands selected for the study had to meet specific criteria to ensure homogeneity: a) terrain with less than 10 % slope, b) soil types limited to Dystric Cambisol (Steigerwald) and Eutric Leptic Cambisol (Plateau), and c) a forest dominated by beech trees (more than 80 % of the species) with no human intervention since 2018.

The forest area corresponding to these criteria was overlaid with a 60 m x 60 m grid. 240 plots were chosen for sampling - 120 each in the Steigerwald and the Plateau. On each plot, a central tree that varied in social position (dominant to subordinate), size (in terms of diameter), and forest structure (single to multi-layered) was selected. (Figure 4). Each sampling point averaged approximately four trees, including the central tree and its neighbors, as defined by their canopy interactions.



(a)

(b)

(c)

Figure 4 Exemplary overview of selected mature beech stands; (a) single-layer stand, (b) single-layer stand with regeneration, (c) multi-layer stand. Pictures from July 2021. Figure taken from [Mathes et al. \(2024\)](#).

Data were collected during winter 2020/2021 (leaf-off) and summer 2021 (leaf-on). A mobile laser scanner (ZEB HORIZON, GeoSLAM Ltd., UK) was used in winter to capture three-dimensional data of the forest within a 30 m radius of each central tree. The spiral scanning methodology was extended at intervals with increasing radii of 7 m, 14 m, 21 m, 28 m, and 35 m ([Figure 5](#)).

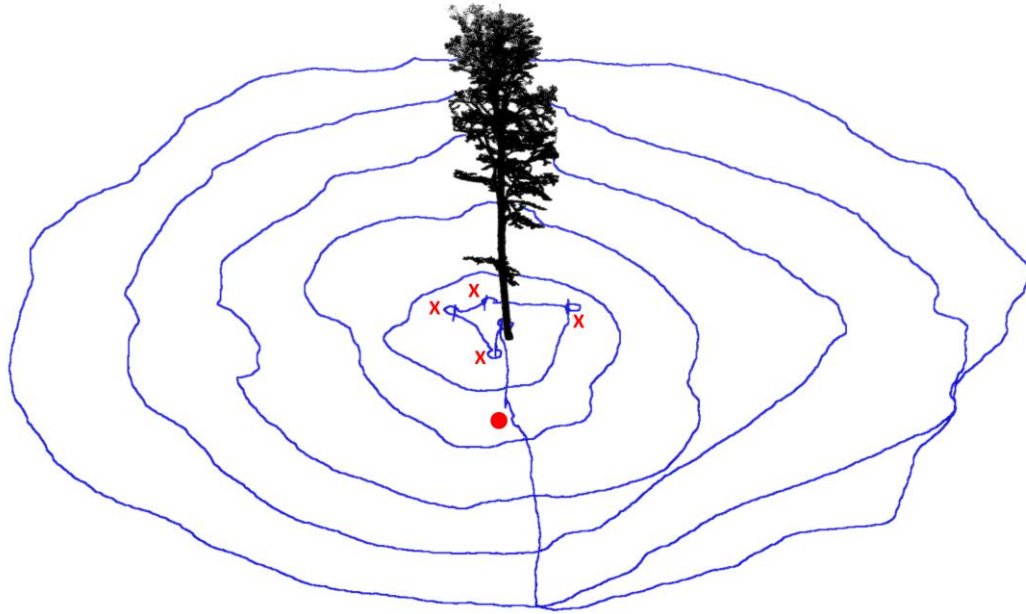


Figure 5 The walking path used with the mobile laser scanner to capture the forest stand on a plot (blue line). The red dot marks the start and end points of the scan. The scan path started in the south and went directly north to the central tree before the surrounding neighboring trees, marked with a red X, were scanned. The spiral scan method was extended at regular intervals with radii of 7 m, 14 m, 21 m, 28 m, and 35 m. The central tree is highlighted in this figure as an example of the point cloud.

During winter, two core samples were taken from each tree at breast height (increment borer: Haglöf Mora Coretax, diameter 5.15 mm). These samples were taken at 90° intervals from the north and east. During the summer, the vitality of the sample trees was assessed by crown condition. Trees were assigned to defoliation classes, categorized in 5 % increments. A tree with full foliage was scored 0 %, while a tree with no foliage was scored 100 % (Figure 6). This assessment methodology aligns with the forest status assessment approach used in Germany (Wellbrock and Eickenscheidt, 2018). The social position assessment was based on the approach by Kraft (1884). We combined Kraft's classes 1 and 2 into the "dominant" social position and Kraft's classes 4 and 5 into the "subordinate" social position. Kraft's class 3 will be further referred to as "intermediate". Crown competition was also recorded, ranging from 'crowded' canopies to the more widely spaced 'discontinuous' canopy structures.



(a) (b) (c) (d)

Figure 6 Beech trees with different degrees of crown defoliation. From a very vital crown (a) to a very thinned crown (d). Pictures from July 2021.

7.3 Data processing

7.3.1 Occlusion in laser scanning point clouds (Paper I)

The mobile laser scanner data was processed using GeoSLAM HUB 6.1 for SLAM registration. Scans were exported in .laz format and processed using the R package 'lidR' ([Roussel et al., 2020](#)). Point clouds around specific tree collectives were clipped to a 30 m x 40 m area. Ground points were classified using the ground segmentation algorithm ([Zhang et al., 2016](#)), and point heights were normalized using the spatial interpolation algorithm (interpolation is done using a k-nearest neighbor approach with an inverse-distance weighting). The point cloud was voxelized to 1 cm resolution to manage the data volume and aligned using CloudCompare software (version 2.11.3, cloudcompare.org, EDF R&D, Paris, France).

Twenty trees per species were identified for each scan from the resulting point cloud. Trees were segmented using LiDAR360 ([GreenValley International, Ltd., 2019](#)) and manually corrected using Cloud Compare software. Metrics were derived from each tree point cloud, including total height, diameter at breast height, maximum crown projection area, corresponding height, crown volume, and surface area. The diameter at breast height was determined using circular fitting and the height from the maximum z-value of the point cloud. The crown base, maximum crown projection area, crown volume, and crown surface area were also calculated, with all morphologies determined using a voxel size of 1 cm.

Six circular subplots of a 5 m radius were clipped from each scan for forest structure analysis. Relative point counts within these subplots were calculated by dividing the point clouds into 1-meter-thick horizontal slices and counting each point. The mean point count

for each height layer across the six subplots was determined, normalizing the maximum mean value observed in the winter scans as 100 %, with other values proportionally adjusted.

The spatial distribution of points was analyzed using the Clark-Evans (CE) index, a measure of object distribution in space ([Clark and Evans, 1954](#)). This index assesses the horizontal spread of points to evaluate clumping or regularity. Theoretically, the values of the CE index range from 0, indicating extreme clumping (all points at a singular location), to 2.1491, signifying a strictly regular hexagonal pattern. Values below 1.0 suggest clumping, around 1.0 indicate randomness, and above 1.0 point towards a regular distribution. The analysis was conducted using the "spatstat" package in R ([Baddeley and Turner, 2005](#)), with horizontal strata projected onto a plane by nullifying the z-values of each voxel. Duplicates were removed, and the Donnelly edge correction was applied to mitigate edge bias ([Donnelly, 1978, Pommerening and Stoyan, 2006](#)).

The box-dimension was employed to measure structural complexity in the forest ([Seidel, 2018](#)), simultaneously considering object density and their three-dimensional distribution. Calculations for the box-dimension were based on the respective point clouds of the subplots, incorporating the maximum tree height as the upper limit and the voxel size set (ranging from 5-50 cm) as the lower limit. This dimension was computed for three distinct horizontal forest strata (1-12 m, 13-24 m, 25-36 m) and the overall forest.

Relative point counts, the CE index, and the box-dimension were derived for voxel sizes of 5 cm, 10 cm, 20 cm, and 50 cm edge lengths.

7.3.2 Effect of single tree morphology and forest structure on drought stress response of beech (Paper II, III)

Tree core samples

To determine annual ring widths, tree cores were cut horizontally along the ring direction using a core microtome ([Gärtner and Nievergelt, 2010](#)) and then air-dried. The ring widths were then measured to within 0.01 mm. This measurement was done using a LINTAB 5 measuring table (Rinntech, Heidelberg, Germany) equipped with a Leica MZ 6 stereomicroscope (Wetzlar, Germany) and the TSAP-Win software (Rinntech, Version 4).

Cross-dating was performed on samples from cores with clearly visible annual rings. A default value of 0.01 mm was used in cases where annual rings were missing. The average of the measurements from two cores taken from one tree was calculated to set up a chronology for each tree.

Stable isotope analysis ($\delta^{13}\text{C}$)

For stable isotope analysis ($\delta^{13}\text{C}$) of the years 2016-2020, annual rings were isolated from tree cores taken in the northern direction of each stem. Rings were coarsely segmented and then finely ground using a ball mill (MM200, Retsch, Haan, Germany). To minimize potential bias from plastic microtubes, stainless steel microvials (BioSpec, Bartlesville, USA) and four-millimeter stainless steel balls were used. For $\delta^{13}\text{C}$ measurements, wood samples were weighed into tin capsules. These samples were combusted in an elemental analyser (NA 1110; Carlo Erba, Milan, Italy, and Vario Pyro Cube, Elementar, Hanau, Germany). This system was coupled to an isotope ratio mass spectrometer (Delta Plus; Finnigan MAT and IsoPrime 100, IsoPrime, Stockport, UK). The resulting measurements were then compared to a laboratory standard CO_2 gas, previously calibrated against a secondary isotope standard (IAEA- CH_6 for $\delta^{13}\text{C}$, calibration accuracy: 0.06 % SD). To improve precision, a solid internal laboratory standard (SILS) of wheat flour was used and calibrated against these references, with long-term precision below 0.2‰. Carbon isotope data are presented as $\delta^{13}\text{C}$ relative to the international Vienna Pee Dee Belemnite (VPDB) standard using the equation: $\delta^{13}\text{C} [\text{‰}] = [(R_{\text{sample}}/R_{\text{standard}}) - 1] \times 1000$, where R_{sample} and R_{standard} represent the ratios of $^{13}\text{C}/^{12}\text{C}$ in the sample and standard, respectively.

Laser scan data

The data collected by the mobile laser scanner were first processed using the GeoSLAM HUB software to perform the SLAM registration. Each point cloud was clipped to a 30 m radius around its central tree. Ground points were classified using the ground segmentation algorithm ([Zhang *et al.*, 2016](#)) and normalized using the spatial interpolation algorithm, using a k-nearest neighbor approach with inverse distance weighting. The dataset was next voxelized to a resolution of 1 cm^3 . The point clouds of individual trees were then identified and extracted using LiDAR360 software (GreenValley International, Ltd., 2019), based on the method of [Li *et al.* \(2012\)](#). However, complications arose in segmenting certain trees, such as incorrect or imprecise point assignments, requiring manual post-processing using CloudCompare software (Version 2.11.3, cloudcompare.org, EDF R&D, Paris, France). Metrics such as tree height, crown diameter, and crown volume were derived from the resulting individual tree point clouds using LiDAR360. The Hegyi index, a distance-dependent competition index, was also calculated considering the nearest ten neighbors identified by their trunk coordinates.

The 30 m radius of the point cloud was chosen to analyze the entire forest structure, complemented by a 10 m radius to study the immediate neighborhood. To assess the effects of direct solar radiation on beech trees, the point cloud with a ten-meter radius was reduced to its southern half, termed "Semicircle," for additional analysis. ([Figure 7](#)). The point

clouds were voxelized to a resolution of 20 cm, which proved to be a good compromise between accuracy and occlusion reduction in the first part of this thesis.

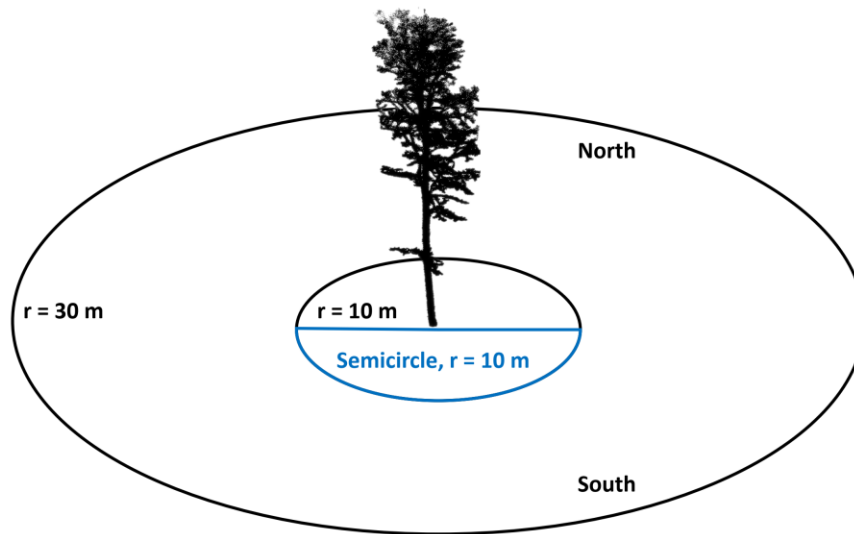


Figure 7 Overview of the respective cutting radii. In addition to the point cloud with a radius of 30 m, a point cloud with a radius of 10 m was used, and a “semicircle” reducing the 10 m point cloud to the southern half around the central tree. Figure taken from [Mathes et al. \(2024\)](#).

Spatial point distribution in this study was quantified using the Clark and Evans aggregation index (CE index), calculated using the spatstat R package ([Baddeley and Turner, 2005](#)). Evenness and skewness analyses were conducted to further explore the distribution characteristics within the forest ([Figure 8](#)). These analyses focused on the distribution patterns of the CE index, the tree height distribution, and the diameter at breast height (dbh) distribution of a plot. This assessment was performed across the three different point cloud radii, 30 m, 10 m, and the 10 m semicircular radius. The box-dimension, which reflects the complexity of the forest structure, was also calculated for each of these point clouds, according to the methodology described in [Seidel \(2018\)](#).

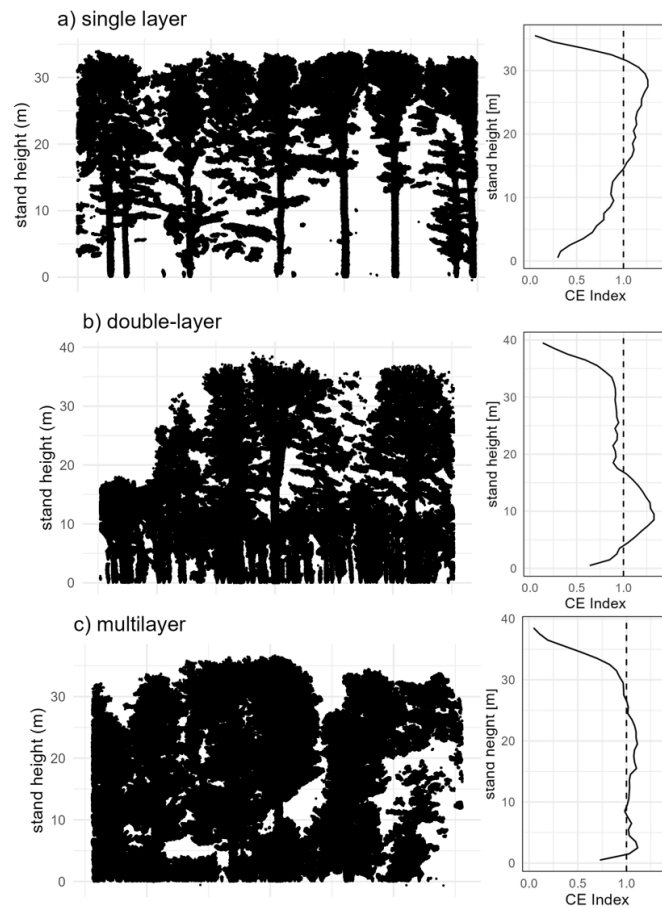


Figure 8 Overview of exemplary selected stands (cross-section through the laser scan point clouds) and how their vertical space-filling can be characterized using the CE index. (a) single-layer stand, (b) double-layer stand, (c) multilayer stand. Figure taken from [Mathes et al. \(2024\)](#).

7.3.3 Intra-annual variation of the $\delta^{13}\text{C}$ signal

In addition to the inter-annual $\delta^{13}\text{C}$ signals described above, the intra-annual variation of the $\delta^{13}\text{C}$ signals was measured. In winter 2022, cores were taken from twelve trees in the Plateau and in the Steigerwald. Six cores were selected for either high or low resistance index, according to [Mathes et al. \(2023a\)](#). These cores were sectioned using a core microtome ([Gärtner and Nievergelt, 2010](#)), scanned at high resolution, and measured using CooRecorder software version 9.8.1.

The experimental setup used a laser ablation isotope ratio mass spectrometry (LA-IRMS) system consisting of a UV laser (Teledyne LSX-213 G2+, Nd:YAG laser; wavelength 213 nm), a sample chamber (isoScell, Terra Analytic, Alba Iulia, Romania), a combustion oven, a Cryoflex trace gas system (Sercon, Crewe, UK) to collect the produced CO_2 with liquid nitrogen (LN_2) traps, a GC column (Rt-Q-Bond column, Restek, 0.53 mm ID, 30 m, 20 μm), and an IRMS for $\delta^{13}\text{C}$ measurement (HS2022, Sercon, Crewe, UK). The laser is aimed at a wood sample in a sealed chamber with settings of fluence 4 J/cm^2 ,

laser output 22.5 %, 20 Hz. Within each annual ring, ten shots were programmed. These gases and particles were then transported via helium to an oven to completely oxidize all carbon to CO₂. This CO₂, after drying in a Nafion trap, was collected in two trap stages and analyzed through a GC column that separated CO₂ from other gases. Finally, the $\delta^{13}\text{C}$ of the CO₂ was measured by IRMS. The $\delta^{13}\text{C}$ signals of these cores were explicitly analyzed for the years 2016 to 2022. The analyses were performed at the Swiss Federal Institute for Forest, Snow, and Landscape Research WSL; details of the measurement procedure can be found in [Saurer *et al.* \(2023\)](#).

7.4 Statistical analysis

7.4.1 Occlusion in laser scanning point clouds (Paper I)

A paired Wilcoxon rank sum test with Bonferroni adjusted p-values was used to analyze differences in single tree morphologies and forest structure metrics. This approach was chosen because the data did not consistently show a normal distribution or homogeneity of variance for all variables examined. A significance level of $p < 0.05$ was used for all statistical analyses.

7.4.2 Effect of single tree morphology and forest structure on drought stress response of beech (Paper II, III)

Increment and $\delta^{13}\text{C}$ signal analysis

The growth increment analysis for 2016-2020 aimed to exclude aging effects and focus on drought effects. Relative increments were calculated against the maximum value per tree during this period. The Kruskal-Wallis test was used to identify differences in growth and $\delta^{13}\text{C}$ signal, followed by post-hoc analysis using the Wilcoxon rank sum test with Bonferroni corrected p-value.

Resistance Indices

The Resistance Index (RT) was calculated to measure the impact of water stress-induced growth reduction from 2016 to 2020. The index was derived by dividing the arithmetic means of 2020 and 2019 by those of 2016 and 2017. Two indices were calculated: the Resistance Index for annual Basal Area Increment (Resistance Index BAI) and the $\delta^{13}\text{C}$ signal (Resistance Index $\delta^{13}\text{C}$). Values of RT BAI and RT $\delta^{13}\text{C}$ below 1 indicate a reduction

in radial growth and stomatal conductance due to prolonged drought. For the forest structure analysis, the mean and standard deviation of these indices and defoliation were calculated for each plot.

Regression analysis methods

GAM was used for regression analysis to investigate the relationship between annual basal area increment (BAI), resistance indices (RT BAI, RT $\delta^{13}\text{C}$), competition intensity (Hegyi-Index), and tree morphological variables. Model selection was based on Akaike's corrected information criterion with a Gaussian data family and identity link function. The number of knots was limited to three, adjusted by generalized cross-validation (R package MuMIn ([Bartoń, 2022](#))).

Drought-responsive trees were identified based on resistance indices for logistic regression analysis. Trees were classified for reduced or increased RT BAI and lower or higher RT $\delta^{13}\text{C}$ discrimination. Logistic regression was performed on a balanced dataset, with model accuracy and selection using the R package MuMIn and evaluated with the caret package ([Kuhn, 2022](#)).

Statistical analysis of canopy closure and regional differences

Differences between canopy closure levels and study regions were analyzed using the Wilcoxon rank-sum test with Bonferroni-corrected p-values, which was chosen due to the lack of normal distribution and homogeneity of variance for all variables studied.

Implementation of non-linear models

After z-transforming the variables, a Boruta feature selection analysis (R package “Boruta” ([Kursa and Rudnicki, 2010](#))) identified key stand structural variables for explaining RT BAI and RT $\delta^{13}\text{C}$. These variables were incorporated into a generalized additive model (GAM) using the restricted maximum likelihood (REML) method (R package “mgcv” ([Wood, 2011](#))). The model set a maximum of three knots to prevent overfitting, with automated adaptation via generalized cross-validation. Concurvity was checked to ensure reliable estimates.

Multiple logistic regression focused on extreme values of the resistance indices to investigate relationships between tree morphological variables, resistance indices, and defoliation. For this analysis, the highest and lowest 10 % of plots regarding drought response were selected. Model selection was guided by Akaike's information criterion (AIC) (R package “bestglm” ([McLeod et al., 2020](#))), and variance inflation factor was used to assess multicollinearity. The Tjur R^2 measured predictive power, and Odds Ratios (ORs) were calculated to evaluate associations (R package “sjPlot” ([Lüdecke, 2023](#))).

7.4.3 Intra-annual variation of the $\delta^{13}\text{C}$ signal

The Mann-Whitney U test was used to examine potential differences in the intra-annual $\delta^{13}\text{C}$ signal between regions and groups categorized by high or low resistance index. This non-parametric statistical test was chosen because of the violation of assumptions for parametric tests and its robustness to outliers. The results of this test helped to evaluate whether the region or the resistance index had a significant effect on the intra-annual $\delta^{13}\text{C}$ signal.

7.5 Overview

This section provides a comprehensive overview of the data sets collected during this dissertation (Table 2). It includes information on the types of data collected, their geographic locations, and the time of data collection. Each dataset is linked to the specific research papers to which it contributed.

Table 2 Overview of the data sets and their use in the dissertation's peer-reviewed publications.

Type of Data	Geographical Location	Time of Data Collection	Used in Paper
Mobile Laser Scanner Point Clouds	Kranzberg Forest, Plateau, Steigerwald; Germany	Summer and Winter 2020/2021	Paper I, II, III
Tree Ring Widths	Plateau, Steigerwald; Germany	Winter 2020/2021	Paper II, III
Isotope Signals	Plateau, Steigerwald; Germany	Winter 2020/2021	Paper II, III
Forest Structure, Crown Condition Surveys	Plateau, Steigerwald; Germany	Summer 2021	Paper II, III
Intra-annual $\delta^{13}\text{C}$ signal	Plateau, Steigerwald; Germany	Winter 2022/2023	-

All analyses in this thesis were performed using R 4.3.0 ([R Core Team, 2023](#)). Visualizations were created using the R package "ggplot2" ([Wickham, 2016](#)).

8 Results

This chapter presents the main results of the three papers on which this thesis is based. In addition, the intra-annual trend of the $\delta^{13}\text{C}$ signal is presented in a subchapter.

8.1 Occlusion in laser scanning point clouds (Paper I)

Analysis of spruce and beech tree point clouds revealed apparent morphological differences at the individual tree level, especially between ground scans and full scans. Ground scans had less detail in the upper part of the canopy compared to full scans (Figure 9 (1, 2) vs. Figure 9 (3, 4)). Seasonal changes, especially the presence or absence of leaves, affected the appearance of beech trees more than spruce trees (Figure 9 a vs. Figure 9 b).

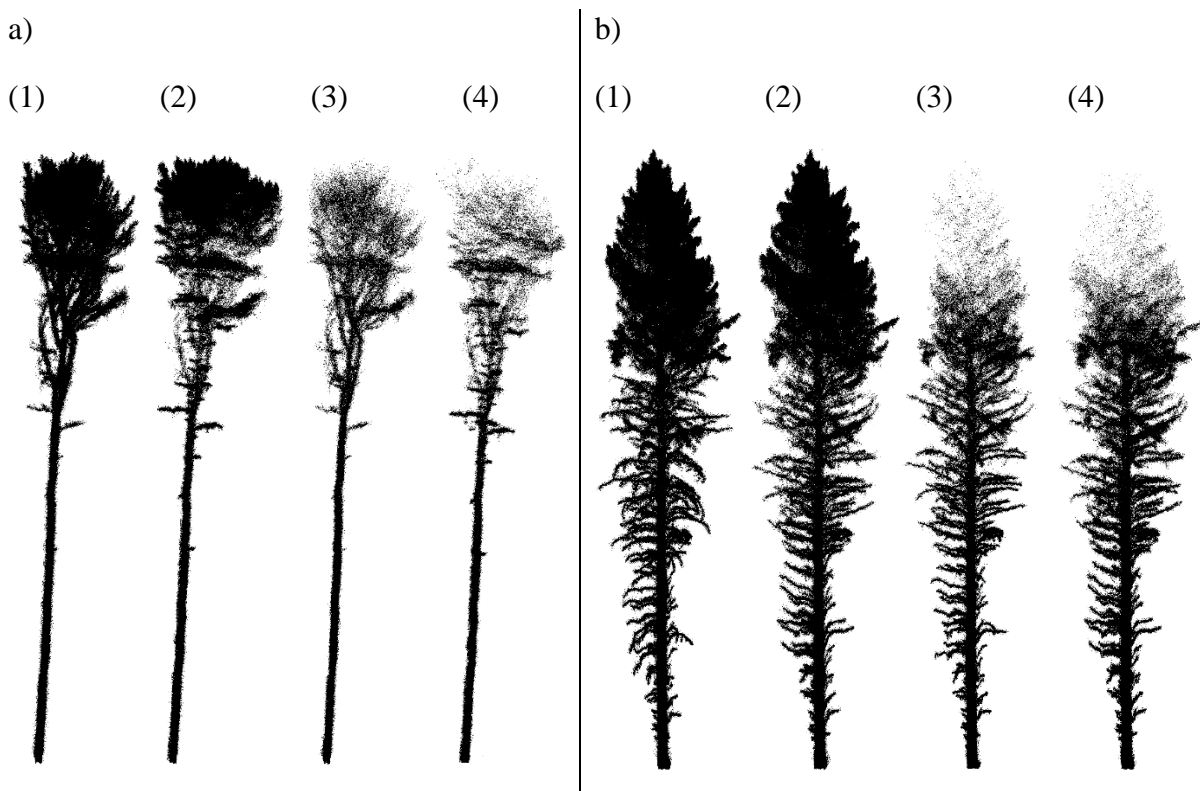


Figure 9 Single tree point clouds resulting from different scanning times and methods. Figures a) (1)-(4) show the same beech and figures b) (1)-(4) show the same spruce. The individual tree silhouettes were derived from the scans full scan winter (1), full scan summer (2), ground scan winter (3), ground scan summer (4). Figure taken from [Mathes et al. \(2023b\)](#).

The seasonal comparison at the individual tree level partially confirmed the observed visual differences. The total tree height for beech was slightly lower in summer scans than in winter scans. For Norway spruce, however, significant seasonal differences were observed for maximum crown projection area, crown volume, and crown area, all smaller on average

in winter 2020/2021 than in summer 2020. No significant differences were observed for total tree height and height of maximum crown projection area in Norway spruce.

There was a pronounced differentiation in structural complexity between the seasons at the stand level. Box-dimension, as an indicator of structural complexity, showed significant seasonal variation. For spruce, box-dimension values were larger in summer than in winter, indicating a more complex structure during the growing season. In contrast, beech showed larger box-dimension values in the crown area in winter.

Methodological comparisons between ground scans and full scans indicated that full scans typically resulted in a more comprehensive capture of structural complexity, especially in the upper height ranges of the trees. Larger box-dimension values were obtained from full scans compared to ground scans. In addition, full scans were more effective at capturing more points over the entire height range of the trees, particularly in the canopy regions.

As the voxel size increased from 5 cm to 50 cm, the CE index showed that the divergence between the ground and full scan trend lines decreased with increasing voxel size (Figure 10). With increasing voxel size, there was a general increase in CE index values over each height section. This increase suggests a more regular spatial arrangement of voxels because of increasing size. In addition, the height threshold, indicating a tendency toward regular distribution, shifted slightly downward with decreasing spatial resolution, while the maxima of the corresponding curves shifted upward.

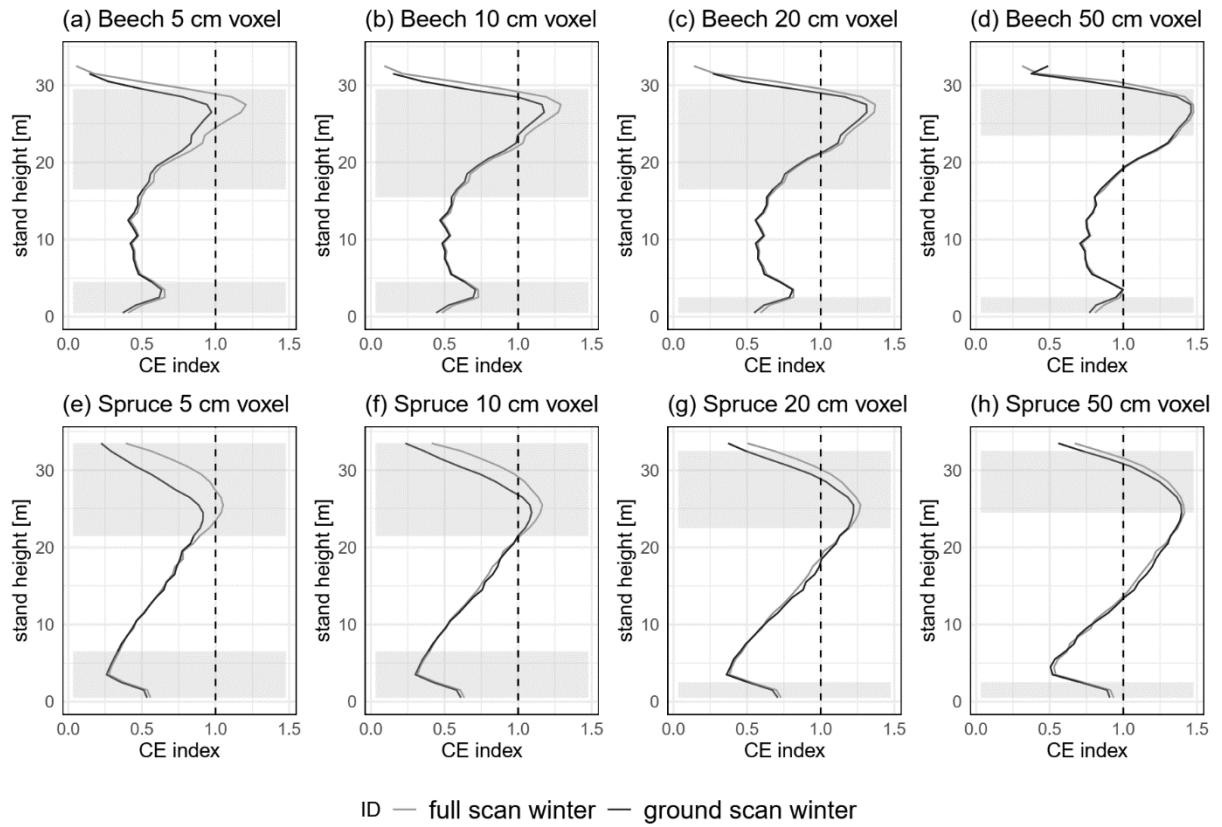


Figure 10 The CE indices for beech (a)-(d) and spruce (e)-(h) stands for the ground and full scans from winter over the height range. The black curve shows the plot for the ground scan, and the gray curve for the full scan ($n=6$, respectively). Shaded in gray is the height range in which the scans differ significantly from each other. Figure taken from [Mathes et al. \(2023b\)](#).

8.2 Effect of single tree morphology on drought stress response of beech (Paper II)

During the 2018-2020 drought period, drought conditions pronouncedly influenced the growth dynamics of dominant tree species (Figure 11). Specifically, dominant beech trees showed an increase in radial growth increment during the first drought year of 2018. However, as the drought persisted into 2019, a marked decrease in growth rate was observed, falling below the metrics recorded in 2016 and 2017. This trend continued in 2020. In contrast, the radial increment of subordinate beech trees in 2020 was similar to previous years, except 2016, which showed a significant deviation from 2017, 2018, and 2019 metrics.

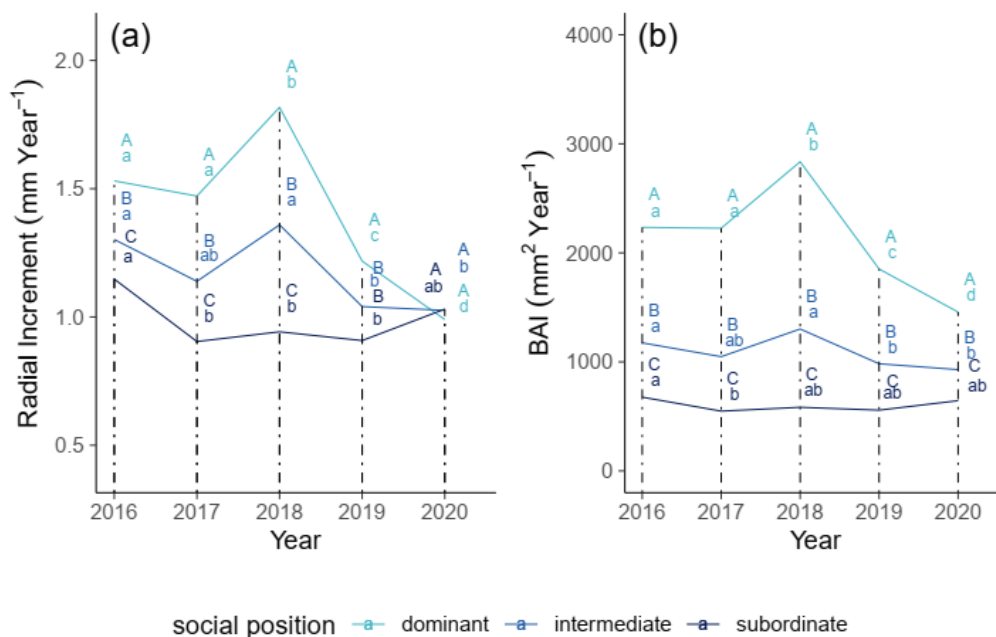


Figure 11 Increments for the years 2016-2020 in dependence of social position for the annual (a) radial increment for the entire collective and (b) basal area increment (BAI). Lowercase letters (a, b, c, d) indicate significant differences across the years for the respective social position. Capital letters (A, B, C) show significant differences between social positions within the same year. Sample size for the specific social position: dominant ($n = 620$), intermediate ($n = 175$), subordinate ($n = 195$). Figure taken from [Mathes et al. \(2023a\)](#).

When data were analyzed by study areas, radial growth trends among trees of identical social positions in the two regions showed consistency. A consistent decrease in mean relative diameter growth was documented within the dominant cohort, with apparent differences between drought-free (2016, 2017) and drought-affected (2019, 2020) years. Regarding the $\delta^{13}\text{C}$ isotopic signature, it was found that trees with lower social dominance

exhibited increased $\delta^{13}\text{C}$ discrimination (Figure 12). This discrimination increased from drought-free to drought-affected years.

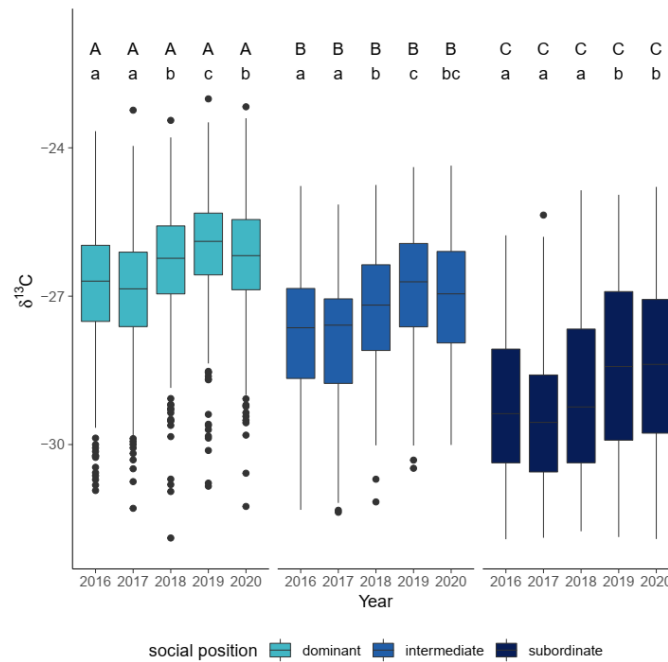


Figure 12 $\delta^{13}\text{C}$ values across the years 2016-2020 for trees of the different social positions. Lowercase letters (a, b, c) indicate significant differences within a social position. Capital letters (A, B, C) show significant differences between social positions within the same year. Sample size for the specific social position: dominant (n = 620), intermediate (n = 175), subordinate (n = 185). Figure taken from [Mathes et al. \(2023a\)](#).

No significant variance in RT $\delta^{13}\text{C}$ was detected among social positions when evaluating resistance indices based on social position. All social positions responded to the drought period. In contrast, a clear trend in resistance values of the BAI was observed from dominant to subordinate tree classes.

No clear relationships between morphological traits and resistance indices were found within the entire sample set. However, when the focus was narrowed to specific subsets of trees with pronounced resistance indices, somewhat stronger morphological distinctions were observed. Trees with distinct single tree morphologies, such as increased DBH or height, were predisposed to reduced growth under drought conditions.

In the competitive context, there was a decrease in basal area growth associated with increased competition. The magnitude of this competitive effect was found to be temporally variable. Following the 2018 drought, particularly in 2020, the detrimental effects of competition on growth metrics were weakened. Specifically, trees in highly competitive environments experienced increased growth during drought intervals compared to pre-drought periods. The influence of competitive dynamics on ^{13}C discrimination was found to be less deterministic.

8.3 Effect of forest structure on drought stress response of beech (Paper III)

In the two study regions, beech forests showed distinct defoliation, growth decline, and changes in $\delta^{13}\text{C}$ signals during the 2018-2020 drought period compared to pre-drought conditions. Defoliation was significant in both regions, with 51 % and 35 % leaf mass loss in the Plateau and Steigerwald, respectively (Table 3). Growth reduction was significantly more pronounced in the Plateau, although differences between regions were not statistically significant. The $\delta^{13}\text{C}$ signal showed no significant differences between the regions.

Table 3 Mean and standard deviation (sd) of defoliation, Resistance Index BAI (RT BAI), and Resistance Index $\delta^{13}\text{C}$ (RT $\delta^{13}\text{C}$) per plot for both study areas. An asterisk (*) marks significant differences between the two study areas. A plus (+) marks significant deviations from 0 % for defoliation or from 1 for the RT values. The total sample size for Plateau and Steigerwald was $n = 120$. Table taken from [Mathes et al. \(2024\)](#).

Study region	mean defoliation (%)	sd defoliation (%)	mean RT BAI	sd RT BAI	mean RT $\delta^{13}\text{C}$	Sd RT $\delta^{13}\text{C}$
Plateau	0.51*+	0.15*	0.87+	0.38*	0.97+	0.03
Steigerwald	0.35*+	0.09*	0.93+	0.29*	0.97+	0.03

With increasing canopy openness, there were significant changes in defoliation in both regions (Figure 13). However, variations in canopy closure did not lead to significant changes in BAI and $\delta^{13}\text{C}$ resistance indices during the drought period.

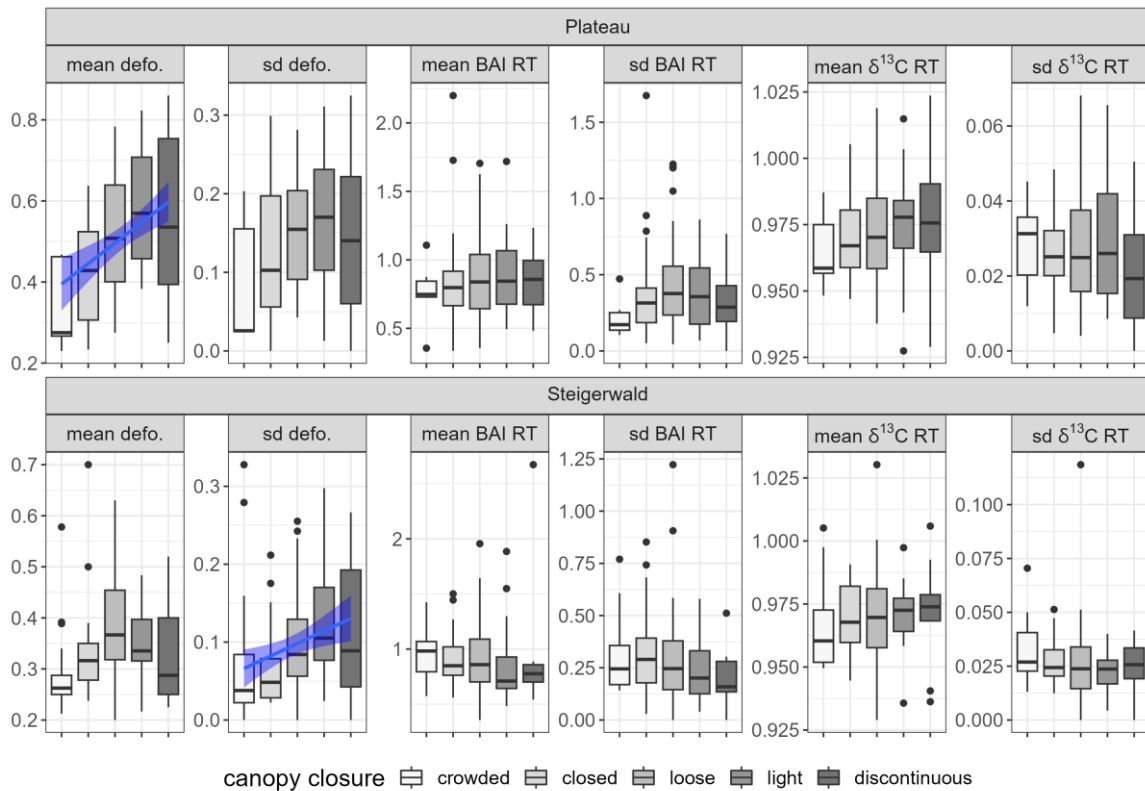


Figure 13 Relationship between crown closure and defoliation (defo.) and resistance indices (RT) BAI resp. $\delta^{13}\text{C}$ (mean and standard deviation (sd) per plot) for the two study areas, Plateau (upper row) and Steigerwald (lower row). The blue trend line is based on a linear model and only plotted for the models where the slope parameter significantly differs from zero. The blue bands around the solid lines indicate the 95 % confidence interval. $n = 240$. Figure taken from [Mathes et al. \(2024\)](#).

Regarding forest structure, no significant differences were observed between multi-layer and single- or double-layer beech stands concerning defoliation and resistance indices. Although some differences in mean defoliation were observed in the Plateau, these were not statistically significant.

Boruta analysis of forest structure variables derived from laser scanning data identified several key variables, but the overall predictive power for defoliation and resistance indices (BAI, $\delta^{13}\text{C}$) remained low. The best model was for mean defoliation within a 30 m radius in the Steigerwald, with an adjusted R^2 of 0.29.

Logistic regression models highlighted the Hegyi index as a crucial variable for explaining drought resistance, while box-dimension and CE evenness were relevant for specific aspects of drought resistance. The results indicated that lower box-dimension and higher competition increased the likelihood of an elevated mean RT BAI during drought. The Hegyi index also significantly influenced the standard deviation of RT BAI, indicating more significant variability in tree growth during drought. However, models for the $\delta^{13}\text{C}$ isotope showed low explanatory power. Conversely, the models for mean defoliation showed a higher fit, with significant effects of both box-dimension and CE evenness.

8.4 Intra-annual variation of the $\delta^{13}\text{C}$ signal

The intra-annual trend of the $\delta^{13}\text{C}$ signal showed pronounced variation within and across the years (Figure 14). During each drought year from 2018 to 2020, there was an increase in the $\delta^{13}\text{C}$ signal, followed by a decrease at the beginning of the following year. An exception to this pattern occurred in 2017, where $\delta^{13}\text{C}$ values decreased throughout the year.

The mean trend lines for the two groups, categorized by high or low resistance index, showed similar patterns, although trees with a lower resistance index tended to have higher $\delta^{13}\text{C}$ values. Analysis of the means showed significant differences between these groups in the middle of the 2016 growing season and toward the end of the 2018 growing season, the first year of drought.

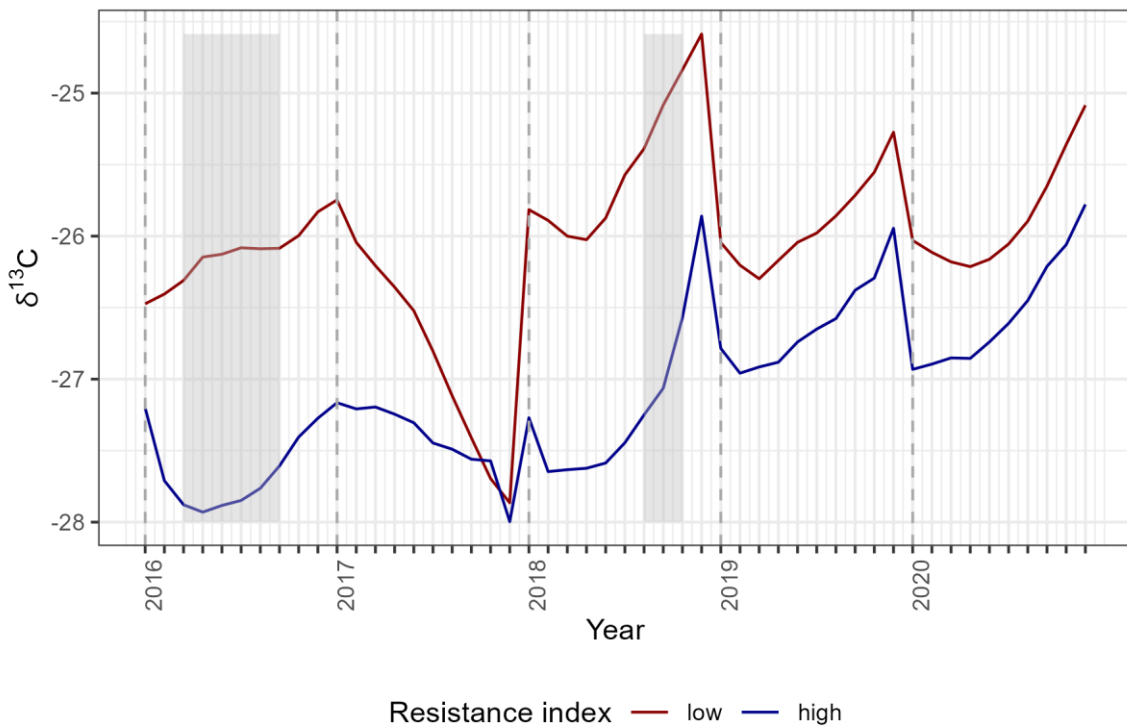


Figure 14 Intra-annual variation of $\delta^{13}\text{C}$ values differentiated by their resistance index. The lines represent the means of the $\delta^{13}\text{C}$ values for 'resistance index low' (dark red) and 'resistance index high' (dark blue) based on six individual measurements. Ten individual measurements were made within each ring. Gray bands indicate periods with significant differences between the two groups (Mann-Whitney U test). Vertical dashed lines mark the beginning of a new growing season. $n=12$.

The examination of $\delta^{13}\text{C}$ values from the Plateau and Steigerwald regions from 2016 to 2020 revealed broadly similar patterns (Figure 15). The intra-annual pattern of $\delta^{13}\text{C}$ values for both regions showed a comparable trend and no significant differences. However, there was a tendency for trees in the Steigerwald region to experience less drought stress over the observation period compared to those in the Plateau.

During the three drought years (2018-2020), a marked increase in $\delta^{13}\text{C}$ values was observed towards the end of each year. In 2016, this increase was less pronounced in both regions, and in 2017, the trend was even reversed, indicating a decrease in drought stress as the growing season progressed.

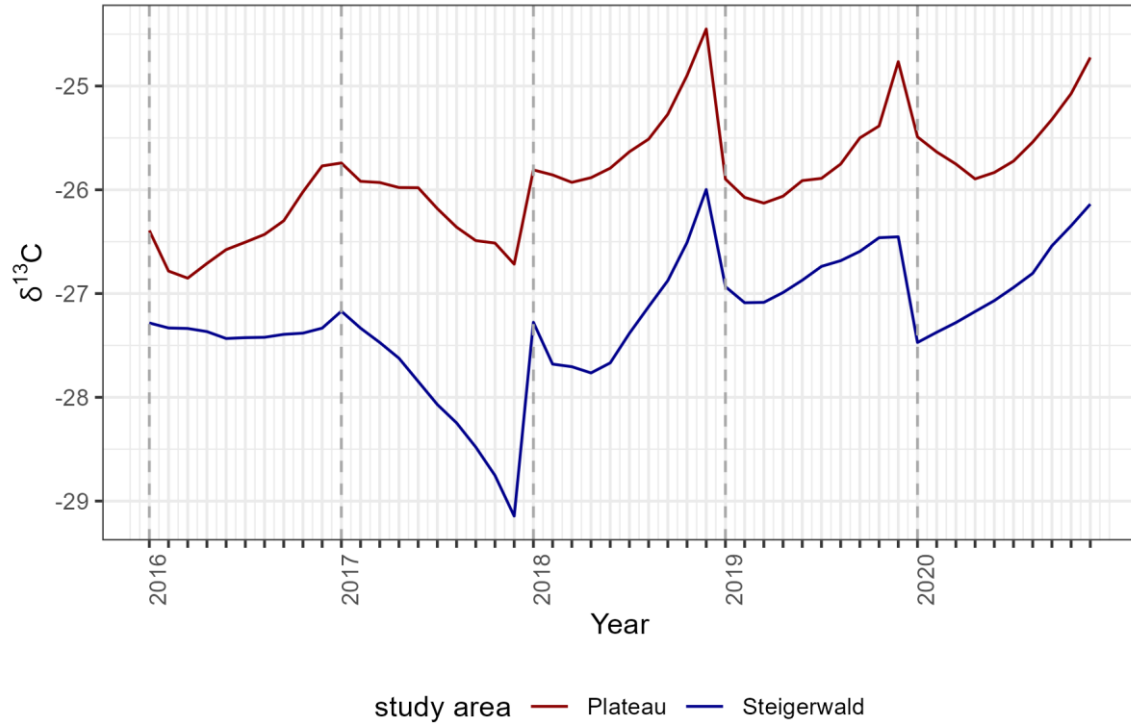


Figure 15 Intra-annual variation of $\delta^{13}\text{C}$ values between the Plateau (dark red) and Steigerwald (dark blue) study over the study period from 2016 to 2020. The lines represent the average $\delta^{13}\text{C}$ values in each region based on six measurements. Ten individual measurements were made within each ring. Vertical dashed lines mark the beginning of a new vegetation period. The lines are not statistically different (Mann-Whitney U test). $n=12$.

9 Discussion

9.1 Occlusion in laser scanning point clouds (Paper I)

9.1.1 Seasonal comparison

In the seasonal comparison of single tree morphologies and forest structures, occlusion effects were detected for individual trees and entire stands of beech and spruce, confirming hypotheses H1.1 and H1.2. In particular, beech trees exhibited lower height measurements during the summer scans, a phenomenon attributed to their dense canopy, which prevented the laser beams from fully reaching the treetops. This effect is consistent with the high crown plasticity of Beech trees, which leads them to form dense canopies with extensive green foliage in the lower stem areas during growing seasons due to their shade tolerance ([Masarovicová and štefančík, 1990](#), [Dieler and Pretzsch, 2013](#)). Conversely, although spruce trees form dense canopies, they tend to lose needles in lower stem sections under dense conditions due to light deficiency ([Matyssek et al., 2010](#)), resulting in less occlusion compared to beech.

Despite pronounced occlusion, no significant differences were observed in other crown morphologies of beech, such as the height of maximum crown projection area, crown projection area, crown volume, and crown surface area. This may be due to the availability of complete winter scans as a reference, which helped to correctly assign points to specific trees despite sparse data in the upper crown area. However, spruce showed unexpected morphological variation between summer and winter scans, suggesting that the noise inherent in laser scanning and the algorithmic processing used to calculate metrics can cause small but significant differences in tree morphology ([Hyypä et al., 2020](#), [Trzeciak and Brilakis, 2021](#)). The mobile laser scanner used in this study is known to have high noise levels, especially at longer distances. The accuracy of MLS scans at a distance of 5 m is about 20 times lower than that of TLS, with the range noise of the scanning device estimated to be around ± 30 mm ([GeoSLAM, 2020](#), [Trzeciak and Brilakis, 2021](#)). This noise level resulted in deviations in diameter at breast height measurements that were larger than the specified range noise and consistent with findings suggesting a maximum error of up to 4 cm ([Hunčaga et al., 2020](#)).

At the stand level, box-dimension values for each season were within plausible ranges for both tree species ([Seidel et al., 2019](#), [Seidel et al., 2020](#), [Stiers et al., 2020](#), [Willim et al., 2020](#)). Seasonal variations in the box-dimension values were observed for both tree species. For beech, these variations could be attributed to foliage and environmental influences such as slight leaf movement, which amplifies noise and results in more scattered point clouds in leaf-bearing trees compared to leaf-off trees ([Guzmán et al., 2020](#), [Neudam et al., 2022](#)). At

the stand level, occlusion of beech was particularly pronounced in the canopy layer during summer scans, resulting in smaller box-dimension values in the 26-36 m height range. In summary, there were differences in single tree morphology and forest structure of beech stands. Contrary to initial expectations, similar differences were also found for spruce, leading to the rejection of hypotheses H1.1 and H1.2.

9.1.2 Methodological comparison

One result of the methodological comparison focusing on individual tree morphologies was that both beech and spruce had lower heights when scanned only from the ground, as hypothesis H1.3 assumed. This result is mainly attributed to the more pronounced occlusion effects in ground scans, where biomass obstructs the laser beams, leading to incomplete detection of the upper parts of the canopy. For spruce, an evergreen species with a pyramidal crown shape, this height difference was more pronounced than for beech. This difference may be influenced by the evergreen nature of spruce and its crown shape, which makes it difficult to detect the top of the tree in dense stands. The high tree density of the study area (639-926 trees per hectare, standing stem volume of 802-981 m³/ha) further limited the visibility of the crown to the laser beams.

Due to occlusion, other crown morphologies derived from ground scans were smaller than those derived from full scans. In spruce, for parameters such as height of maximum crown projection area, maximum crown projection area, and crown area. For beech, a similar pattern was observed only for the crown area. In contrast, the crown volume was larger when scanned from the ground only. This unexpected result can be partly attributed to the noise inherent in the mobile laser scanner and the methods used to calculate crown morphology. In particular, the convex hull method, which creates a large enveloping hull around the canopy, can significantly change the derived metrics from only minor differences in the point clouds ([Yan *et al.*, 2019](#)). In combination with noise, this method is likely to be a contributing factor to the observed differences.

The extent to which these differences are relevant for future research depends on the specific research question and the level of accuracy required. Compared to traditional measurement methods associated with more significant uncertainty, such as vertex height measurements ([Stereńczak *et al.*, 2019](#)), the MLS technique is a robust tool for determining single tree morphologies. Differences in single tree morphologies were small, although occasionally significant, with occlusion effects causing a systematic underestimation of tree height of approximately 1.04 % for beech and 2.19 % for spruce in the methodological comparison. Since not all canopy-related single tree morphologies were smaller when scanned from the ground only, hypothesis H1.3 must be rejected.

The methodological comparison for both tree species at the forest structure level showed that the biomass of the canopy was not recorded as well when scanning only from the ground. Lower proportions of detected points and lower values for the CE index and box-dimension evidence this. This finding supports hypothesis H1.4, which is consistent with the expectation that reduced laser penetration into the upper canopy layers due to occlusion leads to the underestimation of the stand structural variables. Differences were also observed in the lower range despite both scans being conducted in close temporal proximity under identical weather conditions. This variance is attributed to unavoidable noise in the data, such as that introduced during SLAM (Simultaneous Localization and Mapping) processing, small wind gusts, etc. In a full scan, each object in the stand is scanned from a greater variety of perspectives and distances than in a ground scan. [Trzeciak and Brilakis \(2021\)](#) found that object recognition, mainly of edges and corners, becomes increasingly difficult as the distance from the object increases. The additional viewpoints in the full scans likely led to increased blurring during the SLAM process, resulting in increased noise in these scans.

Concerning spatial resolution, hypothesis H1.5 postulated that increasing voxel size could mitigate the loss of information in the upper canopy layers. This hypothesis was confirmed as the differences between the datasets (ground scan vs. full scan) decreased with increasing voxel size. However, even at a point cloud resolution of 50 cm, some differences persisted, especially in terms of relative point counts. For the CE index, a reduction in spatial resolution resulted in larger values per height level. Consequently, comparisons between different resolutions, such as 5 cm and 20 cm for the CE index, may reveal differences of similar magnitude to those observed in other studies comparing different forest types ([Stiers et al., 2020](#), [Willim et al., 2020](#)). This highlights the importance of considering the spatial resolution of point clouds when comparing stand structural variables. Notably, the overall characteristics and trends of the curves, such as the number of maxima and minima, are largely preserved, which is critical for accurately characterizing forest structure. The choice of spatial resolution thus represents a typical trade-off situation. A voxel size of 20 cm is an appropriate compromise to reduce the effect of occlusion on the data.

9.2 Effect of single tree morphology on drought stress response of beech (Paper II)

9.2.1 Growth reaction in dependence of social position

The study examined the effects of the 2018-2020 drought years on the diameter increment patterns of dominant beech trees, confirming the first hypothesis (H2.1.1) that the radial growth response of beech trees to drought stress depends on their social position. However, the response patterns were more complex than expected. Contrary to expectations, the severe drought of 2018 led to an increase, rather than a decrease, in growth. The "carry-over effect" could explain this phenomenon, where stored carbon reserves, predeveloped buds, and water reserves allow for increased growth in the first year of drought ([Hackett-Pain et al., 2015](#), [Chakraborty et al., 2021](#)). Furthermore, wood formation occurs early in the growing season, with approximately 75 % of the total annual ring in beech trees formed by the end of June ([Čufar et al., 2008](#), [Michelot et al., 2012](#)). The onset of drought stress in late June 2018 may explain why growth was not severely affected that year.

In the subsequent years of 2019 and 2020, the ongoing drought resulted in a decrease in diameter increment compared to 2016, 2017, and 2018. This decrease could be attributed to reduced carbon reserves formed in the first year of drought, which affected tree ring width in subsequent years as the drought persisted. Similar patterns were observed following the historic drought of 2003 in the Steigerwald region, where a more pronounced reduction in radial growth occurred in the following year, 2004 ([Zimmermann et al., 2020](#)). In addition, droughts affect both above- and belowground plant compartments, particularly reducing fine root biomass ([Meier and Leuschner, 2008](#)), likely contributing to reduced water and nutrient uptake in the years following 2018.

Additionally, beech mast events could limit growth. Moderate to high masting was observed in 2016, 2018, and 2020 ([StMELF, 2019, 2020](#)), and previous research has linked drought-associated seed production to reduced radial growth in beech ([Hackett-Pain et al., 2017](#)). While this was not evident in 2018 (when an increase in growth was observed), it can be confirmed for 2020. The reduction in growth during this year could be attributed to both masting and drought, as beech fruit production relies on current photoassimilates, independent of old carbon reserves ([Hoch et al., 2013](#)), and is more pronounced in dominant trees. The significant growth reduction in dominant trees may indicate that some individual trees have crossed a tipping point, not necessarily in 2018, but due to prolonged drought conditions. Some trees showed no growth or even died.

In contrast, the growth of subordinate trees remained relatively constant over the study period from 2016 to 2020. This suggests that the severe drought of 2018 to 2020 did not intensify existing environmental limitations for this group. Subordinate trees, although

responding to reduced water availability (as indicated by $\delta^{13}\text{C}$ signals), may benefit from reduced competitive pressure during drought years. The stress on neighboring dominant trees could facilitate the performance of understory trees by stabilizing their growth. This effect could suggest a stabilizing role of understory trees in the ecosystem, provided that their presence does not increase stress on dominant trees. An alternative explanation could be Liebig's Law of the Minimum, which postulates that the subordinate trees, limited primarily by light availability, are less responsive to drought conditions ([Odum, 1959](#)).

9.2.2 Growth reaction in dependence of the study area

In the Steigerwald, trees adapted to a slightly cooler climate and deeper, water-storing soils showed higher radial growth in 2018 than in the Plateau. This pattern is consistent with [Walthert *et al.* \(2021\)](#), who found that deep soil water reserves helped mitigate drought stress in beech trees that year.

However, in 2019 and 2020, growth declines were similar between study sites, challenging the idea that trees on drier sites are better adapted to drought ([Bolte *et al.*, 2016](#), [Cuervo-Alarcon *et al.*, 2021](#)). This suggests that the prolonged drought event overcame differences in habitat or forest history, resulting in similar drought responses among all beech trees studied. This uniform response indicates the potential for severe drought to function as an ecosystem tipping point. It rejects hypothesis H2.1.2, which suggested that trees in warmer, drier climates on flat sites would be less affected in their growth by drought.

9.2.3 $\delta^{13}\text{C}$ signature in dependence of social position

Analyses of the relationship between the $\delta^{13}\text{C}$ signature and social position showed that subordinate trees had lower $\delta^{13}\text{C}$ values, possibly due to the assimilation of CO_2 emitted by respiration, which is depleted in ^{13}C closer to the ground surface ([Berry *et al.*, 1997](#)). In addition, variations in light access affect $\delta^{13}\text{C}$ values, with studies showing an increase in $\delta^{13}\text{C}$ with higher irradiance ([Farquhar *et al.*, 1989](#), [Hanba *et al.*, 1997](#)). More intense competition resulting in greater shading is associated with lower $\delta^{13}\text{C}$ values ([Mölder *et al.*, 2011](#)). Temperature also influences $\delta^{13}\text{C}$, with higher summer temperatures leading to higher $\delta^{13}\text{C}$ values ([Porter *et al.*, 2009](#)). Subordinate trees, shielded by the canopy of dominant trees, are less exposed to temperature extremes and benefit from the cooler interior forest climate.

For dominant trees, the $\delta^{13}\text{C}$ signal increased during drought-influenced years (2018-2020), suggesting altered stomatal conductance in response to increased drought stress. However,

contrary to expectations, $\delta^{13}\text{C}$ values in 2020 were lower than in 2019 and not different from 2018, even though 2020 was very dry. This could be due to increased defoliation, as observed in 2020, where reduced foliage may have been better supplied with water, resulting in a lower $\delta^{13}\text{C}$ signal. Defoliation in beech, an anisohydric species, is a response to drought stress and xylem dehydration but can lead to additional damage, such as sunburn or beetle infestation ([Brück-Dyckhoff *et al.*, 2019](#), [Schuldt *et al.*, 2020](#)).

For the subordinate collective, a significant increase in $\delta^{13}\text{C}$ values was observed in 2019 and 2020, coinciding with a decrease in the growth of the dominant trees. This suggests that these trees also experienced drought stress, indicating resistance to one-year droughts but susceptibility to persistent multi-year droughts. The exact cause, whether different light conditions or altered stomatal conductance, remains unclear but highlights that prolonged droughts affect all social classes of beech trees, potentially acting as a tipping point for the species. In summary, hypothesis H2.2, that drought-related $\delta^{13}\text{C}$ isotope signals differ between social classes, was supported, although $\delta^{13}\text{C}$ trends were similar across years.

9.2.4 Effect of morphological differences to drought resistance

When resistance was defined as the ratio of basal area increment in 2019-2020 compared to 2016-2017, there were no clear correlations between resistance and tree morphology across the dataset. This finding contradicts expectations and suggests that tree morphology may not significantly influence resistance. However, existing literature suggests that this is unlikely ([Bennett *et al.*, 2015](#), [Stovall *et al.*, 2019](#)). An explanation could be that other factors, such as soil variability, pathogens, or genetics, could overshadow morphological response patterns.

A focused analysis of trees with a stronger response to the drought period showed that RT BAI tended to decrease with increasing height and social position. This pattern, where more giant beech trees with extensive crowns are more susceptible to drought, is consistent with the "structural overshoot" theory, which suggests that trees can grow beyond their sustainable capacity under favorable conditions, making them more vulnerable during water shortages ([Jump *et al.*, 2017](#)). Their greater exposure to radiation and wind increases hydraulic stress ([Skomarkova *et al.*, 2006](#), [Bennett *et al.*, 2015](#), [Grote *et al.*, 2016](#)). When RT $\delta^{13}\text{C}$ was considered, there were less significant correlations with morphological variables. However, more giant trees with larger box-dimensions had lower resistance, possibly because a larger photosynthetically active area requires more resources. However, non-significant models for canopy area and volume challenge this explanation.

Contrary to expectations, more giant trees in the upper canopy, which are expected to use water more rapidly and experience more drought stress, had a higher probability of having

a higher RT $\delta^{13}\text{C}$. This could be because these trees shed more leaves, reducing stress on the hydraulic system and allowing for a better supply of the remaining leaves. Another explanation for the diffuse response pattern, which is not strongly related to morphological variables, could be that the severe and prolonged droughts overwhelmed differences that might be apparent under milder drought conditions. This is supported by the observation that RT $\delta^{13}\text{C}$ decreased similarly across social positions. Therefore, hypothesis H2.3, suggesting significant morphological influences on drought resistance, can only be partially accepted. Significant morphological variables affecting resistance were identified in a subset of the data but with limited scope and accuracy.

9.2.5 Competitive environment and its effect on tree performance

Competition, which can be managed through silvicultural treatments such as thinning, significantly affects tree growth. Basal area increment (BAI) was highly dependent on the level of competition faced by each tree, supporting the silvicultural principle that growth is enhanced by removing competitors ([e.g., Chakraborty *et al.*, 2021](#)). However, prolonged drought was observed to reduce the influence of competition. Despite their initial advantages, such as better access to light and more extensive root systems, trees with low competition showed declining performance over time during prolonged droughts. This suggests that their competitive advantages become detrimental under drought conditions. On the other hand, trees under highly competitive pressure showed less change in basal area increment. This could be due to more drought-damaged neighbors, freeing up resources for these suppressed trees, or because water use by dominant trees decreased under stress, leaving a similar amount for suppressed trees. As a result, hypothesis H2.4, that reduced competition mitigates the effects of drought, cannot be fully accepted for prolonged drought scenarios. The extreme nature of the drought may have overwhelmed the competitive advantage of dominant trees due to their higher resource requirements for maintaining greater biomass.

9.3 Effect of forest structure on drought stress response of beech (Paper III)

9.3.1 Response of beech forests to prolonged drought

The results indicate that beech forests in both study areas responded to the drought period with defoliation, reduced growth, and changes in the $\delta^{13}\text{C}$ signature, consistent with findings from other studies (e.g., [Rohner et al. \(2021\)](#) or [Walthert et al. \(2021\)](#)). Defoliation in beech is a stress response due to its anisohydric stomatal regulation and cavitation-sensitive xylem ([Schuldt et al., 2020](#), [Arend et al., 2022](#), [Weithmann et al., 2022](#)). Less leaf mass and thus reduced photosynthetic capacity led to a decrease in radial increment during the drought period, as confirmed by several studies ([Scharnweber et al., 2020](#), [Debel et al., 2021](#)). In addition, an elevated $\delta^{13}\text{C}$ signature in both study areas indicated water stress.

Comparing the two study areas, the Plateau experienced higher mean crown defoliation, suggesting greater drought sensitivity due to limited water availability on the shallower soils ([Chakraborty et al., 2013](#), [Weber et al., 2013](#), [Klesse et al., 2022](#)). Legacy effects from past droughts may have contributed to this increased sensitivity ([Kannenbergh et al., 2020](#), [Neycken et al., 2022](#)). However, differences in $\delta^{13}\text{C}$ signatures between regions were insignificant, possibly due to similarly high-stress levels across plots during the extreme drought. Overall, the hypothesis that beech stands in both regions would respond to drought with defoliation, growth reduction, and an increase in $\delta^{13}\text{C}$ signature is accepted.

9.3.2 Effects of stand structure on the drought response

The results indicate a relationship between crown closure and defoliation in beech forests, particularly in the Plateau. An increase in defoliation with decreasing crown closure suggests that more open canopies may make beech trees more vulnerable to drought. Open canopies expose trees to direct sunlight, which can lead to adverse effects such as sun scald and predispose trees to further disturbances such as beetle infestation (e.g., *Agrilus viridis* L.), potentially triggering a cascade of damage ([Manion, 1981](#), [Brück-Dyckhoff et al., 2019](#)). In addition, defoliation increases the risk of future tree mortality ([Petit-Cailleux et al., 2021](#)). It creates canopy gaps that increase temperatures and decrease humidity in the forest, which could worsen drought stress and further increase defoliation.

Contrary to initial expectations, no significant changes in the resistance indices BAI and $\delta^{13}\text{C}$ in response to canopy closure were observed. Reduced leaf mass was expected to decrease radial increment and an altered $\delta^{13}\text{C}$ signature due to reduced photosynthesis. However, the lack of such effects could be attributed to the compensatory influence of

increased space for the remaining trees, which could offset the effects of reduced crown foliage. Moreover, the remaining crown could still receive sufficient water and nutrients, allowing for adequate sugar production for wood formation and preventing an altered $\delta^{13}\text{C}$ signature. This observation is consistent with [Roloff's \(1986\)](#) findings that damaged beech trees do not always show reduced growth rates. Furthermore, [Weithmann et al. \(2022\)](#) describe that the extreme drought event in 2018 led to the development of smaller leaves with improved water use efficiency in sun-exposed canopies. However, severely defoliated beech trees remain highly susceptible to pathogens and wood decay, which affects stem stability and break resistance ([Purahong et al., 2021](#), [Langer and Bußkamp, 2023](#)). Hypothesis H3.2 was partially supported, confirming the association between open canopies and increased defoliation but not finding the expected more significant growth decline and more pronounced $\delta^{13}\text{C}$ signature. This suggests that the effects of drought on beech forests may be more diverse than previously thought.

Hypothesis H3.3 postulated that multi-layer beech forests would show lower canopy defoliation and higher resistance (as measured by tree growth and $\delta^{13}\text{C}$ signature) than single-layer forests. However, the results did not support this hypothesis. There was no significant difference in drought response between multi-layer and single-layer forests. There were no significant correlations for the 30-meter cutting radius, which represents the forest structure, the 10-meter cutting radius, which represents the immediate neighborhood, and the 10-meter semicircle immediately to the south, which assesses the potential effects of direct sunlight on beech trees. This finding suggests that the relationship between forest structure, defoliation, and resistance indices is more complex than initially thought.

More robust relationships were identified by focusing on a subset of the data. For example, plots with more tree competition were more likely to have increased resistance in basal area growth. This may be due to smaller trees competing with more giant trees, as is often the case in stands with abundant understory. Under prolonged drought conditions, growth partitioning may favor smaller trees ([Bose et al., 2022](#), [Mathes et al., 2023a](#), [Pretzsch et al., 2023](#)). Stands with a mix of dominant and subordinate beech trees were more resistant and may recover more quickly from drought. The results also indicated that stands with smaller box-dimensions, characterized by lower complexity, have a higher likelihood of maintaining average BAI. These could be selectively thinned stands where treatments are focused on selected trees.

The models on $\delta^{13}\text{C}$ signal responses with mean competition as a determining factor yielded low explanatory power, consistent with [Rothenbühler et al. \(2021\)](#), who also found no systematic differences in $\delta^{13}\text{C}$ tree-ring records between dead and live trees. In conclusion, hypothesis 3.3 was rejected as the results provided limited evidence that multi-layer beech forests are less susceptible to canopy defoliation or more drought-resistant than single-layer forests.

9.4 Intra-annual variation of the $\delta^{13}\text{C}$ signal

The $\delta^{13}\text{C}$ signal of beech varies during the year, reflecting changes in environmental conditions (Figure 14 and Figure 15). In particular, the observed increases in $\delta^{13}\text{C}$ values within the dry years 2018-2020 indicated an increased drought stress situation. A substantial rise in $\delta^{13}\text{C}$ values was observed mainly in the second half of the growing season, which can be interpreted as an exhaustion of the soil water reserves accumulated during the winter half-year. [Sarris *et al.* \(2013\)](#) also attribute the increase of $\delta^{13}\text{C}$ values in *Pinus halepensis* in dry years to the fact that the productive growing seasons are mainly limited to early to mid-spring and mid-to-late autumn. Thus, the latewood absorbs the carbon sequestered and stored during the drought-induced summer dormancy, resulting in high $\delta^{13}\text{C}$ values.

The influence of interannual changes in water availability on wood $\delta^{13}\text{C}$ has already been described ([Warren *et al.*, 2001](#), [Leavitt, 2002](#), [Kagawa *et al.*, 2003](#)). The observed intra-annual decrease in $\delta^{13}\text{C}$ values in 2017 could, therefore, be due to a sufficient water supply of the vegetation and corresponds to the pattern observed for beech by [Helle and Schleser \(2004\)](#). The minimum $\delta^{13}\text{C}$ values are found in the latewood of the annual ring. At the end of the annual ring, the $\delta^{13}\text{C}$ values increase again. This increase in $\delta^{13}\text{C}$ marks the gradual transition to storage-dependent growth ([Helle and Schleser, 2004](#)). [Skomarkova *et al.* \(2006\)](#) state that 10 to 20 % of a beech annual ring seems to be influenced by the carbon cycle of the previous year.

The $\delta^{13}\text{C}$ values tend to be higher in the Plateau, which could be attributed to the shallower soils and lower precipitation compared to the Steigerwald. The low expression of significant differences between the groups formed (study area, resistance index) indicates a high variability of responses at the individual tree level, which underlines the complexity of adaptation mechanisms to different environmental conditions ([Weigel *et al.*, 2023](#)).

The observed variability of the $\delta^{13}\text{C}$ signal within one year may lead to uncertainties when using isotope data averaged over one year or measured separately for latewood and earlywood. Especially in the case of tiny annual rings, an imprecise separation at the annual ring boundary of the core may lead to a bias of the signal.

9.5 Effect of drought stress on beech wood quality

The significant crown defoliation observed in this study suggests that wood quality may also be affected, as described by [Langer and Bußkamp \(2023\)](#). Therefore, the current damage to beech trees is also associated with several economic challenges, such as increased harvesting costs due to the increased proportion of crown deadwood, reduced timber

revenues due to the rapidly progressing timber degradation, and missed optimal harvesting time.

[Stimmelmayer \(2022\)](#) examined the central trees of this study concerning wood quality to determine whether drought stress - recognizable by changes such as defoliation, a changed $\delta^{13}\text{C}$ signature, or a decline in growth - also affects wood quality. The study used the methodology of acoustic and electrical resistance tomography, originally developed for tree inspection in traffic safety and has only been used to a limited extent in forestry. The results showed that these tomographic methods provide insights into the trunk's interior but have limited information about wood quality. Acoustic tomography, suitable for diagnosing pronounced defects such as cavities or decay, revealed only a few defects in the wood of the beech trunks examined in this study. On the other hand, electrical resistance tomography provided a more detailed picture of the trunk's interior. However, the interpretations are unclear due to the variability of the electrical conductivity of the red heartwood ([Hanskötter, 2004](#)). Beech trees in the Plateau appear to have a high proportion of red heart and decay, with understory beech affected and trees with large stem diameters. There is also evidence that crown defoliation is reflected in changes in stem moisture distribution. Beech trees with a large diameter at breast height are particularly affected, as they show an increased variation in electrical resistance tomograms, which could be interpreted as a consequence of embolisms. Furthermore, beech trees with fragile cores show, on average, larger stem diameters and pronounced crown defoliation. This can be interpreted as an effect of moisture reduction in the process of heavy defoliation. The study by [Stimmelmayer \(2022\)](#) illustrates the complexity of assessing wood quality under dry stress conditions and the limitations of tomography as a method for investigating wood quality in standing trees.

9.6 Response of other tree species to the 2018-2020 drought event

Strong but heterogeneous effects of the 2018-2020 drought on Central European forest ecosystems have also been demonstrated for other tree species ([Buras et al., 2020](#)). [Thom et al. \(2023\)](#) found that the average annual growth rate of trees decreased by about 41 % for Bavaria, Germany, during the exceptional drought event 2018-2020. Of the twenty tree species studied, thirteen showed significant growth losses. In particular, the conifer species *Picea abies* and *Pinus sylvestris* were more vulnerable than the deciduous species *Fagus sylvatica*, *Quercus robur*, and *Quercus petraea*. For Norway spruce, [Schmied et al. \(2022\)](#) found that high structural diversity in a tree's environment favors growth and improves its performance under drought. More giant trees in the study were more climate-sensitive. The pronounced sensitivity of spruce and pine to drought may be due to their isohydric behavior, which manifests in reduced photosynthesis and thus reduced production of photoassimilates

for growth during drought, in contrast to anisohydric species such as beech ([Martínez-Sancho et al., 2017](#)). While effective stomatal regulation provides protection during short-term droughts by reducing water demand ([Hartmann, 2011](#)), it could prove counterproductive for spruce during prolonged droughts, leading to premature stomatal closure and making trees vulnerable to carbon deficiency ([Hartmann, 2011](#), [Lévesque et al., 2013](#), [Hartl-Meier et al., 2014](#), [Vitasse et al., 2019](#)).

[Senf et al. \(2020\)](#) show that drought is an important factor in tree mortality on a continental scale and suggest that a future increase in drought could trigger widespread tree mortality in Europe. [Spiecker and Kahle \(2023\)](#) also conclude that forest tree mortality in the Black Forest primarily depends on the climatic water balance, which shows a strongly decreasing trend from 1954 to 2020. Contrary to expectations that site diversity and factors such as forest structure and tree species composition significantly influence mortality, the data suggest that trees respond similarly to changes regardless of site and stand factors. [Süßel and Brüggemann \(2021\)](#), based on findings from the drought year 2018, suggest that several *Quercus robur* L. stands in the Rhine-Main valley will be threatened by severe forest mortality in the coming decades. Successive droughts pose a significant threat to forests under climate change, even in forest ecosystems with comparatively good water supply, like floodplain forests with tree species such as *Quercus robur* L., *Acer pseudoplatanus* L., and *Fraxinus excelsior* L. ([Schnabel et al., 2022](#)). Overall, a potential reduction in the vigor of Central European tree species under more intense droughts due to climate change can be expected to shift the distribution of tree species in Europe ([Allen et al., 2010](#), [Buras and Menzel, 2018](#)).

9.7 Mitigating drought stress through species interactions

One strategy for adapting forests to climate change may be to use silvicultural measures to create mixed and structurally rich forests. The survival risk can be distributed among complementary tree species with different requirements. Therefore, a structurally rich stand can recover more quickly after disturbances and is considered more climate-resilient. Silvicultural guidelines such as those of [Utschig et al. \(2011\)](#) recommend the conversion of monospecific forests into more stable mixed forests to adapt to climate change. Although greater tree diversity is not systematically correlated with increased drought resistance ([Grossiord, 2020](#)), studies suggest that integrating other tree species, such as silver fir (*Abies alba*) or oak species, into beech forests can increase the drought tolerance of beech ([Jonard et al., 2011](#), [Lebourgeois et al., 2013](#), [Metz et al., 2016](#), [Magh et al., 2019](#)). The benefits of these mixed stands increase with tree size ([Schwarz and Bauhus, 2019](#)). A possible explanation for this could be the "hydraulic lift" or "hydraulic redistribution" that has been

observed in various ecosystems, including mixed beech forests ([Zapater *et al.*, 2011](#), [Töchterle *et al.*, 2020](#)). This phenomenon occurs when there is a pronounced water gradient between the roots and the soil, for example, during periods of drought, which can lead to the release of water from the roots. Therefore, as climate change continues, tree species diversity should be promoted at all stages of stand development. In particular, regeneration should take place at an early stage, with emphasis on introducing species other than beech.

10 Conclusion

In this thesis, the influence of single tree morphology and forest structure on the response of European beech to drought stress in the years 2018 to 2020 was analyzed using a combination of mobile laser scanning technology and retrospective analyses of radial increment and $\delta^{13}\text{C}$ signal. The thesis consists of two main parts:

The first part of the thesis focused on detecting single tree morphology and forest structure using mobile laser scanning ([Paper I](#)). By using a crane to make full scans, we could quantify the occlusion effect apparent in the ground scans in more detail. The results showed that occlusion was pronounced in the canopy region of the stands. For single tree morphologies, occlusion plays a role, especially when extracting single tree point clouds from the entire point cloud. Relying solely on a single ground scan in the leaf-on state made accurate and comparable extraction of beech trees challenging. The noise of the laser scanner, in combination with the algorithms used to calculate the metrics, affected the morphology of the individual trees. Overall, no very pronounced differences could be detected for the crown-related variables. However, occlusion-induced biases were most evident in height estimates, with a methodological comparison revealing an underestimation of approximately 1.04 % for beech and 2.19 % for spruce.

At the stand level, significant information was lost in the canopy region when scanning from the ground only. Increasing the voxel size can compensate for this loss of information but at the cost of losing detail in the point clouds. The results suggest that the voxelization of point clouds with a voxel size of 20 cm effectively reduces occlusion effects while preserving essential information. The quantification of information loss in this thesis serves as a basic framework for adjusting ground scans to account for the occlusion effect. The first part of the thesis is intended to raise awareness of the occlusion effect in mobile laser scanning and to encourage further research and improvement in this area.

The second part of the thesis was dedicated to investigating the influence of single tree morphology and forest structure on the response of European beech to drought stress ([Paper II](#) and [Paper III](#)). Beech suffered significantly from the 2018-2020 drought period, with pronounced crown defoliation, reduced growth, and changes in the $\delta^{13}\text{C}$ signature compared to the pre-drought period. The intensity of the 2018-2020 drought event was so severe that it appears to have overridden many known rules and drivers of forest ecology and forest dynamics (social position, morphology, competition). The drought disproportionately affected the dominant tree community, the very trees targeted by forest management approaches and previously considered as anchors of stability against weather extremes, especially storms. This could lead to increased mortality of large trees, increased interior forest temperatures, and exacerbated drought stress. This is a typical pattern known for tipping points.

However, understory trees provide some consistency in growth during drought periods. They also play a crucial role in regulating the microclimate within the forest stand. Therefore, forest management strategies should consider measures to promote and enhance the understory to ensure the stability of the forest ecosystem.

The results showed a correlation between canopy closure and defoliation, particularly in the Plateau, suggesting that beech is more susceptible to drought in more open canopies. In contrast, the effectiveness of forest management practices in reducing the effects of drought stress, as indicated by basal area increment and $\delta^{13}\text{C}$ values, appears to be limited. On average, neighboring trees and forest structures had a minimal effect on drought resistance. The severity of drought stress was not significantly reduced by an open or a closed forest canopy. However, forests with a greater structural complexity tended to have higher resistance, possibly due to the understory compensating for some losses in the upper canopy. This finding highlights the importance of maintaining and promoting structural diversity in beech forests. This includes promoting a mix of tree ages and sizes to create a more resilient forest structure that can withstand drought. Multi-layered forests with a substantial understory can help mitigate the effects of canopy defoliation through drought damage in the following tree layer, which would otherwise increase the susceptibility to the next drought. The remarkable variation in the data may reflect a wide range of adaptability and intraspecific diversity within beech populations, suggesting some degree of adaptation to extreme climatic conditions such as those observed during the 2018-2020 drought period. For this adaptive process, an early regeneration of the beech forests could be of advantage. During thinning and other silvicultural treatments, priority should be given to maintaining and promoting drought-tolerant and vigorous individuals. This may include selecting trees based on growth patterns, as well as health indicators (crown defoliation) and other characteristics. At the same time, however, quality timber production should not be neglected.

In addition, introducing a diversity of tree species could further strengthen the forest's ability to adapt to environmental stresses. Although beech is the dominant broadleaf species in Central Europe, the increasing frequency and intensity of droughts may make it necessary to introduce or promote more drought-resistant species in forests. There will be fewer rather than more sites within the beech optimum in Germany. Increasing the diversity of tree species and provenances could increase forest ecosystems' long-term stability and functionality in the face of climate change. Silvicultural measures such as group selection create different conditions that favor regeneration and the development of tree species mixtures, limiting the intervention to specific areas and leaving the rest of the site untreated. The results highlight the importance of adaptive silvicultural practices that consider changing climatic conditions, although the overall potential to reduce drought stress appears limited.

Ongoing research and monitoring are essential to understanding the complex interactions between forest structure, species composition, and drought-related climatic stressors. Overall, the results of this thesis contribute to a better understanding of how beech trees respond to drought events. This understanding is essential for the conservation of beech forests in the face of climate change and contributes to the knowledge of the ecological resilience of forests. Nevertheless, recurrent multi-year droughts, such as the 2018-2020 event, are expected to permanently change growth dynamics, stand structure, and species composition in forests.

11 References

- Abegg, M., Kükenbrink, D., Zell, J., Schaepman, M. and Morsdorf, F. 2017 Terrestrial Laser Scanning for Forest Inventories—Tree Diameter Distribution and Scanner Location Impact on Occlusion. *Forests* **8**, 184.
- Adams, H.D., Collins, A.D., Briggs, S.P., Vennetier, M., Dickman, L.T. and Sevanto, S.A. *et al.* 2015 Experimental drought and heat can delay phenological development and reduce foliar and shoot growth in semiarid trees. *Global Change Biol* **21**, 4210–4220.
- Allen, C.D., Macalady, A.K., Chenchouni, H., Bachelet, D., McDowell, N. and Vennetier, M. *et al.* 2010 A global overview of drought and heat-induced tree mortality reveals emerging climate change risks for forests. *Forest Ecology and Management* **259**, 660–684.
- Arend, M., Link, R.M., Zahnd, C., Hoch, G., Schuldt, B. and Kahmen, A. 2022 Lack of hydraulic recovery as a cause of post-drought foliage reduction and canopy decline in European beech. *New Phytologist* **234**, 1195–1205.
- Aussenac, G. 2000 Interactions between forest stands and microclimate: Ecophysiological aspects and consequences for silviculture. *Ann. For. Sci.* **57**, 287–301.
- Aussenac, G. and Granier, A. 1988 Effects of thinning on water stress and growth in Douglas-fir. *Canadian Journal of Forest Research* **18**, 100–105.
- Baddeley, A. and Turner, R. 2005 spatstat: An R Package for Analyzing Spatial Point Patterns. *Journal of Statistical Software* **12**, 1–42.
- Barnosky, A.D., Hadly, E.A., Bascompte, J., Berlow, E.L., Brown, J.H. and Fortelius, M. *et al.* 2012 Approaching a state shift in Earth's biosphere. *Nature* **486**, 52–58.
- Bartoń, K. 2022 MuMIn: Multi-Model Inference. R package version 1.46.0.
- Bauwens, S., Bartholomeus, H., Calders, K. and Lejeune, P. 2016 Forest Inventory with Terrestrial LiDAR: A Comparison of Static and Hand-Held Mobile Laser Scanning. *Forests* **7**, 127.
- Bayer, D., Seifert, S. and Pretzsch, H. 2013 Structural crown properties of Norway spruce (*Picea abies* [L.] Karst.) and European beech (*Fagus sylvatica* [L.]) in mixed versus pure stands revealed by terrestrial laser scanning. *Trees* **27**, 1035–1047.
- Bennett, A.C., McDowell, N.G., Allen, C.D. and Anderson-Teixeira, K.J. 2015 Larger trees suffer most during drought in forests worldwide. *Nature plants* **1**, 1–5.
- Berry, S.C., Varney, G.T. and Flanagan, L.B. 1997 Leaf $\delta^{13}\text{C}$ in *Pinus resinosa* trees and understory plants: variation associated with light and CO₂ gradients. *Oecologia* **109**, 499–506.

- Bigler, C. and Vitasse, Y. 2021 Premature leaf discoloration of European deciduous trees is caused by drought and heat in late spring and cold spells in early fall. *Agricultural and Forest Meteorology* **307**, 108492.
- Bolte, A., Czajkowski, T., Coccozza, C., Tognetti, R., Miguel, M. de and Pšidová, E. *et al.* 2016 Desiccation and Mortality Dynamics in Seedlings of Different European Beech (*Fagus sylvatica* L.) Populations under Extreme Drought Conditions. *Frontiers in plant science* **7**, 751.
- Bose, A.K., Rohner, B., Bottero, A., Ferretti, M. and Forrester, D.I. 2022 Did the 2018 megadrought change the partitioning of growth between tree sizes and species? A Swiss case-study. *Plant biology (Stuttgart, Germany)* **24**, 1146–1156.
- Bosela, M., Štefančík, I., Marčíš, P., Rubio-Cuadrado, Á. and Lukac, M. 2021 Thinning decreases above-ground biomass increment in central European beech forests but does not change individual tree resistance to climate events. *Agricultural and Forest Meteorology* **306**, 108441.
- Bréda, N., Granier, A. and Aussenac, G. 1995 Effects of thinning on soil and tree water relations, transpiration and growth in an oak forest (*Quercus petraea* (Matt.) Liebl.). *Tree physiology* **15**, 295–306.
- Bréda, N., Huc, R., Granier, A. and Dreyer, E. 2006 Temperate forest trees and stands under severe drought: a review of ecophysiological responses, adaptation processes and long-term consequences. *Ann. For. Sci.* **63**, 625–644.
- Brooks, J.R. and Mitchell, A.K. 2011 Interpreting tree responses to thinning and fertilization using tree-ring stable isotopes. *The New phytologist* **190**, 770–782.
- Brück-Dyckhoff, C., Petercord, R. and Schopf, R. 2019 Vitality loss of European beech (*Fagus sylvatica* L.) and infestation by the European beech splendour beetle (*Agilus viridis* L., Buprestidae, Coleoptera). *Forest Ecology and Management* **432**, 150–156.
- Bundesministerium für Ernährung und Landwirtschaft (BMEL). 2021 *Waldbericht der Bundesregierung* 2021. https://www.bmel.de/SharedDocs/Downloads/DE/Broschueren/waldbericht2021.pdf?__blob=publicationFile&v=11 (accessed on 20 July, 2023).
- Buras, A. and Menzel, A. 2018 Projecting Tree Species Composition Changes of European Forests for 2061-2090 Under RCP 4.5 and RCP 8.5 Scenarios. *Frontiers in plant science* **9**, 1986.
- Buras, A., Rammig, A. and Zang, C.S. 2020 Quantifying impacts of the 2018 drought on European ecosystems in comparison to 2003. *Biogeosciences* **17**, 1655–1672.
- Calev, A., Zoref, C., Tzukerman, M., Moshe, Y., Zangy, E. and Osem, Y. 2016 High-intensity thinning treatments in mature *Pinus halepensis* plantations experiencing prolonged drought. *Eur J Forest Res* **135**, 551–563.

- Caudullo, G., Welk, E. and San-Miguel-Ayanz, J. 2017 Chorological maps for the main European woody species. *Data in brief* **12**, 662–666.
- Chakraborty, T., Reif, A., Matzarakis, A. and Saha, S. 2021 How Does Radial Growth of Water-Stressed Populations of European Beech (*Fagus sylvatica* L.) Trees Vary under Multiple Drought Events? *Forests* **12**, 129.
- Chakraborty, T., Saha, S. and Reif, A. 2013 Decrease in Available Soil Water Storage Capacity Reduces Vitality of Young Understorey European Beeches (*Fagus sylvatica* L.)-A Case Study from the Black Forest, Germany. *Plants* **2**, 676–698.
- Clark, P.J. and Evans, F.C. 1954 Distance to nearest neighbour as a measure of spatial relationships in populations. *Ecology* **35**, 445–453.
- Copernicus Climate Change Service. 2024 *2023 is the hottest year on record, with global temperatures close to the 1.5°C limit*. <https://climate.copernicus.eu/copernicus-2023-hottest-year-record> (accessed on 28 January, 2024).
- Corcobado, T., Cech, T.L., Brandstetter, M., Daxer, A., Hüttler, C. and Kudláček, T. *et al.* 2020 Decline of European Beech in Austria: Involvement of Phytophthora spp. and Contributing Biotic and Abiotic Factors. *Forests* **11**, 895.
- Čortan, D., Nonić, M. and Šijačić-Nikolić, M. 2019 Phenotypic Plasticity of European Beech from International Provenance Trial in Serbia. *Forests of Southeast Europe Under a Changing Climate* **65**, 333–351.
- Cuervo-Alarcon, L., Arend, M., Müller, M., Sperisen, C., Finkeldey, R. and Krutovsky, K.V. 2021 A candidate gene association analysis identifies SNPs potentially involved in drought tolerance in European beech (*Fagus sylvatica* L.). *Sci Rep* **11**, 2386.
- Čufar, K., Prislan, P., Luis, M. de and Gričar, J. 2008 Tree-ring variation, wood formation and phenology of beech (*Fagus sylvatica*) from a representative site in Slovenia, SE Central Europe. *Trees* **22**, 749–758.
- D'Amato, A.W., Bradford, J.B., Fraver, S. and Palik, B.J. 2013 Effects of thinning on drought vulnerability and climate response in north temperate forest ecosystems. *Ecological applications : a publication of the Ecological Society of America* **23**, 1735–1742.
- Dassot, M., Constant, T. and Fournier, M. 2011 The use of terrestrial LiDAR technology in forest science: application fields, benefits and challenges. *Annals of Forest Science* **68**, 959–974.
- Debel, A., Meier, W.J.-H. and Bräuning, A. 2021 Climate Signals for Growth Variations of *F. sylvatica*, *P. abies*, and *P. sylvestris* in Southeast Germany over the Past 50 Years. *Forests* **12**, 1433.

- Del Campo, A.D., Otsuki, K., Serengil, Y., Blanco, J.A., Yousefpour, R. and Wei, X. 2022 A global synthesis on the effects of thinning on hydrological processes: Implications for forest management. *Forest Ecology and Management* **519**, 120324.
- Del Martinez Castillo, E., Zang, C.S., Buras, A., Hacket-Pain, A., Esper, J. and Serrano-Notivoli, R. *et al.* 2022 Climate-change-driven growth decline of European beech forests. *Communications biology* **5**, 163.
- Deutscher Wetterdienst (DWD). 2022a *Lufttemperatur: vieljährige Mittelwerte 1991 - 2020*.
https://www.dwd.de/DE/leistungen/klimadatendeutschland/mittelwerte/temp_9120_SV_html.html;jsessionid=9F4792D80B666AA6CF1C9A2384B77AAF.live31081?view=nasPublication&nn=16102 (accessed on 29 June, 2022).
- Deutscher Wetterdienst (DWD). 2022b *Niederschlag: vieljährige Mittelwerte 1991 - 2020*.
https://www.dwd.de/DE/leistungen/klimadatendeutschland/mittelwerte/nieder_9120_SV_html.html;jsessionid=9F4792D80B666AA6CF1C9A2384B77AAF.live31081?view=nasPublication&nn=16102 (accessed on 29 June, 2022).
- Diaconu, D., Kahle, H.-P. and Spiecker, H. 2017 Thinning increases drought tolerance of European beech: a case study on two forested slopes on opposite sides of a valley. *Eur J Forest Res* **136**, 319–328.
- Dieler, J. and Pretzsch, H. 2013 Morphological plasticity of European beech (*Fagus sylvatica* L.) in pure and mixed-species stands. *Forest Ecology and Management* **295**, 97–108.
- Dobbertin, M., Eilmann, B., Bleuler, P., Giuggiola, A., Graf Pannatier, E. and Landolt, W. *et al.* 2010 Effect of irrigation on needle morphology, shoot and stem growth in a drought-exposed *Pinus sylvestris* forest. *Tree Physiol* **30**, 346–360.
- Donnelly, K. 1978 *Simulation to determine the variance and edge-effect of total nearest neighbour distances*. In: Hodder I. (ed.) *Simulation methods in Archeology: 91–95*. Cambridge Press, London.
- Ehbrecht, M., Schall, P., Juchheim, J., Ammer, C. and Seidel, D. 2016 Effective number of layers: A new measure for quantifying three-dimensional stand structure based on sampling with terrestrial LiDAR. *Forest Ecology and Management* **380**, 212–223.
- Ellenberg, H. and Leuschner, C. 2010 *Vegetation Mitteleuropas mit den Alpen: In ökologischer, dynamischer und historischer Sicht; 203 Tabellen*. 6th edn. Ulmer, 1333 p.
- European Commission. 2019 The European green deal.
- FAO - Food and Agriculture Organization of the United Nations. 2014 *World reference base for soil resources 2014: International soil classification system for naming soils and creating legends for soil maps*. FAO.

- Farquhar, G.D., Ehleringer, J.R. and Hubick, K.T. 1989 Carbon isotope discrimination and photosynthesis. *Annual review of plant physiology and plant molecular biology*, 503–537.
- Forest Europe. 2020 *State of Europe's Forests: Ministerial Conference on the Protection of Forests in Europe*, 394 p.
- Frenne, P. de, Lenoir, J., Luoto, M., Scheffers, B.R., Zellweger, F. and Aalto, J. *et al.* 2021 Forest microclimates and climate change: Importance, drivers and future research agenda. *Global change biology* **27**, 2279–2297.
- Friedlingstein, P., O'Sullivan, M., Jones, M.W., Andrew, R.M., Bakker, D.C.E. and Hauck, J. *et al.* 2023 Global Carbon Budget 2023. *Earth Syst. Sci. Data* **15**, 5301–5369.
- Gärtner, H. and Nievergelt, D. 2010 The core-microtome: A new tool for surface preparation on cores and time series analysis of varying cell parameters. *Dendrochronologia* **28**, 85–92.
- Gebhardt, T., Häberle, K.-H., Matyssek, R., Schulz, C. and Ammer, C. 2014 The more, the better? Water relations of Norway spruce stands after progressive thinning. *Agricultural and Forest Meteorology* **197**, 235–243.
- GeoSLAM. 2020 *ZEB HORIZON User Guide V1.0*, 24 p.
- Giuggiola, A., Bugmann, H., Zingg, A., Dobbertin, M. and Rigling, A. 2013 Reduction of stand density increases drought resistance in xeric Scots pine forests. *Forest Ecology and Management* **310**, 827–835.
- Grams, T.E.E., Hesse, B.D., Gebhardt, T., Weigl, F., Rötzer, T. and Kovacs, B. *et al.* 2021 The Kroof experiment: realization and efficacy of a recurrent drought experiment plus recovery in a beech/spruce forest. *Ecosphere* **12**.
- GreenValley International, Ltd. 2019 *LiDAR360; Software*.
- Grossiord, C. 2020 Having the right neighbors: how tree species diversity modulates drought impacts on forests. *New Phytologist* **228**, 42–49.
- Grote, R., Gessler, A., Hommel, R., Poschenrieder, W. and Priesack, E. 2016 Importance of tree height and social position for drought-related stress on tree growth and mortality. *Trees* **30**, 1467–1482.
- Guzmán, Q.J.A., Sharp, I., Alencastro, F. and Sánchez-Azofeifa, G.A. 2020 On the relationship of fractal geometry and tree–stand metrics on point clouds derived from terrestrial laser scanning. *Methods Ecol Evol* **11**, 1309–1318.
- Hacket-Pain, A.J., Friend, A.D., Lageard, J.G.A. and Thomas, P.A. 2015 The influence of masting phenomenon on growth–climate relationships in trees: explaining the influence of previous summers' climate on ring width. *Tree Physiol* **35**, 319–330.

- Hackett-Pain, A.J., Lageard, J.G.A. and Thomas, P.A. 2017 Drought and reproductive effort interact to control growth of a temperate broadleaved tree species (*Fagus sylvatica*). *Tree Physiol* **37**, 744–754.
- Hanba, Y.T., Mori, S., Lei, T.T., Koike, T. and Wada, E. 1997 Variations in leaf $\delta^{13}\text{C}$ along a vertical profile of irradiance in a temperate Japanese forest. *Oecologia* **110**, 253–261.
- Hansen, J.E., Sato, M., Simons, L., Nazarenko, L.S., Sangha, I. and Kharecha, P. *et al.* 2023 Global warming in the pipeline. *Oxf Open Clim Chang* **3**.
- Hanskötter, B. 2004 *Diagnose fakultativer Farbkerne an stehender Rotbuche (Fagus sylvatica L.) mittels Elektrischer Widerstandstomographie*. 1st edn. Cuvillier Verlag, 138 p.
- Hardt Ferreira Dos Santos, V.A., Modolo, G.S. and Ferreira, M.J. 2020 How do silvicultural treatments alter the microclimate in a Central Amazon secondary forest? A focus on light changes. *Journal of environmental management* **254**, 109816.
- Hari, V., Rakovec, O., Markonis, Y., Hanel, M. and Kumar, R. 2020 Increased future occurrences of the exceptional 2018-2019 Central European drought under global warming. *Sci Rep* **10**, 12207.
- Hartl-Meier, C., Dittmar, C., Zang, C. and Rothe, A. 2014 Mountain forest growth response to climate change in the Northern Limestone Alps. *Trees* **28**, 819–829.
- Hartmann, H. 2011 Will a 385 million year-struggle for light become a struggle for water and for carbon? - How trees may cope with more frequent climate change-type drought events. *Global Change Biol* **17**, 642–655.
- Hedwall, P.-O., Brunet, J., Nordin, A. and Bergh, J. 2013 Changes in the abundance of keystone forest floor species in response to changes of forest structure. *J Vegetation Science* **24**, 296–306.
- Helle, G. and Schleser, G.H. 2004 Beyond CO₂-fixation by Rubisco – an interpretation of $\delta^{13}\text{C}$ / $\delta^{12}\text{C}$ variations in tree rings from novel intra-seasonal studies on broad-leaf trees. *Plant Cell Environ* **27**, 367–380.
- Hoch, G., Siegwolf, R.T.W., Keel, S.G., Körner, C. and Han, Q. 2013 Fruit production in three masting tree species does not rely on stored carbon reserves. *Oecologia* **171**, 653–662.
- Hunčaga, M., Chudá, J., Tomašík, J., Slámová, M., Koreň, M. and Chudý, F. 2020 The Comparison of Stem Curve Accuracy Determined from Point Clouds Acquired by Different Terrestrial Remote Sensing Methods. *Remote Sensing* **12**, 2739.
- Hyypä, E., Yu, X., Kaartinen, H., Hakala, T., Kukko, A., Vastaranta, M. and Hyypä, J. 2020 Comparison of Backpack, Handheld, Under-Canopy UAV, and Above-Canopy UAV Laser Scanning for Field Reference Data Collection in Boreal Forests. *Remote Sensing* **12**, 3327.

- Hyypä, J., Holopainen, M. and Olsson, H. 2012 Laser Scanning in Forests. *Remote Sensing* **4**, 2919–2922.
- IPCC Intergovernmental Panel on Climate Change (ed). 2018 *Global warming of 1.5°C. An IPCC Special Report on the impacts of global warming of 1.5°C above pre-industrial levels and related global greenhouse gas emission pathways, in the context of strengthening the global response to the threat of climate change, sustainable development, and efforts to eradicate poverty*. In Press, 630 p.
- Jacobs, M., Rais, A. and Pretzsch, H. 2021 How drought stress becomes visible upon detecting tree shape using terrestrial laser scanning (TLS). *Forest Ecology and Management* **489**, 118975.
- Jonard, F., André, F., Ponette, Q., Vincke, C. and Jonard, M. 2011 Sap flux density and stomatal conductance of European beech and common oak trees in pure and mixed stands during the summer drought of 2003. *Journal of Hydrology* **409**, 371–381.
- Jump, A.S., Ruiz-Benito, P., Greenwood, S., Allen, C.D., Kitzberger, T. and Fensham, R. *et al.* 2017 Structural overshoot of tree growth with climate variability and the global spectrum of drought-induced forest dieback. *Global Change Biol* **23**, 3742–3757.
- Kagawa, A., Naito, D., Sugimoto, A. and Maximov, T.C. 2003 Effects of spatial and temporal variability in soil moisture on widths and $\delta^{13}\text{C}$ values of eastern Siberian tree rings. *J. Geophys. Res.* **108**.
- Kannenbergh, S.A., Schwalm, C.R. and Anderegg, W.R.L. 2020 Ghosts of the past: how drought legacy effects shape forest functioning and carbon cycling. *Ecology letters* **23**, 891–901.
- Klesse, S., Wohlgemuth, T., Meusburger, K., Vitasse, Y., Arx, G. von and Lévesque, M. *et al.* 2022 Long-term soil water limitation and previous tree vigor drive local variability of drought-induced crown dieback in *Fagus sylvatica*. *The Science of the total environment* **851**, 157926.
- Kohler, M., Sohn, J., Nägele, G. and Bauhus, J. 2010 Can drought tolerance of Norway spruce (*Picea abies* (L.) Karst.) be increased through thinning? *European Journal of Forest Research* **129**, 1109–1118.
- Kraft, G. 1884 *Beiträge zur Lehre von den Durchforstungen, Schlagstellungen und Lichtungshieben*. Klindworth.
- Kramer, K., Ducousso, A., Gömöry, D., Hansen, J.K., Ionita, L. and Liesebach, M. *et al.* 2017 Chilling and forcing requirements for foliage bud burst of European beech (*Fagus sylvatica* L.) differ between provenances and are phenotypically plastic. *Agricultural and Forest Meteorology* **234-235**, 172–181.
- Kuhn, M. 2022 caret: Classification and Regression Training. R package version 6.0-92.

- Kursa, M.B. and Rudnicki, W.R. 2010 Boruta: Wrapper Algorithm for All Relevant Feature Selection. *Journal of Statistical Software* **36**, 1–13.
- Lagergren, F., Lankreijer, H., Kučera, J., Cienciala, E., Mölder, M. and Lindroth, A. 2008 Thinning effects on pine-spruce forest transpiration in central Sweden. *Forest Ecology and Management* **255**, 2312–2323.
- Langer, G.J. and Bußkamp, J. 2023 Vitality loss of beech: a serious threat to *Fagus sylvatica* in Germany in the context of global warming. *J Plant Dis Prot* **130**, 1101–1115.
- Leavitt, S.W. 2002 Prospects for reconstruction of seasonal environment from tree-ring $\delta^{13}C$: baseline findings from the Great Lakes area, USA. *Chemical Geology* **192**, 47–58.
- Lebourgeois, F., Gomez, N., Pinto, P. and Mérian, P. 2013 Mixed stands reduce *Abies alba* tree-ring sensitivity to summer drought in the Vosges mountains, western Europe. *Forest Ecology and Management* **303**, 61–71.
- Lee, B.-U., Jeon, H.-G., Im, S. and Kweon, I.S. 2019 Depth Completion with Deep Geometry and Context Guidance. In *2019 International Conference on Robotics and Automation (ICRA)*. IEEE, pp. 3281–3287.
- Leuschner, C., Fuchs, S., Wedde, P., Rütger, E. and Schuldt, B. 2024 A multi-criteria drought resistance assessment of temperate *Acer*, *Carpinus*, *Fraxinus*, *Quercus*, and *Tilia* species. *Perspectives in Plant Ecology, Evolution and Systematics* **62**, 125777.
- Leuschner, C., Weithmann, G., Bat-Enerel, B. and Weigel, R. 2023 The Future of European Beech in Northern Germany—Climate Change Vulnerability and Adaptation Potential. *Forests* **14**, 1448.
- Lévesque, M., Saurer, M., Siegwolf, R., Eilmann, B., Brang, P., Bugmann, H. and Rigling, A. 2013 Drought response of five conifer species under contrasting water availability suggests high vulnerability of Norway spruce and European larch. *Global Change Biol* **19**, 3184–3199.
- Li, L., Mu, X., Soma, M., Wan, P., Qi, J. and Hu, R. *et al.* 2021 An Iterative-Mode Scan Design of Terrestrial Laser Scanning in Forests for Minimizing Occlusion Effects. *IEEE Trans. Geosci. Remote Sensing* **59**, 3547–3566.
- Li, W., Guo, Q., Jakubowski, M.K. and Kelly, M. 2012 A New Method for Segmenting Individual Trees from the Lidar Point Cloud. *photogramm eng remote sensing* **78**, 75–84.
- Liang, X., Kankare, V., Hyypä, J., Wang, Y., Kukko, A. and Haggrén, H. *et al.* 2016 Terrestrial laser scanning in forest inventories. *ISPRS Journal of Photogrammetry and Remote Sensing* **115**, 63–77.

- Lindner, M., Maroschek, M., Netherer, S., Kremer, A., Barbati, A. and Garcia-Gonzalo, J. *et al.* 2010 Climate change impacts, adaptive capacity, and vulnerability of European forest ecosystems. *Forest Ecology and Management* **259**, 698–709.
- Lovell, J.L., Jupp, D., Newnham, G.J. and Culvenor, D.S. 2011 Measuring tree stem diameters using intensity profiles from ground-based scanning lidar from a fixed viewpoint. *ISPRS Journal of Photogrammetry and Remote Sensing* **66**, 46–55.
- Lüdecke, D. 2023 sjPlot: Data Visualization for Statistics in Social Science.
- Lüttschwager, D. and Jochheim, H. 2020 Drought Primarily Reduces Canopy Transpiration of Exposed Beech Trees and Decreases the Share of Water Uptake from Deeper Soil Layers. *Forests* **11**, 537.
- LWF - Bayerische Landesanstalt für Wald und Forstwirtschaft. 2005 *Waldatlas Bayern*, 137 p.
- Magh, Bonn, Grote, Burzlaff, Pfautsch and Rennenberg. 2019 Drought Superimposes the Positive Effect of Silver Fir on Water Relations of European Beech in Mature Forest Stands. *Forests* **10**, 897.
- Manion, P.D. 1981 *Tree disease concepts*. Prentice-Hall, Inc.
- Martín-Benito, D., Del Río, M., Heinrich, I., Helle, G. and Cañellas, I. 2010 Response of climate-growth relationships and water use efficiency to thinning in a *Pinus nigra* afforestation. *Forest Ecology and Management* **259**, 967–975.
- Martínez-Sancho, E., Dorado-Liñán, I., Hacke, U.G., Seidel, H. and Menzel, A. 2017 Contrasting Hydraulic Architectures of Scots Pine and Sessile Oak at Their Southernmost Distribution Limits. *Frontiers in plant science* **8**, 598.
- Masarovicová, E. and štefančík, L. 1990 Some ecophysiological features in sun and shade leaves of tall beech trees. *Biol Plant* **32**, 374–387.
- Mathes, T., Seidel, D. and Annighöfer, P. 2023a Response to extreme events: do morphological differences affect the ability of beech (*Fagus sylvatica* L.) to resist drought stress? *Forestry (Lond)* **96**, 355–371.
- Mathes, T., Seidel, D., Häberle, K.-H., Pretzsch, H. and Annighöfer, P. 2023b What Are We Missing? Occlusion in Laser Scanning Point Clouds and Its Impact on the Detection of Single-Tree Morphologies and Stand Structural Variables. *Remote Sensing* **15**, 450.
- Mathes, T., Seidel, D., Klemmt, H.-J., Thom, D. and Annighöfer, P. 2024 The effect of forest structure on drought stress in beech forests (*Fagus sylvatica* L.). *Forest Ecology and Management* **554**, 121667.
- Matyssek, R., Fromm, J., Rennenberg, H. and Roloff, A. 2010 *Biologie der Bäume: Von der Zelle zur globalen Ebene*. Verlag Eugen Ulmer, 349 p.

- McDowell, N.G., Adams, H.D., Bailey, J.D., Hess, M. and Kolb, T.E. 2006 Homeostatic maintenance of ponderosa pine gas exchange in response to stand density changes. *Ecological Applications* **16**, 1164–1182.
- McDowell, N.G., Adams, H.D., Bailey, J.D. and Kolb, T.E. 2007 The role of stand density on growth efficiency, leaf area index, and resin flow in southwestern ponderosa pine forests. *Canadian Journal of Forest Research* **37**, 343–355.
- McLeod, A.I., Xu, C. and Lai, Y. 2020 *bestglm: Best Subset GLM and Regression Utilities*.
- Meier, I.C. and Leuschner, C. 2008 Genotypic variation and phenotypic plasticity in the drought response of fine roots of European beech. *Tree Physiol* **28**, 297–309.
- Metz, J., Annighöfer, P., Schall, P., Zimmermann, J., Kahl, T., Schulze, E.-D. and Ammer, C. 2016 Site-adapted admixed tree species reduce drought susceptibility of mature European beech. *Global change biology* **22**, 903–920.
- Meyer, P., Spînu, A.P., Mölder, A. and Bauhus, J. 2022 Management alters drought-induced mortality patterns in European beech (*Fagus sylvatica* L.) forests. *Plant biology (Stuttgart, Germany)* **24**, 1157–1170.
- Michelot, A., Simard, S., Rathgeber, C., Dufrêne, E. and Damesin, C. 2012 Comparing the intra-annual wood formation of three European species (*Fagus sylvatica*, *Quercus petraea* and *Pinus sylvestris*) as related to leaf phenology and non-structural carbohydrate dynamics. *Tree Physiol* **32**, 1033–1045.
- Mölder, I., Leuschner, C. and Leuschner, H.H. 2011 $\delta^{13}\text{C}$ signature of tree rings and radial increment of *Fagus sylvatica* trees as dependent on tree neighborhood and climate. *Trees* **25**, 215–229.
- Neudam, L., Annighöfer, P. and Seidel, D. 2022 Exploring the Potential of Mobile Laser Scanning to Quantify Forest Structural Complexity. *Front. Remote Sens.* **3**.
- Neycken, A., Scheggia, M., Bigler, C. and Lévesque, M. 2022 Long-term growth decline precedes sudden crown dieback of European beech. *Agricultural and Forest Meteorology* **324**, 109103.
- Nilsen, P. and Strand, L.T. 2008 Thinning intensity effects on carbon and nitrogen stores and fluxes in a Norway spruce (*Picea abies* (L.) Karst.) stand after 33 years. *Forest Ecology and Management* **256**, 201–208.
- Nussbaumer, A., Meusburger, K., Schmitt, M., Waldner, P., Gehrig, R. and Haeni, M. *et al.* 2020 Extreme summer heat and drought lead to early fruit abortion in European beech. *Sci Rep* **10**, 5334.
- Odum, E.P. 1959 Fundamentals of Ecology. *Journal of Range Management* **12**, 313.

- Petit-Cailleux, C., Davi, H., Lefèvre, F., Garrigue, J., Magdalou, J.-A. and Hurson, C. *et al.* 2021 Comparing statistical and mechanistic models to identify the drivers of mortality within a rear-edge beech population. *Peer Community Journal* **1**.
- Pommerening, A. and Stoyan, D. 2006 Edge-correction needs in estimating indices of spatial forest structure. *Can. J. For. Res.* **36**, 1723–1739.
- Porter, T.J., Pisaric, M.F.J., Kokelj, S.V. and Edwards, T.W.D. 2009 Climatic Signals in $\delta^{13}\text{C}$ and $\delta^{18}\text{O}$ of Tree-rings from White Spruce in the Mackenzie Delta Region, Northern Canada. *Arctic, Antarctic, and Alpine Research* **41**, 497–505.
- Pretzsch, H., Ahmed, S., Rötzer, T., Schmied, G. and Hilmers, T. 2023 Structural and compositional acclimation of forests to extended drought: results of the KROOF throughfall exclusion experiment in Norway spruce and European beech. *Trees*, 1–21.
- Pretzsch, H., Bauerle, T., Häberle, K.H., Matyssek, R., Schütze, G. and Rötzer, T. 2016 Tree diameter growth after root trenching in a mature mixed stand of Norway spruce (*Picea abies* [L.] Karst) and European beech (*Fagus sylvatica* [L.]). *Trees* **30**, 1761–1773.
- Pretzsch, H., Biber, P., Uhl, E., Dahlhausen, J., Rötzer, T. and Caldentey, J. *et al.* 2015 Crown size and growing space requirement of common tree species in urban centres, parks, and forests. *Urban Forestry & Urban Greening* **14**, 466–479.
- Pretzsch, H., Grams, T., Häberle, K.H., Pritsch, K., Bauerle, T. and Rötzer, T. 2020 Growth and mortality of Norway spruce and European beech in monospecific and mixed-species stands under natural episodic and experimentally extended drought. Results of the KROOF throughfall exclusion experiment. *Trees* **34**, 957–970.
- Pretzsch, H., Rötzer, T., Matyssek, R., Grams, T.E.E., Häberle, K.-H. and Pritsch, K. *et al.* 2014 Mixed Norway spruce (*Picea abies* [L.] Karst) and European beech (*Fagus sylvatica* [L.]) stands under drought: from reaction pattern to mechanism. *Trees* **28**, 1305–1321.
- Purahong, W., Tanunchai, B., Wahdan, S.F.M., Buscot, F. and Schulze, E.-D. 2021 Molecular Screening of Microorganisms Associated with Discolored Wood in Dead European Beech Trees Suffered from Extreme Drought Event Using Next Generation Sequencing. *Plants* **10**, 2092.
- R Core Team. 2023 R: A Language and Environment for Statistical Computing, Vienna, Austria.
- Rakovec, O., Samaniego, L., Hari, V., Markonis, Y., Moravec, V. and Thober, S. *et al.* 2022 The 2018–2020 Multi-Year Drought Sets a New Benchmark in Europe. *Earth's Future* **10**.

- Rohner, B., Kumar, S., Liechti, K., Gessler, A. and Ferretti, M. 2021 Tree vitality indicators revealed a rapid response of beech forests to the 2018 drought. *Ecological Indicators* **120**, 106903.
- Roloff, A. 1986 *Morphologie der Kronenentwicklung von Fagus sylvatica L. (Rotbuche) unter besonderer Berücksichtigung möglicherweise neuartiger Veränderungen*. Dissertation.
- Rothenbühler, S., Walthert, L., Saurer, M., Gärtner, H., Gessler, A. and Rigling, A. *et al.* 2021 *Assessing drought-induced mortality of European beech and Scots pine in the Valais, Switzerland*.
- Roussel, J.-R., Auty, D., Coops, N.C., Tompalski, P., Goodbody, T.R. and Meador, A.S. *et al.* 2020 lidR: An R package for analysis of Airborne Laser Scanning (ALS) data. *Remote Sensing of Environment* **251**, 112061.
- Ruehr, N.K., Law, B.E., Quandt, D. and Williams, M. 2014 Effects of heat and drought on carbon and water dynamics in a regenerating semi-arid pine forest: a combined experimental and modeling approach. *Biogeosciences* **11**, 4139–4156.
- Ryding, J., Williams, E., Smith, M. and Eichhorn, M. 2015 Assessing Handheld Mobile Laser Scanners for Forest Surveys. *Remote Sensing* **7**, 1095–1111.
- Sankey, T. and Tatum, J. 2022 Thinning increases forest resiliency during unprecedented drought. *Sci Rep* **12**, 9041.
- Sarris, D., Siegwolf, R. and Körner, C. 2013 Inter- and intra-annual stable carbon and oxygen isotope signals in response to drought in Mediterranean pines. *Agricultural and Forest Meteorology* **168**, 59–68.
- Saurer, M., Sahlstedt, E., Rinne-Garmston, K.T., Lehmann, M.M., Oettli, M., Gessler, A. and Treydte, K. 2023 Progress in high-resolution isotope-ratio analysis of tree rings using laser ablation. *Tree physiology* **43**, 694–705.
- Scharnweber, T., Manthey, M., Criegee, C., Bauwe, A., Schröder, C. and Wilmking, M. 2011 Drought matters – Declining precipitation influences growth of *Fagus sylvatica* L. and *Quercus robur* L. in north-eastern Germany. *Forest Ecology and Management* **262**, 947–961.
- Scharnweber, T., Smiljanic, M., Cruz-García, R., Manthey, M. and Wilmking, M. 2020 Tree growth at the end of the 21st century - the extreme years 2018/19 as template for future growth conditions. *Environ. Res. Lett.* **15**, 74022.
- Schmied, G., Hilmers, T., Uhl, E. and Pretzsch, H. 2022 The Past Matters: Previous Management Strategies Modulate Current Growth and Drought Responses of Norway Spruce (*Picea abies* H. Karst.). *Forests* **13**, 243.

- Schnabel, F., Purrucker, S., Schmitt, L., Engelmann, R.A., Kahl, A. and Richter, R. *et al.* 2022 Cumulative growth and stress responses to the 2018-2019 drought in a European floodplain forest. *Global Change Biol* **28**, 1870–1883.
- Schuldt, B., Buras, A., Arend, M., Vitasse, Y., Beierkuhnlein, C. and Damm, A. *et al.* 2020 A first assessment of the impact of the extreme 2018 summer drought on Central European forests. *Basic and Applied Ecology* **45**, 86–103.
- Schwarz, J.A. and Bauhus, J. 2019 Benefits of Mixtures on Growth Performance of Silver Fir (*Abies alba*) and European Beech (*Fagus sylvatica*) Increase With Tree Size Without Reducing Drought Tolerance. *Front. For. Glob. Change* **2**.
- Seidel, D. 2018 A holistic approach to determine tree structural complexity based on laser scanning data and fractal analysis. *Ecology and evolution* **8**, 128–134.
- Seidel, D., Ammer, C. and Puettmann, K. 2015 Describing forest canopy gaps efficiently, accurately, and objectively: New prospects through the use of terrestrial laser scanning. *Agricultural and Forest Meteorology* **213**, 23–32.
- Seidel, D., Annighöfer, P., Ehbrecht, M., Magdon, P., Wöllauer, S. and Ammer, C. 2020 Deriving Stand Structural Complexity from Airborne Laser Scanning Data—What Does It Tell Us about a Forest? *Remote Sensing* **12**, 1854.
- Seidel, D., Ehbrecht, M., Annighöfer, P. and Ammer, C. 2019 From tree to stand-level structural complexity — Which properties make a forest stand complex? *Agricultural and Forest Meteorology* **278**, 107699.
- Senf, C., Buras, A., Zang, C.S., Rammig, A. and Seidl, R. 2020 Excess forest mortality is consistently linked to drought across Europe. *Nat Commun* **11**, 6200.
- Senf, C. and Seidl, R. 2021 Persistent impacts of the 2018 drought on forest disturbance regimes in Europe. *Biogeosciences* **18**, 5223–5230.
- Serra-Maluquer, X., Mencuccini, M. and Martínez-Vilalta, J. 2018 Changes in tree resistance, recovery and resilience across three successive extreme droughts in the northeast Iberian Peninsula. *Oecologia* **187**, 343–354.
- Skomarkova, M.V., Vaganov, E.A., Mund, M., Knohl, A., Linke, P., Boerner, A. and Schulze, E.-D. 2006 Inter-annual and seasonal variability of radial growth, wood density and carbon isotope ratios in tree rings of beech (*Fagus sylvatica*) growing in Germany and Italy. *Trees* **20**, 571–586.
- Sohn, J.A., Saha, S. and Bauhus, J. 2016 Potential of forest thinning to mitigate drought stress: A meta-analysis. *Forest Ecology and Management* **380**, 261–273.
- Spiecker, H. and Kahle, H.-P. 2023 Climate-driven tree growth and mortality in the Black Forest, Germany-Long-term observations. *Global change biology* **29**, 5908–5923.

- Stereńczak, K., Mielcarek, M., Wertz, B., Bronisz, K., Zajączkowski, G. and Jagodziński, A.M. *et al.* 2019 Factors influencing the accuracy of ground-based tree-height measurements for major European tree species. *Journal of environmental management* **231**, 1284–1292.
- Stiers, M., Annighöfer, P., Seidel, D., Willim, K., Neudam, L. and Ammer, C. 2020 Quantifying the target state of forest stands managed with the continuous cover approach – revisiting Möller's “Dauerwald” concept after 100 years. *Trees, Forests and People* **1**, 100004.
- Stimmelmayer, M. 2022 *Relationship between drought stress, vitality and wood quality in beech forests (Fagus sylvatica L.)*. Master thesis, Technical University of Munich, unpublished, 156 p.
- StMELF - Bayerische Staatsministerium für Ernährung, Landwirtschaft und Forsten. 2023 *Ergebnisse der Waldzustandserhebung 2022*, 21 p.
- StMELF - Bayerisches Staatsministerium für Ernährung, Landwirtschaft und Forsten. 2019 *Ergebnisse der Waldzustandserhebung 2019*, 21 p.
- StMELF - Bayerisches Staatsministerium für Ernährung, Landwirtschaft und Forsten. 2020 *Waldbericht 2020*, 40 p.
- Stovall, A.E.L., Shugart, H. and Yang, X. 2019 Tree height explains mortality risk during an intense drought. *Nature communications* **10**, 4385.
- Süßel, F. and Brüggemann, W. 2021 Tree water relations of mature oaks in southwest Germany under extreme drought stress in summer 2018. *Plant Stress* **1**, 100010.
- Thom, D., Buras, A., Heym, M., Klemmt, H.-J. and Wauer, A. 2023 Varying growth response of Central European tree species to the extraordinary drought period of 2018 – 2020. *Agricultural and Forest Meteorology* **338**, 109506.
- Thom, D., Sommerfeld, A., Sebald, J., Hagge, J., Müller, J. and Seidl, R. 2020 Effects of disturbance patterns and deadwood on the microclimate in European beech forests. *Agricultural and Forest Meteorology* **291**, 108066.
- Thonfeld, F., Gessner, U., Holzwarth, S., Kriese, J., Da Ponte, E., Huth, J. and Kuenzer, C. 2022 A First Assessment of Canopy Cover Loss in Germany's Forests after the 2018–2020 Drought Years. *Remote Sensing* **14**, 562.
- Thünen-Institut - Dritte Bundeswaldinventur - Ergebnisdatenbank. 2012 <https://bwi.info>, Aufruf am: 19.06.2023; Auftragskürzel: 77Z1JI_L235of_2012_bi, Archivierungsdatum: 2014-6-10 16:7:59.927. Überschrift: Vorrat [m³/ha] nach Land und Baumaltersklasse, Filter: Baumartengruppe=Buche ; Jahr=2012 ;
- Töchterle, P., Yang, F., Rehschuh, S., Rehschuh, R., Ruehr, N.K., Rennenberg, H. and Dannenmann, M. 2020 Hydraulic Water Redistribution by Silver Fir (*Abies alba* Mill.) Occurring under Severe Soil Drought. *Forests* **11**, 162.

- Trochta, J., Král, K., Janík, D. and Adam, D. 2013 Arrangement of terrestrial laser scanner positions for area-wide stem mapping of natural forests. *Can. J. For. Res.* **43**, 355–363.
- Trzeciak, M. and Brilakis, I. 2021 Comparison of accuracy and density of static and mobile laser scanners. 2021 European Conference on Computing in Construction, 2021 European Conference on Computing in Construction. Ixia, Rhodes, Greece, July 25-27.
- Utschig, H., Neufanger, M. and Zanker, T. 2011 Das 100-Baum-Konzept als Einstieg für Durchforstungsregeln in Mischbeständen. *Allg. Forstz. Waldwirtsch. Umweltvorsorge AFZ-Der Wald AFZ*, 4–6.
- van der Maaten, E. 2013 Thinning prolongs growth duration of European beech (*Fagus sylvatica* L.) across a valley in southwestern Germany. *Forest Ecology and Management* **306**, 135–141.
- van der Woude, A.M., Peters, W., Joetzjer, E., Lafont, S., Koren, G. and Ciais, P. *et al.* 2023 Temperature extremes of 2022 reduced carbon uptake by forests in Europe. *Nat Commun* **14**, 6218.
- van der Zande, D., Jonckheere, I., Stuckens, J., Verstraeten, W.W. and Coppin, P. 2008 Sampling design of ground-based lidar measurements of forest canopy structure and its effect on shadowing. *Canadian Journal of Remote Sensing* **34**, 526–538.
- Vitasse, Y., Bottero, A., Cailleret, M., Bigler, C., Fonti, P. and Gessler, A. *et al.* 2019 Contrasting resistance and resilience to extreme drought and late spring frost in five major European tree species. *Global Change Biol* **25**, 3781–3792.
- Walentowski, H. 2006 *Handbuch der natürlichen Waldgesellschaften Bayerns: Ein auf geobotanischer Grundlage entwickelter Leitfaden für die Praxis in Forstwirtschaft und Naturschutz*. 2nd edn. Verl. Geobotanica, 441 p.
- Walthert, L., Ganthaler, A., Mayr, S., Saurer, M., Waldner, P. and Walser, M. *et al.* 2021 From the comfort zone to crown dieback: Sequence of physiological stress thresholds in mature European beech trees across progressive drought. *The Science of the total environment* **753**, 141792.
- Warren, C.R., McGrath, J.F. and Adams, M.A. 2001 Water availability and carbon isotope discrimination in conifers. *Oecologia* **127**, 476–486.
- Weber, P., Bugmann, H., Pluess, A.R., Walthert, L. and Rigling, A. 2013 Drought response and changing mean sensitivity of European beech close to the dry distribution limit. *Trees* **27**, 171–181.
- Weigel, R., Bat-Enerel, B., Dulamsuren, C., Muffler, L., Weithmann, G. and Leuschner, C. 2023 Summer drought exposure, stand structure, and soil properties jointly control the growth of European beech along a steep precipitation gradient in northern Germany. *Global change biology* **29**, 763–779.

- Weithmann, G., Link, R.M., Banzragch, B.-E., Würzberg, L., Leuschner, C. and Schuldt, B. 2022 Soil water availability and branch age explain variability in xylem safety of European beech in Central Europe. *Oecologia* **198**, 629–644.
- Wellbrock, N. and Eickenscheidt, N. 2018 *Leitfaden und Dokumentation zur Waldzustandserhebung in Deutschland*. Johann Heinrich von Thünen-Institut.
- Whitehead, D., Jarvis, P.G. and Waring, R.H. 1984 Stomatal conductance, transpiration, and resistance to water uptake in a Pinussylvestris spacing experiment. *Canadian Journal of Forest Research* **14**, 692–700.
- Wickham, H. 2016 *ggplot2: Elegant Graphics for Data Analysis*. Springer-Verlag New York.
- Willim, K., Stiers, M., Annighöfer, P., Ehbrecht, M., Ammer, C. and Seidel, D. 2020 Spatial Patterns of Structural Complexity in Differently Managed and Unmanaged Beech-Dominated Forests in Central Europe. *Remote Sensing* **12**, 1907.
- Wood, S.N. 2011 Fast stable restricted maximum likelihood and marginal likelihood estimation of semiparametric generalized linear models. *Journal of the Royal Statistical Society (B)* **73**, 3–36.
- Yan, Z., Liu, R., Cheng, L., Zhou, X., Ruan, X. and Xiao, Y. 2019 A Concave Hull Methodology for Calculating the Crown Volume of Individual Trees Based on Vehicle-Borne LiDAR Data. *Remote Sensing* **11**, 623.
- Yousefpour, R., Augustynczyk, A.L.D., Reyer, C.P.O., Lasch-Born, P., Suckow, F. and Hanewinkel, M. 2018 Realizing Mitigation Efficiency of European Commercial Forests by Climate Smart Forestry. *Sci Rep* **8**, 345.
- Zapater, M., Hossann, C., Bréda, N., Bréchet, C., Bonal, D. and Granier, A. 2011 Evidence of hydraulic lift in a young beech and oak mixed forest using 18O soil water labelling. *Trees* **25**, 885–894.
- Zellweger, F., Frenne, P. de, Lenoir, J., Vangansbeke, P., Verheyen, K. and Bernhardt-Römermann, M. *et al.* 2020 Forest microclimate dynamics drive plant responses to warming. *Science (New York, N.Y.)* **368**, 772–775.
- Zhang, W., Qi, J., Wan, P., Wang, H., Xie, D., Wang, X. and Yan, G. 2016 An Easy-to-Use Airborne LiDAR Data Filtering Method Based on Cloth Simulation. *Remote Sensing* **8**, 1–22.
- Zimmermann, L., Raspe, S., Dietrich, H.-P. and Wauer, A. 2020 Dürreperioden und ihre Wirkung auf Wälder. *LWF aktuell*, 18–23.

12 Appendices

12.1 Paper I



Article

What Are We Missing? Occlusion in Laser Scanning Point Clouds and Its Impact on the Detection of Single-Tree Morphologies and Stand Structural Variables

Thomas Mathes ^{1,*}, Dominik Seidel ², Karl-Heinz Häberle ³, Hans Pretzsch ^{4,5} and Peter Annighöfer ¹

¹ Professorship of Forest and Agroforest Systems, Technical University of Munich, Hans-Carl-v.-Carlowitz-Platz 2, D-85354 Freising, Germany

² Spatial Structures and Digitization of Forests, Faculty of Forest Sciences and Forest Ecology, University of Göttingen, Büsgenweg 1, D-37077 Göttingen, Germany

³ Restoration Ecology, Technical University of Munich, Emil-Ramann-Str. 6, D-85354 Freising, Germany

⁴ Forest Growth and Yield Science, Technical University of Munich, Hans-Carl-von-Carlowitz-Platz 2, D-85354 Freising, Germany

⁵ Sustainable Forest Management Research Institute iuFOR, Valladolid University, 47002 Valladolid, Spain

* Correspondence: thomas.mathes@tum.de

Abstract: Laser scanning has revolutionized the ability to quantify single-tree morphologies and stand structural variables. In this study, we address the issue of occlusion when scanning a spruce (*Picea abies* (L.) H.Karst.) and beech (*Fagus sylvatica* L.) forest with a mobile laser scanner by making use of a unique study site setup. We scanned forest stands (1) from the ground only and (2) from the ground and from above by using a crane. We also examined the occlusion effect by scanning in the summer (leaf-on) and in the winter (leaf-off). Especially at the canopy level of the forest stands, occlusion was very pronounced, and we were able to quantify its impact in more detail. Occlusion was not as noticeable as expected for crown-related variables but, on average, resulted in smaller values for tree height in particular. Between the species, the total tree height underestimation for spruce was more pronounced than that for beech. At the stand level, significant information was lost in the canopy area when scanning from the ground alone. This information shortage is reflected in the relative point counts, the Clark–Evans index and the box dimension. Increasing the voxel size can compensate for this loss of information but comes with the trade-off of losing details in the point clouds. From our analysis, we conclude that the voxelization of point clouds prior to the extraction of stand or tree measurements with a voxel size of at least 20 cm is appropriate to reduce occlusion effects while still providing a high level of detail.

Keywords: mobile laser scanner; forest structure; accuracy; voxel size; *Fagus sylvatica* L.; *Picea abies* (L.) H.Karst



Citation: Mathes, T.; Seidel, D.; Häberle, K.-H.; Pretzsch, H.; Annighöfer, P. What Are We Missing? Occlusion in Laser Scanning Point Clouds and Its Impact on the Detection of Single-Tree Morphologies and Stand Structural Variables. *Remote Sens.* **2023**, *15*, 450. <https://doi.org/10.3390/rs15020450>

Academic Editor: Huaqiang Du

Received: 19 December 2022

Revised: 9 January 2023

Accepted: 10 January 2023

Published: 12 January 2023



Copyright: © 2023 by the authors. Licensee MDPI, Basel, Switzerland. This article is an open access article distributed under the terms and conditions of the Creative Commons Attribution (CC BY) license (<https://creativecommons.org/licenses/by/4.0/>).

1. Introduction

Laser scanning has revolutionized the ability to quantify single-tree morphologies and stand structural variables, e.g., [1–3]. By using terrestrial laser scanners, the structures of trees and stands can be recorded more quickly and accurately than with conventional methods [4]. During the last several years, this technology has opened new opportunities for environmental scientists and foresters [5]. The aboveground structure of a forest is one of the key features of forest ecosystems and especially influences which ecosystem services are provided by the system. For example, Gough et al. [6] found a significant influence of the forest structure on forest productivity, and Bauhus et al. [7] observed its effects on forest stability and resilience. Moreover, the forest structure is related to biodiversity, e.g., [8,9], and to microclimate regulation, e.g., [10,11].

For forest inventory purposes, single-tree morphologies, such as the tree height and diameter at breast height, can be derived from laser scanner data, e.g., [12]. One advantage

is that such classic variables can be measured faster and more efficiently with laser scanners. However, it is also possible to quantify characteristics that have hardly been measurable to date. The technique has also enabled more precise and efficient ways of measuring crown morphologies, such as the height of the maximum crown projection area, the maximum crown projection area, the crown volume and the crown surface area. These are of interest for several tree physiological relationships (e.g., [13]). Jacobs et al. [14] showed, on the basis of laser scan data, that drought stress affects the crown size and tree height.

Lidar-based scanners are currently the dominant solution for outdoor mobile mapping [15]. For many forestry-related questions, laser scan data are either collected from the ground or from the air. When scanning from the ground, there are basically two different approaches: terrestrial laser scanning (TLS) and mobile laser scanning (MLS), also often called handheld personal laser scanning (HPLS). In TLS, the three-dimensional point cloud is achieved through single scans with a fixed viewpoint [16] or by combining multiple single scans [17]. Since multiple scan locations are required to accurately capture the forest structure and to reduce occlusion, the method is time-consuming and costly. MLS, on the other hand, is faster and therefore more cost-efficient [18]. This technology uses an inertial measurement unit to determine the position of a laser while the laser takes distance measurements of its surroundings.

When scanning from the air, the scanner is attached to an aircraft, for example, an unmanned aerial vehicle (drone) or a light aircraft (airborne laser scanning (ALS)). ALS has a high area coverage but, presently, still has a lower point cloud resolution than terrestrial/mobile laser scanning from the ground. Additionally, difficulties arise in obtaining detailed tree structures due to canopy occlusion [19]. Mobile laser scanners, on the other hand, are well suited for scanning forest stands and individual trees with a high level of detail, e.g., [20,21].

Aerial scans and ground-based scans are limited to a single perspective of the forest, either from above or below the canopy. This necessarily results in an occlusion effect, e.g., [22,23]. It remains unclear how much information is missed by being restricted to one perspective and how this affects tree and stand structural variables derived from laser scans. Most likely, the amount of information missed due to occlusion depends on the distribution of biomass in space. Especially dense stands can be assumed to be susceptible to either approach [24].

Beech (*Fagus sylvatica* L.) is a tree species that forms very dense stands due to its high shade tolerance and pronounced development of shade leaves [25]. Such canopies can act as shields against laser beams even at lower stand heights. Spruce (*Picea abies* (L.) H.Karst.) also forms dense canopies but loses its needles in lower stem sections under dense stand conditions due to the lack of light. In both cases and for both species, laser scanners are likely unable to detect the upper crown due to occlusion when scanning from the ground during the vegetation period. In winter, on the other hand, beech trees shed their leaves, whereas spruce trees do not lose their needles. Due to increased visibility in winter, the accessibility of beech canopies with laser beams from the ground should be better for beech than for spruce in the leaf-off period.

To obtain stable estimations of structural and morphological variables, the issue of occlusion is often addressed by reducing the spatial resolution of the point cloud based on so-called voxelization, e.g., [26,27]. Voxelization has the potential to compensate for occlusion and the spatial variation in the point cloud density with distance from the scanner to a certain degree, depending on the voxel size. However, voxelization is also accompanied by a loss of detail in the point cloud and an increase in space-filling estimates. While voxels should not be too small to ensure reduced occlusion, they should also not be too large to prevent severe losses in resolution. A voxel size of 10 or 20 cm side length is often chosen as a compromise [22,27,28].

In this study, we intended to address the issue of occlusion in mobile laser scanning from the ground by making use of a study site with the possibility of scanning a forest stand from below and above. The aim was to quantify the potential loss of information

and to detect the pattern showing where information is lost and how the loss changes with different voxel sizes. To do this, we scanned forest stands (1) from the ground only and (2) from the ground and from above by using the crane experiment KROOF [29]. We also examined the seasonal effect for beech by scanning in the summer (leaf-on) and winter (leaf-off) seasons.

The hypotheses of this work were driven by two assumptions. First, the effect of occlusion (information loss) in deciduous species is stronger in summer than in winter because the leaves reduce the visibility of the upper parts of the crown (seasonal comparison). Second, there is occlusion in the tree crown when scanning only from the ground. Even under the best conditions (no leaves), an occlusion effect remains due to the lack of perspectives of the objects of interest from above (methodological comparison). The specific hypotheses were:

Seasonal comparison

H1. For beech, the occlusion effect leads to significant differences in single-tree morphologies when comparing summer to winter ground scans; for spruce, there are no significant differences.

H2. For beech stands, the occlusion effect results in a significant difference in stand complexity when comparing summer to winter scans; for spruce, there is no significant difference.

Methodological comparison

H3. For single trees, the occlusion effect leads to smaller values for canopy morphologies of all trees (e.g., lower height and smaller crown volume) when scanned only from the ground.

H4. For stands, the occlusion effect results in an underestimation of the stand structural variables when scanned only from the ground.

H5. For stand-specific variables, the occlusion effect is reduced in importance as the resolution of the data decreases (voxel size increases).

2. Materials and Methods

2.1. Study Area

The study area was located in the Kranzberg Forest (48°25′09.8″N; 11°39′39.8″E) in the southern part of Germany, about 35 km northeast of Munich [30]. Within the forest, there is the unique Kranzberg Forest Roof (KROOF) experiment on an area of 0.5 ha [31]. The KROOF experiment was originally designed as a drought stress experiment. In addition to water retention by roofs, a canopy crane had been installed at the KROOF experimental site (Figure 1c). This allows research to be conducted at heights of up to 45 m. In this study, this crane was used to complement the ground scans with scans from above the forest canopy.

The mixed stand primarily consists of pure tree groups of Norway spruce (*Picea abies* (L.) H.Karst.) and European beech (*Fagus sylvatica* L.) trees that were planted in 1951 ± 2 y and 1931 ± 4 y, respectively [29]. These two tree species are among the most common tree species in Germany, with forested area shares of 25% for spruce and 16% for beech [32], and are coniferous and deciduous, respectively. According to inventory data for the KROOF site, beech trees had a height of about 28 m and spruce trees had a height of about 32 m on average [31]. The average diameter at breast height (dbh) was about 29 cm for beech and about 35 cm for spruce [31]. In total, there were 639–926 trees per ha with a stand basal area of 54.0–60.1 m²·ha⁻¹, a standing stem volume of 802–981 m³·ha⁻¹, and a mean periodic volume increment (1998–2016) of 19.4–26.3 m³·ha⁻¹·y⁻¹ [33].



Figure 1. The mobile laser scanner in the start position (a) and attached to the crane (b). During operation, it was lifted over the canopy and moved smoothly over the canopy of the forest stand. Figure (c) shows the crane itself.

2.2. Data Collection

Data were collected in the pure sections of spruce and beech stands. The two areas selected for scanning each had a size of $30\text{ m} \times 40\text{ m}$ (1200 m^2). The areas were scanned during two different seasons of the year, in summer 2020 (during the vegetation period, leaf-on for deciduous trees) and in winter 2020/2021 (leaf-off for deciduous trees). There was nearly no growth between summer and winter scans, and we can also exclude possible influences of the different treatments of the drought experiment. To record the plots, we used the ZEB HORIZON mobile laser scanner (GeoSLAM Ltd., Nottingham, UK). The ZEB HORIZON mobile scanner is able to scan objects up to a distance of 100 m from the scanning device using the time-of-flight principle and SLAM (simultaneous localization and mapping) technology (e.g., [34]). As a data collector, Velodyne VLP-16 multibeam LiDAR is embedded in the device. The wavelength of the laser was 903 nm, the scan rate was 300,000 points per second and the range noise was $\pm 30\text{ mm}$ with expected system accuracies of 1–3 cm. Each scan followed the same predefined scanning procedure.

First, the specific areas (beech and spruce) were only scanned from the ground, following a predefined walking pattern (Figure 2a), further referred to as the “ground scan”. For the second scan, the same walking path was used as for the first scan (with otherwise identical conditions) but was then complemented by a canopy scan. To do this, the scanner was attached to the crane and moved up vertically over the top of the canopy (Figure 1) while operating. The crane was then set in motion horizontally by turning it clockwise and moving the scanner along the horizontal crane axis. This allowed the area to be scanned from above and below within one single scan (Figure 2b). This scan is further referred to as the “full scan”. The starting point of the scans was always the same. In total, 8 different scans were performed (2 plots (beech and spruce), 2 conditions (ground scan and full scan) and 2 seasons (summer and winter)). The scans were performed under optimal weather conditions (no wind, fog, rain, or frost).

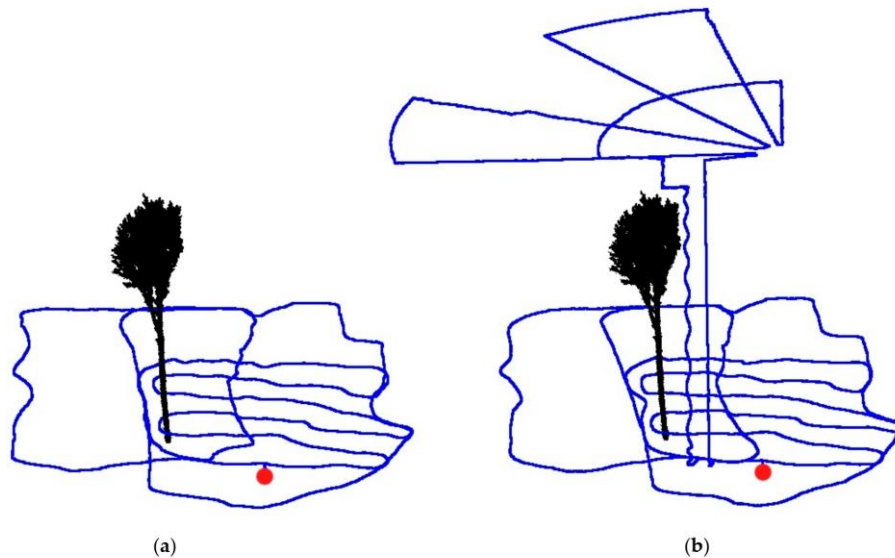


Figure 2. The walking paths (blue lines) for the beech plot for the two scan conditions, (a) ground scan and (b) full scan. The red dot indicates the same starting point in each scan. The walking path on the ground is identical. A beech tree is shown as an example for better orientation.

2.3. Data Processing

The data collected by the mobile laser scanner were first processed using the manufacturer-specific software GeoSLAM HUB 6.1 [35], which means that actual SLAM registration was performed. This was carried out with the default software configuration, turning off any additional sharpening or filtering. After preprocessing, the individual scans were exported in the .laz file format. The R package “lidR” [36] was used to further process the exported point clouds. The point clouds were clipped to the specific tree collective (area size 30 m × 40 m). Ground points were then classified using the Ground Segmentation Algorithm [37]. With the Spatial Interpolation Algorithm (interpolation is performed using a k-nearest neighbor approach with inverse-distance weighting), the heights of the points were normalized. To reduce the amount of data, the point cloud was initially voxelized to a resolution of 1 cm (representative voxel size of 1 cm³). To ensure that the point clouds of the different scans overlapped exactly, they were aligned using CloudCompare software (version 2.11.3, cloudcompare.org, EDF R&D, Paris, France).

From the remaining point cloud, the point clouds of 20 single trees per species and scan were identified. Trees were then pre-cut using the software LiDAR360 [38]. The tree segmentation algorithm used was developed based on the method described by Li et al. [39]. Each tree was manually postprocessed using Cloud Compare software for better quality. The full scan from winter was used as a reference for segmenting the same trees from the ground-based scans. By overlaying the single-tree point clouds, it was possible for each point to be assigned to the correct tree, even for scans that recorded very few points in the upper canopy.

From each single-tree point cloud, the following single-tree morphological variables were calculated: total tree height (tth), diameter at breast height (dbh), height of maximum crown projection area (hcpa), maximum crown projection area (cpa), crown volume (crvol) and crown surface area (csa). The dbh was determined using circular fitting (height range of 1.29–1.31 m) (R package “circular” [40]), and the height was obtained from the maximum z-value of each point cloud. The crown base was defined as the height where the horizontal

cross-section of the crown first reached five times the base area of the tree. The maximum crown projection area (cpa) and corresponding height (h_{cpa}) were calculated where a horizontal cross-section of 20 cm thickness reached its maximum value. The crown volume and crown surface area were computed using a convex hull around the remaining point cloud above the crown base (R package “geometry” [41]). All single-tree morphologies were calculated with a voxel size of 1 cm.

From each scan, we clipped six circular subplots with a radius of 5 m at identical points for stand structure analysis. For these subplots, we calculated the relative point counts in three-dimensional space, the Clark–Evans index and the box dimension, as described below. We calculated the change in the point counts with height relative to the respective maximum value (relative point counts). For this calculation, we cut 1 m thick horizontal slices from the point clouds and determined the number of points for each of them. For each height layer, the mean value for each of the 6 subplots was calculated. The largest mean value for the respective winter scans (ground scan and full scan) was defined as 100%, and all other values were calculated in relation to the largest value.

We used the aggregation index from Clark and Evans [42] to calculate the spatial description of the point distribution (CE index). The CE index is widely used to characterize forest structures, e.g., [26,27]. The CE index examines the horizontal distribution of objects for clumping or regularity. The calculated value theoretically ranges from 0 (strongest clumping, where all objects are at the same point) to 2.1491 (strictly regular hexagonal pattern). Aggregation values less than 1.0 indicate a tendency towards clumping, values around 1.0 indicate a random distribution, and values above 1.0 indicate a tendency towards a regular distribution. The calculation was performed with the R package “spatstat” [43]. Before the calculation, we projected the 1 m thick horizontal strata onto a plane by setting the z-value of each voxel to zero. Duplicate voxels were deleted. To avoid edge bias, Donnelly edge correction was applied [44,45].

The box dimension can be used as a measure of the structural complexity of forests [46] and is often used to differentiate different forest structures, e.g., [26,27]. It considers the density and three-dimensional distribution of objects at the same time. The box dimension was calculated based on specific subplot point clouds. We used the maximum tree height as the upper cut-off. The lower cut-off, which is the smallest box-edge length used in the box-dimension calculation, was defined as the respective voxel size tested (5–50 cm). We calculated the box dimensions for three horizontal forest strata of each 3D point cloud (1–12 m, 13–24 m and 25–36 m), as well as for the overall forest. Details on the box dimension can be found in Seidel [46] and Sarkar and Chaudhuri [47].

The relative point counts, the Clark–Evans index and the box dimension were derived for voxels of 5 cm (5 cm³), 10 cm (1 dm³), 20 cm (8 dm³) and 50 cm (125 dm³) edge lengths.

2.4. Data Analysis

To determine differences in the single-tree morphologies and metrics for the stand structure, we used the paired Wilcoxon rank-sum test with Bonferroni-corrected *p*-values, since the normal distribution and the homogeneity of variance could not be confirmed for all of the studied variables. The significance level of *p* < 0.05 was chosen for all statistical tests conducted in this study. All statistical procedures were performed using R 4.1.2 [48].

3. Results

3.1. Visual Assessment of Single-Tree Point Clouds

Clear morphological differences between the point clouds of spruce and beech could already be detected visually at the single-tree level (Figure 3a vs. Figure 3b). These differences were apparent between the ground scans and the full scans (Figure 3(1,2) vs. Figure 3(3,4)). The point clouds of the ground scans (Figure 3(3,4)) lose much detail in the upper parts of single-tree crowns. Additionally, the effects of seasonality could be detected visually to a certain extent for beech, obviously less so for spruce: for the full scans, Figure 3a(1) shows a smaller, more narrow crown appearance in the winter, when

there are no leaves, compared to the summer (Figure 3a(2)), when there are leaves on the tree. However, differences could also be detected between the seasons from the visual inspection of ground scans: when comparing Figure 3a(3,4), the point cloud density in the upper crown layer seems to decrease even more in summer compared to winter. Such differences could not be detected visually for spruce (Figure 3b(3,4)).

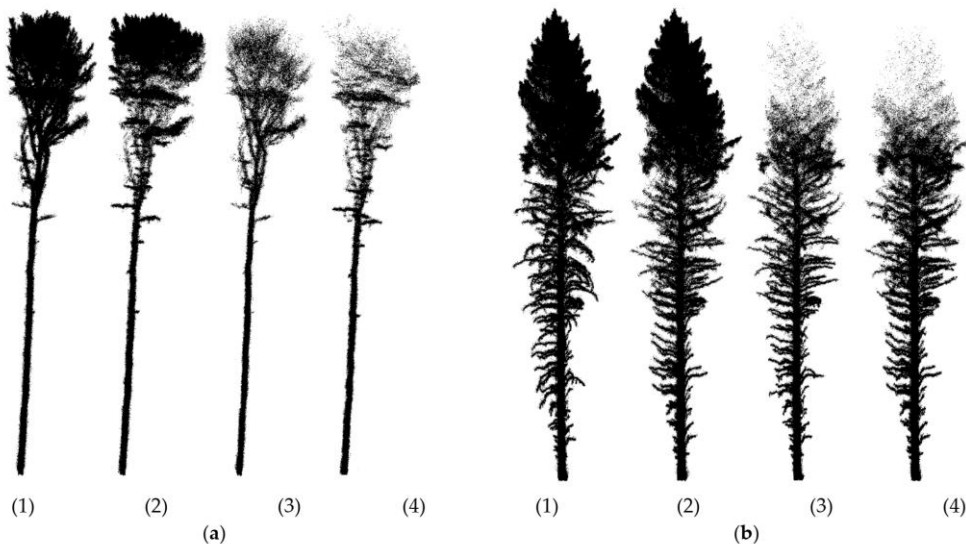


Figure 3. Single-tree point clouds resulting from different scanning times and methods. Figure (a) (1–4) shows the same beech, and figure (b) (1–4) shows the same spruce. The individual tree silhouettes were derived from the full scan in winter (1), full scan in summer (2), ground scan in winter (3), and ground scan in summer (4).

3.2. Seasonal Comparison

3.2.1. Single-Tree Morphologies (H1)

The seasonal comparison at the single-tree level only partly confirms the visual impressions of Figure 3, namely, that the single-tree morphologies in the respective scans differ depending on the season in which they were recorded (Figure 4). The overall differences were not very pronounced for the crown-related variables, which were derived from the part of the point clouds where the occlusion effect was most noticeable when scanning from the ground. Only the total tree height of beech trees was estimated to be slightly lower on average for the summer scans compared to the winter scans. Other crown-related variables were not significantly different for beech (hcpa, cpa, crvol, and csa, cf. Figure 4, Beech c–f). In addition to the total tree height, the dbh of beech trees was also significantly bigger in summer 2020 than in winter 2020/2021 (cf. Figure 4, Beech a; Table S1). We could also detect significant differences for spruce scans (bottom row in Figure 4) for the diameter at breast height, the maximum crown projection area, the crown volume and the crown surface area, which were all smaller on average in winter 2020/2021 than in summer 2020. No significant differences were found in the total tree height or the height of the maximum crown projection area. Table S1 shows the mean differences \pm standard deviations between ground scans in summer and ground scans in winter for both tree species and whether the difference is significant between the species.

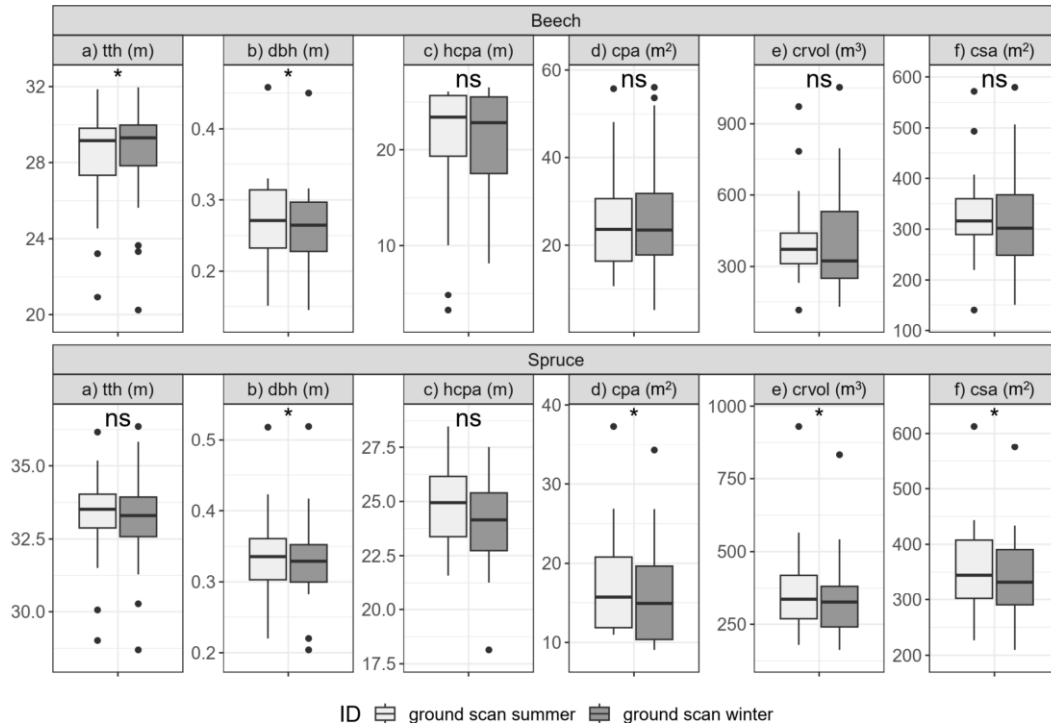


Figure 4. Seasonal comparison of single-tree morphologies of beech and spruce ($n = 20$ for each species). Shown are the total tree height (tth) (a), diameter at breast height (dbh) (b), height of maximum crown projection area (hcpa) (c), maximum crown projection area (cpa) (d), crown volume (crvol) (e) and crown surface area (csa) (f) for ground scans conducted in winter and summer. Asterisks indicate significant differences between scans (*: $p \leq 0.05$; ns: $p > 0.05$).

3.2.2. Stand Structure (H2)

Pronounced seasonal differences in stand structural complexity could be found for whole stands when comparing the winter and summer ground scans (Figure 5). The box dimension was significantly influenced by the seasonal effect. Across all height ranges of the point clouds, the values of the box dimension differed significantly. In addition, there were also species-specific differences. While the box dimension of spruce (Figure 5, bottom row) was always larger in summer than in winter, the picture was slightly different for beech (Figure 5, upper row). For beech, the box-dimension values from the winter ground scans were larger for the highest point cloud layer (25–36 m) compared to the summer ground scans. The largest values for the box dimension were found in the medium height range of 13–24 m for the stands of both species. The differences in the box dimension at resolutions of 10, 20 and 50 cm are shown in Figure S1. At these resolutions, the same trends seen at the 5 cm resolution are observed. However, these are not that pronounced. In particular, for beech, the pronounced difference in the 25–36 m height range at a 5 cm resolution becomes progressively smaller with reduced resolution.

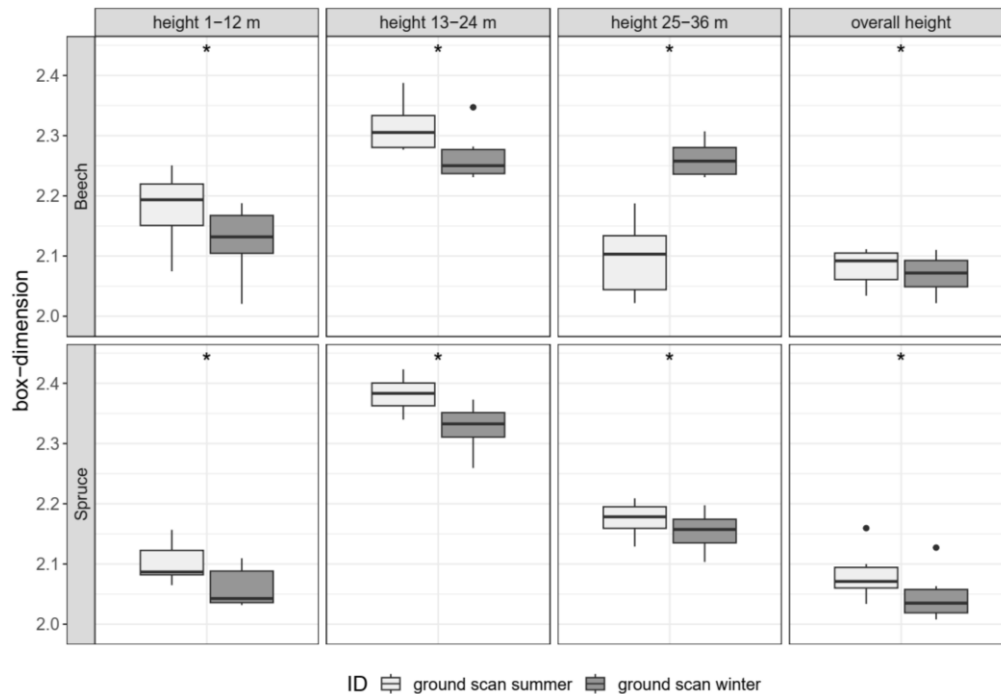


Figure 5. Seasonal comparison of different point cloud sections for the beech and spruce stands across the winter and summer ground scans. The boxplots are based on six circular subplots, each with a radius of 5 m. Shown are the box dimensions for point cloud sections of 1–12 m, 13–24 m and 25–36 m and the total point cloud. Asterisks indicate significant differences between the scans (*: $p \leq 0.05$). The resolution of the point cloud was 5 cm.

3.3. Methodological Comparison

3.3.1. Single-Tree Morphologies (H3)

The methodological comparison of the two scanning methods (ground scan and full scan) in winter, the optimal scanning season, shows differences in the single-tree morphologies (Figure 6). The resulting total tree height was lower on average when scanning from the ground (Figure 6, left column) for both tree species. The effect was more pronounced for spruce than for beech (Table 1). The same is true for the crown surface area. Furthermore, for beech, the derived diameter at breast height was smaller and the crown volume was larger for the ground scans compared to the full scans (Table 1). For spruce, significant differences were especially found in the height of the maximum crown projection area and the maximum crown projection area itself (Figure 6, Spruce(c,d)).

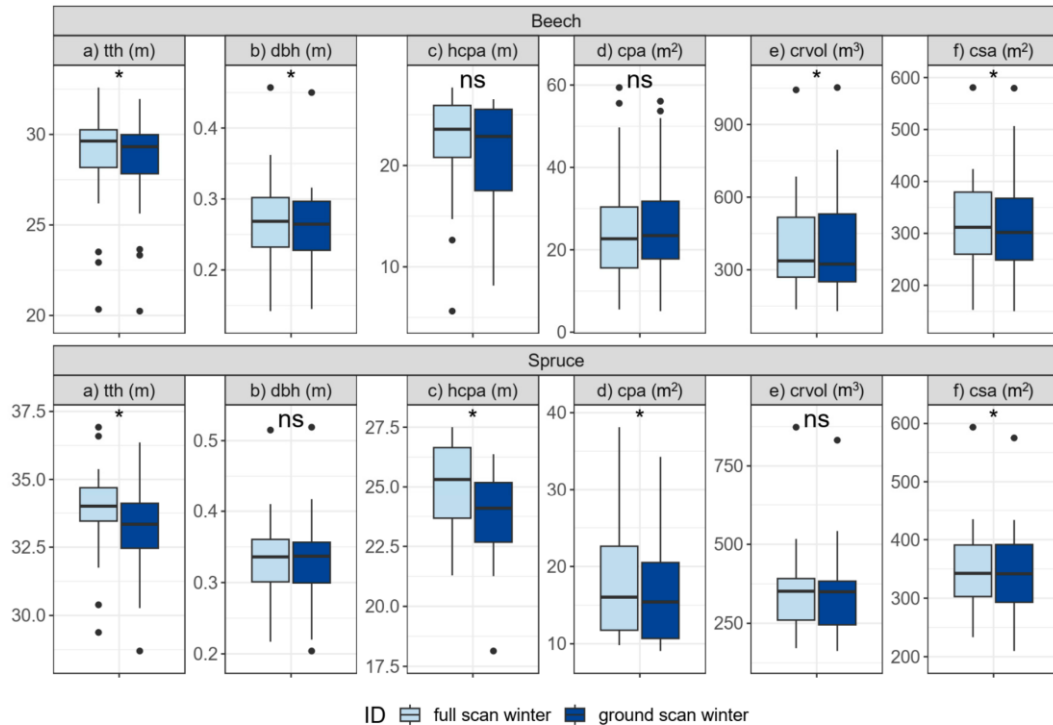


Figure 6. Methodological comparison between the ground scans and full scans conducted in winter of the single-tree morphologies of beech and spruce ($n = 20$ for each species). Shown are the total tree height (tth) (a), diameter at breast height (dbh) (b), height of maximum crown projection area (hcpa) (c), maximum crown projection area (cpa) (d), crown volume (crvol) (e) and crown surface area (csa) (f) for both winter scans. Asterisks indicate significant differences between the scans (*: $p \leq 0.05$; ns: $p > 0.05$).

Table 1. Mean difference \pm standard deviation between the full scan in winter and the ground scan in winter for beech and spruce ($n = 20$ for each species). The data are presented in absolute (abs.) and relative values (rel. in %). Listed are the single-tree morphological variables total tree height (tth), diameter at breast height (dbh), height of maximum crown projection area (hcpa), maximum crown projection area (cpa), crown volume (crvol) and crown surface area (csa). The p-value indicates whether the difference is significant between beech and spruce.

	Beech (abs.)	Beech (rel.)	Spruce (abs.)	Spruce (rel.)	p-Value
tth (m)	-0.30 ± 0.34	-1.04 ± 1.20	-0.74 ± 0.45	-2.19 ± 1.34	0.001
dbh (m)	-0.01 ± 0.01	-3.35 ± 5.02	0.00 ± 0.01	-0.18 ± 2.42	0.025
hcpa (m)	-0.88 ± 2.78	-4.00 ± 12.68	-1.24 ± 2.41	-4.94 ± 9.58	0.685
cpa (m ²)	$+0.43 \pm 5.68$	$+1.59 \pm 21.16$	-1.12 ± 1.44	-6.42 ± 8.23	0.602
crvol (m ³)	$+4.85 \pm 103.09$	$+1.22 \pm 26.00$	-3.88 ± 17.47	-1.11 ± 4.98	0.052
csa (m ²)	-2.31 ± 41.29	-0.73 ± 12.98	-5.97 ± 13.31	-1.72 ± 3.84	0.445

When analyzing the differences in the morphological variables of both species, they were surprisingly similar (Table 1). However, besides the dbh, one especially significant difference could be found between the species: namely, the total tree height underestimation for spruce was more pronounced than that for beech. For all other variables, the p-value is above the significance level of 0.05, and the effect size is hence in a similar range for both species.

3.3.2. Stand structure (H4)

The methodological comparison at the stand level shows that the values of the box dimension were larger in the full scan compared to the ground scan for both tree species (Figure 7). The values in the lower two height ranges for both tree species were close together (1–12 m and 13–24 m) (first two columns in Figure 7). However, the differences were clearly greater in the upper height range of 25–36 m, where a lot of information on the structural complexity is lost. Here, the full scans result in a significantly higher box dimension, with the effect being slightly larger for spruce than for beech. Additionally, for the full point clouds, the box dimension is significantly larger for the full scans compared to the ground scans (last column in Figure 7).

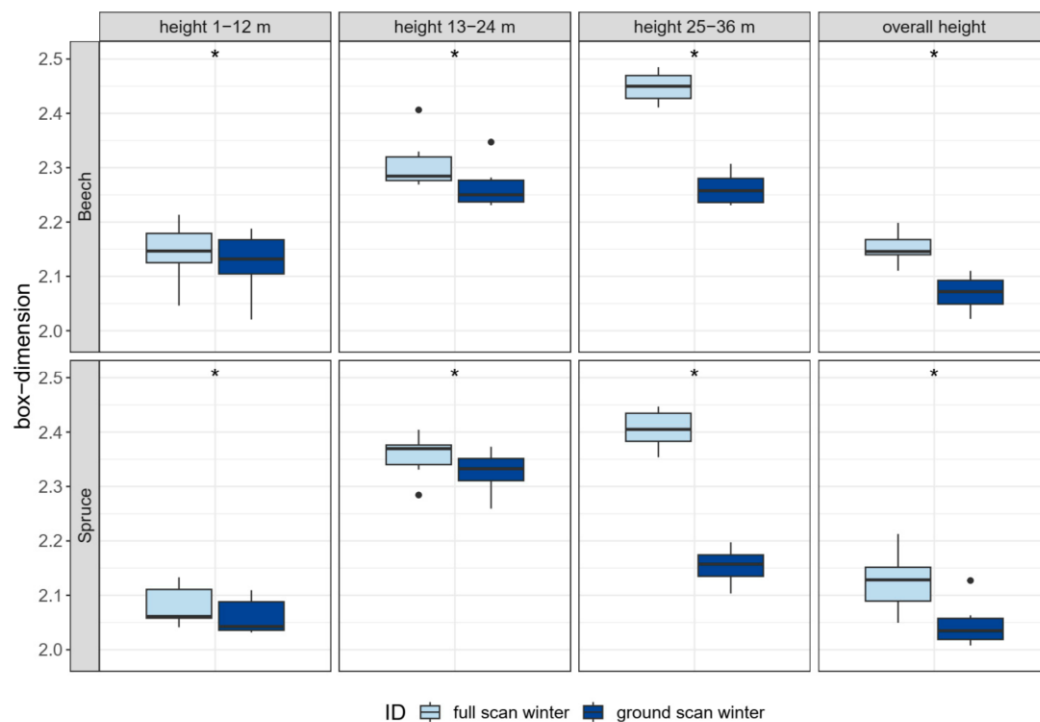


Figure 7. Methodological comparison of different point cloud sections for the beech and spruce stands between the ground scans and full scans conducted in winter. The boxplots are based on six circular subplots, each with a radius of 5 m. Shown are the box dimensions for point cloud sections of 1–12 m, 13–24 m and 25–36 m and the total point cloud. Asterisks indicate significant differences between the scans (*: $p \leq 0.05$). The resolution of the point cloud was 5 cm.

An analysis of the relative point counts with height also showed that significantly fewer points were recorded over almost the entire height spectrum when scanning from the

ground compared to the full scan (Figure 8a,b). The difference was particularly apparent in the crown regions of the stands for both tree species. At heights where the maximum number of points (100%) for the full scans were recorded (27 m for beech and 28 m for spruce), they only accounted for 16% for beech and 8% for spruce on a relative scale at the corresponding heights. The heights at which the maximum number of points were reached were lower in the ground scans than in the full scans for beech and spruce.

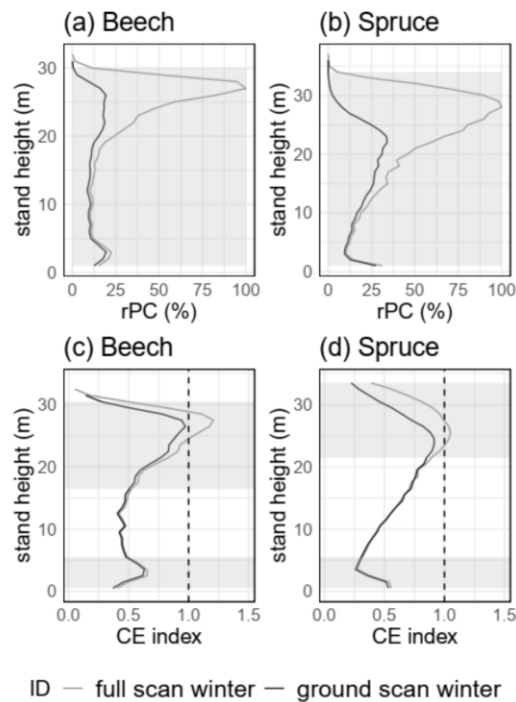


Figure 8. Methodical comparison between the ground scans and full scans conducted in winter for relative point counts (rPC) (a,b) and CE indices (c,d) over the height range. The black curve shows the counts for the ground scan, and the gray curve shows those for the full scan. The curves are based on six circular subplots, each with a radius of 5 m. Shaded in gray is the height range in which the scans differ significantly from each other. The resolution of the point clouds was 5 cm.

Similar trends were found for the CE index, but the trends were more consistent (Figure 8c,d). The CE values for both tree species were highest in the crown area, indicating that the points were more regularly distributed in space there. When comparing the ground scans to the full scans, the scans in the lower height range hardly differ from each other. For the higher parts of the stand, the CE values diverge. For the full scans, the regularity in the distribution pattern further increased in the higher canopy layers (gray lines in Figure 8c,d). The difference starts to become significant at a height of 17 m for beech, (Figure 8c) and at 22 m for spruce (Figure 8d). Additionally, for the ground scans, the CE index for both tree species remains below 1.0 over the entire height range.

3.3.3. Spatial Resolution (H5)

The observed loss of information in the ground scan point clouds (e.g., Figures 7 and 8) decreases with decreasing spatial resolution, i.e., with increasing voxel size. In Figure 9, this is exemplified by the relative point counts. When increasing the voxel size from 5 cm

to 50 cm, the trend lines of the ground and full scans become increasingly similar; i.e., for a voxel size of 5 cm, the number of points in the canopy was underestimated, which becomes less and less pronounced from 10 cm voxels through 20 cm voxels to 50 cm voxels. This was true for both tree species. However, even at 50 cm voxels, significant differences in the canopy range remain between the point counts of the ground scans and full scans.

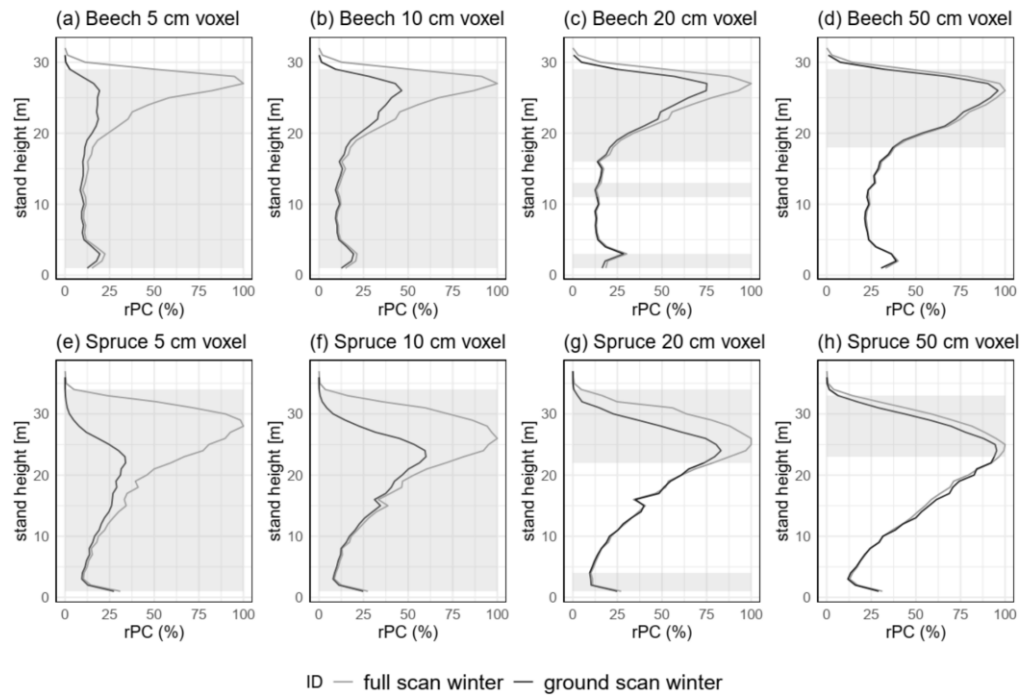


Figure 9. The relative point counts (rPC) with height for beech (a–d) and spruce (e–h) stands for the ground and full scans from winter. The black curve shows the relative counts over the height range for the ground scans, and the gray curve shows those for the full scans. The curves are based on six circular subplots, each with a radius of 5 m. Shaded in gray is the height range in which the scans differ significantly from each other.

For changing resolutions, the CE index (Figure 10) shows a similar picture to rPC (Figure 9), namely, that an increasing voxel size decreases the divergence between the trend lines of the ground and full scans. However, the initial differences between the CE values were not as pronounced to start out with, meaning that the CE values point in a very similar direction, even at a voxel resolution of 5 cm. In addition, the CE index values generally increase in each height section with increasing voxel size. The arrangement of voxels in space becomes more and more regular due to the effect of increasing the voxel size. The height threshold, above which the tendency towards a regular distribution is indicated, shifts slightly downward with decreasing spatial resolution. At the same time, the maxima of the respective curves shift upward (Figure 10a–d). For spruce, it was similar (Figure 10e–h).

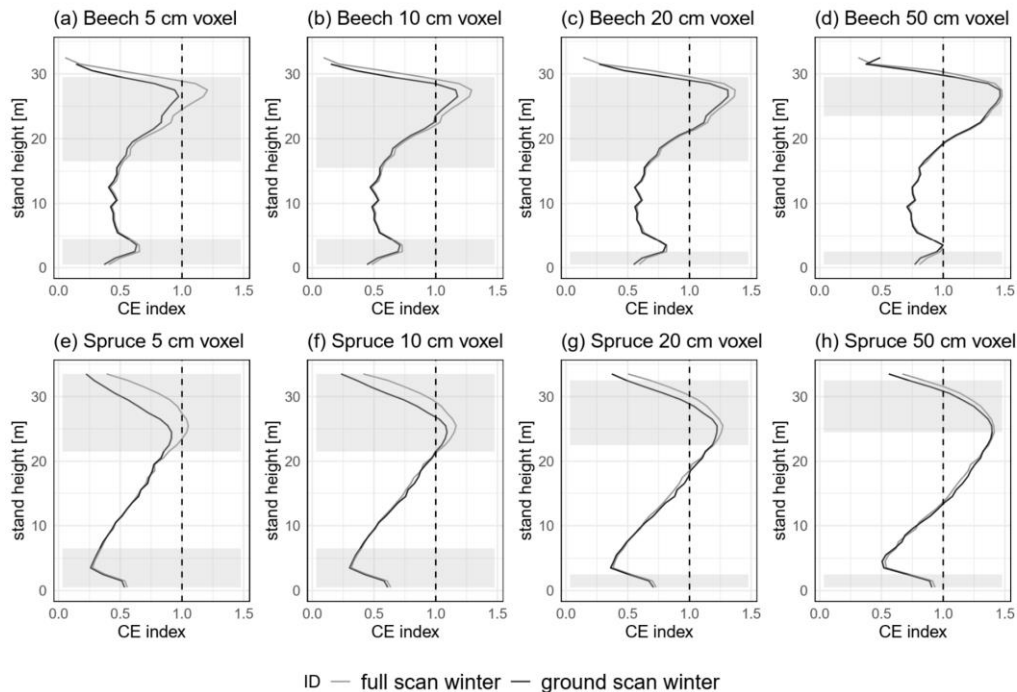


Figure 10. CE indices for beech (a–d) and spruce (e–h) stands for the ground and full scans from winter over the height range. The black curve shows the plot for the ground scan, and the gray curve shows the plot for the full scan. The curves are based on six circular subplots, each with a radius of 5 m. Shaded in gray is the height range in which the scans differ significantly from each other.

The differences in the box dimension at resolutions of 10, 20 and 50 cm are presented in Figure S2. With a lower resolution, the same trends seen with the 5 cm resolution are observed. However, the significance range differs and is generally not as pronounced.

4. Discussion

4.1. Seasonal Comparison

In the seasonal comparison (summer and winter), occlusion effects could be detected in the data for single trees and whole stands (Figures 3–5), as assumed with H1 and H2. The tree heights of beech were especially affected by the time of scanning (Figure 4 and Table S1). They were lower for beech in summer, most likely because the dense canopies of beech trees prevented sufficient laser beams from reaching the top sections of the trees on average. Beech is a tree species with high crown plasticity [49]. As a result, beech forms a dense canopy and develops many green leaves in the lower part of the stem during the vegetation period due to its higher shade tolerance, e.g., [50]. Spruce also forms dense canopies but loses its needles in lower stem sections under dense stand conditions due to the lack of light [25,51]. For beech, the greater photosynthetically active mass in the lower canopy results in a greater reduction in the laser beam compared to spruce.

However, we could not detect any differences in the other crown morphological variables of beech (hcpa, cpa, crvol and csa). Here, we would have expected larger deviations, because the ground scan in summer was strongly thinned out in the upper crown area, and the crown architectures were no longer easily recognizable. An explanation for why

no differences appeared could be that the full scans from winter were available as orientations when the trees were manually cut out from the point cloud. With the full scan from winter, the points could be assigned to the correct tree. However, the upper crown area was still only very sparsely populated with points, and without the full winter scan reference, it would have been unclear which tree they belong to. However, overall, the three-dimensional space of the single-tree point cloud was occupied in such a way (cf. Figure 3a(4)) that the algorithms used calculated very similar single-tree morphologies, although the occlusion was pronounced.

We did not expect any differences for spruce, because growth was already complete when the summer scan was performed at the end of August 2020, and the winter scan was performed before the start of the 2021 growing season. So, no major growth should have taken place between the summer and winter scans. Initially, we could not detect such differences visually since this species does not shed its needles in winter (Figure 3b(3,4)). However, the results show that even more single-tree morphological variables differ from each other than for beech (Figure 4). This could indicate that the noise of the laser scanner in combination with the algorithm used to calculate the metrics affect the morphologies of the individual trees in such a way that even two identical scans in a row result in slightly different values. The differences are small, but still significant (Figure 4 and Table S1). MLS scans are known for their comparatively high level of noise [52]. The accuracy of MLS scans at a distance of 5 meters is about 20 times lower than those produced by TLS [53]. The range noise (noise along an axis perpendicular to the target) of the device used in this study is estimated to be around ± 30 mm, according to the manufacturer [54]. Trzeciak and Brilakis [53] found that the range noise of the ZEB Horizon scanner was 40–50 mm at 40 meters. Based on these numbers, the scanner has an error of approx. $\pm 0.1\%$ (4/4000 cm). The deviations we observed for the dbh measurement, for which we can exclude an occlusion effect, are on average 3.08% for beech and 1.04% for spruce in the seasonal comparison (Table S1) (methodological comparison: beech: 3.35%; spruce 0.18% (Table 1)). The deviations we determined are therefore larger than the specified range noise from Trzeciak and Brilakis [53] and are more in line with the findings of Hunčaga et al. [55] according to which the dbh could be determined with a maximum error of up to 4 cm.

At the stand level (Figure 5), the values of the box dimension (>2) for each season are within a plausible range for both tree species, e.g., [27,56,57]. Depending on the season (winter or summer), we found different values of the box dimension in both tree species. In the case of beech, this could be due to the foliage. It is also conceivable that environmental influences such as slight leaf shaking, which cannot be avoided, even when there is no wind, could additionally amplify the noise. Neudam et al. [20] and Guzmán et al. [58] also concluded that leaf-bearing trees produce more scattered point clouds than leafless trees. At the stand level, occlusion is particularly evident in the canopy layer of beech trees (Figure 5). The crown architecture is only captured to a limited extent in the summer scan, which is reflected by smaller values for the box dimension in the height range from 26 to 36 m (Figure 5, third column above). For the total stand (overall height), the values from the summer scan are, however, larger than those from the winter scan, which is consistent with the findings of previous studies, for example, by Neudam et al. [20]. Seasonal differences in the box dimension of spruce were not expected. We can only explain the deviations in our data as noise in the point cloud.

In summary, we found differences in single-tree morphologies and stand complexity for beech. However, contrary to our expectations, we also found such differences for spruce. Thus, we have to reject hypotheses H1 and H2.

4.2. Methodological Comparison

4.2.1. Single-Tree Morphologies

The comparison between the ground and full scans resulted in lower heights for both tree species when scanned only from the ground, as assumed in H3. This is most likely due to the more strongly pronounced occlusion effects of the crown in the ground scans

(Figure 6a). The laser beams are blocked by the biomass, which means that the upper canopy sections are not fully detected. The very large number of laser beams was not sufficient to determine the same height in the ground and full scans for beech in winter conditions. In the case of spruce, as an evergreen tree species, this difference is greater than in the case of beech. Besides the evergreen condition of spruce, its pyramidal crown could play a role in this finding. In a dense stand, this crown shape makes it very difficult to detect the top of it. In the study area, the density of the trees was also very high (639–926 trees per hectare, standing stem volume of 802–981 m³·ha⁻¹). The visibility of the crown is therefore limited for the laser beams.

We expected the canopy morphologies from the ground scans to be smaller than those from the full scans because of the occlusion. In addition to some height values, this was also true for the height of the maximum crown projection area, maximum crown projection area and crown surface area for spruce. For beech, this was only true for the crown surface area. The crown volume, in contrast, was greater when scanning only from the ground. As with the seasonal comparison, we attribute this result, on the one hand, to the noise of MLS and, on the other hand, to the methods we used to calculate the tree canopy morphologies. For example, the convex hull method spans a relatively large hull around the crown. This in itself can result in relatively large changes in the derived quantities due to only a few differences in points in the point clouds [59], specifically for the crown volume. In combination with the noise, we therefore explain the differences as originating from this.

To what extent the deviations determined in this study are relevant for future studies depends on the research question and its accuracy requirements. Especially since traditional methods, such as vertex height measurements, are also associated with uncertainties [60], which can sometimes be larger, the MLS technique seems to nevertheless be a very suitable tool for determining single-tree morphologies. Overall, the differences in the single-tree morphologies were small, even though they were partly significant. Occlusion effects led to a systematic underestimation only for height, in the range of 1.04% for beech and 2.19% for spruce, regarding the methodological comparison.

4.2.2. Stand Structure

At the level of the stand structure, the methodological comparison for both tree species shows that the biomass in the canopy is not captured as well when scanning only from the ground (Figures 7 and 8). This is reflected by lower proportions of points detected and by lower values for the CE index and the box dimension, especially in the canopy, as we postulated with Hypothesis 4. This is in line with our expectations that the reduced number of laser beams reaching the top canopy layers because of occlusion results in underestimations in this vertical range of the stands. There are also differences in the lower range, although both scans were performed in a direct temporal sequence (both scans were performed within one hour under the same weather conditions). Again, this must be attributed to inevitable noise in the data, e.g., during the SLAM processing itself, due to small wind gusts, etc. In the full scan, each object in the forest stand is scanned from far more different perspectives and distances than in the ground scan. Trzeciak and Brilakis [53] found that edges and corners become less and less recognizable as the distance to the object increases. In the full scan, the additional view from above likely led to increased blurring in object recognition during the SLAM procedure, and as a result, the noise in the full scans increased.

In summary, since not all canopy-related single-tree morphological variables were smaller when only scanning from the ground, we must reject Hypothesis H3. Hypothesis H4, on the other hand, can be accepted, since the ground scans underestimated the upper canopy layers, which significantly affected the stand structural variables.

4.2.3. Spatial Resolution

The problem of losing information in the upper canopy layers and underestimating these ranges could be overcome by increasing the voxel size, as we have assumed with Hypothesis 5 (Figures 9 and 10). As the voxel size increases, the differences between the data sets (ground scan and full scan) decrease. However, even at a point cloud resolution of 50 cm, some of the differences remain in the point clouds between the full and ground scans. These were more pronounced for the relative point counts than the CE index. However, for the CE index, a reduction in spatial resolution resulted in larger values per height level. As a consequence, for example, when comparing the 5 and 20 cm resolution values for the CE index, the differences can reach orders of magnitude, which corresponds to the findings described in other studies between different forest types, e.g., in studies by Stiers et al. [26] and Willim et al. [27]. This underlines the importance of considering the spatial resolution of point clouds when comparing stand structural variables, whereby the characteristics and trends of the respective curves (e.g., the number of maxima and minima of each curve) are mainly maintained, which is again elementary for characterizing the structure of a stand. The choice of spatial resolution here resembles a typical trade-off system. To us, a voxel size of 20 cm seems to be an appropriate size to reduce the effect that occlusion has on the data and still provide enough detail at the forest stand level. The same conclusion was also made by Heidenreich and Seidel [21].

To compensate for the occlusion effect, one could introduce a correction factor across the vertical range of the stand. For studies where a high level of detail is required, it might be useful to combine MLS ground scans with drone scans to mimic the full-scan approach used here. Once the occlusion is determined for a stand type, it could be minimized with correction factors for other ground scans in similar stands. When transferring the results of this work to other forests, it should be considered that the performance of scanning devices depends on the environment, particularly illumination conditions, with sunlight reducing the scanner range [61,62].

Hypothesis H5 (occlusion is reduced as the resolution of the data decreases) can be accepted, since a reduction in the point cloud resolution also reduced the effect of occlusion on stand structural variables (i.e., box dimension, relative point counts and CE index). However, reducing the point cloud resolution also changed the range of the stand structural variables, which needs to be considered when changing the point cloud resolution.

5. Conclusions

By using a crane to produce full scans, we were able to quantify the occlusion effect, apparent in every ground scan, in more detail. The effect was pronounced in the canopy range of the stands. For single-tree morphologies, occlusion plays a role, especially when extracting single-tree point clouds from the entire point cloud. With only a single scan from below, beech trees could not be extracted accurately and comparably. The noise of the laser scanner in combination with the algorithms used to calculate the metrics affected the morphologies of the individual trees. Overall, we could not detect very pronounced differences in the crown-related variables. It is the nature of these variables that they are derived from the parts of point clouds where the occlusion effect is most noticeable when scanning from the ground. However, here, occlusion effects led to a systematic underestimation only for height, in the range of 1.04% for beech and 2.19% for spruce, regarding the methodological comparison.

At the stand level, a significant amount of point information was lost in the canopy range when scanning from the ground alone. Increasing the voxel size can compensate for this loss of information but comes with the trade-off of losing details in the point clouds. From our analysis, we conclude that the voxelization of the point clouds prior to the extraction of stand-specific variables with a voxel size of 20 cm can be appropriate to reduce occlusion effects while still providing enough detail.

The quantification of the information loss in this study could be a basis for future ground scans to be adjusted for the occlusion effect. We hope this paper will increase

the awareness of the occlusion effect of MLS and open the door for further research and improvements in this area.

Supplementary Materials: The following supporting information can be downloaded at: <https://www.mdpi.com/article/10.3390/rs15020450/s1>, Table S1: Mean difference \pm standard deviation between the ground scan in winter and the ground scan in summer for beech and spruce ($n = 20$ for each species). The data are presented in absolute (abs.) and relative values (rel. in %). Listed are the single-tree morphological variables total tree height (tth), diameter at breast height (dbh), height of maximum crown projection area (hcpa), maximum crown projection area (cpa), crown volume (crvol) and crown surface area (csa). The p-value indicates whether the difference is significant between beech and spruce. Figure S1: Seasonal comparison of different point cloud sections for the beech and spruce stands across the winter and summer ground scans depending on different spatial resolutions. The boxplots are based on six circular subplots, each with a radius of 5 m. Shown are the box dimensions for point cloud sections of 1–12 m, 13–24 m and 25–36 m and the total point cloud. Asterisks indicate significant differences between the scans (*: $p \leq 0.05$; ns: $p > 0.05$). Figure S2: Methodological comparison of different point cloud sections for the beech and spruce stands between the ground scans and the full scans conducted in winter depending on different spatial resolutions. The boxplots are based on six circular subplots, each with a radius of 5 m. Shown are the box dimensions for point cloud sections of 1–12 m, 13–24 m and 25–36 m and the total point cloud. Asterisks indicate significant differences between the scans (*: $p \leq 0.05$; ns: $p > 0.05$).

Author Contributions: T.M., D.S. and P.A. conceived the ideas for the study; T.M., D.S., H.P. and P.A. designed the methodology for the study; T.M., D.S. and P.A. analyzed the data; T.M. wrote the first draft of the manuscript; T.M., D.S., K.-H.H., H.P. and P.A. contributed to further versions of the manuscript. All authors have read and agreed to the published version of the manuscript.

Funding: This study was conducted in connection with the project “Effects of forest structures on the drought resilience of individual trees (W049)”, supported by the Bavarian State Ministry of Nutrition, Agriculture and Forestry.

Data Availability Statement: The data presented in this study are available on request from the corresponding author.

Acknowledgments: The research site is owned by the Bavarian State Forest Enterprise, which gave us free access and allowed the experimental setup, which we are grateful for. We thank the Bavarian State Ministry of Nutrition, Agriculture and Forestry for their support and trust. We would like to thank the entire KROOF team, especially Thorsten Grams (AG Ecophysiology for Plants, TUM). We thank Rudolf Harpaintner, Barbara Brunschweiger, Merve Mentese and Ranbir Chakraborty for their support in data preparation. We thank the three anonymous reviewers for their constructive comments on an earlier version of this manuscript.

Conflicts of Interest: The authors declare no conflict of interest.

References

- Seidel, D.; Beyer, F.; Hertel, D.; Fleck, S.; Leuschner, C. 3D-laser scanning: A non-destructive method for studying above-ground biomass and growth of juvenile trees. *Agric. For. Meteorol.* **2011**, *151*, 1305–1311. [[CrossRef](#)]
- Seidel, D.; Ammer, C.; Puettmann, K. Describing forest canopy gaps efficiently, accurately, and objectively: New prospects through the use of terrestrial laser scanning. *Agric. For. Meteorol.* **2015**, *213*, 23–32. [[CrossRef](#)]
- Bayer, D.; Seifert, S.; Pretzsch, H. Structural crown properties of Norway spruce (*Picea abies* [L.] Karst.) and European beech (*Fagus sylvatica* [L.]) in mixed versus pure stands revealed by terrestrial laser scanning. *Trees* **2013**, *27*, 1035–1047. [[CrossRef](#)]
- Pretzsch, H. *Grundlagen der Waldwachstumsforschung*; Springer: Berlin/Heidelberg, Germany, 2019; ISBN 978-3-662-58154-4.
- Newnham, G.J.; Armston, J.D.; Calders, K.; Disney, M.I.; Lovell, J.L.; Schaaf, C.B.; Strahler, A.H.; Danson, F.M. Terrestrial Laser Scanning for Plot-Scale Forest Measurement. *Curr. For. Rep.* **2015**, *1*, 239–251. [[CrossRef](#)]
- Gough, C.M.; Atkins, J.W.; Fahey, R.T.; Hardiman, B.S. High rates of primary production in structurally complex forests. *Ecology* **2019**, *100*, e02864. [[CrossRef](#)]
- Bauhus, J.; Forrester, D.I.; Gardiner, B.; Jactel, H.; Vallejo, R.; Pretzsch, H. Ecological Stability of Mixed-Species Forests. In *Mixed-Species Forests*; Springer: Berlin/Heidelberg, Germany, 2017; pp. 337–382.
- Bohn, F.J.; Huth, A. The importance of forest structure to biodiversity-productivity relationships. *R. Soc. Open Sci.* **2017**, *4*, 160521. [[CrossRef](#)]

9. Lelli, C.; Bruun, H.H.; Chiarucci, A.; Donati, D.; Frascaroli, F.; Fritz, Ö.; Goldberg, I.; Nascimbene, J.; Tøttrup, A.P.; Rahbek, C.; et al. Biodiversity response to forest structure and management: Comparing species richness, conservation relevant species and functional diversity as metrics in forest conservation. *For. Ecol. Manag.* **2019**, *432*, 707–717. [CrossRef]
10. Ehbrecht, M.; Schall, P.; Ammer, C.; Fischer, M.; Seidel, D. Effects of structural heterogeneity on the diurnal temperature range in temperate forest ecosystems. *For. Ecol. Manag.* **2019**, *432*, 860–867. [CrossRef]
11. Kovács, B.; Tinya, F.; Ódor, P. Stand structural drivers of microclimate in mature temperate mixed forests. *Agric. For. Meteorol.* **2017**, *234–235*, 11–21. [CrossRef]
12. Liang, X.; Kankare, V.; Hyypää, J.; Wang, Y.; Kukko, A.; Haggrén, H.; Yu, X.; Kaartinen, H.; Jaakkola, A.; Guan, F.; et al. Terrestrial laser scanning in forest inventories. *ISPRS J. Photogramm. Remote Sens.* **2016**, *115*, 63–77. [CrossRef]
13. Pretzsch, H.; Biber, P.; Uhl, E.; Dahlhausen, J.; Rötzer, T.; Caldentey, J.; Koike, T.; van Con, T.; Chavanne, A.; Seifert, T.; et al. Crown size and growing space requirement of common tree species in urban centres, parks, and forests. *Urban For. Urban Green.* **2015**, *14*, 466–479. [CrossRef]
14. Jacobs, M.; Rais, A.; Pretzsch, H. How drought stress becomes visible upon detecting tree shape using terrestrial laser scanning (TLS). *For. Ecol. Manag.* **2021**, *489*, 118975. [CrossRef]
15. Lee, B.-U.; Jeon, H.-G.; Im, S.; Kweon, I.S. Depth Completion with Deep Geometry and Context Guidance. In Proceedings of the 2019 International Conference on Robotics and Automation (ICRA), Montreal, QC, Canada, 20–24 May 2019; pp. 3281–3287, ISBN 978-1-5386-6027-0.
16. Lovell, J.L.; Jupp, D.; Newnham, G.J.; Culvenor, D.S. Measuring tree stem diameters using intensity profiles from ground-based scanning lidar from a fixed viewpoint. *ISPRS J. Photogramm. Remote Sens.* **2011**, *66*, 46–55. [CrossRef]
17. Dassot, M.; Constant, T.; Fournier, M. The use of terrestrial LiDAR technology in forest science: Application fields, benefits and challenges. *Ann. For. Sci.* **2011**, *68*, 959–974. [CrossRef]
18. Ryding, J.; Williams, E.; Smith, M.; Eichhorn, M. Assessing Handheld Mobile Laser Scanners for Forest Surveys. *Remote Sens.* **2015**, *7*, 1095–1111. [CrossRef]
19. Choi, H.; Song, Y. Comparing tree structures derived among airborne, terrestrial and mobile LiDAR systems in urban parks. *GIScience Remote Sens.* **2022**, *59*, 843–860. [CrossRef]
20. Neudam, L.; Annighöfer, P.; Seidel, D. Exploring the Potential of Mobile Laser Scanning to Quantify Forest Structural Complexity. *Front. Remote Sens.* **2022**, *3*, 861337. [CrossRef]
21. Heidenreich, M.G.; Seidel, D. Assessing Forest Vitality and Forest Structure Using 3D Data: A Case Study from the Hainich National Park, Germany. *Front. For. Glob. Chang.* **2022**, *5*, 121. [CrossRef]
22. Ehbrecht, M.; Schall, P.; Juchheim, J.; Ammer, C.; Seidel, D. Effective number of layers: A new measure for quantifying three-dimensional stand structure based on sampling with terrestrial LiDAR. *For. Ecol. Manag.* **2016**, *380*, 212–223. [CrossRef]
23. Abegg, M.; Kükenbrink, D.; Zell, J.; Schaepman, M.; Morsdorff, F. Terrestrial Laser Scanning for Forest Inventories—Tree Diameter Distribution and Scanner Location Impact on Occlusion. *Forests* **2017**, *8*, 184. [CrossRef]
24. Li, L.; Mu, X.; Soma, M.; Wan, P.; Qi, J.; Hu, R.; Zhang, W.; Tong, Y.; Yan, G. An Iterative-Mode Scan Design of Terrestrial Laser Scanning in Forests for Minimizing Occlusion Effects. *IEEE Trans. Geosci. Remote Sens.* **2021**, *59*, 3547–3566. [CrossRef]
25. Matyssek, R.; Fromm, J.; Rennenberg, H.; Roloff, A. *Biologie der Bäume: Von der Zelle zur Globalen Ebene*; Verlag Eugen Ulmer: Stuttgart, Germany, 2010; ISBN 9783825284503.
26. Stiers, M.; Annighöfer, P.; Seidel, D.; Willim, K.; Neudam, L.; Ammer, C. Quantifying the target state of forest stands managed with the continuous cover approach—revisiting Möller’s “Dauerwald” concept after 100 years. *Trees For. People* **2020**, *1*, 100004. [CrossRef]
27. Willim, K.; Stiers, M.; Annighöfer, P.; Ehbrecht, M.; Ammer, C.; Seidel, D. Spatial Patterns of Structural Complexity in Differently Managed and Unmanaged Beech-Dominated Forests in Central Europe. *Remote Sens.* **2020**, *12*, 1907. [CrossRef]
28. Bèland, M.; Widłowski, J.-L.; Fournier, R.A. A model for deriving voxel-level tree leaf area density estimates from ground-based LiDAR. *Environ. Model. Softw.* **2014**, *51*, 184–189. [CrossRef]
29. Pretzsch, H.; Rötzer, T.; Matyssek, R.; Grams, T.E.E.; Häberle, K.-H.; Pritsch, K.; Kerner, R.; Munch, J.-C. Mixed Norway spruce (*Picea abies* [L.] Karst) and European beech (*Fagus sylvatica* [L.] stands under drought: From reaction pattern to mechanism. *Trees* **2014**, *28*, 1305–1321. [CrossRef]
30. Pretzsch, H.; Bauerle, T.; Häberle, K.H.; Matyssek, R.; Schütze, G.; Rötzer, T. Tree diameter growth after root trenching in a mature mixed stand of Norway spruce (*Picea abies* [L.] Karst) and European beech (*Fagus sylvatica* [L.]). *Trees* **2016**, *30*, 1761–1773. [CrossRef]
31. Grams, T.E.E.; Hesse, B.D.; Gebhardt, T.; Weigl, F.; Rötzer, T.; Kovacs, B.; Hikino, K.; Hafner, B.D.; Brunn, M.; Bauerle, T.; et al. The KROOF experiment: Realization and efficacy of a recurrent drought experiment plus recovery in a beech/spruce forest. *Ecosphere* **2021**, *12*, e03399. [CrossRef]
32. Dritte Bundeswaldinventur—Ergebnisdatenbank. Available online: <https://bwi.info> (accessed on 19 June 2020).
33. Pretzsch, H.; Grams, T.; Häberle, K.H.; Pritsch, K.; Bauerle, T.; Rötzer, T. Growth and mortality of Norway spruce and European beech in monospecific and mixed-species stands under natural episodic and experimentally extended drought. Results of the KROOF throughfall exclusion experiment. *Trees* **2020**, *34*, 957–970. [CrossRef]
34. Bauwens, S.; Bartholomeus, H.; Calders, K.; Lejeune, P. Forest Inventory with Terrestrial LiDAR: A Comparison of Static and Hand-Held Mobile Laser Scanning. *Forests* **2016**, *7*, 127. [CrossRef]

35. GeoSLAM. *GeoSLAM Hub*; GeoSLAM: Nottingham, UK, 2020.
36. Roussel, J.-R.; Auty, D.; Coops, N.C.; Tompalski, P.; Goodbody, T.R.; Meador, A.S.; Bourdon, J.-F.; de Boissieu, F.; Achim, A. lidar: An R package for analysis of Airborne Laser Scanning (ALS) data. *Remote Sens. Environ.* **2020**, *251*, 112061. [[CrossRef](#)]
37. Zhang, W.; Qi, J.; Wan, P.; Wang, H.; Xie, D.; Wang, X.; Yan, G. An Easy-to-Use Airborne LiDAR Data Filtering Method Based on Cloth Simulation. *Remote Sens.* **2016**, *8*, 501. [[CrossRef](#)]
38. GreenValley International, Ltd. *LiDAR360 Software*; GreenValley International, Ltd.: Berkeley, CA, USA, 2019.
39. Li, W.; Guo, Q.; Jakubowski, M.K.; Kelly, M. A New Method for Segmenting Individual Trees from the Lidar Point Cloud. *Photogramm. Eng. Remote Sens.* **2012**, *78*, 75–84. [[CrossRef](#)]
40. Agostinelli, C.; Lund, U. R package Circular: Circular Statistics (Version 0.4-95). 2022. Available online: <https://r-forge.r-project.org/projects/circular/> (accessed on 18 December 2022).
41. Habel, K.; Grasman, R.; Gramacy, R.B.; Mozharovskiy, P.; Sterratt, D.C. *_geometry: Mesh Generation and Surface Tessellation_*. R Package Version 0.4.6.1. 2022. Available online: <https://CRAN.R-project.org/package=geometry> (accessed on 18 December 2022).
42. Clark, P.J.; Evans, F.C. Distance to nearest neighbour as a measure of spatial relationships in populations. *Ecology* **1954**, *35*, 445–453. [[CrossRef](#)]
43. Baddeley, A.; Turner, R. spatstat: An R Package for Analyzing Spatial Point Patterns. *J. Stat. Softw.* **2005**, *12*, 1–42. [[CrossRef](#)]
44. Donnelly, K. Simulation to determine the variance and edge-effect of total nearest neighbour distances. In *Simulation Methods in Archeology*; Hodder, I., Ed.; Cambridge Press: London, UK, 1978; pp. 91–95.
45. Pommerening, A.; Stoyan, D. Edge-correction needs in estimating indices of spatial forest structure. *Can. J. For. Res.* **2006**, *36*, 1723–1739. [[CrossRef](#)]
46. Seidel, D. A holistic approach to determine tree structural complexity based on laser scanning data and fractal analysis. *Ecol. Evol.* **2018**, *8*, 128–134. [[CrossRef](#)]
47. Sarkar, N.; Chaudhuri, B.B. An efficient differential box-counting approach to compute fractal dimension of image. *IEEE Trans. Syst. Man Cybern.* **1994**, *24*, 115–120. [[CrossRef](#)]
48. R Core Team. *R: A Language and Environment for Statistical Computing*; R Foundation for Statistical Computing: Vienna, Austria, 2022; Available online: <https://www.R-project.org/> (accessed on 18 December 2022).
49. Dieler, J.; Pretzsch, H. Morphological plasticity of European beech (*Fagus sylvatica* L.) in pure and mixed-species stands. *For. Ecol. Manag.* **2013**, *295*, 97–108. [[CrossRef](#)]
50. Masarovicová, E.; Štefančík, L. Some ecophysiological features in sun and shade leaves of tall beech trees. *Biol. Plant* **1990**, *32*, 374–387. [[CrossRef](#)]
51. Roloff, A.; Weisgerber, H.; Lang, U.M.; Stimm, B. (Eds.) *Enzyklopädie der Holzgewächse: Handbuch und Atlas der Dendrologie/Begründet von Peter Schütt*; Wiley-VCH: Weinheim, Germany, 2007; ISBN 9783527321414.
52. Hyypä, E.; Yu, X.; Kaartinen, H.; Hakala, T.; Kukko, A.; Vastaranta, M.; Hyypä, J. Comparison of Backpack, Handheld, Under-Canopy UAV, and Above-Canopy UAV Laser Scanning for Field Reference Data Collection in Boreal Forests. *Remote Sens.* **2020**, *12*, 3327. [[CrossRef](#)]
53. Trzeciak, M.; Brilakis, I. Comparison of accuracy and density of static and mobile laser scanners. In Proceedings of the 2021 European Conference on Computing in Construction, Ixia, Rhodes, Greece, 25–27 July 2021. [[CrossRef](#)]
54. GeoSLAM. *ZEB HORIZON User Guide V1.0*; GeoSLAM: Nottingham, UK, 2020.
55. Hunčaga, M.; Chudá, J.; Tomaščík, J.; Slámová, M.; Koreň, M.; Chudý, F. The Comparison of Stem Curve Accuracy Determined from Point Clouds Acquired by Different Terrestrial Remote Sensing Methods. *Remote Sens.* **2020**, *12*, 2739. [[CrossRef](#)]
56. Seidel, D.; Ehbrecht, M.; Annighöfer, P.; Ammer, C. From tree to stand-level structural complexity—Which properties make a forest stand complex? *Agric. For. Meteorol.* **2019**, *278*, 107699. [[CrossRef](#)]
57. Seidel, D.; Annighöfer, P.; Ehbrecht, M.; Magdon, P.; Wöllauer, S.; Ammer, C. Deriving Stand Structural Complexity from Airborne Laser Scanning Data—What Does It Tell Us about a Forest? *Remote Sens.* **2020**, *12*, 1854. [[CrossRef](#)]
58. Guzmán, Q.J.A.; Sharp, I.; Alencastro, F.; Sánchez-Azofeifa, G.A. On the relationship of fractal geometry and tree-stand metrics on point clouds derived from terrestrial laser scanning. *Methods Ecol. Evol.* **2020**, *11*, 1309–1318. [[CrossRef](#)]
59. Yan, Z.; Liu, R.; Cheng, L.; Zhou, X.; Ruan, X.; Xiao, Y. A Concave Hull Methodology for Calculating the Crown Volume of Individual Trees Based on Vehicle-Borne LiDAR Data. *Remote Sens.* **2019**, *11*, 623. [[CrossRef](#)]
60. Stereńczak, K.; Mielcarek, M.; Wertz, B.; Bronisz, K.; Zajączkowski, G.; Jagodziński, A.M.; Ochał, W.; Skorupski, M. Factors influencing the accuracy of ground-based tree-height measurements for major European tree species. *J. Environ. Manag.* **2019**, *231*, 1284–1292. [[CrossRef](#)]

61. Shan, T.; Englot, B. LeGO-LOAM: Lightweight and Ground-Optimized Lidar Odometry and Mapping on Variable Terrain. In Proceedings of the 2018 IEEE/RSJ International Conference on Intelligent Robots and Systems (IROS), Madrid, Spain, 1–5 October 2018; pp. 4758–4765, ISBN 978-1-5386-8094-0.
62. Zhang, J.; Singh, S. LOAM: Lidar Odometry and Mapping in Real-time. In *Robotics: Science and Systems X*; 2014; ISBN 9780992374709. Available online: https://www.ri.cmu.edu/pub_files/2014/7/ji_LidarMapping_RSS2014_v8.pdf (accessed on 18 December 2022).

Disclaimer/Publisher’s Note: The statements, opinions and data contained in all publications are solely those of the individual author(s) and contributor(s) and not of MDPI and/or the editor(s). MDPI and/or the editor(s) disclaim responsibility for any injury to people or property resulting from any ideas, methods, instructions or products referred to in the content.

12.2 Paper II

Note: Please note that this Paper is not open access.

Response to extreme events: do morphological differences affect the ability of beech (*Fagus sylvatica* L.) to resist drought stress?

Thomas Mathes^{1,*}, Dominik Seidel² and Peter Annighöfer¹

¹Professorship of Forest and Agroforest Systems, Technical University of Munich, Hans-Carl-v.-Carlowitz-Platz 2, D-85354 Freising, Germany

²Spatial Structures and Digitization of Forests, Faculty of Forest Sciences and Forest Ecology, University of Göttingen, Büsgenweg 1, D-37077 Göttingen, Germany

*Corresponding author E-mail: thomas.mathes@tum.de

Received 1 February 2022

Adaptive silvicultural approaches intend to develop forests that can cope with changing climatic conditions. Just recently, many parts of Germany experienced 3 years of summer drought in a row (2018–2020). This study analysed the effects of this event on beech (*Fagus sylvatica* L.) in two regions in northern Bavaria, Germany. For this purpose, 990 beech trees were studied on 240 plots in drought-stressed forests. We examined trees of different social position and different size. Their morphology (e.g. tree height, crown volume) was recorded by laser scanning, and drought stress was quantified by tree core sample analyses. In addition to increment analyses, the $\delta^{13}\text{C}$ signal was determined by year. Results show that the dominant tree collective was particularly affected by the drought. They still managed to perform well in 2018, but the radial growth decreased significantly in 2019 and 2020, partly resembling the performance values of subordinate trees. Subordinate trees, on the other hand, provide some consistency in growth during drought years. The drought was so severe that the effects of competition on tree growth began to disappear. The difference in growth of two geographically distinct study areas equalized due to drought. With continuing drought, increasing levels of the $\delta^{13}\text{C}$ signal were detected. Similar patterns at different $\delta^{13}\text{C}$ levels were found across the social positions of the trees. The influence of tree morphological variables on tree resistance to drought showed no clear pattern. Some trends could be found only by focusing on a data subset. We conclude that the intensity of the 2018–2020 drought event was so severe that many rules and drivers of forest ecology and forest dynamics (social position, morphology and competition) were overruled. The influence of morphological differences was shown to be very limited. The weakening of dominant trees could potentially be no longer linear and drought events like the one experienced in 2018–2020 have the potential of acting as tipping points for beech forests.

Introduction

European beech (*Fagus sylvatica* L.) is a widely distributed, ecologically and economically important tree species in central Europe (Ellenberg and Leuschner, 2010). Currently, the species' share in Germany is increasing because it is commonly used to convert conifer forests to mixed broadleaf forests (Thünen-Institut, 2012). However, beech is sensitive to summer droughts like those that recently occurred in central Europe in 2003 and 2018 (Jump *et al.*, 2006; Scharnweber *et al.*, 2011; Brandl *et al.*, 2020; Leuschner, 2020; Schuldt *et al.*, 2020; Maringer *et al.*, 2021; Del Martínez Castillo *et al.*, 2022).

The frequency and severity of droughts will most likely continue to increase in central Europe (Seidl *et al.*, 2017; IPCC, 2018; Hari *et al.*, 2020; Rakovec *et al.*, 2020). This implies major management challenges for many beech-dominated forests in central Europe.

Forest ecosystems in general are particularly vulnerable to extreme climate events due to their relatively slow natural adaptation rates (Allen *et al.*, 2010). During this slow adaptation process, extreme weather events – like temperature extremes – may increasingly become tipping points for the ecosystems (Barnosky *et al.*, 2012). A typical situation known to drive ecosystems towards tipping points is a situation where accelerating change caused by a positive feedback drives the system to a new state (van Nes *et al.*, 2016). Transferred to the beech forests, a tipping point could be defined as a non-reversible change of the species composition. To date, it is not clear whether tipping points preventing a long-term survival for beech as a species have already been reached in some areas in Germany. It also remains unclear to what extent silvicultural measures may help to increase the lifespan of beech-dominated stands to provide a time window to continue converting them to other species over time.

Handling Editor: Dr. Fabian Fassnacht

© The Author(s) 2023. Published by Oxford University Press on behalf of Institute of Chartered Foresters. All rights reserved. For permissions, please e-mail: journals.permissions@oup.com.

In this context, the question arises whether individuals in a stand are equally affected by drought events and if not, which individuals of a stand are more strongly affected than others. One important related variable is the social position of the trees within the stand. Allen *et al.* (2010) and McDowell *et al.* (2008) found that trees with an increased stand space and hence improved resource availability suffer less from drought mortality. Such trees can develop more extensive individual root systems over time, and thereby increase their ability to extract water from the soil during and after drought periods compared with trees in dense stands (Whitehead *et al.*, 1984; Aussenac and Granier, 1988). Diaconu *et al.* (2017) showed that beech trees with a lower social position in a stand are less resilient towards drought events. Similar results regarding the effect of thinning on drought tolerance indices have been presented by Sohn *et al.* (2016) who found that for broadleaves, thinning improved drought resistance.

On the other hand, the water demand of exposed trees increases due to an increased exposure to light and the accompanying transpiration rate (Anders *et al.*, 2006; McDowell *et al.*, 2006). The increased transpiration rates of large trees are related to higher hydraulic stresses in situations with limited water availability. This was often used as an explanation for their greater susceptibility to drought events (Zang *et al.*, 2012; Bennett *et al.*, 2015). Van der Maaten (2012) showed that dominant beech trees are particularly more sensitive to dry conditions compared with intermediate trees.

For understory trees, differing processes may apply. On the one side, in terms of social position, understory trees may appear less vigorous, but could benefit from the shade and microclimate under the canopy of the more dominant but exposed trees. Heat and drought may, for instance, reduce the growth of exposed tall trees in relation to small trees and lead to a more equal size distribution and a more homogeneous vertical structure of the stand (Grote *et al.*, 2016). On the other hand, these individuals are also competing with the dominant trees for the limited resources above- and belowground, and their lower social position could be a disadvantage and result in higher stress levels. Meyer *et al.* (2022) found a shift of tree mortality from suppressed to large tree individuals in response to the 2018/2019 drought. Lüttschwager and Jochheim (2020) conclude that thinning by removing understory trees should be employed to stabilize forests under drought conditions, because dominant trees have more water conservation behaviour and higher adaptability to drought compared with understory trees.

In this context, the role of tree metrics, like tree height, crown volume and leaf area index is discussed as possible allometric characteristics that relate to drought stress for trees (Dobbertin *et al.*, 2010; Adams *et al.*, 2015; Bennett *et al.*, 2015; Seidel *et al.*, 2016; Stovall *et al.*, 2019). For beech, however, there are not many studies in this regard. Tree metrics such as crown diameter, crown area and crown volume could relate to the level of drought stress for various reasons. A larger crown volume, for example, is coupled with a larger leaf mass and consequently with higher transpiration. Variables describing the growth shape of the tree, such as the height to diameter ratio (H/D ratio) or the box-dimension, a measure of structural complexity of the trees (Seidel, 2018) could also be relevant for drought susceptibility. The impact of the soil is also discussed. Weber *et al.* (2013) conclude that beech trees near their dry distribution limit of the species are adapted

to extreme conditions already, while changes in the growth patterns of beech under mesic conditions have to be expected.

In this study, we focused on analysing the effects of drought stress on the growth of individual beech trees. We recorded their social position, structure (diameter, tree height, crown diameter, crown volume and position) and competitive environment using a mobile laser scanner (MLS). We combined this with retrospective analysis techniques targeted towards tree growth. In addition to an increment analysis, we determined the $\delta^{13}\text{C}$ signal of single year rings. The $\delta^{13}\text{C}$ values of year rings have been reported to show drought signals more precisely than tree-ring width alone (Andreu *et al.*, 2008).

The hypotheses of this study address the effects of drought on radial growth (H1), as well as the effects on the $\delta^{13}\text{C}$ signal (H2). Furthermore, we shed light on how morphological differences affect resistance to drought (H3) and whether these effects can be influenced by the management of competition (H4). The specific hypotheses were:

H1.1: The radial growth reaction of beech trees to drought stress depends on their social position.

H1.2: Trees that are accustomed to a warm and dry climate, as well as shallow sites, do not react as strongly to drought events in their radial growth.

H2: The drought-related $\delta^{13}\text{C}$ signal differs between different social positions.

H3: Morphological differences affect resistance to drought indicated by: (1) impact on tree-ring growth and (2) differences in stable carbon isotope signatures.

H4: A lower competitive environment mitigates adverse drought effects.

Materials and methods

Study area

This study was conducted on two sites, referred to as the 'Plateau' and 'Steigerwald'. Both sites were located in two beech-dominated (*F. sylvatica* L.) forest areas in southern Germany (northern Bavaria) (Figure 1).

The first study area, near Würzburg on the Southern Franconian Plateau ('Plateau'), is a low-lying plateau landscape (LWF, 2005). For the reference period 1991–2020, the area has been characterized by a warm dry climate with an average annual temperature of around 10.1°C and an annual average precipitation of 576 mm (cf. Table 1) (DWD, 2022a, b).

According to the World Reference Base for Soil Resources (WRB) (FAO, 2014), the soils of the Plateau are classified as Entic Leptic Cambisol (Clayic) with tendency to Rendzic Leptic Phaeozem (Clayic). These soils are comparably shallow, formed from carbonate-rich parent material (shell-bearing limestone). Their water holding capacity is relatively small, which is why they are classified as moderately dry to moderately fresh (German Soil Classification Working Group (Arbeitskreis Standortkartierung, 2016)). The potential natural vegetation of the Plateau is predominantly Hordelymo-Fagetum and Galio odorati-Fagetum (Walentowski, 2006).

The second study area rises steeply from the flat undulating landscape of the Plateau and is near Bamberg in the Steigerwald region ('Steigerwald'). The region is cooler (8.6°C) and has a

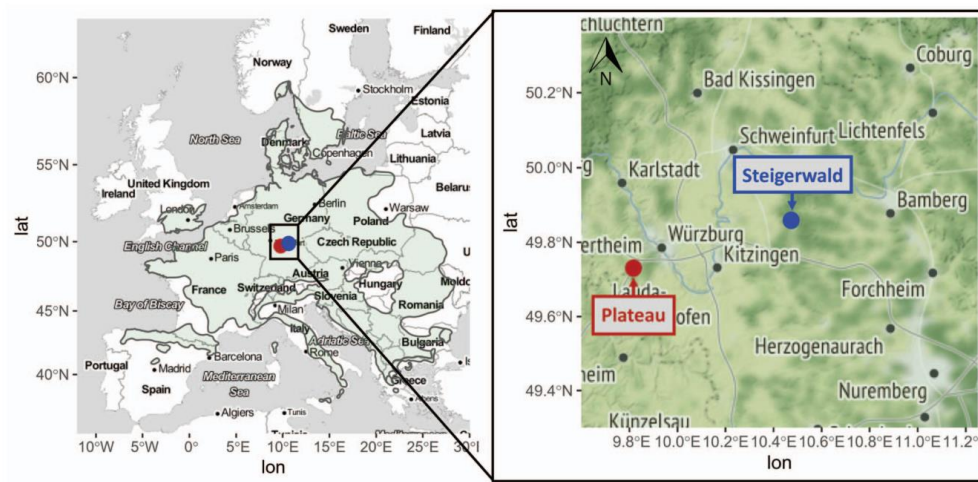


Figure 1 Geographic location of the study sites; the red dot represents the study area on the Southern Franconian Plateau. This area is one of the warmest and driest areas in Germany. A bit more humid and cooler is the Steigerwald (blue dot). The green shading indicates the distribution pattern of European beech (*Fagus sylvatica* L.) in Europe according to Caudullo *et al.* (2017).

Table 1 Main characteristics of the study sites Plateau and Steigerwald presented by climatic, geographic and soil data. The data basis is the Forest Atlas of Bavaria (LWF, 2005) and the climate stations of the German weather service (DWD, 2022a, b). The climate data cited refer to the reference period 1991–2020.

Study site	Plateau	Steigerwald
Latitude, longitude	49.7286, 9.8156	49.8721, 10.4724
Elevation (m.a.s.l.)	270–350	400–460
Geology	Muschelkalk	Keuper
Soils according to the WRB	Entric Leptic Cambisol (Clayic) with tendency to Rendzic Leptic Phaeozem (Clayic)	Dystric Cambisol (Loamic)
Climate	Suboceanic	Suboceanic
Mean annual temperature	10.1°C	8.6°C
Mean annual precipitation	576 mm	802 mm
Potential vegetation/plant association	Hordelymo-Fagetum and Galio odorati-Fagetum	Predominantly Luzulo-Fagetum, but also Galio odorati-Fagetum

higher average precipitation (802 mm) than the Plateau (cf. Table 1) (DWD, 2022a, b). The soils in the Steigerwald have formed on Keuper and are classified as Dystric Cambisol (Loamic). These are deeper than those in the Plateau and consequently have a slightly better water regime (LWF, 2005). The potential natural vegetation of the Steigerwald is predominantly Luzulo-Fagetum, but also Galio odorati-Fagetum (Walentowski, 2006).

In both regions, nutrients are not considered as growth-limiting for European beech, but the summer water supply is. Plateau and Steigerwald experienced pronounced water deficits in the years 2018–2020. Measurements of soil moisture at the Würzburg (Plateau) forest climate station showed that drought stress started here at the end of June in each year (<40 per

cent available water capacity) (Zimmermann and Raspe, 2019; Zimmermann *et al.*, 2020). A summary of the site conditions is presented in Table 1.

Sampling design

The sampling design followed a hierarchical approach, beginning with a pre-stratification based on geodata from a forest management plan. The resulting study area included only stands that met the following characteristics: (a) the slope of the forest sites was <10 per cent to minimize slope and exposure effects, (b) only soils classified as Dystric Cambisol (Steigerwald) and Entric Leptic Cambisol (Plateau) were selected and (c) only stands that were

Table 2 Characterization of the recorded trees; classified according to the two study sites Plateau and Steigerwald. Min = minimum, Max = maximum, SD = standard deviation.

Study site	Plateau				Steigerwald			
	Min	Mean	Max	SD	Min	Mean	Max	SD
Number of trees	464				526			
DBH (cm)	9.0	35.9	84.0	15.2	8.0	43.1	92.0	20.3
Total tree height (m)	6.9	26.3	37.9	5.9	8.8	29.4	42.4	6.9
BAI (cm ² year ⁻¹)	0.6	12.7	68.6	9.4	0.2	19.6	105.4	16.5

mainly composed of beech as dominant tree species (species share >80 per cent), with no silvicultural treatments since 2018 were considered. This was to assure that the forest structure recorded at the end of 2020 would not have been affected by any recent disturbances like thinning.

The potential forest area was then covered with a randomly placed point grid with a resolution of 60 × 60 m. Only sample points that had a minimum distance of 50 m to recently disturbed areas or to the forest edge to minimize edge effects were considered. The coordinates of the point grid were transferred to a Global Positioning System (GPS) device (Garmin GPSMAP 66sr). In the field, a total of 240 trees were selected, 120 in the Steigerwald and 120 on the Plateau. The selection was done in a way that minimized the spatial extent of all the plots within each study area. Trees belonging to different social positions (dominant, subordinate), tree dimensions (small, large timber) and forest structures (single-layered, multi-layered) were selected. For each of these eight possible combinations, 15 samples were selected per study site (2 × 2 × 2 × 15 = 120). In addition to this first 'central' tree, its closest neighbours were also included in the study. These were all the trees that interacted ('touched') in the canopy with the central tree. Depending on the density of the forest, between zero and seven neighbours were identified per central tree. On average, there were about four trees per sample point in total (cf. Table 2).

Data collection

Data collection took place in the winter of 2020/2021 (no leaves on the tree, leaf-off) and in summer of 2021 (during the vegetation period, leaf-on). During the data collection campaign in the winter, the diameter at breast height (DBH) of each sample tree was measured. The social position assessment was based on the approach by Kraft (1884). We combined Kraft's classes 1 and 2 into the 'dominant' social position and Kraft's classes 4 and 5 into the 'subordinate' social position. Kraft's class 3 will be further referred to as 'intermediate'. This addresses potential assignment difficulties during data collection and divides the data into classes that were expected to respond similarly to drought (Grote *et al.*, 2016; Diaconu *et al.*, 2017).

During the summer campaign, the crown condition of the sample trees was assessed, as an important indicator for the vitality of the trees. The assessment was based on assigning the trees to defoliation classes, which are divided in 5 per cent steps. A 0 per cent means the complete foliage of a tree, 100 per cent

means its complete defoliation. The assessment is analogous to the forest status assessment in Germany (Wellbrock and Eickenscheidt, 2018). The approach was carried out by using binoculars. Crown competition was coded as follows: '1' competition from one side, '2' from two sides, '3' from three sides and '4' from four sides.

Three-dimensional (3D) data on the individual trees and the surrounding forest structure were recorded with a MLS (ZEB HORIZON, GeoSLAM Ltd, UK) in leave-off condition for optimal visibility. Today, laser scanning techniques can be used for recording forest structural data efficiently (Seidel *et al.*, 2015). The forest was recorded within a radius of 30 m around the central tree. After starting the scan, the central tree was approached from south to north (for later point cloud orientation), circled with the MLS and marked with a pronounced 'up'-'down' movement of the scanning device for automated identification in the 3D data (for details, see below). Then, the MLS path continued in a spiral manner around the central tree. The radius of the spirals was about 7, 14, 21, 28 and 35 m, respectively. The mobile scanner continuously scans the surroundings up to 70 m from the device using the time-of-flight principle and the simultaneous localization and mapping (SLAM) technology (e.g. Bauwens *et al.*, 2016).

Tree-growth core samples were also collected from each sample tree during the winter campaign. Two core samples from each tree were extracted in an angle of 90° to one another (north and east) at breast height. An increment borer from Mora with 5 mm diameter was used.

Data and sample processing

Laser scan data

The data collected by the MLS were first processed using the manufacturer-specific software GeoSLAM HUB (GeoSLAM, 2020), which means the actual SLAM registration was performed. After pre-processing, the individual scans were exported in the .laz file format. The R package lidR (Roussel *et al.*, 2020) was used to further process the exported point clouds. The point clouds were cut to a radius of 30 m around the stem foot coordinate of the central tree from the respective scans. The ground points were then classified using the Ground Segmentation Algorithm (Zhang *et al.*, 2016). With the Spatial Interpolation Algorithm (interpolation is done using a k-nearest neighbour approach with an inverse-distance weighting), the height of the points was normalized. To further reduce the amount of data, the point cloud was voxelized to a resolution of 1 × 1 × 1 cm (1 cm³). From this remaining

point cloud, the point clouds of single trees were identified and extracted using the software LiDAR360 (GreenValley International, Ltd, 2019). The tree segmentation algorithm used was developed based on the method described by Li *et al.* (2012). However, this segmentation was not successful in all cases, especially not for complex forest structures. In these cases, we manually post-processed the single-tree points clouds with the software CloudCompare (Version 2.11.3, cloudcompare.org, EDF R&D, Paris, France). From the final single-tree point clouds, LiDAR360 was used to calculate tree height, crown diameter, crown area and crown volume for the sample trees. The box-dimension, a measure of the structural complexity of the trees (Seidel, 2018), was calculated based on the single-tree point clouds using the upper cut-off as tree height and a lower cut-off of 10 cm. We considered the nearest 10 neighbours when calculating the Hegyi index (distance-dependent competition index). These were selected based on their tree trunk coordinates.

The total number of trees differs depending on the study sites due to the different number of neighbours. An overview of the total number of sampled trees, their height and basal area increment (BAI) is given in Table 2.

Tree core samples

To measure the width of the annual growth rings, the tree cores were cut horizontally (in the direction of the year rings) with a core microtome developed by the Swiss Federal Institute for Forest, Snow and Landscape Research (Gärtner and Nievergelt, 2010; Schollaen *et al.*, 2017). The cores were then air dried and the ring widths were measured to the nearest 0.01 mm using a measuring table (LINTAB 5; Rinntech, Heidelberg, Germany) with a stereo microscope (MZ 6; Leica, Wetzlar, Germany) and the TSAP-Win software package (Rinntech, Version 4). Cross dating was performed using respective site samples of unambiguous cores. For apparently missing year rings, the value 0.01 mm was entered, to identify them later. A chronology for each tree was built by calculating the arithmetic mean of the two cores of one tree.

Stable isotope analysis ($\delta^{13}\text{C}$)

From the tree core taken in the northern direction of each stem, the annual rings were separated for the years 2016, 2017, 2018, 2019 and 2020 under the microscope using a scalpel. After an initial coarse manual comminution of each year ring (also using the scalpel), the samples were milled to fine powder with a ball mill (MM200, Retsch, Haan, Germany). To exclude bias due to abrasion in plastic microtubes, the samples were transferred to stainless steel microvials (BioSpec, Bartlesville, US) and supplemented with two 4-mm stainless steel balls. These were subsequently clamped in a ball mill, which ground each sample twice for 10 min at a frequency of 25 sec⁻¹. Between millings, the process was paused for 30 sec, to avoid overheating and cool the containers. In case of a sample weight of < 9 mg, the mass loss during milling caused by the electrostatic adhesion of wood to the ball, as well as in the container itself, was sometimes greater than optimal. This mass could not be completely regained after grinding. Therefore, samples with < 9 mg were directly crushed by hand so that they were small enough to be weighed in the mass

spectrometer (Balance: CP2P, Sartorius, Göttingen, Germany). If the weight was < 2 mg, no comminution was performed.

For the measurement of $\delta^{13}\text{C}$, the wood samples were weighed into tin capsules. The samples were combusted in an elemental analyser (NA 1110; Carlo Erba, Milan, Italy and Vario Pyro Cube, Elementar, Hanau, Germany) that was coupled via a ConFlo III reference system to an isotope-ratio mass spectrometer (Delta Plus; Finnigan MAT and IsoPrime 100, IsoPrime, Stockport, UK) and measured against a laboratory working standard CO₂ gas, previously calibrated against a secondary isotope standard (IAEA-CH6 for $\delta^{13}\text{C}$, accuracy of calibration 0.06 per cent SD). Wheat flour as solid internal laboratory standard (SILS) was calibrated against these references and were run after every 10th sample. The long-term precision for the SILS was < 0.2 per cent. Carbon isotope data are presented as $\delta^{13}\text{C}$ relative to the international Vienna Pee Dee Belemnite standard: $\delta^{13}\text{C}$ [%] = $[(R_{\text{sample}}/R_{\text{standard}}) - 1] \times 1000$; where R_{sample} and R_{standard} are the ratios of $^{13}\text{C}/^{12}\text{C}$ in the sample and standard.

Statistical analysis

The growth increment was analysed for the years 2016–2020. This short period allowed excluding possible ageing effects and thereby focusing on the drought effects. The relative increment was calculated in relation to the maximum value observed per tree in the 5-year period.

To determine differences in growth and $\delta^{13}\text{C}$ signal, we used the non-parametric Kruskal–Wallis test, since normal distribution and homogeneity of variance could not be confirmed for the data. For post hoc analysis, we used the Wilcoxon Rank Sum Test with Bonferroni corrected *P*-value. The significance level *P* < 0.05 was chosen for all statistical tests conducted in this study.

Resistance index

As dependent variable, the resistance index (RT) was calculated to quantify the tree-specific degree of water stress-induced growth depression from 2016 to 2020. The index is defined as quotient of the arithmetic mean value from the years 2020 and 2019 in relation to the arithmetic mean value from the years 2016 and 2017. The RT was calculated for the annual BAI (RT BAI) as well as for the $\delta^{13}\text{C}$ signal (RT $\delta^{13}\text{C}$). If the RT BAI < 1, then the arithmetic mean of 2019 and 2020 is smaller than that of 2016 and 2017, and the prolonged drought has resulted in reduced radial growth. A RT $\delta^{13}\text{C}$ < 1 means that the ^{13}C discrimination of 2019 and 2020 is smaller than that of 2016 and 2017. We examined whether this RT correlated with any of the calculated morphological variables. To test whether the RT was affected by social position, we used the Student's *t* test.

Regression analysis

For regression analysis, we used generalized additive models (GAM), since the relationship between response and explanatory variable could not be specified in advance. GAM regressions were used for (i) the analysis of the competition intensity and the annual BAI and (ii) the relationships of the resistance indices (RT BAI, RT $\delta^{13}\text{C}$) and the tree morphological variables. For the latter, the plot ID was set as random effect and the fixed effect variables were the study area, DBH, tree height, crown diameter, crown

area, crown volume, box-dimension and H/D ratio. For each of our dependent variables (RT BAI, RT $\delta^{13}\text{C}$), we first ran all possible model combinations of independent variables using the model dredging function of the R package MuMIn (Bartoń, 2022). The model selection was based on the Akaike information criterion corrected. The data family was set to 'Gaussian' with an 'identity-link function'. The number of knots was set to a maximum of three with automated adaption via generalized cross-validation.

Based on the Resistance Indices, we identified the tree individuals, which showed a pronounced response to drought years. For these individuals, we used a logistic regression model (function glm) with a binary response variable describing the influence of tree morphological variables on the resistance indices. We defined the binary response as follows. For the RT BAI, we classified trees as individuals with 'reduced BAI', if their BAI decreased by 50 per cent or more (RT BAI ≤ 0.5) or as individuals with 'increased BAI', if their BAI doubled (RT BAI ≥ 2). For the RT $\delta^{13}\text{C}$, trees with a value ≤ 0.925 were classified as individuals with 'lower ^{13}C discrimination' and trees with a RT $\delta^{13}\text{C} \geq 1.025$ were classified as individuals with 'higher ^{13}C discrimination'. We calculated the logistic regression for a balanced data set. The binary variable was assigned to an equal number of observations, which were randomly selected (in the groups 'reduced BAI' and 'increased BAI', as well as in the groups 'lower ^{13}C discrimination' and 'higher ^{13}C discrimination' were the same number of trees each). The model selection was also performed with the R package MuMIn, as described above. The accuracy of the models (overall agreement rate averaged over cross-validation iterations) was computed with the R package caret (Kuhn, 2022). All statistical procedures were performed using R 4.1.1 (R Core Team, 2020).

Results

Growth reaction in dependence of social position

The drought years 2018 through 2020 had the greatest impact on the growth of dominant trees (Figure 2a). Although the mean radial increment was not significantly different between 2016 and 2017, the dominant beech trees responded with an increase in increment in the first drought year of 2018. As the drought continued, the increment in 2019 decreased significantly below that of 2016 and 2017. This response pattern continued in 2020. Even though the absolute increment decreased, it initially continued to lie above that of the intermediate or subordinate trees for most years observed, but it finally did not for the year 2020.

The radial increment of the subordinate beech trees in 2020 did not differ from that of the other years. Only the increment of the year 2016 was significantly different from that of the years 2017, 2018 and 2019 (Figure 2a).

Similar trends could be observed for the BAI. Here, however, the BAIs of the dominant trees continued to lie above those of the intermediate or subordinate trees for all the years observed, including 2020 (Figure 2b). The trends across the observed years within the specific social position were similar to Figure 2a (due to the relationship of radial increment and BAI), with the exception that for the subordinate collective, the increments from 2018 to 2020 were no longer significantly different from that of 2016 and 2017.

Growth reaction in dependence of the study area

The radial growth of the individuals within the same social position in the two study areas was quite similar (Figure 3). For the dominant collective (Figure 3a), an overall downward trend was observed in the average relative diameter increment. Values in drought-free years (2016 and 2017) differed significantly from those in 2019 and 2020. Trees in the Steigerwald showed the highest relative diameter increment in the 5-year period in 2018. In contrast, the relative diameter increment on the Plateau continuously decreased. In 2019 and 2020, the increment values of the two study areas did not significantly differ from one another.

For the subordinate trees (Figure 3b), the two study areas did not differ in their values in 2016 and 2020. Looking at the growth trend over the years, the tree relative diameter increment fell below the 2016 level in 2017 and 2018, but recovered in 2019 and 2020, depending on the study area. The trees on the Plateau did not significantly differ anymore from the value recorded in 2016, the trees in the Steigerwald remained at the level of 2017.

$\delta^{13}\text{C}$ signature in dependence of social position

The ^{13}C discrimination differed according to social position (Figure 4). With a decrease in the social dominance of a tree, a lower $\delta^{13}\text{C}$ value was observed, indicating an increase in ^{13}C discrimination. However, the trend across the years was similar for all social classes, increasing from the drought-free years (2016 and 2017) to the drought-influenced years (2018–2020). The mean $\delta^{13}\text{C}$ value for 2018–2020 was higher than that of 2016–2017 for all social positions. Changes between the years were not all significant, but in general, the years 2018–2020 or 2019–2020 were different from 2016 to 2017 (cf. Figure 4).

Resistance in dependence of social position

The RT $\delta^{13}\text{C}$ did not differ between the social positions, but the mean value lay significantly below 1 for all social classes (Figure 5a). The same is true for the RT BAI, which also significantly differed from 1 (Figure 5b). When visually inspecting the boxplot, the significance of the differences appears to be based on the sample size. Also, the RT BAI showed a positive significant trend from the highest (dominant) social position to the lowest (subordinate) (Figure 5b). The values of the 'dominant' and 'intermediate' social position were < 1 (0.812, 0.896) and the mean value from the subordinate trees was greater than 1 (1.118).

Resistance in dependence of morphological differences

For the total number of sample trees, there were no clear trends between tree morphology variables and resistance. Neither for tree-ring growth (RT BAI) (Supplementary Appendices 1 and 2), nor for differences in $\delta^{13}\text{C}$ signature (RT $\delta^{13}\text{C}$) (Supplementary Appendices 3 and 4). The multivariate analysis did not lead to a significant improvement of the models either (Supplementary Appendix 5). Therefore, we focused on the collective of the trees, which showed a strong RT response. When analysing only those trees that responded most notably in RT BAI when comparing the years 2016–2017 and 2019–2020, we found

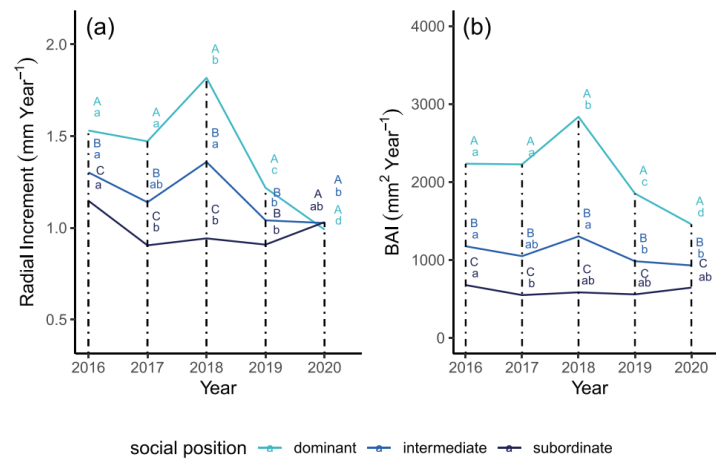


Figure 2 Increments for the years 2016–2020 in dependence of social position for the annual (a) radial increment for the entire collective and (b) BAI. Lowercase letters (a, b, c, d) indicate significant differences across the years for the respective social position. Capital letters (A, B, C) show significant differences between social positions within the same year. Sample size for the specific social position: dominant ($n = 620$), intermediate ($n = 175$), subordinate ($n = 195$).

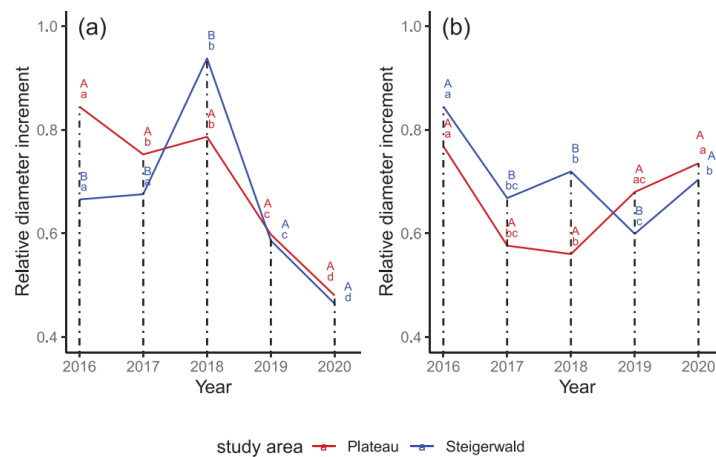


Figure 3 Relative diameter increments of the years 2016–2020 for (a) the dominant collective and (b) the subordinate collective. Lowercase letters (a, b, c, d) indicate significant differences across the years for the respective study area. Capital letters (A, B) show significant differences between study site locations within the same year. Sample size for the study areas: Plateau ($n = 464$), Steigerwald ($n = 526$).

7 out of 11 morphological variables to be significantly different between the two time periods (Figure 6).

The logistic models showed a higher probability of decreased BAI during drought (≤ 0.5) for trees with larger DBH, tree height, crown diameter and observed defoliation (Figure 6a–c, f). The opposite trend could be observed for increasing crown length and H/D ratio (Figure 6d, e).

Model accuracies for the single predictor variables ranged from 0.652 to 0.717. Other metrics examined, such as crown volume and box-dimension, were not significant.

The same analysis using RT $\delta^{13}\text{C}$ led to five significant variables out of 11 (Figure 7). The logistic models showed an increased probability of a higher RT $\delta^{13}\text{C}$ (≥ 1.025) for a higher defoliation and an increasing tree height (Figure 7c, d). The probability of a

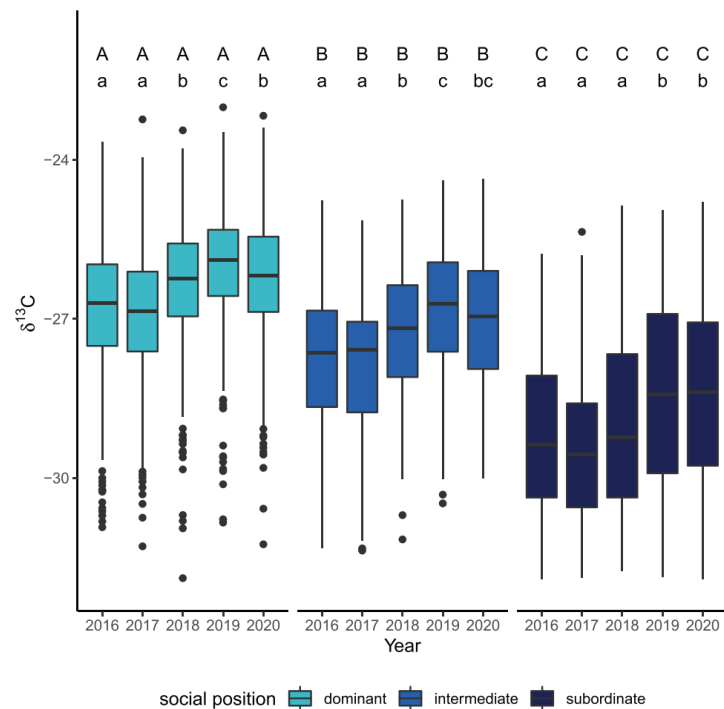


Figure 4 $\delta^{13}\text{C}$ values across the years 2016–2020 for trees of the different social positions. Lowercase letters (a, b, c) indicate significant differences within a social position. Capital letters (A, B, C) show significant differences between social positions within the same year. Sample size for the specific social position: dominant ($n = 620$), intermediate ($n = 175$), subordinate ($n = 185$).

lower RT $\delta^{13}\text{C}$ (≤ 0.925) increased as the crown length and box-dimension increased (Figure 7 a,b).

Model accuracies ranged from only 0.58 to 0.72. Other metrics examined, such as DBH, crown diameter and crown volume, were not significant. Multivariate approaches could also not improve the models (Supplementary Appendix 6).

The trends in Figures 6 and 7 are not primarily influenced by differences in social position. Reducing the models to a specific social position led to similar results with equal trends.

Competitive environment and its effect of tree performance

As is to be expected, increasing competition led to a decrease in BAI, which can be seen by the general negative trend of the data across both study sites in Figure 8. However, the intensity of the competition effect differed between the years. The most apparent differences were found where competition was low (Hegyí index around 0–2). Here, in the years following the drought of 2018 (especially in 2020), the effect of competition on BAI continuously decreased

compared with the years 2016–2018 in both study areas. With increasing competition (Hegyí index > 2), the differences between years and sites disappeared and the overlapping confidence intervals indicated no significant differences (Figure 8).

When considering the RT indices, the effect of competition as explanatory variable also showed a complex pattern (Figure 9). The RT BAI increased with increasing competition, showing that individuals in a highly competitive environment tended to have a higher BAI during the drought years, compared with the pre-drought years (Figure 9a,b). This is true for both competition metrics, namely the Hegyí index and the simpler 'Crown Competition' class used here. The effect of competition on the RT $\delta^{13}\text{C}$ was less obvious and pronounced. The effect of increasing crown competition on the RT $\delta^{13}\text{C}$ (Figure 9d) was significant and negative, but had a very low accuracy of only 0.534, with wide confidence intervals including the equal probability value of 0.5. No significant effect could be found for the Hegyí index as variable (Figure 9c). Thus, the strength of competition obviously has less influence on ^{13}C discrimination.

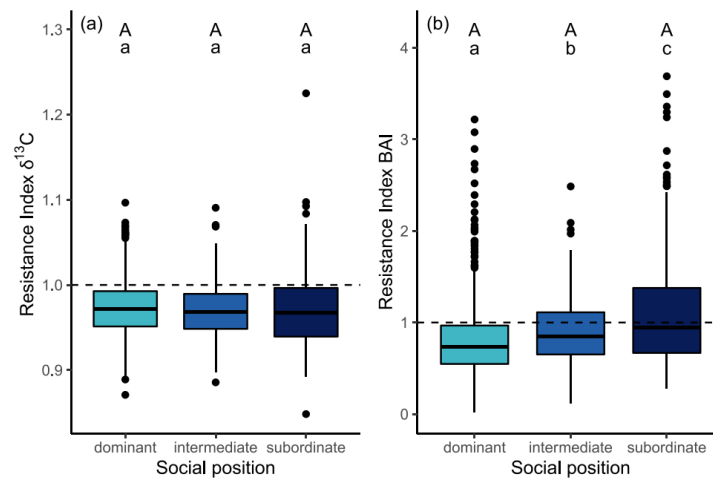


Figure 5 Resistance to drought events in dependence of social position. (a) Shows the RT $\delta^{13}\text{C}$ (b) the RT BAI. Lowercase letters (a, b, c) show significant differences between the social positions. The capital letter A indicates all boxplots whose underlying mean is significantly different from 1. Sample size for the specific social position: dominant ($n = 620$), intermediate ($n = 175$), subordinate ($n = 195$).

Discussion

Growth reaction in dependence of social position

In short, the drought years of 2018–2020 have had the greatest impact on diameter increment patterns of dominant beech trees. These results confirmed the first hypothesis (H1.1), namely that the radial growth reaction of beech trees to drought stress depends on their social position. However, the patterns were not as straightforward as we had anticipated beforehand. In particular, the first heavy drought in 2018 was not followed by a decrease in growth during the vegetation period of 2018, but an increase. The reason could be the ‘carry-over effect’ described, e.g. by Chakraborty *et al.* (2021), Elling *et al.* (2007) and Hackett-Pain *et al.* (2015). Stored carbon reserves, buds already developed and water reserves enable an increased growth in the first year of drought. In addition, wood is formed early in the vegetation period. Čufar *et al.* (2008) and Michelot *et al.* (2012) confirmed that by the end of June, 75 per cent of the total annual ring of beech trees is already formed. Thus, the within-year response of the tree also depends on the time when the drought becomes effective. Data from the Würzburg forest climate station indicate that the drought stress period actually began during the last days of June (Zimmermann and Raspe, 2019). This could explain why drought stress did not have a severe impact on growth in 2018.

In 2019 and 2020, the continued drought led to a decrease in diameter increment for the dominant beech trees, compared with the years 2016 and 2017 (and 2018) (Figure 2). An obvious explanation for this is that less carbon reserves could finally be formed in the first drought year 2018, which then caused a reduction in tree-ring width in the following years, when the drought continued. For the historical drought year of 2003, a stronger

decrease of the radial growth was also only found in the year following the actual drought (2004) in the Steigerwald region (Zimmermann *et al.*, 2020). In addition, drought does not only affect aboveground plant compartments, but also belowground plant compartments. Especially the living fine root biomass is known to decrease first during drought events (Meier and Leuschner, 2008). Reduced fine root mass due to the extreme year 2018 may have caused reduced water as well as nutrient uptake capacity in the following years.

Also, the effects of beech masting, which are known to include temporary growth restriction, must be considered. In the years 2016, 2018 and 2020, medium to high fructification was observed for beech growing in the study areas (StMELF, 2019, 2020). Previous studies observed a severe reduction in radial growth due to the combination of seed production and drought in beech (Hackett-Pain *et al.*, 2017). This could not be verified for 2018 (increase in growth) but could be confirmed for 2020. In this regard, the growth decrease could also be caused by masting in addition to the drought, as beech fruit production is supplied by current photoassimilates, it is independent from old carbon reserves (Hoch *et al.*, 2013) and is higher for dominant trees. Overall, the sharp drop in growth of the dominant collective could already be an indication that a tipping point has been exceeded for some individual trees, not necessarily in 2018 but through the persisting drought. Finally, no growth and even death was registered for some trees.

The growth of the subordinate trees essentially remained constant in our study. Neither the 2018 peak nor the 2019, 2020 growth decrease was evident in this collective. This suggests that the severe drought of 2018–2020 did not have a reinforcing effect, next to all other possible environmental limitations

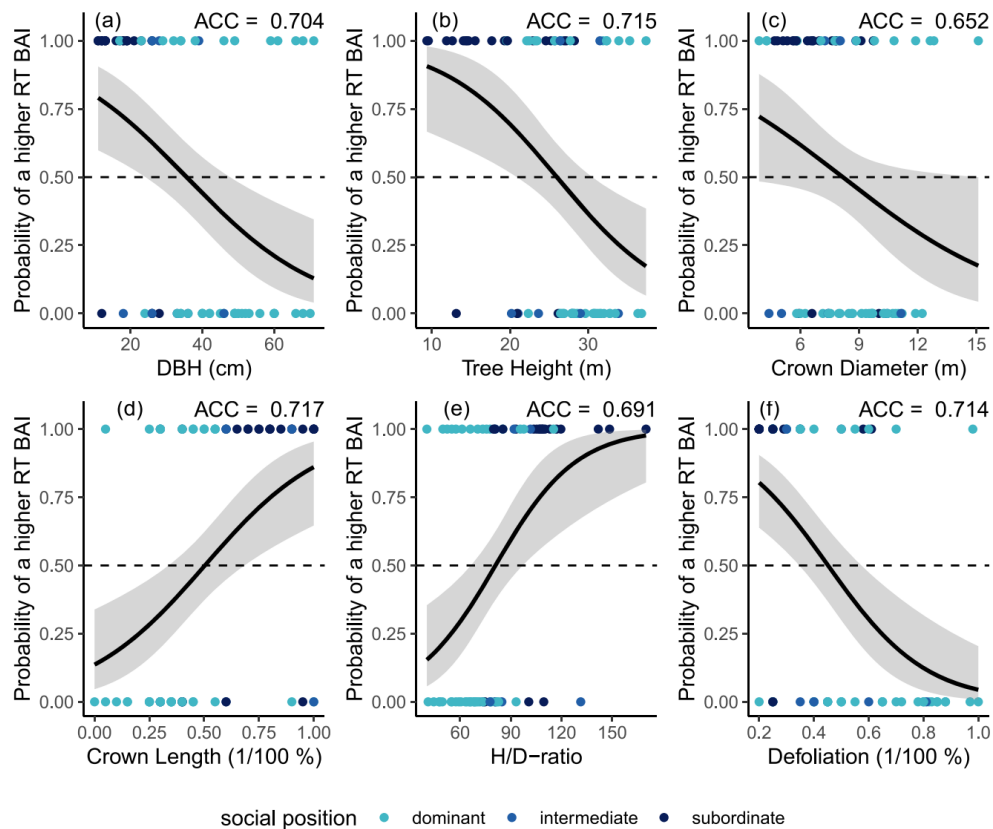


Figure 6 Logistic regression plot for the probability of a higher RT BAI for different variables (a–f). A lower RT BAI was defined as ≤ 0.5 , a higher RT BAI was defined as ≥ 2 . The dashed line indicates the threshold value (probability = 0.5). From each class, 36 trees were selected. All models are significant. Ribbons around solid lines indicate the 95% confidence interval. ACC stands for the accuracy of the specific model.

that this collective of trees is confronted with (possible reduced access to light and nutrients through competition with dominant trees). Possibly, the effect of drought even counterbalances the effect of competition. So even though the understory trees also respond to the reduced water availability (see the $\delta^{13}\text{C}$ pattern in Figure 4), the competitive pressure of their neighbours might decrease in drought years. It could be that the neighbours suffer more strongly from the drought, which in return might increase the performance of the understory trees. This counteracts the drought effect and the performance appears constant. For a collective of trees, this could mean that the understory trees have a stabilizing effect on the ecosystem, as long as their presence does not increase the stress for the dominant trees. We did not explicitly study this here, but this might be an interesting focus for future studies. A further explanation could also simply be Liebig's Law of the Minimum. It states that for an organism the

'essential material available in amounts most closely approaching the critical minimum needed will tend to be the limiting one' (Odum, 1959). Consequently, the subordinate collective, which primarily suffers from lack of light, does not respond strongly to the drought impulse.

Growth reaction in dependence of the study area

The trees in the Steigerwald were adapted to a slightly cooler climate with more precipitation in the past and to deeper soils with a higher water holding capacity. This framework could be the explanation for the significant increase in radial growth in 2018 here (Figure 3). Walthert *et al.* (2021) concluded in their study that water reserves in deep soil layers prevented drought stress in beech trees for the year 2018.

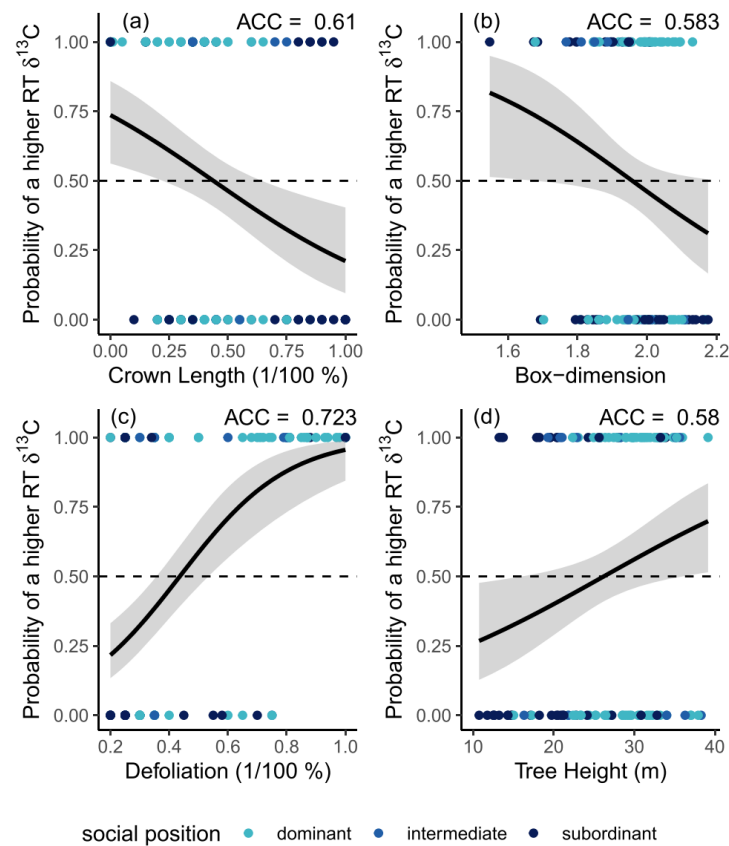


Figure 7 Logistic regression plot for the probability of a higher RT $\delta^{13}\text{C}$ for different variables (a–d). A lower RT $\delta^{13}\text{C}$ was defined as ≤ 0.925 , a higher RT BAI was defined as $\delta^{13}\text{C} \geq 1.025$. The dashed line indicates the threshold value (probability = 0.5). From each class, 61 trees were selected. All models are significant. Ribbons around solid lines indicate the 95% confidence interval. ACC stands for the accuracy of the specific model.

However, it is remarkable that the relative increases between the study areas were no longer significantly different in 2019 and 2020 (Figure 3). In this respect, our results cannot support previous studies stating that trees growing on a dry site were better adapted to drought (Bolte *et al.*, 2016; Cuervo-Alarcon *et al.*, 2021). The observed multi-year drought event seems to have overruled the effects of different growing habitats or forest stand history in view of the relative diameter increment for the whole tree collective, with the result that all beech trees from both sites show similar responses to the drought. This is a further indication for the potential of severe and long-lasting drought events of becoming tipping points for entire systems. Finally, hypothesis H1.2, according to which trees that are accustomed to a warm and dry climate, as well as shallow sites, do not react

as strongly in their radial growth to drought events, could not be accepted.

$\delta^{13}\text{C}$ signature in dependence of social position

Similar to the analysis of radial growth, our results for the $\delta^{13}\text{C}$ signature showed an effect of the social position (Figure 4). One reason for the lower $\delta^{13}\text{C}$ value of the subordinate trees could be the assimilation of CO_2 , which is emitted by respiration. Respiration leads to discrimination of ^{13}C , so atmospheric CO_2 was significantly depleted in ^{13}C closer to the ground surface (Berry *et al.*, 1997). This reduces the abundance of $^{13}\text{CO}_2$ in the air, resulting in more negative $\delta^{13}\text{C}$ values in the lower canopy (Da Silveira *et al.*, 1989; Knohl *et al.*, 2005). Subordinate trees could

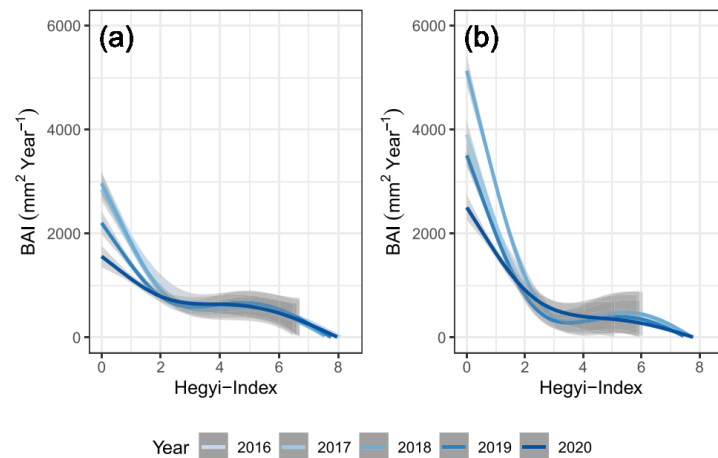


Figure 8 BAI in dependence of Hegyi index of competition from 2016 to 2020 for study area (a) Plateau and (b) Steigerwald. Regression lines are based on GAM models. All trends are significant. The explained deviance decreases over the years. Ribbons around solid lines indicate the 95% confidence interval. Sample size for the study areas: Plateau ($n = 464$), Steigerwald ($n = 526$).

therefore assimilate more ^{13}C -depleted CO_2 , which is consequently reflected in the $\delta^{13}\text{C}$ signature and may explain the observed pattern.

Another mechanism, which could contribute to the observed pattern, is the differences in light access. Several studies showed an increase of $\delta^{13}\text{C}$ in tree biomass with increasing irradiance (Farquhar *et al.*, 1989; Hanba *et al.*, 1997). This is in line with Mölder *et al.* (2011), who found that more intense competition – i.e. greater shading – is associated with a smaller $\delta^{13}\text{C}$ value. But temperature could have had an influence as well. Porter *et al.* (2009) demonstrated a strong positive association between $\delta^{13}\text{C}$ signature and maximum summer temperatures. Subordinate trees are less exposed to temperature peaks compared with dominant trees because they remain in their shadow (under their canopy) and benefit from the forest interior climate during extreme temperature situations.

For the dominant collective, the $\delta^{13}\text{C}$ signal increases for the drought-influenced years (2018–2020). According to Farquhar *et al.* (1989) and Gessler *et al.* (2014), a difference in discrimination can be caused by two factors: (1) altered photosynthetic capacity, e.g. due to different light conditions or (2) altered stomatal conductance. For the years considered in conjunction with the decrease in increment, it is reasonable to interpret this as increased drought stress, hence altered stomatal conductance.

As expected, the tree ring $\delta^{13}\text{C}$ generally increased with drought. The values for the period 2018–2020 were higher than for 2016–2017. But contrary to our expectations, the tree ring $\delta^{13}\text{C}$ did not continue to increase with the drought event continuing to last. For the dominant trees, the values in 2020 were even significantly lower than in 2019 and no longer different from 2018, although 2020 was also very dry. This was also found by Billings *et al.* (2016). We did not expect this, especially because carry-over effects tend to have the opposite direction. An

explanation why this is not so could be the increasing defoliation. In 2020, the trees had less foliage on average due to the two previous drought years (StMELF, 2019; 2020). The lower leaf mass might have been supplied better with water despite the drought, which in turn might have lowered the $\delta^{13}\text{C}$ signal again. This agrees with the subjective impression during the crown assessments that the remaining leaves from those beeches that were already suffering from partial crown die-back often appeared greener than average. Weithmann *et al.* (2021) found evidence that the severe 2018 drought event triggered the formation of smaller leaves with higher water use efficiency in the sun canopy. Therefore, leaf shedding could be a further response to drought, to decrease drought stress. Beech, as an anisohydric species, accepts greater fluctuations in water balance, which is associated with a higher risk of embolism (Choat *et al.*, 2012; Leuschner *et al.*, 2019). During extreme drought, beech does not fully close its stomata and continuously loses water through the leaf surface (Leuschner, 2009; van Wittenberghe *et al.*, 2012). In this respect, defoliation is a response to xylem dehydration (Schuldt *et al.*, 2020; Walthert *et al.*, 2021). Increasing defoliation is, however, often accompanied by damage such as sunburn, beetle infestation (e.g. *Agrilus viridis* L.), etc. (Brück-Dyckhoff, 2017) and can trigger a chain reaction (Manion, 1981), which could be interpreted again as the event's intensity surpassing the species adaptive ability and increasing the risk to function as tipping point for the system.

In the subordinate collective, it is noticeable that the $\delta^{13}\text{C}$ value increased significantly in 2019 and 2020. At the same time, the growth of the dominant trees decreased significantly (Figure 2). It is likely that the available water capacity in the soil dropped to such an extent that these trees also experienced drought stress. It is apparent that the trees did not react significantly in the first year of drought (Figure 3). This could be

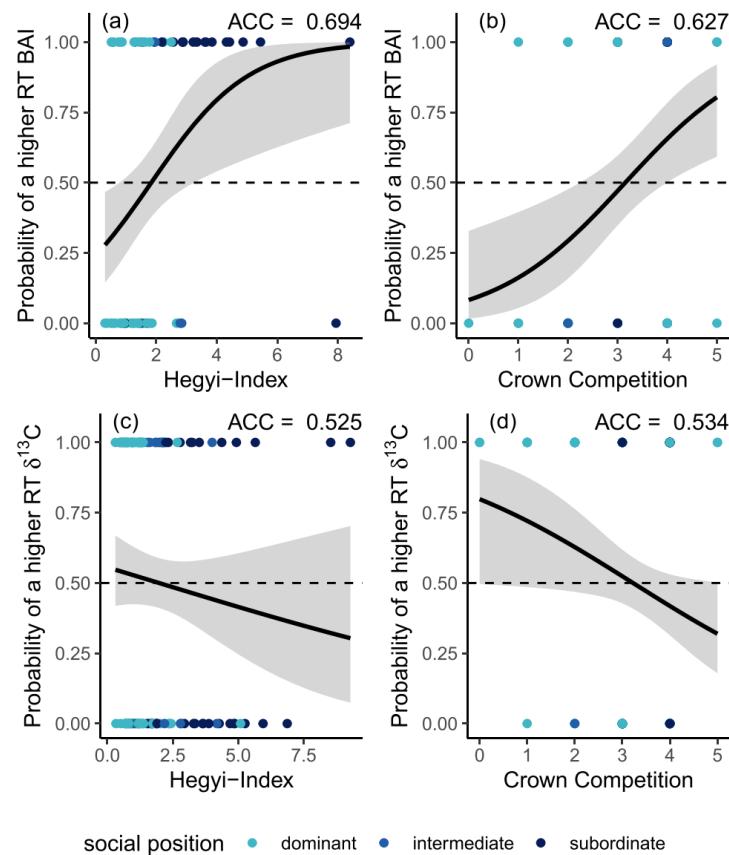


Figure 9 Logistic regression plot for the probability of a higher RT BAI (a, b) and of a higher RT $\delta^{13}C$ (c, d) in dependence of different metrics expressing the competition. A lower RT BAI was defined as ≤ 0.5 , a higher RT BAI was defined as ≥ 2 . A lower RT $\delta^{13}C$ was defined as ≤ 0.925 , a higher RT BAI was defined as $\delta^{13}C \leq 0.925$. The dashed line indicates the threshold value (probability = 0.5). Models a, b, d are significant. Ribbons around solid lines indicate the 95% confidence interval. ACC stands for the accuracy of the specific model.

interpreted as resistance of this collective to 1-year drought stress, simply because they are not as exposed as strongly to radiation as the dominant collective. However, considering the $\delta^{13}C$ signal, persistent multi-year drought finally also seems to have affected the subordinate collective in 2019 and 2020, either due to different light conditions (if overstory trees lost parts of their canopy or shed and developed smaller leaves) or altered stomatal conductance. Which of the factors might be the driving one cannot be concluded here from the data and might be a topic of further research. But again, we can conclude that persistent droughts also affect this collective, again pointing towards the potential of this disturbance to act as tipping point across social tree classes for the species beech. In short, hypothesis H2 – which states that the drought-related $\delta^{13}C$ isotope signal differs

between different social positions – could be accepted, whereas the trend of the $\delta^{13}C$ isotope was similar across the years.

The effect of morphological differences to drought resistance

When defining resistance as a ratio between the tree performance of the years 2019 and 2020 and tree performance of the years 2016 and 2017, no obvious correlations of resistance and tree morphology could be found when analysing the whole dataset of the trees (cf. Appendix). The tree response patterns triggered by the extreme drought were very diffuse. This was against our expectations. One explanation could simply be that tree morphology does not affect resistance.

According to the literature so far, this seems unlikely (Bennett *et al.*, 2015; Stovall *et al.*, 2019). A further explanation is that the morphological response pattern is overruled by other factors, like small scale soil differences, pathogens or tree genetics, which we cannot account for here. Focusing on the group of trees that showed strong differences in 2019–2020 compared with 2016–2017, revealed some differences (Figures 6 and 7).

For this smaller collective, we found that the RT BAI tended to decrease with increasing size and higher social position of the individual. Even though this might seem counterintuitive at first, the results are confirmed by earlier research from Skomarkova *et al.* (2006), according to whom beech trees with large crowns are more sensitive to drought. Due to their height, large trees tend to be more strongly exposed to radiation, wind and heat. In drought years, this exposure can cause more pronounced hydraulic stress than for their shorter neighbours (Lu *et al.*, 1996; Bennett *et al.*, 2015; Grote *et al.*, 2016). This pattern was true for many of the morphological variables but not for the crown volume.

We found even less significant correlations with the morphological variables of a tree considering RT $\delta^{13}\text{C}$. There was no influence of social position, but of crown length, box-dimension, defoliation and tree height. Trees that have a large box-dimension, i.e. a high degree of complexity, that are bigger with larger canopy volume, have a lower resistance. This is in line with the patterns shown by the correlations with the RT BAI. Large dominant trees also have higher box-dimension and therefore tend to show more stress. One explanation could be that as the box-dimension increases, they have to supply a greater photosynthetically active surface through the given branch network (Seidel *et al.*, 2019) and thus are more likely to be stressed. However, non-significant models for canopy area and canopy volume do not confirm this. The increase in the probability (based on the logistic regression model) of a higher RT $\delta^{13}\text{C}$ with tree height was contrary to our expectations. It was assumed that large trees in the upper canopy use water more rapidly and are thus more likely to experience drought stress (Oren *et al.*, 1998; Bennett *et al.*, 2015). However, it could be that these trees have already dropped more of their leaves. The observed trend in defoliation may be a consequence of this. Advanced defoliation was accompanied with higher probability of RT $\delta^{13}\text{C} \geq 1.025$. The tree's hydraulic system, originally designed to supply more leaf mass, manages to supply the remaining leaf mass better.

Finally, a third explanation for the observed diffuse response pattern – apparently not strongly linked to the tree morphological variables – is that the persistent and severe droughts were so strong that they obscured differences that might be apparent under low levels of drought. This is supported by our observations that the RT $\delta^{13}\text{C}$ basically equally dropped below 1 across the social positions. Overall, H3 can only be accepted with restrictions. There were a few significant morphological variables that seemed to affect resistance to drought for a subset of the data, not for all observations, and of these variables, a few with only low accuracy.

Competitive environment and its effect of tree performance

Finally, competition is a factor that can be managed with silvicultural treatments. First, our findings confirm familiar patterns: BAI

depended strongly on the competition each tree was exposed to. This observation confirms the silvicultural assumptions that growth is enhanced by the removal of competitors (Dobbertin *et al.*, 2009; Pretzsch, 2019; Chakraborty *et al.*, 2021). However, our results show that long drought events overrule the effect of competition. Especially the performance of individuals with low competition decreased over time. Under a long-lasting drought, their competitive advantage of better access to light and most likely a larger root system seems to be detrimental over time. Possibly this is to the advantage of the understory. As it appears, the performance of individuals in situations of high competitive pressure did not change as much. One interpretation could be that the neighbours are more damaged by the drought and thus more resources are available for the oppressed tree. Or that the competition remained about the same and with the dominant tree using less water due to the stress, the oppressed trees still had about the same. Overall, hypothesis H4 stating that a lower competitive environment mitigates adverse drought effects, cannot consequently be accepted for the observed prolonged drought. The drought event may have been so severe that the previously important factor of competitive advantage of dominant individuals might have been overruled by higher resource requirements to supply the larger amount of biomass and plant tissue. Once again, this highlights the potential of prolonged drought events to significantly change ecosystem structures in a temperate beech forest and shows the importance of putting classical rules of resistance and stability in context. If the frequency of such events is to increase in the upcoming near future, this could develop into a typical pattern known for tipping points and we might be faced with large ecosystem changes.

Conclusion

Our study confirmed that beech trees in northern Bavaria were severely stressed by prolonged drought. We conclude that the intensity of the 2018–2020 drought event was so severe that many known rules and drivers of forest ecology and forest dynamics (social position, morphology and competition) were overruled. The dominant tree collective was particularly affected by the drought. Hence, the trees that are targeted by forest management approaches and that were so far considered anchors of stability against weather extremes, especially storms, suffered the most.

The increased die-back of large trees opens up the canopy and the forest interior heats up accordingly. This in turn leads to increased drought stress. The weakening of these individuals could potentially be no longer linear in northern Bavarian beech forests and develop into a typical pattern known for tipping points.

Subordinate trees, however, provide some consistency in growth during drought years. Since the drought stress of dominant trees is often also accompanied by defoliation, subordinate trees are of crucial importance. They cool down the stand microclimate (Frenne *et al.*, 2013; Davis *et al.*, 2019; Zellweger *et al.*, 2020) and could thus be aimed at for generating a multi-layered forest. Although adaptation may be possible to a certain extent, it remains unclear whether such drought events overstrain the adaptive capacity of beech systems, if their frequency increases in the near future.

In a further study, we want to analyse the influence of stand structure on the drought stress of beech trees. In this way, we want to investigate the extent to which silvicultural measures can help to increase the lifespan of beech-dominated stands to provide a time window to continue converting them to other species over time.

Supplementary data

Supplementary data are available at *Forestry* online.

Data availability

The data underlying this article will be shared on a reasonable request to the corresponding author.

Acknowledgements

We would like to thank the Bavarian State Forest Enterprise and the municipality of Leinach for providing the study sites. We also thank the Bavarian State Institute of Forestry LWF for providing GIS Data. Rudolf Harpaintner and Felix Glasmann from the Professorship of Forest and Agroforest Systems, Technical University of Munich, for their support in data collection and processing. We sincerely thank Peter Schad for classifying the soils according to the WRB, Thorsten Grams, Yessica Kömel and Rudi Schäufele for performing the isotope analysis. Simone Schäfer-Hecht, Sebastian Damböck, Paul Unkel and Markus Stimmelmayer have contributed to the success of this work with their bachelor and master theses. We thank Ian Burke, Ranbir Chakraborty, Corinne Gonzalez, Merve Mentese, Joachim Thein and Jana Walbaum for their help in the laboratory, and Markus Stimmelmayer for his great support in the summer 2021 field work. We thank the editors and the two anonymous reviewers for their constructive comments on an earlier version of this manuscript, which helped us to improve the quality of the article.

Funding

Bavarian State Ministry of Nutrition, Agriculture and Forestry through the project 'Effects of forest structures on the drought resilience of individual trees (W049)'.

Conflict of interest statement

None declared.

References

Adams, H.D., Collins, A.D., Briggs, S.P., Vennetier, M., Dickman, L.T., Sevanto, S.A., *et al.* 2015 Experimental drought and heat can delay phenological development and reduce foliar and shoot growth in semi-arid trees. *Glob. Chang. Biol.* **21**, 4210–4220.

Allen, C.D., Macalady, A.K., Chenchouni, H., Bachelet, D., McDowell, N., Vennetier, M., *et al.* 2010 A global overview of drought and heat-induced tree mortality reveals emerging climate change risks for forests. *For. Ecol. Manag.* **259**, 660–684.

Anders, S., Müller, J., Augustin, S. and Rust, S. 2006 Die Ressource Wasser im zweischichtigen Nadel-Laub-Mischwald. *Ökologischer Waldumbau in Deutschland* 152–183.

Andreu, L., Planells, O., Gutiérrez, E., Helle, G. and Schleser, G.H. 2008 Climatic significance of tree-ring width and $\delta^{13}\text{C}$ in a Spanish pine forest network. *Tellus B Chem. Phys. Meteorol.* **60**, 771–781.

Standortskartierung, A. 2016 *Forstliche Standortsaufnahme: Begriffe, Definitionen, Einteilungen, Kennzeichnungen, Erläuterungen*. 7th edn. IHW-Verlag, p. 400.

Aussenac, G. and Granier, A. 1988 Effects of thinning on water stress and growth in Douglas-fir. *Can. J. For. Res.* **18**, 100–105.

Barnosky, A.D., Hadly, E.A., Bascombe, J., Berlow, E.L., Brown, J.H., Fortelius, M., *et al.* 2012 Approaching a state shift in Earth's biosphere. *Nature* **486**, 52–58.

Bartoń, K. 2022 *MuMin: Multi-Model Inference. R Package Version 1.46.0*.

Bauwens, S., Bartholomeus, H., Calders, K. and Lejeune, P. 2016 Forest inventory with terrestrial LiDAR: a comparison of static and hand-held mobile laser scanning. *Forests* **7**, 127.

Bayerisches Staatsministerium für Ernährung, Landwirtschaft und Forsten (StMELF). 2019 *Ergebnisse der Waldzustandserhebung*. <https://www.stmelf.bayern.de/>.

Bennett, A.C., McDowell, N.G., Allen, C.D. and Anderson-Teixeira, K.J. 2015 Larger trees suffer most during drought in forests worldwide. *Nat. Plants* **1**, 1–5.

Berry, S.C., Varney, G.T. and Flanagan, L.B. 1997 Leaf $\delta^{13}\text{C}$ in *Pinus resinosa* trees and understory plants: variation associated with light and CO_2 gradients. *Oecologia* **109**, 499–506.

Billings, S.A., Boone, A.S. and Stephen, F.M. 2016 Tree-ring $\delta^{13}\text{C}$ and $\delta^{18}\text{O}$, leaf $\delta^{13}\text{C}$ and wood and leaf N status demonstrate tree growth strategies and predict susceptibility to disturbance. *Tree Physiol.* **36**, 576–588.

Bolte, A., Czajkowski, T., Cocozza, C., Tognetti, R., de Miguel, M., Pšidová, E., *et al.* 2016 Desiccation and mortality dynamics in seedlings of different European beech (*Fagus sylvatica* L.). Populations under extreme drought conditions. *Front. Plant Sci.* **7**, 751.

Brandt, S., Paul, C., Knoke, T. and Falk, W. 2020 The influence of climate and management on survival probability for Germany's most important tree species. *For. Ecol. Manag.* **458**, 117652, 1–9.

Brück-Dyckhoff, C. 2017 *Zur Beteiligung des Buchenprachtkäfers (Agrilus viridis L.) an Vitalitätsverlusten älterer Rotbuchen (Fagus sylvatica L.)*, Dissertation, Technical University of Munich, p. 241.

Caudullo, G., Welk, E. and San-Miguel-Ayanz, J. 2017 Chorological maps for the main European woody species. *Data Brief* **12**, 662–666.

Chakraborty, T., Reif, A., Matzarakis, A. and Saha, S. 2021 How does radial growth of water-stressed populations of European beech (*Fagus sylvatica* L.). Trees vary under multiple drought events? *Forests* **12**, 129.

Choat, B., Jansen, S., Brodribb, T.J., Cochard, H., Delzon, S., Bhaskar, R., *et al.* 2012 Global convergence in the vulnerability of forests to drought. *Nature* **491**, 752–755.

Cuervo-Alarcon, L., Arend, M., Müller, M., Sperisen, C., Finkeldy, R. and Krutovsky, K.V. 2021 A candidate gene association analysis identifies SNPs potentially involved in drought tolerance in European beech (*Fagus sylvatica* L.). *Sci. Rep.* **11**, 2386.

Čufar, K., Prislán, P., Luis, M.d. and Gričar, J. 2008 Tree-ring variation, wood formation and phenology of beech (*Fagus sylvatica*) from a representative site in Slovenia, SE Central Europe. *Trees* **22**, 749–758.

Da Silveira, L., Sternberg, L., Mulkey, S.S. and Wright, S.J. 1989 Ecological interpretation of leaf carbon isotope ratios: influence of respired carbon dioxide. *Ecology* **70**, 1317–1324.

- Davis, K.T., Dobrowski, S.Z., Holden, Z.A., Higuera, P.E. and Abatzoglou, J.T. 2019 Microclimatic buffering in forests of the future: the role of local water balance. *Ecography* **42**, 1–11.
- Del Martinez Castillo, E., Zang, C.S., Buras, A., Hacket-Pain, A., Esper, J., Serrano-Notivol, R., et al. 2022 Climate-change-driven growth decline of European beech forests. *Commun Biol* **5**, 163.
- Deutscher Wetterdienst (DWD). 2022a *Lufttemperatur: vieljährige Mittelwerte 1991–2020*. https://www.dwd.de/DE/leistungen/klimadatendeutschland/mittelwerte/temp_9120_SV_html.html;jsessionid=9F4792D80B666AA6CF1C9A2384B77AAF.live31081?view=nasPublicatio n&nn=16102 (accessed on 29 June, 2022).
- Deutscher Wetterdienst (DWD). 2022b *Niederschlag: vieljährige Mittelwerte 1991–2020*. https://www.dwd.de/DE/leistungen/klimadatendeutschland/mittelwerte/nieder_9120_SV_html.html;jsessionid=9F4792D80B666AA6CF1C9A2384B77AAF.live31081?view=nasPublicatio n&nn=16102 (accessed on 29 June, 2022).
- Diaconu, D., Kahle, H.-P. and Spiecker, H. 2017 Thinning increases drought tolerance of European beech: a case study on two forested slopes on opposite sides of a valley. *Eur. J. Forest Res.* **136**, 319–328.
- Dobbertin, M., Eilmann, B., Bleuler, P., Giugliola, A., Graf Pannatier, E., Landolt, W., et al. 2010 Effect of irrigation on needle morphology, shoot and stem growth in a drought-exposed *Pinus sylvestris* forest. *Tree Physiol.* **30**, 346–360.
- Dobbertin, M., Hug, C. and Waldner, P. 2009 *Kronenverlichtung. Sterberaten und Waldwachstum in Langzeitstudien–Welche Indikatoren beschreiben den Waldzustand am besten: Forum für Wissen 2009*. Swiss Federal Research Institute WSL.
- Ellenberg, H. and Leuschner, C. 2010 *Vegetation Mitteleuropas mit den Alpen: In ökologischer, dynamischer und historischer Sicht; 203 Tabellen*. 6th edn. Ulmer, p. 1333.
- Elling, W., Heber, U., Polle, A. and Beese, F. 2007 *Schädigung von Waldökosystemen: Auswirkungen anthropogener Umweltveränderungen und Schutzmaßnahmen*. 1st edn. Elsevier Spektrum Akademischer Verlag, p. 422.
- Farquhar, G.D., Ehleringer, J.R. and Hubick, K.T. 1989 Carbon isotope discrimination and photosynthesis. *Annu. Rev. Plant Physiol. Plant Mol. Biol.* **50**, 503–537.
- Frenne, P., Rodríguez-Sánchez, F., Coomes, D.A., Baeten, L., Verstraeten, G., Vellend, M., et al. 2013 Microclimate moderates plant responses to macroclimate warming. *Proc. Natl. Acad. Sci. U. S. A.* **110**, 18561–18565.
- Gärtner, H. and Nievergelt, D. 2010 The core-microtome: a new tool for surface preparation on cores and time series analysis of varying cell parameters. *Dendrochronologia* **28**, 85–92.
- GeoSLAM 2020 *GeoSLAM Hub*. Version 6.1.
- Gessler, A., Ferrio, J.P., Hommel, R., Treydte, K., Werner, R.A. and Monson, R.K. 2014 Stable isotopes in tree rings: towards a mechanistic understanding of isotope fractionation and mixing processes from the leaves to the wood. *Tree Physiol.* **34**, 796–818.
- GreenValley International, Ltd 2019 *LiDAR360; Version: v4.1.5. Software*. Green Valley International.
- Grote, R., Gessler, A., Hommel, R., Poschenrieder, W. and Priesack, E. 2016 Importance of tree height and social position for drought-related stress on tree growth and mortality. *Trees* **30**, 1467–1482.
- Hacket-Pain, A.J., Friend, A.D., Lageard, J.G.A. and Thomas, P.A. 2015 The influence of masting phenomenon on growth-climate relationships in trees: explaining the influence of previous summers' climate on ring width. *Tree Physiol.* **35**, 319–330.
- Hacket-Pain, A.J., Lageard, J.G.A. and Thomas, P.A. 2017 Drought and reproductive effort interact to control growth of a temperate broadleaved tree species (*Fagus sylvatica*). *Tree Physiol.* **37**, 744–754.
- Hanba, Y.T., Mori, S., Lei, T.T., Koike, T. and Wada, E. 1997 Variations in leaf $\delta^{13}C$ along a vertical profile of irradiance in a temperate Japanese forest. *Oecologia* **110**, 253–261.
- Hari, V., Rakovec, O., Markonis, Y., Hanel, M. and Kumar, R. 2020 Increased future occurrences of the exceptional 2018–2019 Central European drought under global warming. *Sci. Rep.* **10**, 1–10.
- Hoch, G., Siegwolf, R.T.W., Keel, S.G., Körner, C. and Han, Q. 2013 Fruit production in three masting tree species does not rely on stored carbon reserves. *Oecologia* **171**, 653–662.
- IPCC Intergovernmental Panel on Climate Change (ed.) 2018 *Global Warming of 1.5°C. An IPCC Special Report on the Impacts of Global Warming of 1.5°C above Pre-Industrial Levels and Related Global Greenhouse Gas Emission Pathways, in the Context of Strengthening the Global Response to the Threat of Climate Change, Sustainable Development, and Efforts to Eradicate Poverty*. In Press, p. 630.
- Jump, A.S., Hunt, J.M. and Peñuelas, J. 2006 Rapid climate change-related growth decline at the southern range edge of *Fagus sylvatica*. *Glob. Chang. Biol.* **12**, 2163–2174.
- Knohl, A., Werner, R.A., Brand, W.A. and Buchmann, N. 2005 Short-term variations in $\delta^{13}C$ of ecosystem respiration reveals link between assimilation and respiration in a deciduous forest. *Oecologia* **142**, 70–82.
- Kraft, G. 1884 *Beiträge zur Lehre von den Durchforstungen, Schlagstellungen und Lichtungshieben*. Klindworth.
- Kuhn, M. 2022 *Caret: Classification and Regression Training. R package version 6.0–6.92*.
- Leuschner, C. 2009 *Die Trockenheitsempfindlichkeit der Rotbuche vor dem Hintergrund des prognostizierten Klimawandels*. Jahrbuch der Akademie der Wissenschaften zu Göttingen, Göttingen, pp. 281–296.
- Leuschner, C. 2020 Drought response of European beech (*Fagus sylvatica* L.)—a review. *Perspect. Plant Ecol. Evol. Syst.* **47**, 125576. <https://doi.org/10.1016/j.ppees.2020.125576>.
- Leuschner, C., Wedde, P. and Lübke, T. 2019 The relation between pressure-volume curve traits and stomatal regulation of water potential in five temperate broadleaf tree species. *Ann. For. Sci.* **76**, 1–14.
- Li, W., Guo, Q., Jakubowski, M.K. and Kelly, M. 2012 A new method for segmenting individual trees from the Lidar point cloud. *Photogr. Eng. Remote Sens.* **78**, 75–84.
- Lu, P., Biron, P., Granier, A. and Cochard, H. 1996 Water relations of adult Norway spruce (*Picea abies* (L) Karst) under soil drought in the Vosges mountains: whole-tree hydraulic conductance, xylem embolism and water loss regulation. *Ann. For. Sci.* **53**, 113–121.
- Lüttschwager, D. and Jochheim, H. 2020 Drought primarily reduces canopy transpiration of exposed beech trees and decreases the share of water uptake from deeper soil layers. *Forests* **11**, 537.
- LWF – Bayerische Landesanstalt für Wald und Forstwirtschaft. 2005 *Walddatlas Bayern*, p. 137
- Manion, P.D. 1981 *Tree Disease Concepts*. Prentice-Hall, Inc.
- Maringer, J., Stelzer, A.-S., Paul, C. and Albrecht, A.T. 2021 Ninety-five years of observed disturbance-based tree mortality modeled with climate-sensitive accelerated failure time models. *Eur. J. Forest Res.* **140**, 255–272.
- McDowell, N.G., Adams, H.D., Bailey, J.D., Hess, M. and Kolb, T.E. 2006 Homeostatic maintenance of ponderosa pine gas exchange in response to stand density changes. *Ecol. Appl.* **16**, 1164–1182.
- McDowell, N.G., Pockman, W.T., Allen, C.D., Breshears, D.D., Cobb, N., Kolb, T., et al. 2008 Mechanisms of plant survival and mortality during drought: why do some plants survive while others succumb to drought? *New Phytol.* **178**, 719–739.

- Meier, I.C. and Leuschner, C. 2008 Genotypic variation and phenotypic plasticity in the drought response of fine roots of European beech. *Tree Physiol.* **28**, 297–309.
- Meyer, P., Spînu, A.P., Mölder, A. and Bauhus, J. 2022 Management alters drought-induced mortality patterns in European beech (*Fagus sylvatica* L.) forests. *Plant Biol.* **24**, 1157–1170.
- Michelot, A., Simard, S., Rathgeber, C., Dufrière, E. and Damesin, C. 2012 Comparing the intra-annual wood formation of three European species (*Fagus sylvatica*, *Quercus petraea* and *Pinus sylvestris*) as related to leaf phenology and non-structural carbohydrate dynamics. *Tree Physiol.* **32**, 1033–1045.
- Mölder, I., Leuschner, C. and Leuschner, H.H. 2011 $\delta^{13}\text{C}$ signature of tree rings and radial increment of *Fagus sylvatica* trees as dependent on tree neighborhood and climate. *Trees* **25**, 215–229.
- Odum, E.P. 1959 Fundamentals of ecology. *J. Range Manag.* **12**, 313.
- Oren, R., Phillips, N., Katul, G., Ewers, B.E. and Pataki, D.E. 1998 Scaling xylem sap flux and soil water balance and calculating variance: a method for partitioning water flux in forests. *Ann. For. Sci.* **55**, 191–216.
- Porter, T.J., Pisarcik, M.F.J., Kokelj, S.V. and Edwards, T.W.D. 2009 Climatic signals in $\delta^{13}\text{C}$ and $\delta^{18}\text{O}$ of tree-rings from white spruce in the Mackenzie Delta region, northern Canada. *Arct. Antarct. Alp. Res.* **41**, 497–505.
- Pretzsch, H. 2019 *Grundlagen der Waldwachstumsforschung*. Springer, p. 676.
- R Core Team 2020 R: A Language and Environment for Statistical Computing.
- Rakovec, O., Hari, V., Markonis, Y., Samaniego, L., Hanel, M., Thober, S., et al. 2020 The 2018–2019 European Drought Sets a New Benchmark over 250 Years, EGU General Assembly Conference Abstracts. <https://doi.org/10.5194/egusphere-egu2020-6881>.
- Rinntech Version 4 TSAP-Win, Version: 4 Scientific. Rinntech.
- Roussel, J.-R., Auty, D., Coops, N.C., Tompalski, P., Goodbody, T.R., Meador, A.S., et al. 2020 lidar: an R package for analysis of airborne laser scanning (ALS) data. *Remote Sens. Environ.* **251**, 112061.
- Scharnweber, T., Manthey, M., Criegee, C., Bauwe, A., Schröder, C. and Wilking, M. 2011 Drought matters – declining precipitation influences growth of *Fagus sylvatica* L. and *Quercus robur* L. in North-Eastern Germany. *For. Ecol. Manag.* **262**, 947–961.
- Schollaen, K., Baschek, H., Heinrich, I., Slotta, F., Pauly, M. and Helle, G. 2017 A guideline for sample preparation in modern tree-ring stable isotope research. *Dendrochronologia* **44**, 133–145.
- Schuld, B., Buras, A., Arend, M., Vitasse, Y., Beierkuhnlein, C., Damm, A., et al. 2020 A first assessment of the impact of the extreme 2018 summer drought on central European forests. *Basic Appl. Ecol.* **45**, 86–103.
- Seidel, D. 2018 A holistic approach to determine tree structural complexity based on laser scanning data and fractal analysis. *Ecol. Evol.* **8**, 128–134.
- Seidel, D., Annighöfer, P., Stiers, M., Zemp, C.D., Burkardt, K., Ehbrecht, M., et al. 2019 How a measure of tree structural complexity relates to architectural benefit-to-cost ratio, light availability, and growth of trees. *Ecol. Evol.* **9**, 7134–7142.
- Seidel, D., Schall, P., Gille, M. and Ammer, C. 2015 Relationship between tree growth and physical dimensions of *Fagus sylvatica* crowns assessed from terrestrial laser scanning. *iForest* **8**, 735–742.
- Seidel, H., Schunk, C., Matiu, M. and Menzel, A. 2016 Diverging drought resistance of scots pine provenances revealed by infrared thermography. *Front. Plant Sci.* **7**, 1247.
- Seidl, R., Thom, D., Kautz, M., Martin-Benito, D., Peltoniemi, M., Vacchiano, G., et al. 2017 Forest disturbances under climate change. *Nat. Clim. Chang.* **7**, 395–402.
- Skomarkova, M.V., Vaganov, E.A., Mund, M., Knohl, A., Linke, P., Boerner, A., et al. 2006 Inter-annual and seasonal variability of radial growth, wood density and carbon isotope ratios in tree rings of beech (*Fagus sylvatica*) growing in Germany and Italy. *Trees* **20**, 571–586.
- Sohn, J.A., Saha, S. and Bauhus, J. 2016 Potential of forest thinning to mitigate drought stress: a meta-analysis. *For. Ecol. Manag.* **380**, 261–273.
- StMELF – Bayerisches Staatsministerium für Ernährung, Landwirtschaft und Forsten 2020 *Waldbericht 2020*. Bayerisches Staatsministerium für Ernährung, Landwirtschaft und Forsten, p. 40.
- Stovall, A.E.L., Shugart, H. and Yang, X. 2019 Tree height explains mortality risk during an intense drought. *Nat. Commun.* **10**, 4385.
- Thünen-Institut – Dritte Bundeswaldinventur – Ergebnisdatenbank 2012 <https://bwi.info>, Aufruf am: 19.06.2020, Auftragskürzel: 7721JI_L235of_2012_bi, Archivierungsdatum: 2014-6-10 16:7:59.927. Überschrift: Waldfläche (gemäß Standflächenanteil) [ha] nach Land und Baumartengruppe, Filter: Jahr = 2012.
- van der Maaten, E. 2012 Climate sensitivity of radial growth in European beech (*Fagus sylvatica* L.) at different aspects in southwestern Germany. *Trees* **26**, 777–788.
- van Nes, E.H., Arani, B.M.S., Staal, A., van der Bolt, B., Flores, B.M., Bathiany, S., et al. 2016 What do you mean, 'Tipping Point'? *Trends Ecol. Evol.* **31**, 902–904.
- van Wittenberghe, S., Adriaenssens, S., Staelens, J., Verheyen, K. and Samson, R. 2012 Variability of stomatal conductance, leaf anatomy, and seasonal leaf wettability of young and adult European beech leaves along a vertical canopy gradient. *Trees* **26**, 1427–1438.
- Walentowski, H. 2006 *Handbuch der natürlichen Waldgesellschaften Bayerns: Ein auf geobotanischer Grundlage entwickelter Leitfaden für die Praxis in Forstwirtschaft und Naturschutz*. 2nd edn. Geobotanica, p. 441.
- Walthert, L., Ganthaler, A., Mayr, S., Saurer, M., Waldner, P., Walsler, M., et al. 2021 From the comfort zone to crown dieback: sequence of physiological stress thresholds in mature European beech trees across progressive drought. *Sci. Total Environ.* **753**, 141792, 1–14.
- Weber, P., Bugmann, H., Pluess, A.R., Walthert, L. and Rigling, A. 2013 Drought response and changing mean sensitivity of European beech close to the dry distribution limit. *Trees* **27**, 171–181.
- Weithmann, G., Schuld, B., Link, R.M., Heil, D., Hoerber, S., John, H., et al. 2021 Leaf trait modification in European beech trees in response to climatic and edaphic drought. *Plant Biol.* **24**, 1272–1286.
- Wellbrock, N. and Eickenscheidt, N. 2018 *Leitfaden und Dokumentation zur Waldzustandserhebung in Deutschland*. Johann Heinrich von Thünen-Institut.
- Whitehead, D., Jarvis, P.G. and Waring, R.H. 1984 Stomatal conductance, transpiration, and resistance to water uptake in a *Pinus sylvestris* spacing experiment. *Can. J. For. Res.* **14**, 692–700.
- FAO. 2014 *World Reference Base for Soil Resources 2014: International Soil Classification System for Naming Soils and Creating Legends for Soil Maps*. Food and Agriculture Organization of the United Nations.
- Zang, C., Pretzsch, H. and Rothe, A. 2012 Size-dependent responses to summer drought in scots pine, Norway spruce and common oak. *Trees* **26**, 557–569.
- Zellweger, F., Frenne, P.d. and Coomes, D. 2020 Forest microclimate dynamics drive plant responses to warming. *Science* **368**, 772–775.
- Zhang, W., Qi, J., Wan, P., Wang, H., Xie, D., Wang, X., et al. 2016 An easy-to-use airborne LiDAR data filtering method based on cloth simulation. *Remote Sens.* **8**, 1–22.
- Zimmermann, L. and Raspe, S. 2019 *Jahrhundertsommer* Nr. 3. *LWF aktuell* **119**, 56–58.
- Zimmermann, L., Raspe, S., Dietrich, H.-P. and Wauer, A. 2020 Dürreperioden und ihre Wirkung auf Wälder. *LWF aktuell* **126**, 18–23.

12.3 Paper III

Note: Please note that this Paper is not open access.

Forest Ecology and Management 554 (2024) 121667



Contents lists available at ScienceDirect

Forest Ecology and Management

journal homepage: www.elsevier.com/locate/foreco



The effect of forest structure on drought stress in beech forests (*Fagus sylvatica* L.)

Thomas Mathes^{a,*,}, Dominik Seidel^b, Hans-Joachim Klemmt^c, Dominik Thom^d, Peter Annighöfer^a

^a Professorship of Forest and Agroforest Systems, Technical University of Munich, Hans-Carl-v.-Carlowitz-Platz 2, D-85354 Freising, Germany

^b Spatial Structures and Digitization of Forests, University of Göttingen, Büsgenweg 1, D-37077 Göttingen, Germany

^c Departement "Silviculture and Mountain Forests", Bavarian Forest Institute (LWF), Hans-Carl-v.-Carlowitz-Platz 1, D-85354 Freising, Germany

^d Ecosystem Dynamics and Forest Management Group, Technical University of Munich, Hans-Carl-v.-Carlowitz-Platz 2, D-85354 Freising, Germany

ARTICLE INFO

Keywords:
Resistance
Basal area increment
Stable isotope ($\delta^{13}\text{C}$)
Defoliation
Box-dimension
Clark-Evans

ABSTRACT

The unprecedented drought between 2018 and 2020 had a significant impact on European beech (*Fagus sylvatica* L.) forests in Central Europe. The role of different forest structures in mitigating drought stress remains controversial. This contentious debate prompted our study, in which we aimed to quantify the effect of forest structure on drought stress in beech forests in two ecoregions of northern Bavaria, Germany. Using a mobile laser scanner, we surveyed 240 plots in drought-stressed forests. We analyzed the responses of beech trees to the drought period through radial growth, wood-derived $\delta^{13}\text{C}$ signal, and crown defoliation. Results revealed significant responses of beech forests in both regions to the drought event, including increased crown defoliation, reduced tree growth, and altered $\delta^{13}\text{C}$ signatures compared to pre-drought conditions. Our results show a relationship between crown closure and crown defoliation in beech, suggesting an increased vulnerability of beech to drought in more open canopies. However, the potential for silvicultural intervention to mitigate drought stress, as measured by BAI and $\delta^{13}\text{C}$ signal, appears limited. Neighboring trees and forest structure had little influence on average drought resistance. The $\delta^{13}\text{C}$ signal showed minimal responsiveness to variations in canopy openness, as well as to distinctions between single and multi-layered forests. However, increased structural complexity within stands tended to increase resistance due to the compensatory effects of understorey trees. Future forest management strategies could focus on promoting structural diversity, selecting resilient individuals but also actively enrich the forests with more drought-adapted species to increase the adaptive capacity of beech-dominated forests in the face of changing climate conditions.

1. Introduction

The unprecedented drought during 2018–2020 had severe impacts on forests in Central Europe (Senf and Seidl, 2021; Thonfeld et al., 2022; Thom et al., 2023). Tree mortality of 14 million cubic meters in hardwoods was recorded, with a large proportion of this attributed to European beech (*Fagus sylvatica* L.) (BMEL, 2021). Moreover, severe growth decline (Scharmweber et al., 2020; Leuschner et al., 2023), partial or complete crown dieback, early leaf shedding, and leaf discoloration have been reported for beech (Nussbaumer et al., 2020; Bigler and Vitasse, 2021; Arend et al., 2022; BMEL, 2022). In addition, beech became susceptible to secondary disease attacks leading to mortality in trees with reduced vigor and defense capacity (Corcobado et al.,

2020; Langer and Bußkamp, 2021).

A disturbance hotspot was located in northern Bavaria (StMELF, 2023). In 1986, Plochmann and Hieke (1986) concluded that drought has played only a minor role in the disturbance regime of the forests in Bavaria during the last 200 years. However, with ongoing climate change, the frequency and magnitude of extreme drought events have already increased and will further increase, unless greenhouse gas emissions will be drastically reduced (Hari et al., 2020; Hammond et al., 2022; Rakovec et al., 2022). Because of their comparatively slow natural adaptation rates, forest ecosystems are particularly vulnerable to extreme climatic events (Allen et al., 2010).

The dieback of beech is highly relevant, as it is currently Europe's most abundant deciduous tree species (Forest Europe, 2020). In the near

* Corresponding author.

E-mail address: thomas.mathes@tum.de (T. Mathes).

<https://doi.org/10.1016/j.foreco.2023.121667>

Received 17 September 2023; Received in revised form 17 December 2023; Accepted 20 December 2023

Available online 28 December 2023

0378-1127/© 2023 Elsevier B.V. All rights reserved.

future, beech will become even more important, as its proportion in the regeneration layer is significantly higher than in the old-growth stands, according to the results of many national forest inventories (Forest Europe, 2020). Many beech stands are presently in a mature phase (Thünen-Institut, 2012) and must be adapted to the changing climate. One option could be to increase the resistance or resilience of beech-dominated forests to climate extremes through changes in their structure, induced by silvicultural measures such as thinnings.

However, the effectiveness of thinnings to reduce drought stress is discussed controversially. On the one hand, studies recommend heavy thinnings to mitigate the effects of drought on remaining trees (Laurent et al., 2003; Martín-Benito et al., 2010; Sankey and Tatum, 2022). That is because thinnings reduce total transpiration, interception rates, and competition among trees in the short term, which increases soil water availability and improves root development (Aussenac and Granier, 1988; Lagergren et al., 2008; Sohn et al., 2016b; Gavinet et al., 2019). Positive effects have also been observed in terms of tree growth performance, mortality, and vigor (Bréda et al., 1995; Bréda et al., 2006; Kohler et al., 2010; Brooks and Mitchell, 2011; Gebhardt et al., 2014; Sohn et al., 2016a).

On the other hand, however, adverse effects of thinnings can also occur. A changed radiation regime within the stand or the establishment of vital ground vegetation after thinning can reduce water availability in the soil and increase the water demand of exposed trees, which can offset the positive effects of thinnings (McDowell et al., 2006; Brooks and Mitchell, 2011; Gebhardt et al., 2014; Bosela et al., 2021). In addition, excessive thinning results in reduced structural complexity and a lower attenuating effect of the stand interior climate, which can lead to greater temperature and humidity extremes (Aussenac, 2000; Ehbrecht et al., 2017; Thom et al., 2020). For beech, practical observations indicate that sometimes heavily thinned stands are affected by significant damage such as sun scald or crown defoliation.

Thus, different thinning intensities could be a typical trade-off system that has yet to be accounted for beech. Our study aims to gain in-depth knowledge about the relationship between forest structures and drought stress in beech forests. We seek to complement the scientific fortification for climate-adaptive silviculture in beech-dominated forests and adaptation strategies to climate change. To that end, we are coupling mobile laser scanning techniques and retrospective data analyses in an innovative approach. We accounted for the response of beech trees to the drought period via radial growth, the $\delta^{13}\text{C}$ -signal, and crown defoliation. These indicators provide complementary information as tree rings reveal reduced growth during drought, $\delta^{13}\text{C}$ signals provide information on drought stress and carbon fixation, and crown defoliation indicates drought stress.

For our study, we chose two regions in Northern Bavaria with evidence of site dependence on drought response (Scharnweber et al., 2011; Thom et al., 2023; Weigel et al., 2023). The null hypotheses of this study, which we have listed below, are based on the assumption that many Central European forest enterprises pursue the goal of creating multi-layered forests with their silvicultural concepts (e.g., BaySF, 2011). This objective is based on the assumption that such forests have higher resilience to disturbances, for which there is quit some theoretical reasoning (Seidel and Ammer, 2023). Therefore, we assumed multilayered beech forests were less affected by the drought period from 2018 to 2020. Accordingly, our hypotheses are as follows:

H1. Beech forests in both study regions responded to the drought period with (1) defoliation, (2) growth decline, and (3) an increase in the $\delta^{13}\text{C}$ signature.

H2. With increasing canopy openness, (1) defoliation and (2) growth decline was greater, and (3) the $\delta^{13}\text{C}$ signature was more pronounced.

H3. Multi-layered beech forests exhibited (1) lower canopy defoliation and (2) higher resistance (as measured by tree growth and $\delta^{13}\text{C}$ signature) to the drought period compared to single-layered forests.

2. Materials and methods

2.1. Study area

This study was conducted in two ecoregions of northern Bavaria ("Plateau" and "Steigerwald"). The first study area, located near Würzburg (Latitude: 49.7286 N, Longitude: 9.8156E (WGS 84)), is on the Southern Franconian Plateau ("Plateau"). During the reference period of 1991–2020, this area exhibited a warm-dry climate, with an average annual temperature of approximately 10.1 °C and an average annual precipitation sum of 576 mm (DWD, 2022a, 2022b). According to the World Reference Base for Soil Resources (FAO, 2014), the soils in the Plateau are classified as Eutric Leptic Cambisol (Clayic) with a tendency towards Rendzic Leptic Phaeozem (Clayic). These soils are relatively shallow and originate from shell-bearing limestone. Due to their limited water-holding capacity, they are categorized as moderately dry to moderately fresh (Arbeitskreis Standortkartierung, 2016).

The second study area is located near Bamberg in the Steigerwald region ("Steigerwald") (Latitude: 49.8721 N, Longitude: 10.4724E). Compared to the Plateau, this region has a cooler climate with an average temperature of 8.6 °C and a higher average precipitation sum of 802 mm (DWD, 2022a, 2022b). The soils in the Steigerwald region have developed on Keuper and are classified as Dystric Cambisol (Loamic). These soils are deeper than those of the Plateau, resulting in a higher water-holding capacity (LWF, 2005). The Plateau and the Steigerwald experienced significant water deficits between 2018 and 2020 (Thom et al., 2023). Additional site information can be found in Mathes et al. (2023a).

2.2. Sampling design

For this study, only stands that met the following criteria were considered, in order to minimize differences in stand and site conditions: a) slopes below 10% were selected, b) soils were classified as Dystric Cambisol (Steigerwald) and Eutric Leptic Cambisol (Plateau), and c) stands were dominated by beech (species share > 80%), and without silvicultural treatments since 2018. The latter ensured that the forest structure recorded by the end of 2020 was not recently influenced by human disturbances such as thinning.

With a randomly chosen first point, a grid with a 60 × 60 m resolution was placed over this potential forest area. 240 plots were selected for fieldwork, with an equal distribution of 120 plots in both study regions. The selection criteria for the plots included a minimum distance of 50 m from recently disturbed areas or forest edges to minimize the influence of edge effects. The chosen plots aimed to represent various combinations of social positions of the trees (dominant, subordinate), tree dimensions (diameter at breast height (dbh)), and forest structures (single-layered, double-layered/multi-layered) (Fig. 1). The classification of trees into dominant and subordinate categories is based on the approach developed by Kraft (1884), as detailed in Mathes et al. (2023a). In this classification, Kraft's classes 1 and 2 are termed 'dominant', while classes 4 and 5 are termed 'subordinate'. Specifically, 15 sample trees (central trees) were selected for each of the eight possible combinations (2 social positions × 2 tree dimensions × 2 canopy layers) per study site, resulting in 120 samples. Apart from these "central" trees, their closest neighbors were also included in the study. These neighboring trees, all European beech (*Fagus sylvatica* L.), were those that "touched" the central tree with their crowns. Depending on forest density, zero to seven neighbors were selected, resulting in an average of approximately four trees per plot in total.

2.3. Data collection

We collected all field data during winter 2020/2021 (leaf-off) and summer 2021 (leaf-on). A mobile laser scanner (MLS) (ZEB HORIZON, GeoSLAM Ltd., UK) captured three-dimensional data of individual trees

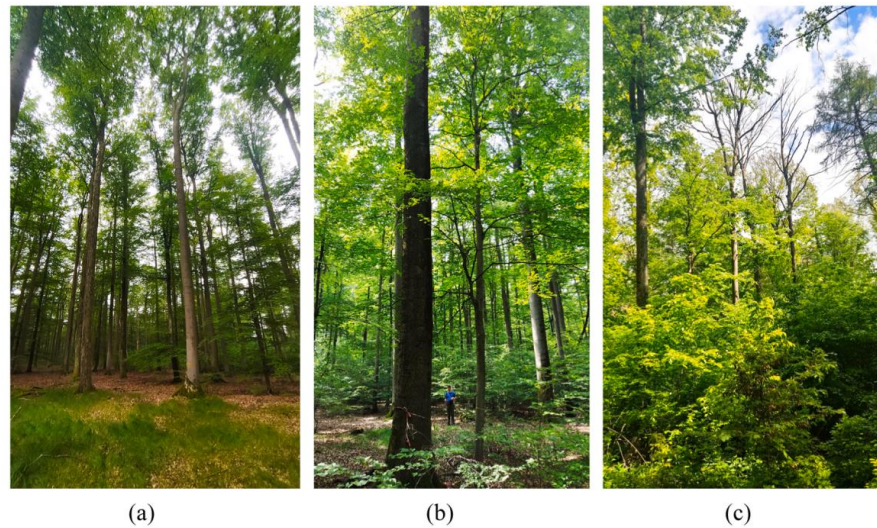


Fig. 1. Exemplary overview of selected mature beech stands; (a) single-layer stand, (b) single-layer stand with regeneration, (c) right: multi-layer stand. Pictures from July 2021, by T. Mathes.

and the surrounding forest structure during the leaf-off season. The MLS was used to scan the forest within a 30 m radius around the central tree. Beginning from the south, the MLS path systematically spiraled around the central tree, progressively increasing the radii at approximately 7 m, 14 m, 21 m, 28 m, and 35 m. Using the time-of-flight principle during scanning and SLAM (simultaneous localization and mapping) technology during post-processing, the mobile scanner continuously captured the surroundings up to a range of 100 m from the device.

During the winter campaign, two core samples per tree were extracted at breast height (1.3 m) from each sample tree using a standard increment borer (Haglöf Mora Coretax, diameter 5.15 mm) with a 90° angle between them (north and east directions).

In the summer campaign, the crown conditions of the sample trees were assessed as an indicator of their vitality. The assessment involved assigning the trees to defoliation classes categorized in 5% steps. A rating of 0% indicated complete foliage, while 100% represented complete defoliation. This assessment methodology aligns with the forest status assessment approach used in Germany (Wellbrock and Eickenscheidt, 2018). In addition, the crown closure was visually assessed and classified into different levels: "crowded" when crowns interlock deeply, "closed" when crowns touch each other, "loose" when crown spacing is less than a crown width, "light" when crown spacing equals a crown width, and "discontinuous" crown closure when the crown spacing exceeds a crown width.

2.4. Data processing

2.4.1. Tree core samples

The width of the annual growth rings was determined by horizontally cutting the tree cores in the ring direction using a core microtome. The cores were then air-dried, and their ring widths were measured to the nearest 0.01 mm. This measurement was performed using a measuring table (LINTAB 5; Rinntech, Heidelberg, Germany) equipped with a stereo microscope (MZ 6; Leica, Wetzlar; Germany) and the TSAP-Win software (Rinntech, Version 4). Cross-dating was performed using site samples of cores whose annual rings were clearly recognizable. In instances where annual rings were missing, a standardized value of

0.01 mm was assumed. The average measurement of the two cores taken from each tree was computed to build a chronology for each tree.

2.4.2. Stable Isotope Analysis ($\delta^{13}\text{C}$)

The tree cores taken in the northern direction of each stem provided annual rings for the years 2016–2020. The samples were finely powdered using a ball mill (MM200, Retsch, Haan, Germany). To minimize potential bias from plastic microtubes, stainless steel microvials (BioSpec, Bartlesville, USA) and four-millimeter stainless steel balls were used. The microvials were clamped in the ball mill, subjecting each sample to two ten-minute grinding cycles at a frequency of 25 s⁻¹, with a 30-second pause between cycles to prevent overheating.

For $\delta^{13}\text{C}$ measurement, the wood samples were weighed into tin capsules. The samples were combusted in an elemental analyzer (NA 1110; Carlo Erba, Milan, Italy, and Vario Pyro Cube, Elementar, Hanau, Germany) connected to an isotope-ratio mass spectrometer (Delta Plus; Finnigan MAT and IsoPrime 100, Isoprime, Stockport, UK) through a ConFlo III reference system. The measurements were compared against a laboratory working standard CO₂ gas, previously calibrated against a secondary isotope standard (IAEA-CH6 for $\delta^{13}\text{C}$, calibration accuracy: 0.06% SD). A solid internal laboratory standard (SILS) of wheat flour was calibrated against these references and ran after every tenth sample. The long-term precision for the SILS was below 0.2%. Carbon isotope data are presented as $\delta^{13}\text{C}$ relative to the international Vienna Pee Dee Belemnite (VPDB) standard using the equation: $\delta^{13}\text{C} [\text{‰}] = [(R_{\text{sample}}/R_{\text{standard}}) - 1] \times 1000$, where R_{sample} and R_{standard} represent the ratios of $^{13}\text{C}/^{12}\text{C}$ in the sample and standard, respectively.

2.4.3. Laserscan data

Each point cloud was clipped to a 30 m radius around its respective central tree (R package "lidR" (Roussel et al., 2020)). The ground points were classified with the Ground Segmentation Algorithm (Zhang et al., 2016). The height of the points was normalized using the Spatial Interpolation Algorithm (interpolation was done using a k-nearest neighbor approach with an inverse-distance weighting). The point clouds were then voxelized to a resolution of 20 cm. Mathes et al. (2023b) showed that a voxel size of 20 cm is appropriate to reduce

occlusion effects while still providing enough detail.

The 30 m cutting radius around the central tree was chosen to analyze the entire stand structure. In addition, the 10 m radius was analyzed to study the direct neighborhood. To quantify possible effects of direct solar radiation on the beech trees, the point cloud with the ten-meter radius was reduced to the southern half (“Semicircle”) and exported as another point cloud for further analysis (Fig. 2).

We used the aggregation index by Clark and Evans (Clark and Evans, 1954) to calculate the spatial description of the point distribution (CE index) (comp. Fig. 3). The CE index is widely used to characterize forest structures (e.g., Willim et al., 2020). It examines the horizontal distribution of objects for clumping or regularity. The calculated value theoretically ranges from 0 (strongest clumping, where all objects are at the same point) to 2.1491 (strictly regular hexagonal pattern). Aggregation values less than 1.0 indicate a tendency toward clumping, values around 1.0 indicate a random distribution and values above 1.0 indicate a trend toward a regular distribution. Before calculating the CE index, we projected the 1 m thick horizontal strata onto a plane by setting the z-value of each voxel to zero. Duplicate voxels were deleted. To avoid edge bias, Donnelly edge correction was applied (Donnelly, 1978). The calculation was performed with the R package “spatstat” (Baddeley and Turner, 2005).

The box-dimension is a valuable metric for assessing the structural complexity of trees or forests (Seidel, 2018; Seidel and Ammer, 2023). It is commonly employed to distinguish between different forest structures, as demonstrated in previous studies (e.g., Stiers et al., 2020). This metric considers the density and three-dimensional distribution of objects simultaneously. Box-dimensions were calculated for the entire forest. The upper threshold for this calculation was determined by the maximum tree height, while the lower threshold, which determines the minimum box edge length used in the box dimension calculation, was defined as the voxel size.

Furthermore, the specific point clouds were processed using LiDAR360 software (GreenValley International, Ltd, 2019) to identify and extract individual trees. The tree segmentation algorithm applied was based on the method described by Li et al. (2012). From the resulting single tree point clouds, LiDAR360 was used to calculate tree height, the diameter at breast height (dbh), as well as to determine the positions of the sample trees. The Hegyi index, a distance-dependent competition index, was calculated based on the positions of the trees, considering the nearest ten neighbors determined by their tree trunk coordinates.

Furthermore, we utilized evenness (R Package “vegan” (Oksanen et al., 2022)) and skewness (R Package “e1071” (Meyer et al., 2023)) measures to assess (1) the distribution of the CE index with height and (2) the dbh and height distribution per plot. Evenness was employed to quantify the uniform distribution of the respective variable. Values closer to one indicate a high level of uniformity. Additionally, we calculated the skewness to identify any potential disproportionalities. Negative values indicate left-skewed distributions, representing a disproportional filling in the canopy layers for the CE index. In contrast, positive values indicate right-skewed distributions, indicating disproportional filling in the lower stand layers for the CE index. Values closer to zero suggest a more homogeneous distribution. For each of the three point clouds (30 m, 10 m, semicircle 10 m), we calculated the evenness and skewness of the CE index (CE skewness, CE evenness), as well as for the dbh- and the height- distribution per plot (dbh skewness, dbh evenness, height skewness, height evenness). Furthermore, the box-dimension, the mean dbh and height per plot, and the mean Hegyi index per plot were calculated (see Table 1).

2.5. Statistical analysis

2.5.1. Statistical tests

To determine differences between the individual canopy closure levels and the study regions, we used the Wilcoxon rank sum test with Bonferroni corrected p-values since normal distribution and homogeneity of variance could not be confirmed for all the studied variables. The significance level $p < 0.05$ was chosen for all statistical tests conducted in this study.

2.5.2. Resistance indices

To assess the tree-specific impact of water stress-induced growth reduction from 2016 to 2020, the Resistance Index (RT) was employed as the dependent variable. The index was computed by taking the ratio of the arithmetic mean values from 2020 and 2019 to the arithmetic mean values from 2016 and 2017. Modifying the resistance index was required since the drought period considered here was not a singular event for one year but lasted three years (2018–2020). Two Resistance indices were calculated: the Resistance Index for annual basal area increment (Resistance Index BAI) and the Resistance Index for the $\delta^{13}\text{C}$ signal (Resistance Index $\delta^{13}\text{C}$). A value of RT BAI less than 1 indicates that the average growth for 2019 and 2020 is lower than that for 2016 and 2017, suggesting reduced radial growth due to prolonged drought.

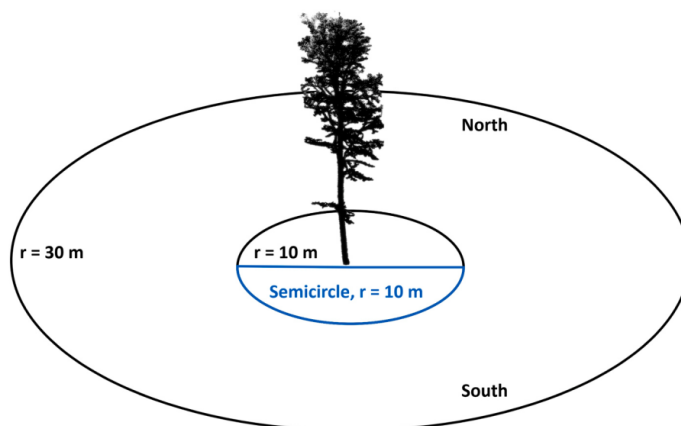


Fig. 2. Overview of the respective cutting radii. In addition to the point cloud with a radius of 30 m, a point cloud with a radius of 10 m was used, and a “semicircle” reducing the 10 m point cloud to the southern half around the central tree.

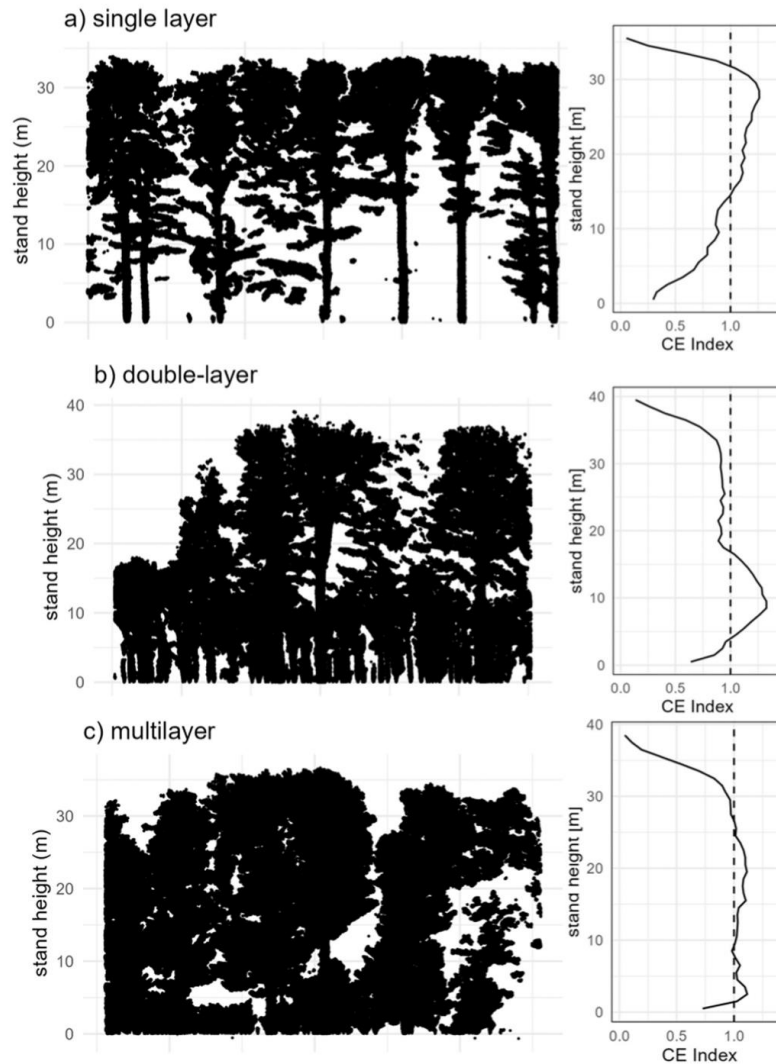


Fig. 3. Overview of exemplary selected stands (cross-section through the laser scan point clouds) and how their vertical space-filling can be characterized using the CE index. (a) single-layer stand, (b) double-layer stand, (c) multilayer stand.

Similarly, a value of $RT \delta^{13}C$ less than 1 indicates that the $\delta^{13}C$ discrimination for 2019 and 2020 is smaller than that for 2016 and 2017, suggesting a reduced stomata conductivity and potentially increased stress due to prolonged drought. We calculated the mean and standard deviation of the Resistance indices and the defoliation for each plot (mean BAI RT, sd BAI RT, mean $\delta^{13}C$ RT, sd $\delta^{13}C$ RT, mean defoliation, sd defoliation).

2.5.3. Non-linear models

After the z-transformation of all variables, the entire dataset underwent a Boruta analysis (R package “Boruta” (Kursa and Rudnicki, 2010)), a machine learning feature selection method. This analysis

helped identify which stand structural variables are potentially important to explain BAI and $\delta^{13}C$. These variables were then utilized to develop a generalized additive model (GAM). GAM is a flexible modeling approach accommodating non-linear relationships between predictors and the response variable. By incorporating the selected variables into the GAM framework and employing the restricted maximum likelihood (REML) method, an accurate estimation of model parameters while accounting for potential random effects was achieved. The data family was set to ‘Gaussian’ with an ‘identity-link function.’ (R package “mgcv” (Wood, 2011)). The number of knots was set to a maximum of three to avoid overfitting, with automated adaptation via generalized cross-validation. We tested concavity to identify potential

Table 1

The calculated variables per plot (z-transformed) with their mean and standard deviation (sd) for all plots.

variable	unit	mean	sd
mean dbh	meter	0.29	0.08
dbh skewness	-	1.00	0.94
dbh evenness	-	0.96	0.01
mean height	meter	22.23	4.78
height skewness	-	-0.15	1.08
height evenness	-	0.99	0.01
CE skewness	-	-1.04	0.60
CE evenness	-	0.98	0.01
box-dimension	-	2.36	0.04
Hegyi index	-	1.63	0.81

interpretation issues and unstable estimates.

In a subsequent analysis, we employed multiple logistic regression to further investigate the relationship between tree morphological variables and the resistance indices and defoliation. In this analysis, we focused on extreme values only to reduce data noise and obtain more robust associations, ultimately examining the plots that demonstrated the most pronounced reaction to the drought. To that end, we selected 10% of all plots that experienced the lowest and greatest drought response in terms of BAI, $\delta^{13}\text{C}$, and defoliation, respectively. Akaike's Information Criterion (AIC) was utilized to identify the explanatory variables of the most parsimonious model (R package "bestglm" (McLeod et al., 2020)). Subsequently, we investigated multicollinearity among the explanatory variables using a variance inflation factor. The Tjur R^2 was used to measure predictive power in multiple logistic regression models, quantifying the percentage difference in probabilities between observed events and random chance. Using Tjur R^2 also allows for evaluating the individual effect size of predictors in logistic regression.

Based on the multiple logistic regression analysis results, we used Odds Ratios (ORs) to assess the association between the independent variables and the resistance indices, respectively defoliation values (R package "sjPlot" (Lüdecke, 2023)). ORs indicate how the probability of the outcome changes with a one-unit increase in the independent variable. A value greater than 1 indicates a positive relationship, where an increase in the independent variable leads to higher odds and a higher probability of the outcome occurring. Conversely, a value less than 1 implies a negative relationship, where an increase in the independent variable is associated with lower odds and a lower probability of the outcome. ORs enable quantifying these relationships' strengths and direction while considering multiple variables in the logistic regression model.

In the study, all data were z-transformed for analysis. For all analyses, we employed the R language and environment for statistical computing in version 4.3.0 (R Core Team, 2023). We used the R package "ggplot2" (Wickham, 2016) for visualizations.

3. Results

3.1. Beech forests in both study regions responded to the drought period (H1)

In response to the 2018–2020 drought period, both study regions exhibited distinct defoliation, growth decline, and changes in the $\delta^{13}\text{C}$

signature compared to pre-drought (2016–2017) conditions (Table 2). Defoliation was evident in both regions and significantly differed from zero ($p < 0.01$). Additionally, both study regions experienced a decrease in growth, as evidenced by a BAI RT significantly less than 1 ($p < 0.01$). Finally, the divergence in $\delta^{13}\text{C}$ RT was significantly different from pre-drought conditions ($p < 0.01$).

Comparing the two study regions, beech trees lost about half of their original leaf mass (51%) in the Plateau, while they lost only 35% of their leaves in the Steigerwald ($p < 0.01$) (Table 2). The standard deviation was also significantly greater in the Plateau than in the Steigerwald ($p < 0.01$). The decline in growth was more pronounced in the Plateau, although the differences between the regions were not statistically significant ($p = 0.16$). The standard deviation of BAI was higher in the Plateau than in the Steigerwald ($p = 0.01$), indicating greater variability in growth response. The $\delta^{13}\text{C}$ signal showed no significant differences between the Plateau and the Steigerwald (mean: $p = 0.17$, sd: $p = 0.98$).

3.2. Canopy openness and drought response (H2)

With increasing canopy opening, significant changes in defoliation were observed for both study regions (Fig. 4). However, in contrast to these results, changes in canopy closure did not result in significant changes in BAI and $\delta^{13}\text{C}$ resistance indices for both study regions in response to the 2018–2020 drought period compared to pre-drought (2016–2017) conditions (slope parameter of the linear model: Plateau BAI RT (mean: $p = 0.50$, sd: $p = 0.54$), Plateau $\delta^{13}\text{C}$ (mean: $p = 0.18$, sd: $p = 0.50$); Steigerwald BAI RT (mean: $p = 0.77$, sd: $p = 0.10$), Steigerwald $\delta^{13}\text{C}$ (mean: $p = 0.33$, sd: $p = 0.11$)).

We observed a significant increase in defoliation for the beech trees in the Plateau with increasing canopy openness (Fig. 4, top left) ($p < 0.01$). In the Steigerwald, the closure levels "crowded" and "loose", as well as "crowded" and "light" differed significantly from each other. However, the slope parameter of the linear model was not significantly different from zero ($p = 0.19$) (Fig. 4, bottom left). The larger interquartile range for the Plateau indicates that the dispersion of observations was more pronounced than that in the Steigerwald. In the Steigerwald, the slope of the linear model in the standard deviation of defoliation was significantly different from zero ($p = 0.03$, Plateau $p = 0.05$).

3.3. Stand structure and drought response (H3)

3.3.1. Stand layers

We found no significant differences between multi-layer beech stands with respect to (1) canopy defoliation and (2) resistance (as indicated by tree growth and $\delta^{13}\text{C}$ signature) to the drought period compared to single or two-layered stands (Fig. 5). The most pronounced differences were found in the Plateau, with differences in mean defoliation ($p = 0.10$) and standard deviation of defoliation ($p = 0.08$) between single and multi-layered stands. In the Steigerwald, the most notable associations were found with respect to differences in mean defoliation ($p = 0.22$).

3.3.2. Stand structure variables

To classify the relationship between the forest structure variables derived from the laser scanning data on defoliation and resistance indices (BAI, $\delta^{13}\text{C}$), Boruta analysis identified several important

Table 2

Mean and standard deviation (sd) of defoliation, Resistance Index BAI, and Resistance Index $\delta^{13}\text{C}$ per plot for both study areas. An asterisk (*) marks significant differences between the two study areas. A plus (+) marks significant deviations from 0% for defoliation or from 1 for the RT values. The total sample size for Plateau and Steigerwald was $n = 120$.

Study region	mean defoliation (%)	sd defoliation (%)	mean BAI RT	sd BAI RT	mean $\delta^{13}\text{C}$ RT	sd $\delta^{13}\text{C}$ RT
Plateau	0.51 * +	0.15 *	0.87 +	0.38 *	0.97 +	0.03
Steigerwald	0.35 * +	0.09 *	0.93 +	0.29 *	0.97 +	0.03

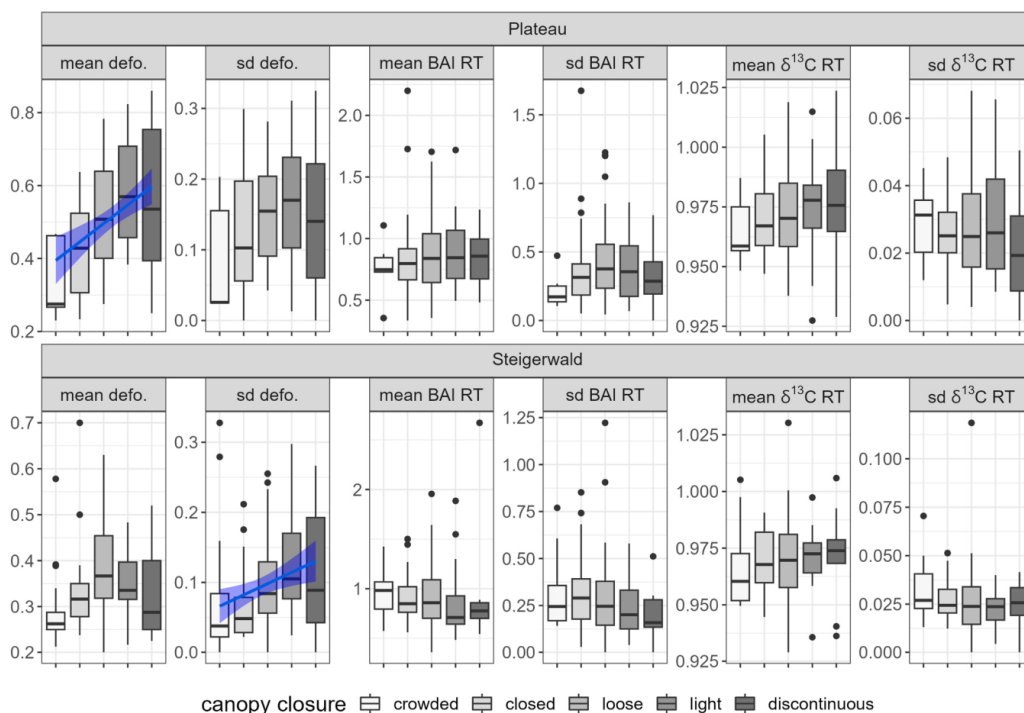


Fig. 4. Relationship between crown closure and defoliation (defo.) and resistance indices BAI resp. $\delta^{13}\text{C}$ (mean and standard deviation (sd) per plot) for the two study areas, Plateau (upper row) and Steigerwald (lower row). The blue trend line is based on a linear model and only plotted for the models where the slope parameter significantly differs from zero. The blue bands around the solid lines indicate the 95% confidence interval. $n = 240$.

variables (Table 3). However, the overall predictive power of the models was low. The best model was for mean defoliation with R^2 of 0.29 for the 30 m radius in the Steigerwald (Table 3). For these point clouds, the response patterns in basal area increment (mean BAI RT) were also best explained ($R^2 = 0.13$). Responses of the stable isotope $\delta^{13}\text{C}$ (mean $\delta^{13}\text{C}$ RT, sd $\delta^{13}\text{C}$ RT) could hardly be explained for both study regions. Analysis of the south-exposed 10 m semicircle did not improve the explanatory power of the models and is therefore not included in Table 3.

To increase the explanatory power of the models, we focused on the collective of plots that showed the most pronounced response to the 2018–2020 drought period, focusing on the 30 m cutting radius (Table 4). The multiple logistic regression models indicated that the most important variable explaining drought resistance was the Hegyi index. In contrast, box-dimension and CE evenness explained only specific aspects of drought resistance. Regarding the response in basal area increment, our results indicate that plots with lower box-dimension and higher mean competition had a higher probability of experiencing an increased mean Resistance Index BAI (BAI RT) during the drought period (Tjur's $R^2 = 0.17$) (Table 4, left). A one-unit increase in box-dimension was associated with a 58% decrease in the probability of higher mean BAI RT during drought (odds ratio: 0.42). On the other hand, a one-unit increase in the Hegyi index was associated with a 115% increase in the probability of higher mean BAI RT during the drought period (odds ratio: 2.15). Similarly, the Hegyi index significantly influenced the standard deviation of BAI RT. An odds ratio of 7.61 indicated a higher probability of greater variation in tree growth during

the drought period.

Regarding the stable carbon isotope $\delta^{13}\text{C}$ (mean $\delta^{13}\text{C}$ RT, sd $\delta^{13}\text{C}$ RT), the explanatory power of the models was relatively low, with a Tjur's R^2 of 0.06 for mean $\delta^{13}\text{C}$ RT and a Tjur's R^2 of 0.09 for sd $\delta^{13}\text{C}$ RT (Table 4, middle).

In contrast, models for mean defoliation show a higher goodness of fit (Tjur's $R^2 = 0.41$) (Table 4, right). Our results indicate significant effects of both box-dimension and CE evenness. A one-unit increase in box-dimension corresponds to a 175% higher probability of increased mean defoliation, while a one-unit increase in CE evenness results in a 207% higher probability of the same. Conversely, the Hegyi index shows a non-significant association with mean defoliation, suggesting a 73% lower probability of increased defoliation with a one-unit increase in the index. Next, the defoliation standard deviation, CE evenness significantly influences variability, indicating a 110% higher probability of increased variability. Similarly, the Hegyi index has an odds ratio of 2.34, indicating a 134% higher probability of increased variability. However, with a p-value of 0.06, it falls close to the statistical significance threshold.

4. Discussion

4.1. The response of beech forests to prolonged drought

Our results underline that beech forests in both study areas responded to the drought period with defoliation, reduced growth, and changes in the $\delta^{13}\text{C}$ signature (Table 2). Defoliation of beech trees during drought

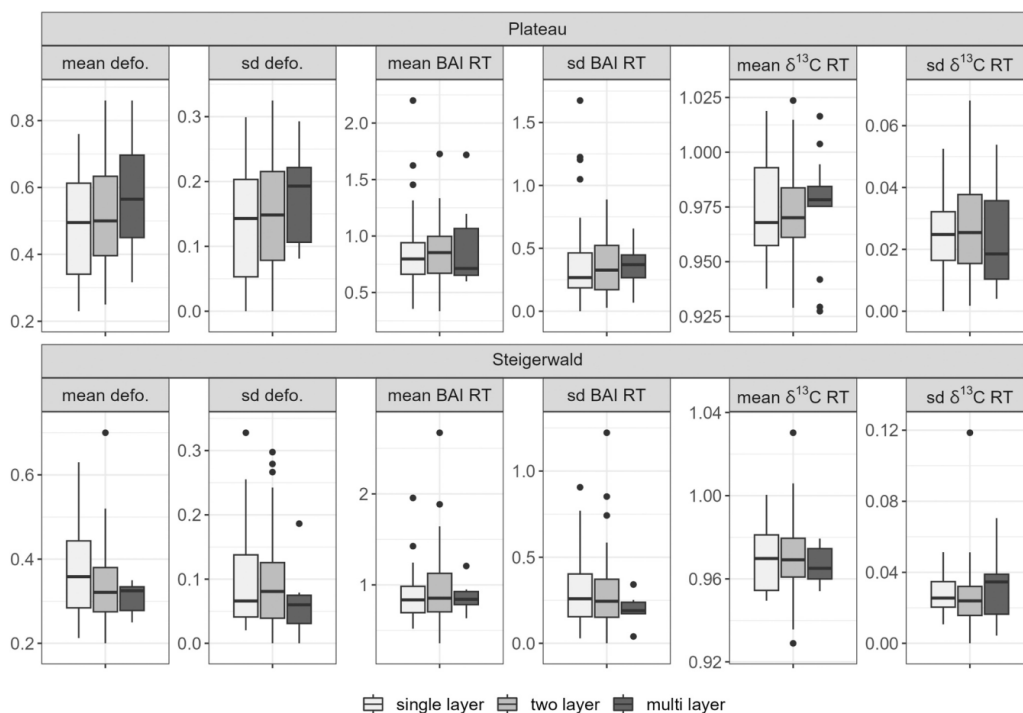


Fig. 5. Relationship between stand layers and defoliation (defo.) and resistance indices BAI resp. $\delta^{13}\text{C}$ (mean and standard deviation (sd) per plot) for the two study areas, Plateau (upper row) and Steigerwald (lower row). There is no significant difference among stands with a different number of stand layers. $n = 240$.

Table 3

The number of important variables classified by Boruta analysis to explain the Resistance indices (mean BAI RT, sd BAI RT, mean $\delta^{13}\text{C}$ RT, sd $\delta^{13}\text{C}$ RT) and the defoliation per plot (mean defo, sd defo). Results are shown for both study areas and two cutting radii (10 m, 30 m). The summary of the generalized additive models (GAM) based on the important variables, with the deviation explained by the model (DE) and the adjusted R² (adj.) are also shown. $n = 240$.

variable	mean BAI RT	sd BAI RT	mean $\delta^{13}\text{C}$ RT	sd $\delta^{13}\text{C}$ RT	mean defoliation	sd defoliation
Plateau 10 m						
Number of important variables	2	3	1	0	3	6
DE (%)	14.2	15.5	8.7	-	21.9	21.6
R ² (adj.)	0.12	0.13	0.07	-	0.19	0.16
Steigerwald 10 m						
Number of important variables	3	5	0	1	7	0
DE (%)	4.2	15.1	-	3.7	28.3	-
R ² (adj.)	0.02	0.11	-	0.02	0.23	-
Plateau 30 m						
Number of important variables	3	3	1	0	3	2
DE (%)	12.0	11.9	8.7	-	23.9	14.2
R ² (adj.)	0.10	0.09	0.07	-	0.21	0.12
Steigerwald 30 m						
Number of important variables	6	5	0	2	5	2
DE (%)	18.8	13.3	-	3.4	32.7	10.6
R ² (adj.)	0.13	0.08	-	0.02	0.29	0.09

has also been observed in several other studies, including Rohner et al. (2021) or Walther et al. (2021). The cause of crown defoliation may be due to anisohydric regulation of leaf stomata associated with the cavitation-sensitive xylem of beech (Schuldt et al., 2020). This regulatory mechanism allows stomata to remain open even under drought conditions, allowing beech to maintain photosynthesis. However, this strategy risks disrupting water flow in the xylem vessels and forming embolisms, leading to partial crown loss and ultimately tree mortality

(Arend et al., 2022; Weithmann et al., 2022). Thus, defoliation is a stress response to drought (Wohlgenuth et al., 2020), driven by anisohydric water potential regulation and limited hydraulic conductivity.

Furthermore, our results indicate that the lack of leaf mass, coupled with limited photosynthetic capacity, leads to reduced growth in response to the drought period, as observed by Scharnweber et al. (2020), Debel et al. (2021), and Bräker (1991), who found a correlation between crown foliage and stem radial growth. However, a decline in

Table 4

Overview of the results of the multiple logistic regression models for both study regions. The explanatory variables are the probability of a higher mean/sd BAI RT and $\delta^{13}\text{C}$ RT, as well as the mean/sd defoliation. Odds ratios less than 1 indicate that an increase in the explanatory variable is associated with a decrease in the probability of the response variable during drought. Conversely, values greater than 1 signify that an increase in the explanatory variable is associated with a higher probability of an increase in the response variable during drought. $n = 48$.

	Probability of a higher mean BAI RT		Probability of a higher sd in BAI RT		Probability of a higher mean $\delta^{13}\text{C}$ RT		Probability of a higher sd in $\delta^{13}\text{C}$ RT		Probability of a higher mean defoliation		Probability of a higher sd in defoliation	
	Odds Ratios	p-values	Odds Ratios	p-values	Odds Ratios	p-values	Odds Ratios	p-values	Odds Ratios	p-values	Odds Ratios	p-values
box-dimension	0.42	0.02							2.75	0.04		
CE evenness									3.07	0.03	2.10	0.04
Hegyi-Index	2.15	0.05	7.61	< 0.01	0.61	0.11	2.15	0.05	0.27	0.06	2.34	0.06
R ² Tjur	0.17		0.34		0.06		0.09		0.41		0.12	

growth is expected across much of the species' range (Del Martinez Castillo et al., 2022). In addition, beech trees in both study areas show an elevated $\delta^{13}\text{C}$ signature, indicating water stress during the drought period (Vannoppen et al., 2020; Bhusal et al., 2021).

The effects of drought in the two study regions were not fully consistent. We observed higher mean crown defoliation in the Plateau. The increased sensitivity to drier sites may indicate that these stands are more susceptible to drought due to limited water availability (Chakraborty et al., 2013; Weber et al., 2013; Klesse et al., 2022). Thus, the available field capacity is lower in the Plateau (Eutric Leptic Cambisol (Clayic)) compared to the Steigerwald (Dystric Cambisol (Loamic)). Under normal conditions, trees mainly extract water from the uppermost soil layers, but during droughts, deciduous trees in particular modify their water uptake strategy by increasingly using roots in deeper soil layers (Brinkmann et al., 2019; Meusburger et al., 2022). Consequently, beech trees in the Plateau, where they grow on shallow soils, often face challenges reaching water reservoirs. Predispositions from the 2003 or 2015 drought may have persisted as a legacy effect, hindering tree recovery and resulting in carbon losses due to impaired photosynthetic and hydraulic function (Kannenberg et al., 2020). Thus, beech vitality may have already been reduced for an extended period of time (Neycken et al., 2022).

The higher standard deviation in the Plateau observed for both mean defoliation and mean BAI RT indicates the presence of individuals experiencing significant stress while others are less affected. This result could be due to an ongoing adaptation process of beech trees to changing climatic conditions, as the Plateau is one of the warmest and hottest regions in Germany (Walentowski et al., 2014). Pfenninger et al. (2021) found genetic differences within the same stand that explain the extent to which a beech tree can withstand and recover from drought.

In terms of the $\delta^{13}\text{C}$ signature, no discernible differences between the regions were found. This finding is noteworthy, particularly as Chakraborty et al. (2022) reported that trees from dry plots showed a higher response to drought and climatic dependency than less-dry plots. Due to the extreme nature of the drought, it is plausible that all plots experienced relatively similar levels of drought stress in our study. Overall, we can accept our hypothesis H1, suggesting that beech stands in both study regions responded to the drought period with (1) defoliation, (2) growth reduction, and (3) an increase in $\delta^{13}\text{C}$ signature.

4.2. Effects of stand structure on the drought response

Our results indicate a relationship between crown closure and crown defoliation in beech forests (Fig. 4). Particularly in the Plateau, a significant increase in defoliation was observed with decreasing crown closure, suggesting that a more open canopy may lead to increased vulnerability of beech trees to drought. A more open canopy leads to greater exposure of individual trees to direct sunlight, which can cause detrimental effects such as sun scald (Brück-Dyckhoff, 2017). Predisposed trees are more likely to experience subsequent disturbances, such as beetle infestations (e.g. *Agritus viridis* L.), which can subsequently trigger a chain reaction (Manion, 1981). The degree of crown defoliation

also increases the likelihood of future tree mortality (Petit-Cailleux et al., 2021). Dieback or increased defoliation of large trees results in gaps in the canopy, leading to increased temperatures and lower air humidity in the interior of the forest (Thom et al., 2020). This situation could potentially exacerbate drought stress and increase defoliation. In such cases, the role of understory trees becomes critical. These trees have the capacity to cool the forest stand and to decrease the vapor pressure deficit (Zellweger et al., 2020), which safeguards ecological processes and biodiversity (Frenne et al., 2013). Thus, the establishment of multi-layered forest structures mitigates the risk of losing the capacity to buffer weather extremes.

Contrary to our expectations, the resistance indices BAI and $\delta^{13}\text{C}$ did not change significantly in relation to canopy closure. We expected reduced leaf mass to cause growth decline and an altered $\delta^{13}\text{C}$ signature. The lack of such effects may be due to the compensatory influence of increased space for the remaining trees, which mitigates the effects of reduced crown foliage. The remaining canopy could receive adequate water and nutrients, facilitating sufficient sugar production for wood formation and preventing an altered $\delta^{13}\text{C}$ signature. This finding is consistent with the research of Roloff (1986), suggesting that damaged beech trees do not always have reduced growth rates. This observation is also consistent with subjective assessments of crown condition, indicating that the remaining leaves of partially defoliated beech trees often show a healthier green color compared to the average. Weithmann et al. (2022) describe that the extreme drought event 2018 triggered the development of smaller leaves, with improved water use efficiency in the sun-exposed canopy. At the same time, it should not be underestimated that severely defoliated beech trees are highly susceptible to pathogens, including those that severely degrade wood (Purahong et al., 2021). Stem stability and breakage resistance of affected trees are significantly reduced (Langer and Bußkamp, 2023). Overall, we must reject hypothesis H2. While the facet of the hypothesis "the more open the canopy, the more significant the defoliation" was supported, the rest of the hypothesis (greater growth decline and more pronounced $\delta^{13}\text{C}$ signature) was not supported.

Hypothesis H3 postulated that multi-layer beech forests, compared to single-layer forests, would exhibit (1) lower crown defoliation and (2) higher resistance (as measured by tree growth and $\delta^{13}\text{C}$ signature) to the drought period. However, the results show that the relationship between crown structure and defoliation and resistance indices is more complex than originally assumed. No significant difference existed between multi-layered and single-layered forests in their response to the observed drought period (Fig. 5). Even when additional stand variables were considered (Table 3). We found no strong correlations for the 30 m cutting radius, which represents stand structure, the 10 m cutting radius, which quantifies direct neighborhood, and the 10 m semicircle directly to the south, which quantifies potential effects of direct solar radiation on beech trees.

By focusing on a subset of the data, namely the respective minimum and maximum values, we were able to identify more robust relationships (Table 4). The reason for this could be that a thinning intensity of about 50% of the stand density has been identified as the threshold at which

hydrological processes are significantly affected (Del Campo et al., 2022). When analyzing the subset of data, it was initially unexpected that plots with higher tree competition had a higher probability of an increased resistance in basal area growth, considering other authors such as Chakraborty et al. (2021) came to the opposite conclusion. The explanation for our result may be that on these specific plots, several smaller individuals compete with a few larger individuals, as is the case in stands with abundant understory. The mean Hegyi index is high, reflecting instances where smaller trees are positioned close to dominant trees. In a previous study, we showed that it is mainly the dominant collective that suffers during drought (Mathes et al., 2023a). However, subordinate trees had an overall higher growth stability during drought years. During prolonged drought there might be a growth partitioning in favor of smaller trees (Bose et al., 2022; Pretzsch et al., 2023). This is consistent with the result that the probability of a higher standard deviation in BAI RT also increases with increasing competition, since in such cases the plot is characterized by a mixture of dominant and subordinate beech trees. Such stands are expected to be more resilient, allowing them to recover more quickly from droughts like the one examined in this study. The probability of an increase in mean BAI RT decreases with box-dimension. Stands with smaller box-dimension are characterized by lower complexity (Neudam et al., 2022). Combined with the results on mean competition, this indicates that single-layered stands with high diameter differentiation have a higher probability of maintaining their average BAI. These could be stands that have been selectively thinned, where the intervention is focused on a selected tree, leaving the rest of the area untreated.

Regarding the response of the $\delta^{13}\text{C}$ signal, where mean competition was the determining factor, the Tjur R^2 values remained relatively low with a maximum of 0.09. The models struggled to adequately explain the variability in the $\delta^{13}\text{C}$ signal of beech trees. Similarly, Rothenbühler et al. (2021) could not identify any systematic differences in the $\delta^{13}\text{C}$ tree-ring records between dead and live trees.

We observed that the mean crown defoliation increased with higher box-dimension. A higher box-dimension implies a more even vertical and horizontal distribution of biomass within plots. Consistent with these findings, the probability of a higher defoliation is also correlated with an increase in CE evenness, meaning that biomass is more evenly distributed across all vertical layers. These forest structures could result from a shelterwood-like cutting approach. Canopy openings after cuttings may also drive an increased crown defoliation, for instance, due to a high predisposition from sun scald. Accordingly, our results show that a decrease in competition is associated with an increased probability of more severe crown defoliation. This suggests that the probability of significant defoliation increases in exposed beech stands. Therefore, adequate stem shading, including a well-developed understory and mid-canopy layer, might be essential. During the thinning phase, this can be achieved by concepts based on individual-tree selection thinnings. Methods such as group selection cutting (German: "Femelschlag") cuttings might be an option during the regeneration phase. This contributes to increased structural diversity, leading to distinct differences between neighboring trees of different age and size, resulting in the formation of uneven-aged forests (Brang et al., 2014; Schall et al., 2018). In conclusion, we had to reject Hypothesis 3 because there was limited evidence that multi-layered beech forests have less canopy defoliation or greater resistance (as measured by tree growth and $\delta^{13}\text{C}$ signature) to the drought period than single-layered forests.

5. Conclusion

European beech (*Fagus sylvatica* L.) suffered significantly from the 2018–2020 drought period. We identified a pronounced crown defoliation, reduced growth, and changes in the $\delta^{13}\text{C}$ signature compared to the pre-drought period. We found a relationship between crown closure and crown defoliation in beech, particularly in the Plateau where reduced crown closure was significantly associated with increased

defoliation. This suggests an increased vulnerability of beech to drought in more open canopies. However, the potential for silvicultural intervention to mitigate drought stress, as measured by BAI and the $\delta^{13}\text{C}$ signal, appears limited. Neighboring trees and forest structure had a weak influence on average drought resistance. Neither open nor closed forest structure could significantly alleviate drought stress. Stands with greater structural complexity tended to have higher resistance, as the understory may compensate some of the upper canopy loss. The substantial variability within the data may indicate high plasticity and intraspecific variation in beech, suggesting some degree of adaptation to climate extremes as experienced from 2018–2020. Such adaptation could occur evolutionarily through natural regeneration. From this perspective, it may be useful to regenerate beech stands at an early stage. In addition to beech, other tree species should be considered that may increase the adaptive capacity.

For further silvicultural treatments in regenerating stands, group selection cuttings could be an option to create different environmental conditions. It may be critical to limit the intervention to specific areas and leave the rest of the site untreated. Trees with high vitality should be selected during the thinning phase. The shading of the trunks necessary to produce high quality wood from the selected trees could be provided by understorey trees, thus simultaneously improving the microclimate of the forest. More research is needed on these silvicultural practices, such as at what stand age or what role weather plays during and after silvicultural treatments.

Overall, the results of this study contribute to a better understanding of how beech trees respond to drought events. This understanding is essential for the conservation of beech forests in the face of climate change and contributes to the knowledge of the ecological resilience of forests. Nevertheless, recurring multi-year droughts, like the event from 2018–2020, can be expected to lead to permanent changes in growth dynamics, stand structures and species compositions in forests.

Funding

This work was supported by the Bavarian State Ministry of Nutrition, Agriculture, and Forestry through the project "Effects of forest structures on the drought resilience of individual trees (W049)."

CRediT authorship contribution statement

Annighöfer Peter: Writing – review & editing, Methodology, Funding acquisition, Conceptualization. **Mathes Thomas:** Writing – review & editing, Writing – original draft, Methodology, Conceptualization. **Seidel Dominik:** Writing – review & editing, Methodology, Conceptualization. **Klemmt Hans-Joachim:** Writing – review & editing. **Thom Dominik:** Writing – review & editing, Methodology.

Declaration of Competing Interest

The authors declare that they have no known competing financial interests or personal relationships that could have appeared to influence the work reported in this paper.

Data availability

Data will be made available on request.

Acknowledgments

We want to thank the Bavarian State Forest Enterprise and the municipality of Leinach for providing the study sites. We also thank the Bavarian State Institute of Forestry LWF for providing GIS Data. Rudolf Harpaintner from the Professorship of Forest and Agroforest Systems, Technical University of Munich, for his data collection and processing support. We sincerely thank Peter Schad for classifying the soils

according to the WRB and Yessica Kömel, and Rudi Schäufele for performing the isotope analysis. Simone Schäfer-Hecht, Sebastian Damböck, Paul Unkel, and Markus Stimmelmayer have contributed to the success of this work with their bachelor and master theses. Thanks to Ian Burke, Ranbir Chakraborty, Corinne Gonzalez, Merve Mentese, Joachim Thein, and Jana Walbaum for their help in the laboratory. Many thanks to Markus Stimmelmayer for his outstanding support during the fieldwork in the summer of 2021. We thank the two anonymous reviewers for their constructive comments on an earlier version of this manuscript.

References

- Allen, C.D., Macalady, A.K., Chenchouni, H., Bachelet, D., McDowell, N., Vennetier, M., et al., 2010. A global overview of drought and heat-induced tree mortality reveals emerging climate change risks for forests. *For. Ecol. Manag.* 259, 660–684.
- Arbeitskreis Standortskartierung, 2016. Forstliche Standortsaufnahme: Begriffe, Definitionen, Einteilungen, Kennzeichnungen, Erläuterungen, 7th edn. IHW-Verlag, p. 400.
- Arend, M., Link, R.M., Zahnd, C., Hoch, G., Schuldt, B., Kahmen, A., 2022. Lack of hydraulic recovery as a cause of post-drought foliage reduction and canopy decline in European beech. *N. Phytol.* 234, 1195–1205.
- Aussenac, G., 2000. Interactions between forest stands and microclimate: Ecophysiological aspects and consequences for silviculture. *Ann. Sci.* 57, 287–301.
- Aussenac, G., Granier, A., 1988. Effects of thinning on water stress and growth in Douglas-fir. *Can. J. For. Res.* 18, 100–105.
- Baddeley, A., Turner, R., 2005. spatstat: An R Package for Analyzing Spatial Point Patterns. *J. Stat. Softw.* 12, 1–42.
- BaySF - Bayerische Staatsforsten. 2011 Grundsätze für die Bewirtschaftung von Buchen – und Buchenmischbeständen im Bayerischen Staatswald, 100 p.
- Bhusal, N., Lee, M., Lee, H., Adhikari, A., Han, A.R., Han, A., Kim, H.S., 2021. Evaluation of morphological, physiological, and biochemical traits for assessing drought resistance in eleven tree species. *Sci. Total Environ.* 779, 146466.
- Bigler, C., Vitasse, Y., 2021. Premature leaf discoloration of European deciduous trees is caused by drought and heat in late spring and cold spells in early fall. *Agric. For. Meteorol.* 307, 108492.
- BMEL - Bundesministerium für Ernährung und Landwirtschaft. 2022 Ergebnisse der Waldzustandserhebung 2021, 76 p.
- Bose, A.K., Rohner, B., Bottero, A., Ferretti, M., Forrester, D.I., 2022. Did the 2018 megadrought change the partitioning of growth between tree sizes and species? A Swiss case-study. *Plant Biol. (Stuttg., Ger.)* 24, 1146–1156.
- Bosela, M., Stefančík, I., Marčíš, P., Rubio-Cuadrado, A., Lukac, M., 2021. Thinning decreases above-ground biomass increment in central European beech forests but does not change individual tree resistance to climate events. *Agric. For. Meteorol.* 306, 108441.
- Bräker, O.U. 1991 Der Radialzuwachs an unterschiedlich belaubten Buchen in zwei Beständen bei Zürich und Basel, 427–433.
- Brang, P., Spathelf, P., Larsen, J.B., Bauhus, J., Bonc ina, A., Chauvin, C., et al., 2014. Suitability of close-to-nature silviculture for adapting temperate European forests to climate change. *For. (Lond.)* 87, 492–503.
- Bréda, N., Granier, A., Aussenac, G., 1995. Effects of thinning on soil and tree water relations, transpiration and growth in an oak forest (*Quercus petraea* (Matt.) Liebl.). *Tree Physiol.* 15, 295–306.
- Bréda, N., Huc, R., Granier, A., Dreyer, E., 2006. Temperate forest trees and stands under severe drought: a review of ecophysiological responses, adaptation processes and long-term consequences. *Ann. Sci.* 63, 625–644.
- Brinkmann, N., Eugster, W., Buchmann, N., Kahmen, A., 2019. Species-specific differences in water uptake depth of mature temperate trees vary with water availability in the soil. *Plant Biol. (Stuttg., Ger.)* 21, 71–81.
- Brooks, J.R., Mitchell, A.K., 2011. Interpreting tree responses to thinning and fertilization using tree-ring stable isotopes. *N. Phytol.* 190, 770–782.
- Brück-Dyckhoff, C. 2017 Zur Beteiligung des Buchenprachtkäfers (*Agritus viridis* L.) an Vitalitätsverlusten älterer Rotbuchen (*Fagus sylvatica* L.). Dissertation, 241 p.
- Bundesministerium für Ernährung und Landwirtschaft (BMEL). 2021 Waldbericht der Bundesregierung 2021. (https://www.bmel.de/SharedDocs/Downloads/DE/Br oschueren/waldbericht2021.pdf?_blob=publicationFile&v=11) (accessed on 20 July, 2023).
- Chakraborty, T., Saha, S., Reif, A., 2013. Decrease in Available Soil Water Storage Capacity Reduces Vitality of Young Understorey European Beeches (*Fagus sylvatica* L.)—A Case Study from the Black Forest, Germany. *Plants* 2, 676–698.
- Chakraborty, T., Reif, A., Matzarakis, A., Saha, S., 2021. How Does Radial Growth of Water-Stressed Populations of European Beech (*Fagus sylvatica* L.) Trees Vary under Multiple Drought Events? *Forests* 12, 129.
- Chakraborty, T., Reif, A., Matzarakis, A., Helle, G., Faßnacht, F., Saha, S., 2022. Carbon and oxygen dual-isotopes in tree rings indicate alternative physiological responses opted by European beech trees to survive drought stress. *Scand. J. For. Res.* 37, 295–313.
- Clark, P.J., Evans, F.C., 1954. Distance to nearest neighbour as a measure of spatial relationships in populations. *Ecology* 35, 445–453.
- Corcobado, T., Cech, T.L., Brandstetter, M., Daxer, A., Hüttler, C., Kudláček, T., et al., 2020. Decline of European Beech in Austria: Involvement of Phytophthora spp. and Contributing Biotic and Abiotic Factors. *Forests* 11, 895.
- Debel, A., Meier, W.J.-H., Bräuning, A., 2021. Climate Signals for Growth Variations of *F. sylvatica*, *P. abies*, and *P. sylvestris* in Southeast Germany over the Past 50 Years. *Forests* 12, 1433.
- Del Martinez Castillo, E., Zang, C.S., Buras, A., Hackett-Pain, A., Esper, J., Serrano-Notivol, R., et al., 2022. Climate-change-driven growth decline of European beech forests. *Commun. Biol.* 5, 163.
- Deutscher Wetterdienst (DWD). 2022a Lufttemperatur: vieljährige Mittelwerte 1991 - 2020. (https://www.dwd.de/DE/leistungen/klimadatendeutschland/mittelwerte/temp_9120_SV_html.html?sessionid=9F4792D80B666AA6GFC1C9A2384B77AAF.live31081?view=na&Publication&nn=16102) (accessed on 29 June, 2022).
- Deutscher Wetterdienst (DWD). 2022b Niederschlag: vieljährige Mittelwerte 1991 - 2020. (https://www.dwd.de/DE/leistungen/klimadatendeutschland/mittelwerte/nieder_9120_SV_html.html?sessionid=9F4792D80B666AA6GFC1C9A2384B77AAF.live31081?view=na&Publication&nn=16102) (accessed on 29 June, 2022).
- Donnelly, K., 1978. Simulation to determine the variance and edge-effect of total nearest neighbour distances. In: Hodder, I. (Ed.), *Simulation methods in Archeology*. Cambridge Press, London, pp. 91–95.
- Ehbrecht, M., Schall, P., Ammer, C., Seidel, D., 2017. Quantifying stand structural complexity and its relationship with forest management, tree species diversity and microclimate. *Agric. For. Meteorol.* 242, 1–9.
- FAO - Food and Agriculture Organization of the United Nations, 2014. World reference base for soil resources 2014: International soil classification system for naming soils and creating legends for soil maps. FAO.
- Forest Europe. 2020 State of Europe's Forests, 394 p.
- Frenne, P., de, Rodríguez-Sánchez, F., Coomes, D.A., Baeten, L., Verstraeten, G., Vellend, M., et al., 2013. Microclimate moderates plant responses to macroclimate warming. *Proc. Natl. Acad. Sci. USA* 110, 18561–18565.
- Gavin, J., Ourcival, J.-M., Limousin, J.-M., 2019. Rainfall exclusion and thinning can alter the relationships between forest functioning and drought. *N. Phytol.* 223, 1267–1279.
- Gebhardt, T., Häberle, K.-H., Matyssek, R., Schulz, C., Ammer, C., 2014. The more, the better? Water relations of Norway spruce stands after progressive thinning. *Agric. For. Meteorol.* 197, 235–243.
- GreenValley International, Ltd. 2019 LiDAR360; Software.
- Hammond, W.M., Williams, A.P., Abatzoglou, J.T., Adams, H.D., Klein, T., López, R., et al., 2022. Global field observations of tree die-off reveal hotter-drought fingerprint for Earth's forests. *Nat. Commun.* 13, 1761.
- Hari, V., Rakovec, O., Markonis, Y., Hanel, M., Kumar, R., 2020. Increased future occurrences of the exceptional 2018–2019 Central European drought under global warming. *Sci. Rep.* 10, 12207.
- Kannenber, S.A., Schwalm, C.R., Anderegg, W.R.L., 2020. Ghosts of the past: how drought legacy effects shape forest functioning and carbon cycling. *Ecol. Lett.* 23, 891–901.
- Klesse, S., Wohlgemuth, T., Meusburger, K., Vitasse, Y., Arx, G. von, Lévesque, M., et al., 2022. Long-term soil water limitation and previous tree vigor drive local variability of drought-induced crown dieback in *Fagus sylvatica*. *Sci. Total Environ.* 851, 157926.
- Kohler, M., Sohn, J., Nägele, G., Bauhus, J., 2010. Can drought tolerance of Norway spruce (*Picea abies* (L.) Karst.) be increased through thinning? *Eur. J. For. Res.* 129, 1109–1118.
- Kraft, G., 1884. Beiträge zur Lehre von den Durchforstungen, Schlagstellungen und Lichtungshieben. Klindworth.
- Kursa, M.B., Rudnicki, W.R., 2010. Boruta: Wrapper Algorithm for All Relevant Feature Selection. *J. Stat. Softw.* 36, 1–13.
- Lagergren, F., Lanckreijer, H., Kučera, J., Cienciala, E., Mölder, M., Lindroth, A., 2008. Thinning effects on pine-spruce forest transpiration in central Sweden. *For. Ecol. Manag.* 255, 2312–2323.
- Langer, G.J., Bußkamp, J., 2021. Fungi Associated With Woody Tissues of European Beech and Their Impact on Tree Health. *Front. Microbiol.* 12, 702467.
- Langer, G.J., Bußkamp, J., 2023. Vitality loss of beech: a serious threat to *Fagus sylvatica* in Germany in the context of global warming. *J. Plant Dis. Prot.* 130, 1101–1115.
- Laurent, M., Antoine, N., Joël, G., 2003. Effects of different thinning intensities on drought response in Norway spruce (*Picea abies* (L.) Karst.). *For. Ecol. Manag.* 183, 47–60.
- Leuschner, C., Weithmann, G., Bat-Enerel, B., Weigel, R., 2023. The Future of European Beech in Northern Germany—Climate Change Vulnerability and Adaptation Potential. *Forests* 14, 1448.
- Li, W., Guo, Q., Jakubowski, M.K., Kelly, M., 2012. A New Method for Segmenting Individual Trees from the Lidar Point Cloud. *Photo Eng. Remote Sens.* 78, 75–84.
- Lüdtke, D. 2023 sjPlot: Data Visualization for Statistics in Social Science.
- LWF - Bayerische Landesanstalt für Wald und Forstwirtschaft. 2005 Waldatlas Bayern, 137 p.
- Manion, P.D., 1981. Tree disease concepts. Prentice-Hall, Inc.
- Martín-Benito, D., Del Río, M., Heinrich, I., Helle, G., Cañellas, I., 2010. Response of climate-growth relationships and water use efficiency to thinning in a *Pinus nigra* afforestation. *For. Ecol. Manag.* 259, 967–975.
- Mathes, T., Seidel, D., Annighöfer, P., 2023a. Response to extreme events: do morphological differences affect the ability of beech (*Fagus sylvatica* L.) to resist drought stress? *Forestry: An International Journal of Forest Research* 96 (3), 355–371. <https://doi.org/10.1093/forestry/cpac056>.
- Mathes, T., Seidel, D., Häberle, K.-H., Pretzsch, H., Annighöfer, P., 2023b. What Are We Missing? Occlusion in Laser Scanning Point Clouds and Its Impact on the Detection of Single-Tree Morphologies and Stand Structural Variables. *Remote Sens.* 15, 450.
- McDowell, N.G., Adams, H.D., Bailey, J.D., Hess, M., Kolb, T.E., 2006. Homeostatic maintenance of ponderosa pine gas exchange in response to stand density changes. *Ecol. Appl.* 16, 1164–1182.

- McLeod, A.I., Xu, C. and Lai, Y. 2020 bestglm: Best Subset GLM and Regression Utilities. Meusburger, K., Trotsiuk, V., Schmidt-Walter, P., Baltensweiler, A., Brun, P., Bernhard, F., et al., 2022. Soil-plant interactions modulated water availability of Swiss forests during the 2015 and 2018 droughts. *Glob. Change Biol.* 28, 5928–5944.
- Meyer, D., Dimitriadou, E., Hornik, K., Weingessel, A., Leisch, F., Chang, C.-C. and Lin, C.-C. 2023 e1071: Misc Functions of the Department of Statistics, Probability Theory Group (Formerly: E1071), TU Wien. CRAN.
- Neudam, L., Annighöfer, P., Seidel, D., 2022. Exploring the Potential of Mobile Laser Scanning to Quantify Forest Structural Complexity. *Front. Remote Sens* 3, 861337.
- Neycken, A., Scheggia, M., Bigler, C., Lévesque, M., 2022. Long-term growth decline precedes sudden crown dieback of European beech. *Agric. For. Meteorol.* 324, 109103.
- Nussbaumer, A., Meusburger, K., Schmitt, M., Waldner, P., Gehrig, R., Haeni, M., et al., 2020. Extreme summer heat and drought lead to early fruit abortion in European beech. *Sci. Rep.* 10, 5334.
- Oksanen, J., Simpson, G.L., Blanchet, F.G., Kindt, R., Legendre, P. and Minchin, P.R. et al. 2022 vegan: Community Ecology Package. CRAN.
- Petit-Cailleux, C., Davi, H., Lefèvre, F., Garrigue, J., Magdalou, J.-A., Hurson, C., et al., 2021. Comparing statistical and mechanistic models to identify the drivers of mortality within a rear-edge beech population. *Peer Community J.* 1.
- Pfenninger, M., Reuss, F., Kiebler, A., Schönnenbeck, P., Caliendo, C., Gerber, S., et al., 2021. Genomic basis for drought resistance in European beech forests threatened by climate change. *eLife* 10.
- Plochmann, R., Hieke, C., 1986. Schadereignisse in den Wäldern Bayerns. Eine Zusammenstellung der forstlichen Literatur seit Beginn des 18. Jahrhunderts: Forstliche Forschungsberichte München. Band 71, 161.
- Pretzsch, H., Ahmed, S., Rötzer, T., Schmieđ, G., Hilmers, T., 2023. Structural and compositional acclimation of forests to extended drought: results of the KROOF throughfall exclusion experiment in Norway spruce and European beech. *Trees* 1–21.
- Purahong, W., Tanunchai, B., Wahdan, S.F.M., Buscot, F., Schulze, E.-D., 2021. Molecular Screening of Microorganisms Associated with Discolored Wood in Dead European Beech Trees Suffered from Extreme Drought Event Using Next Generation Sequencing. *Plants* 10, 2092.
- R Core Team. 2023 R: A Language and Environment for Statistical Computing, Vienna, Austria.
- Rakovec, O., Samaniego, L., Hari, V., Markonis, Y., Moravec, V., Thober, S., et al., 2022. The 2018–2020 Multi-Year Drought Sets a New Benchmark in Europe. *Earth's Future* 10.
- Rohner, B., Kumar, S., Liechti, K., Gessler, A., Ferretti, M., 2021. Tree vitality indicators revealed a rapid response of beech forests to the 2018 drought. *Ecol. Indic.* 120, 106903.
- Roloff, A. 1986 Morphologie der Kronenentwicklung von *Fagus sylvatica* L. (Rotbuche) unter besonderer Berücksichtigung möglicherweise neuartiger Veränderungen. Dissertation.
- Rothenbühler, S., Walthert, L., Saurer, M., Gärtner, H., Gessler, A. and Rigling, A. et al. 2021 Assessing drought-induced mortality of European beech and Scots pine in the Valais, Switzerland.
- Roussel, J.-R., Auty, D., Coops, N.C., Tompalski, P., Goodbody, T.R., Meador, A.S., et al., 2020. lidar: An R package for analysis of Airborne Laser Scanning (ALS) data. *Remote Sens. Environ.* 251, 112061.
- Sankey, T., Tatum, J., 2022. Thinning increases forest resiliency during unprecedented drought. *Sci. Rep.* 12, 9041.
- Schall, P., Gossner, M.M., Heinrichs, S., Fischer, M., Boch, S., Prati, D., et al., 2018. The impact of even-aged and uneven-aged forest management on regional biodiversity of multiple taxa in European beech forests. *J. Appl. Ecol.* 55, 267–278.
- Scharnweber, T., Smiljanic, M., Cruz-García, R., Manthey, M., Wilmking, M., 2020. Tree growth at the end of the 21st century - the extreme years 2018/19 as template for future growth conditions. *Environ. Res. Lett.* 15, 74022.
- Scharnweber, T., Manthey, M., Criegee, C., Bauwe, A., Schröder, C., Wilmking, M., 2011. Drought matters – Declining precipitation influences growth of *Fagus sylvatica* L. and *Quercus robur* L. in north-eastern Germany. *For. Ecol. Manag.* 262, 947–961.
- Schuldt, B., Buras, A., Arend, M., Vitasse, Y., Beierkuhnlein, C., Damm, A., et al., 2020. A first assessment of the impact of the extreme 2018 summer drought on Central European forests. *Basic Appl. Ecol.* 45, 86–103.
- Seidel, D., 2018. A holistic approach to determine tree structural complexity based on laser scanning data and fractal analysis. *Ecol. Evol.* 8, 128–134.
- Seidel, D., Ammer, C., 2023. Towards a causal understanding of the relationship between structural complexity, productivity, and adaptability of forests based on principles of thermodynamics. *For. Ecol. Manag.* 544, 121238.
- Senf, C., Seidl, R., 2021. Persistent impacts of the 2018 drought on forest disturbance regimes in Europe. *Biogeosciences* 18, 5223–5230.
- Sohn, J.A., Saha, S., Bauhus, J., 2016b. Potential of forest thinning to mitigate drought stress: A meta-analysis. *For. Ecol. Manag.* 380, 261–273.
- Sohn, J.A., Hartig, F., Kohler, M., Huss, J., Bauhus, J., 2016a. Heavy and frequent thinning promotes drought adaptation in *Pinus sylvestris* forests. *Ecol. Appl.* a Publ. Ecol. Soc. Am. 26, 2190–2205.
- Stiers, M., Annighöfer, P., Seidel, D., Willim, K., Neudam, L., Ammer, C., 2020. Quantifying the target state of forest stands managed with the continuous cover approach – revisiting Möller's "Dauerwald" concept after 100 years. *Trees, For. People* 1, 100004.
- StMELF - Bayerische Staatsministerium für Ernährung, Landwirtschaft und Forsten. 2023 Ergebnisse der Waldzustandserhebung 2022, 21 p.
- Thom, D., Buras, A., Heym, M., Klemmt, H.-J., Wauer, A., 2023. Varying growth response of Central European tree species to the extraordinary drought period of 2018 – 2020. *Agric. For. Meteorol.* 338, 109506.
- Thom, D., Sommerfeld, A., Sebal, J., Hage, J., Müller, J., Seidl, R., 2020. Effects of disturbance patterns and deadwood on the microclimate in European beech forests. *Agric. For. Meteorol.* 291, 108066.
- Thonfeld, F., Gessner, U., Holzwarth, S., Kriese, J., Da Ponte, E., Huth, J., Kuenzer, C., 2022. A First Assessment of Canopy Cover Loss in Germany's Forests after the 2018–2020 Drought Years. *Remote Sens.* 14, 562.
- Thünen-Institut - Dritte Bundeswaldinventur - Ergebnisdatenbank. 2012 <https://bwi.info>, Aufruf am: 19.06.2023; Auftragskürzel: 7721JL1235of_2012_bi, Archivierungsdatum: 2014-6-10 16:7:59.927. Überschrift: Vorrat [m³/ha] nach Land und Baumaltersklasse, Filter: Baumartengruppe=Buche; Jahr=2012;
- Vannoppen, A., Treyde, K., Boeckx, P., Kint, V., Ponette, Q., Verheyen, K., Muys, B., 2020. Tree species diversity improves beech growth and alters its physiological response to drought. *Trees* 34, 1059–1073.
- Walentowski, H., Falk, W., Mette, T., Kunz, J., Bräuning, A., Meinardus, C., et al., 2014. Assessing future suitability of tree species under climate change by multiple methods: a case study in southern Germany. *Ann. - Res.* 60.
- Walthert, L., Ganthaler, A., Mayr, S., Saurer, M., Waldner, P., Walser, M., et al., 2021. From the comfort zone to crown dieback: Sequence of physiological stress thresholds in mature European beech trees across progressive drought. *The. Sci. Total Environ.* 753, 141792.
- Weber, P., Bugmann, H., Pluess, A.R., Walthert, L., Rigling, A., 2013. Drought response and changing mean sensitivity of European beech close to the dry distribution limit. *Trees* 27, 171–181.
- Weigel, R., Bat-Enerel, B., Dulamsuren, C., Muffler, L., Weithmann, G., Leuschner, C., 2023. Summer drought exposure, stand structure, and soil properties jointly control the growth of European beech along a steep precipitation gradient in northern Germany. *Glob. Change Biol.* 29, 763–779.
- Weithmann, G., Link, R.M., Banzragh, B.-E., Würzburg, L., Leuschner, C., Schuldt, B., 2022. Soil water availability and branch age explain variability in xylem safety of European beech in Central Europe. *Oecologia* 198, 629–644.
- Wellbrock, N. and Eickenscheidt, N. 2018 Leitfaden und Dokumentation zur Waldzustandserhebung in Deutschland. Johann Heinrich von Thünen-Institut.
- Wickham, H., 2016. ggplot2: Elegant Graphics for Data Analysis. Springer-Verlag New York.
- Willim, K., Stiers, M., Annighöfer, P., Ehbrecht, M., Ammer, C., Seidel, D., 2020. Spatial Patterns of Structural Complexity in Differently Managed and Unmanaged Beech-Dominated Forests in Central Europe. *Remote Sens.* 12, 1907.
- Wohlgemuth, T., Kistler, M., Aymon, C., Hagedorn, F., Gessler, A., Gossner, M.M., et al., 2020. Früher Laubfall der Buche während der Sommertrockenheit 2018: Resistenz oder Schwächesyndrom? *Schweiz. Z. für Forstwes.* 171, 257–269.
- Wood, S.N., 2011. Fast stable restricted maximum likelihood and marginal likelihood estimation of semiparametric generalized linear models. *J. R. Stat. Soc. (B)* 73, 3–36.
- Zellweger, F., Frenne, P., de, Lenoir, J., Vangansbeke, P., Verheyen, K., Bernhardt-Römermann, M., et al., 2020. Forest microclimate dynamics drive plant responses to warming. *Sci. (N. Y., N. Y.)* 368, 772–775.
- Zhang, W., Qi, J., Wan, P., Wang, H., Xie, D., Wang, X., Yan, G., 2016. An Easy-to-Use Airborne LiDAR Data Filtering Method Based on Cloth Simulation. *Remote Sens.* 8, 1–22.

12.4 Student projects

Stimmelmayer, M. (2022, MSc.): Relationship between drought stress, vitality, and wood quality in beech forests (*Fagus sylvatica* L.)

Damböck, S. (2021, BSc.): Influence of forest structure on drought stress of European beech (*Fagus sylvatica* L.)

Sackmann S. (2023, BSc.): Response of European beech (*Fagus sylvatica* L.) to droughts in 2018 to 2020 and 2022 – Core analyses of the years 2021 and 2022

Schäfer-Hecht, S. (2021, BSc.): Effects of drought stress on the growth of beeches in Franconia

Unkel, P. (2022, BSc.): The influence of tree metrics on drought resistance of European beech (*Fagus sylvatica* L.) in the dry years 2018, 2019, and 2020 - detection and evaluation using mobile laser scanning